

# Integrating non-visual effects of light in the automated daylight-responsive control of blinds and electric lighting

Présentée le 26 novembre 2021

Faculté de l'environnement naturel, architectural et construit  
Laboratoire d'énergie solaire et physique du bâtiment  
Programme doctoral en énergie

pour l'obtention du grade de Docteur ès Sciences

par

**Marta BENEDETTI**

Acceptée sur proposition du jury

Dr J. Van Herle, président du jury  
Prof. J.-L. Scartezzini, Dr M. Münch, directeurs de thèse  
Prof. C. Cajochen, rapporteur  
Dr R. Ferrini, rapporteur  
Dr J. Wienold, rapporteur

*A ship in harbor is safe, but that is not what ships are built for.*

- John A. Shedd





# Acknowledgements

---

Now that my thesis and my wonderful time at EPFL have come to an end, here is my occasion to express my sincere gratitude to all the people who helped me to reach this goal in many ways:

My thesis supervisor, Prof. Jean-Louis Scartezzini, for giving me the fantastic opportunity to carry on this thesis at LESO-PB, for guiding me with his immense wisdom and experience, for always being supportive throughout the entire journey of my PhD.

Prof. Mirjam Münch, whom I have been so lucky to call my co-supervisor. Despite being quite demanding at times (and she is aware of that!), her contribution was crucial to make this thesis successful: I am beyond grateful to her for providing me with great advice, guidance and encouragement, and for introducing to me the fascinating world of chronobiology and knowledge in statistics. Even though due to Covid-19 I could not join her in New Zealand for my 6-months fellowship, she never left me alone and we had countless Zoom meetings. Thank you Mirjam for being my anchor through all this time.

The jury members of my doctoral exam: Dr. Jan Van Herle, Prof. Christian Cajochen, Dr. Rolando Ferrini and Dr. Jan Wienold, for giving interesting and constructive feedback on my thesis, which helped to enhance its quality.

Dr. Lenka Maierová for her practical help in the design and preparation of the study, and for her involvement in interpreting the results.

The Swiss Innovation Agency Innosuisse and the Board of the Swiss Federal Institutes for ensuring the necessary funding for my research work.

Prof. Christoph Schierz and Dr. Stefan Wolf at the Technical University of Ilmenau, for lending two 'Luxblick' devices, which allowed to record very important data in my study and thus added great quality to my work. I also thank Dr. Christina Schmidt for providing the codes to interpret the cognitive tests results, and Valentin Tissot-Daguette for help in extracting and processing some of the monitored data.

All the 34 participants in my study, for their commitment and compliance to the rules.

Laurent Deschamps and the IT team at LESO-PB, for providing excellent technical support with hardware and software, for their fundamental help in the design and maintenance of an experimental setup of exceptional quality. Thank you for being available to help me with any issue in the shortest

## Acknowledgements

---

delay. The same holds for Pierre Loesch: thank you for your assistance in setting up the testbed and the devices for my study, and for being there any time I needed your help.

Marlene Muff and Barbara Smith, for helping me especially with the administrative procedures, always with a kind smile on their face.

My former colleague, predecessor and dear friend Ali Motamed for being an excellent reference and collaborator, and also an irreplaceable office mate during my earlier years. He paved the way to my research while being a great example of commitment and hard work, and we had much fun together.

All my colleagues and friends at LESO-PB and around: Anna Krammer, Pietro Florio, Alina Walch, Dan Assouline and Claudia Bongiovanni, Dasaraden Mauree, Roberto Castello, Yujie Wu, Olivia Bouvard, Jing Gong, Jérémy Fleury, Luc Burnier, Maxime Lagier, Kavan Javanroodi, Dasun Perera, and all the people who passed by the lab in these years. I received so much from every one of them: from fruitful collaboration in research projects to great company and friendship during trips, parties, sport training and races, coffee and lunch breaks. I will miss you and will forever cherish the memories of many adventures and experiences we had together.

Dr. Andreas Schöler for several inspirational and pleasant discussions on various topics, for the music rehearsals, for his encouragement, intelligence and positive attitude.

Manuele, for hosting me in your home and for putting up with my crises over these last few months, for encouraging me to do my best and believe a bit more in my abilities. Thank you for your presence, your love, and for simply being the best life partner I have ever wished for.

Last but not least, my family: my parents Mara and Paolo and my sister Giulia. Le parole non possono esprimere tutta la mia gratitudine. Grazie a voi che siete da sempre il mio porto sicuro, le mie radici. Grazie per tutto l'amore, la comprensione e l'incoraggiamento che mi avete sempre dato.

Marta Benedetti  
Lausanne, November 12, 2021



# Abstract

---

The use of daylight in buildings is important because it significantly contributes to energy savings by reducing the use of electric lighting and space heating. It also impacts on biological functions and on well-being. Indeed, light not only allows vision, but also has non-visual effects on human physiology: for instance, light is the primary time cue for the circadian entrainment of the biological rhythms to the 24-hour environmental time.

This thesis is focused on two aspects: the automated control of daylighting in buildings, and the examination of its impact on non-visual functions in a semi-realistic office study. The overall hypotheses for this thesis were that a strategy including a daylight-responsive automated controller for indoor lighting combined with an advanced daylighting room design is beneficial for non-visual functions, it can maintain sound visual comfort and lead to low electric energy demand. The main aims of this work were: 1) to set-up an automated control system for integrated daylight and electric lighting; 2) to test its effects on circadian rhythms, cognitive performance and visual comfort in a balanced cross-over study with young participants, and 3) to evaluate its impact on energy demand. To achieve the first aim, an automated controller for venetian blinds and electric lighting was designed to provide optimal indoor lighting conditions according to dynamic preset target levels of illuminance. The controller was based on real-time assessment of lighting conditions by high dynamic range (HDR) vision sensors placed next to the desk at the eye level. In a next step, the automated controller was implemented in a well-daylit office room (*Test* room) and compared with a *Reference* room corresponding to a standard working space without automated control (and a lower window-to-wall ratio). A total of 34 young participants spent five consecutive days (8h/day during normal office hours) in each of the two rooms. Lighting conditions in the room were continuously monitored, and individual light exposures were recorded by wearable devices. Several physiological outcome measures (sleep/wake times, salivary hormonal concentrations, skin temperatures) were obtained. Simultaneously, cognitive performance (on auditive computer tasks), as well as subjective comfort and well-being were repeatedly assessed.

The results showed that vertical illuminance was significantly higher in the *Test* room compared to the *Reference* room, especially in the morning hours until the early afternoon, while visual comfort was always ensured. The higher illuminance in the first part of the day led to a faster accumulation of the daily light dose: 50% of the maximum accumulated illuminance was reached on average 50 minutes earlier in the *Test* than in the *Reference* room.

Concomitantly with higher illuminance, the timing of the circadian rhythms (assessed by the onset

## Abstract

---

of melatonin secretion and peripheral heat loss through the skin) was advanced by approximately 20-30 minutes in the *Test* room. On the other hand, participants overall performed better in the *Reference* room, especially in summer. The overall electricity demand for space heating and lighting decreased by 9.6% in the *Test* room with respect to the *Reference* room.

To summarise, these findings indicate that the lighting strategy had phase-advancing effects on circadian rhythms, which might be a useful real-setting treatment for circadian sleep-wake disorders which have become more frequent in young adults nowadays. Further work is needed to establish optimal lighting for cognitive performance across different seasons of the year.

**Keywords:** daylighting, automated control system, non-visual effects, circadian rhythms, melatonin, cortisol, skin temperature, glare, energy consumption, electric lighting.

## Abstract (italiano)

---

L'uso della luce naturale negli edifici è importante perché contribuisce al risparmio energetico riducendo l'uso dell'illuminazione elettrica e del riscaldamento. Ha anche un impatto sulle funzioni biologiche e sul benessere. Infatti, la luce non solo permette di vedere, ma ha anche effetti "non visivi" sulla fisiologia umana: ad esempio, è la principale indicazione temporale per la sincronizzazione dei ritmi biologici circadiani con l'ambiente esterno.

Questa tesi affronta due aspetti: il controllo automatico dell'illuminazione negli edifici, e l'esame del suo impatto sulle funzioni non visive in uno studio semi-realistico. È stato ipotizzato che un sistema di controllo automatico dell'illuminazione in un ufficio con sistemi avanzati di luce naturale offre vantaggi per le funzioni non visive e il comfort visivo, mantenendo una bassa domanda energetica. Gli obiettivi principali di questo lavoro erano: 1) programmare un sistema di controllo automatico integrante illuminazione naturale ed elettrica; 2) testarne gli effetti su ritmi circadiani, prestazioni cognitive e comfort visivo in uno studio cross-over con giovani partecipanti; 3) valutarne l'impatto sul consumo energetico. Per raggiungere il primo obiettivo, è stato progettato un controllo automatico per schermature veneziane e illuminazione elettrica per fornire condizioni luminose ottimali secondo livelli di illuminamento dinamici preimpostati. Il controllo si basava sulla valutazione in tempo reale delle condizioni luminose da parte di sensori di visione ad alta gamma dinamica posti accanto alla postazione di lavoro. In una fase successiva, il controllo automatico è stato applicato in un ufficio "Test" e confrontato con un ufficio "Reference", rappresentante un tipico ufficio non automatizzato. 34 giovani partecipanti hanno trascorso 5 giorni consecutivi (8 ore al giorno) in ognuno dei due uffici. Le condizioni di illuminamento sono state monitorate continuamente, mentre le esposizioni individuali alla luce erano registrate da dispositivi indossabili. Sono state raccolte varie misure fisiologiche (tempi di sonno/veglia, concentrazioni ormonali salivari, temperature della pelle). Le prestazioni cognitive (su test auditivi al computer) così come il comfort soggettivo sono stati valutati ripetutamente.

I risultati mostrano un illuminamento significativamente più alto nell'ufficio *Test* che nell'ufficio *Reference*, soprattutto dalle ore mattutine fino al primo pomeriggio, pur mantenendo il comfort visivo. Il maggiore illuminamento nella prima parte della giornata ha portato ad un accumulo più veloce della dose individuale di luce giornaliera: il 50% dell'illuminamento accumulato veniva raggiunto in media 50 minuti prima nell'ufficio *Test* che nell'ufficio *Reference*.

Parallelamente, il timing dei ritmi circadiani (indicato dall'inizio della secrezione di melatonina e dalla perdita di calore periferica attraverso la pelle) è stato anticipato di circa 20-30 minuti nell'ufficio *Test*. D'altra parte, la performance cognitiva è stata migliore nella stanza *Reference*, specialmente

## Abstract (italiano)

---

in estate. Il consumo energetico per riscaldamento e illuminazione è diminuito del 9.6% nell'ufficio *Test* rispetto all'ufficio *Reference*.

Lo studio indica che la strategia di illuminazione ha anticipato la fase dei ritmi circadiani, rivelandosi un trattamento potenzialmente utile per i disturbi circadiani di sonno-veglia, diventati più frequenti nei giovani di oggi. Ulteriori approfondimenti sono necessari per stabilire l'illuminazione ottimale per le prestazioni cognitive nelle diverse stagioni dell'anno.

**Parole chiave:** luce naturale, sistemi di automazione, effetti non visivi, ritmi circadiani, melatonina, cortisolo, temperatura della pelle, abbagliamento, consumo energetico, illuminazione elettrica.



# Contents

---

<b>List of Figures</b>	<b>ix</b>
<b>List of Tables</b>	<b>xiii</b>
<b>Nomenclature</b>	<b>xv</b>
<b>1 Introduction</b>	<b>1</b>
1.1 Context . . . . .	1
1.1.1 Daylighting in buildings . . . . .	1
1.1.2 The impact of light on humans . . . . .	2
1.2 Problem statement . . . . .	4
1.3 Research questions . . . . .	5
1.4 Thesis objectives . . . . .	5
1.5 Significance of the thesis . . . . .	6
1.6 Thesis overview . . . . .	7
<b>2 Daylighting control in buildings</b>	<b>9</b>
2.1 Background . . . . .	9
2.1.1 Photometric measurements . . . . .	9
2.1.2 Visual comfort and glare risk assessment . . . . .	11
2.1.3 High Dynamic Range (HDR) sensors . . . . .	13
2.1.4 Daylight in offices . . . . .	16
2.1.5 Hypotheses . . . . .	20
2.2 Automated controller for venetian blinds and electric lighting . . . . .	21
2.2.1 Experimental setup . . . . .	21
2.2.2 Continuous monitoring of indoor lighting conditions . . . . .	27
2.2.3 Sensors, actuators and control platform . . . . .	29
2.2.4 The control algorithm . . . . .	29
2.2.5 Summary of the controller steps . . . . .	37
2.2.6 The <i>Reference</i> room . . . . .	38
2.2.7 Data collection and analysis . . . . .	40
2.3 Results . . . . .	43

## Contents

---

2.3.1	Lighting conditions in the office rooms . . . . .	43
2.3.2	Room temperature . . . . .	45
2.3.3	Electric energy consumption . . . . .	46
2.4	Summary and discussion . . . . .	48
2.4.1	Lighting conditions and DGP monitoring . . . . .	49
2.4.2	Considerations on room temperature . . . . .	50
2.4.3	Electric energy demand . . . . .	51
<b>3</b>	<b>Impact of light on humans</b>	<b>53</b>
3.1	Background . . . . .	53
3.1.1	The visual system . . . . .	53
3.1.2	The non-visual system . . . . .	55
3.1.3	Circadian entrainment . . . . .	60
3.1.4	Non-visual effects of light . . . . .	63
3.1.5	Experimental studies with dynamic office lighting . . . . .	68
3.1.6	Hypotheses . . . . .	69
3.2	Experimental study with young participants . . . . .	70
3.2.1	Screening procedure and participants . . . . .	70
3.2.2	Study protocol . . . . .	71
3.2.3	Study measures . . . . .	72
3.2.4	Statistical analysis . . . . .	79
3.3	Results . . . . .	81
3.3.1	Lighting conditions in the office rooms . . . . .	81
3.3.2	Individual light exposure at the eye . . . . .	83
3.3.3	Salivary hormones . . . . .	87
3.3.4	Distal-proximal skin temperature gradient . . . . .	91
3.3.5	Cognitive performance . . . . .	96
3.3.6	Subjective assessments (VAS/VCS) . . . . .	102
3.3.7	Thermal comfort . . . . .	104
3.3.8	Visual comfort . . . . .	106
3.3.9	Correlation analysis . . . . .	109
3.4	Summary and discussion . . . . .	110
<b>4</b>	<b>Practical implementation in an open-plan office</b>	<b>115</b>
4.1	Motivation . . . . .	115
4.2	The SolAce unit at NEST . . . . .	116
4.3	Experimental setup . . . . .	118
4.4	First monitoring results . . . . .	120

4.5	The control algorithm . . . . .	120
4.6	Aims and future directions . . . . .	120
<b>5</b>	<b>General discussion and conclusion</b>	<b>125</b>
5.1	Achievements and discussion . . . . .	125
5.2	Limitations . . . . .	127
5.3	Summary . . . . .	128
5.4	Outlook . . . . .	129
	 <b>Bibliography</b>	 <b>131</b>
<b>A</b>	<b>Fuzzy Logic Controller for top blind</b>	<b>153</b>
A.1	Fuzzy variables and membership functions . . . . .	153
A.2	Rules of the FLC . . . . .	155
<b>B</b>	<b>Questionnaires: VAS/VCS</b>	<b>157</b>
<b>C</b>	<b>Correlation analysis and subjective comfort</b>	<b>161</b>
<b>D</b>	<b>Control platforms at LESO-PB and NEST</b>	<b>165</b>
	 <b>Curriculum Vitae</b>	 <b>169</b>



## List of Figures

---

1.1	Conceptual scheme: important aspects which need to be integrated for an optimal office lighting. . . . .	4
1.2	Conceptual figure: the three research areas of this interdisciplinary doctoral thesis. .	6
2.1	HDR vision sensors and Glare Meter . . . . .	14
2.2	Simplified schematic overview of an office at the LESO experimental building. . . .	15
2.3	Luminance map captured by the VIP sensor placed close to the user sitting at the desk	15
2.4	The new Glare Meter interface . . . . .	16
2.5	Outdoor view of the southern façade of the LESO building on EPFL campus. The red circles indicate the two office rooms at the second floor which were used during the experiments (left: <i>Reference</i> room, right: <i>Test</i> room). . . . .	21
2.6	Indoor view of the two office rooms . . . . .	22
2.7	Candle power distribution of luminaires . . . . .	23
2.8	Spectral power distribution of the electric lighting fixtures . . . . .	24
2.9	Dimming curves: vertical (a) and horizontal work plane (b) illuminance vs. relative power of the luminaires. . . . .	26
2.10	a) Photograph of the VIP (left) and IcyCAM (middle) vision sensors and spectrometer (right) mounted on the support next to the office desk; b) Exemplary photograph of the work space set-up of the two office rooms. . . . .	27
2.11	Schematic overview of the <i>Test</i> room. The <i>Reference</i> room was identical except that the ADS was covered (see section 2.2.6). . . . .	28
2.12	SPD (between 380 and 780nm, coloured with the approximate colours in the visible spectrum) measured at the desk on a vertical plane at the approximate eye level, at 1.20m height above the floor: a) daylight only, electric lighting switched off; b) mix of daylight and electric lighting. . . . .	28
2.13	Preset dynamic target vertical illuminance curve at the eye level ( $E_{v,target}$ ) throughout the working day, from 8:00 to 18:00. . . . .	30
2.14	Scheme of the information flow and decision making of the automated control platform	31
2.15	Geometry of the <i>Test</i> room (LE2201) for the computation of the blind positions. .	33
2.16	Scheme of input and output variables of the FLC for the top blind . . . . .	33
2.17	The "error" $eE_v$ (y-axis) as a function of $E_{v,measure}$ (x-axis). . . . .	35

## List of Figures

---

2.18	Geometry of the blinds for calculation of the slat angle . . . . .	36
2.19	Execution block diagram of the controller . . . . .	39
2.20	Control box for electric lighting and temperature set point . . . . .	40
2.21	Average time course of vertical illuminance during the day . . . . .	43
2.22	Average time course of Daylight Glare Probability during the day . . . . .	44
2.23	Time course of melanopic Equivalent Daylight Illuminance (EDI), averaged across days for each condition (mean $\pm$ SEM); n=80 for both conditions. . . . .	45
2.24	Time course of room temperature averaged across days . . . . .	45
2.25	Bar charts of total energy demand . . . . .	46
2.26	Bar charts of electric lighting energy demand . . . . .	47
2.27	Bar charts of electric energy demand for space heating . . . . .	47
2.28	Bar charts of sky type during the study (total number of day for each sky type) and outside temperature . . . . .	48
3.1	Simplified scheme of light detection in the retina for vision . . . . .	54
3.2	Standardized relative spectral sensitivity curves for photopic ( $V(\lambda)$ ) and scotopic vision ( $V'(\lambda)$ ). Used with permission: van Bommel [2019b]. . . . .	55
3.3	Relative spectral sensitivity functions of the human photoreceptors . . . . .	56
3.4	Two main neuronal pathways in response to light which are signalled to different brain areas: 'visual' path (red) and 'non-visual' path (cyan) to the SCN. . . . .	57
3.5	Qualitative representation of daily rhythms of melatonin and cortisol secretion in humans . . . . .	58
3.6	Daily circadian rhythm of core body temperature shown on a double-plotted (2-day) scale . . . . .	59
3.7	Schematic diagram of the impact of ancestral versus modern day light exposure and social constraints on sleep patterns . . . . .	61
3.8	Reproduced from [Wright et al., 2013]: averaged light exposure (on a log-scale) for study participants during the week of natural light/dark exposure while camping (black line) and during the week in the built environment with electric lighting (grey line). . . . .	63
3.9	Reproduced from Beersma et al. [2009] (adapted from original: [Khalsa et al., 2003]): Phase-Response Curve (PRC) to a bright light stimulus of 10000 lux. . . . .	65
3.10	Overview of the 4-week study protocol . . . . .	73
3.11	Wearable light sensor device "Luxblick" . . . . .	74
3.12	Wireless skin temperature sensors (i-Buttons, Maxim Integrated, USA) . . . . .	75
3.13	Actigraphy watch "ActTrust" by Condor Instruments (www.condorinst.com.br). . . . .	78
3.14	Time course of photopic vertical illuminance $E_v$ and melanopic EDI in the office rooms. . . . .	82
3.15	Time course of averaged individual photopic illuminance ( $E_v$ ) grouped by condition . . . . .	83

3.16 Dose-response curves for accumulated individual $E_v$ from wearable devices (fitted sigmoidal curves) . . . . .	85
3.17 Bar charts of individual $E_v$ from wearable devices (mean $\pm$ SEM) grouped by season	86
3.18 Time course of averaged individual illuminance ( $E_v$ ) from wearable devices across both conditions, grouped by season . . . . .	87
3.19 Diurnal profile of melatonin concentration . . . . .	88
3.20 Box plots for melatonin secretion onset and offset times . . . . .	89
3.21 Diurnal profile of cortisol concentration (mean $\pm$ SEM) . . . . .	90
3.22 Bar chart of all cortisol concentration grouped by season and condition . . . . .	90
3.23 24-hour time course of the DPG . . . . .	91
3.24 DPG evening rise . . . . .	92
3.25 DPG morning decline . . . . .	93
3.26 Phase angle of entrainment between DPG rise and sleep onset and between DPG decline and wake time . . . . .	94
3.27 Bar charts of fastest 10% reaction times (RT) in the PVT . . . . .	97
3.28 Plots of 3-back accuracy scores . . . . .	98
3.29 Plots of 2-back accuracy scores . . . . .	99
3.30 Plots of 0-back accuracy scores . . . . .	100
3.31 Plots of Mental Effort Rating Scale (MERS) . . . . .	101
3.32 Plots of subjective sleepiness . . . . .	103
3.33 Bar chart of mood rating . . . . .	103
3.34 Bar charts of room temperature . . . . .	104
3.35 Bar chart and line plot of subjective thermal comfort. . . . .	105
3.36 Time courses for room temperature and subjective thermal comfort . . . . .	106
3.37 Bar charts of DGP (mean $\pm$ SEM) grouped by condition (a) and by condition and season (b) . . . . .	107
3.38 Plots of subjective glare (mean $\pm$ SEM) grouped by condition (a), by season and condition (b); c) time course averaged across 5 days and aligned relative to midsleep.	108
3.39 Time course of the Daylight Glare Probability (DGP) index and subjective visual comfort ratings . . . . .	109
4.1 Outdoor view of the NEST building in Dübendorf. The SolAce unit at the second floor of the building is indicated by the red rectangle. . . . .	116
4.2 a) Plan of SolAce; b) indoor view of the working space; c) the living space. . . . .	117
4.3 Working and chilling in SolAce . . . . .	118
4.4 Motorized venetian blinds in the open plan office. . . . .	118
4.5 a) Glare Meter installed on the ceiling; b) greyscale image captured by the sensor .	119

## List of Figures

---

4.6	a) Glare Meter installed on the computer screen; b) greyscale image captured by the sensor. . . . .	119
4.7	First monitoring results in SolAce: vertical illuminance (a), Daylight Glare Probability (b) and average luminance of the work plane (c) . . . . .	122
4.8	Execution diagram of the first version of the control system for blinds and electric lighting in the SolAce unit. . . . .	123
5.1	Indoor view of the open plan office in the SolAce unit, described in Chapter 4. . .	129
A.1	Fuzzy variable eDGP. . . . .	153
A.2	Fuzzy variable eDGP. . . . .	153
A.3	Fuzzy variable $E_v$ . . . . .	154
A.4	Fuzzy variable Presence. . . . .	154
A.5	Fuzzy variable Altitude. . . . .	154
A.6	Fuzzy variable TopBlind. . . . .	155
B.1	Example of questions (screenshots) included in the surveys with Visual Analogue Scale (VAS). . . . .	159
B.2	Mental Effort Rating Scale (MERS). During the study, participants were asked to indicate their perceived effort in executing the cognitive task session. . . . .	160
C.1	Correlation table . . . . .	161
C.2	Heat plots of room temperature and subjective thermal comfort assessments . . .	162
C.3	3D plots of room temperature and subjective thermal comfort . . . . .	163
C.4	Heat plots representing DGP and subjective visual comfort (glare ratings) in all seasons and conditions for all participants, averaged across days . . . . .	164
D.1	Schematic overview of the physical platform of the control system applied in the two rooms of LESO-PB. . . . .	166
D.2	Schematic overview of the data communication platform set up for the control of blinds and lighting at SolAce (courtesy of Valentin Trana and Laurent Deschamps)	167



## List of Tables

---

2.1	Principal radiometric and photometric quantities; table adapted from [Goodman, 2009]. Abbreviations for international standard (SI) units: W = Watt; sr = steradian; lm = lumen; cd = candela; m = meter. . . . .	10
2.2	Categorization of DGP values [Technical Committee CEN/TC 169 "Light and Lighting", 2018]. . . . .	13
2.3	Main characteristics of the installed electric lighting fixtures (identical in both rooms); lm = lumen, K = Kelvin, W = Watt. . . . .	23
2.4	Photometric and $\alpha$ -opic quantities calculated from the two spectral power distributions of the luminaires (Figure 2.8), using the CIE toolbox [Commission Internationale de l'Éclairage (CIE), 2018]. . . . .	24
2.5	Relative power (RP) of ceiling-mounted and standing luminaire and corresponding measured vertical illuminance ( $E_v$ ) and horizontal illuminance on the work plane ( $E_h$ ). All the reported values are means of at least 3 measurements per each dimming step. . . . .	26
2.6	The output variable of the FLC: the top blind position. The variable could take decimal values between 0 (for completely closed) to 1 (completely open). . . . .	35
2.7	Possible scenarios for top blind control, where $\theta$ is the actual sun height and $\theta''$ and $\theta'''$ are critical angles shown in Figure 2.15. The calculated values of these critical angles are: $\theta'' = 60^\circ$ , $\theta''' = 35^\circ$ . . . . .	35
2.8	Commands to electric lighting according to the "lacking" vertical illuminance ' $E_v$ '. . . . .	37
3.1	Scores of the screening questionnaires . . . . .	71
3.2	Results for light recordings: $E_v$ = photopic illuminance, EDI = equivalent (D65) daylight illuminance (lux, SPD derived from the SPD assessed by the spectrometer), both assessed on a vertical plane at the approximate eye level during office hours; individual $E_v$ from wearable light sensor devices during the entire waking period including office hours (mean $\pm$ SD across days and participants). P-value: main effect of <i>condition</i> . . . . .	84
3.3	Summary of sleep times and melatonin and DPG results from study measures in the two conditions . . . . .	95

**List of Tables**

---

3.4 Summary of results of cognitive performance tasks (mean values  $\pm$  SD). RT are shown in ms and accuracy is shown as score (see section 3.2.3); ns = not significant ( $p>0.05$ ). . . . . 100

3.5 Summary of results for subjective sleepiness, mood and comfort assessment (mean  $\pm$  SD) . . . . . 109

B.1 List of questions included in the surveys (VAS/VCS) to which participants were required to answer at regular intervals during the days in the office rooms. The questions were presented to the participants in French (here in italics). . . . . 158

## Nomenclature

---

ADS		Anidolic Daylighting System
CAR		Cortisol Awakening Response
CBT		Core Body Temperature
CCT	[K]	Correlated Colour Temperature
CIE		<i>Commission Internationale de l'Éclairage</i>
DGI	[%]	Daylight Glare Index
DGP	[%]	Daylight Glare Probability
DLMO		Dim Light Melatonin Onset
DPG	[°C]	Distal-to-Proximal skin Temperature Gradient
DSPS		Delayed Sleep Phase Syndrome
EDI	[lux]	Equivalent Daylight Illuminance
$E_{e, mel}$	[W/m <sup>2</sup> ]	Melanopic irradiance
$E_h$	[lux]	Horizontal illuminance (on the work plane)
ELR	[mW/lm]	Efficacy of Luminous Radiation
ESS		Epworth Sleepiness Scale
$E_v$	[lux]	Vertical illuminance (at the eye level)
FLC		Fuzzy Logic Controller
HDR		High Dynamic Range
HO		Horne and Östberg
ipRGCs		intrinsically photosensitive Retinal Ganglion Cells
MCTQ		Munich ChronoType Questionnaire
MERS		Mental Effort Rating Scale
PSQI		Pittsburgh Sleep Quality Index

**Nomenclature**

---

PVT		Psychomotor Vigilance Task
RT	[ms]	Reaction Time
SCN		Suprachiasmatic Nucleus
SD		Standard Deviation
SEM		Standard Error of the Mean
SPD		Spectral Power Distribution
VAS		Visual Analogue Scale
VCS		Visual Comfort Scale
VM		Virtual Machine
WWR	[%]	Window-to-Wall Ratio

# 1

## Introduction

---

### 1.1 Context

#### 1.1.1 Daylighting in buildings

Daylight in non-residential buildings brings several advantages and there are many reasons why it should be used as a primary source of illumination. Firstly, it has a positive impact on energy savings [Ruck et al., 2000]. The use of daylighting in non-residential buildings has the potential to reduce the electricity demand for lighting from 50% to 80% [Bodart & De Herde, 2002], and therefore offers a serious opportunity for reducing Greenhouse Gases (GHG) and CO<sub>2</sub> emissions [Jenkins & Newborough, 2007].

However, maximising the use of daylighting can also lead to problems for building occupants. One of the main issues is glare, which is caused by direct sunlight or reflections on the surfaces, generating visual discomfort. In the absence of a properly designed controller for solar protection, users typically close the blinds to prevent such unpleasant situations and, they often keep them closed even more and longer than necessary.

In general, office occupants seem rather reluctant in pro-actively regulating shadings and lighting, which often leads to poor indoor daylight availability and more frequent use of electric lighting. Indeed, Paule et al. [2015] showed that office occupants adjust the blinds less than two times per week, regardless of the façade orientation or season of the year. In the same study, the authors also found that on average 57% of the window surface was covered by blinds, which made the use of electric lighting mandatory for work places located further from the window [Paule et al., 2015]. The lack of daylight influx in buildings might increase energy consumption, as occupants tend to use more electric lighting. This suggests that daylight contribution to indoor lighting could be optimized (also depending on geographical latitude and climate), for example by using automated control systems for shadings [Tsangrassoulis & Li, 2018].

Nowadays, no disseminated technology exists to assess discomfort glare in real-time. The use of camera-like sensors that capture luminance in the field of view, identify the glare sources and assess glare indexes provides an accurate real-time monitoring of the lighting conditions in the room [Borisuit et al., 2011, 2012; Motamed et al., 2015]. Incorporating such devices in an automated

control system for blinds and electric lighting in an office room has already demonstrated to maintain visual comfort in an ideal range while minimising energy demand [Motamed, 2017].

### 1.1.2 The impact of light on humans

As another important aspect, several studies gave evidence that access to natural light at the workplace improves well-being of occupants [Boyce et al., 2003; Beute & de Kort, 2014]. A sufficient daylight exposure during the day also improves sleep quality, work performance, job satisfaction and mood [Newsham et al., 2009; Figueiro et al., 2017; Boubekri et al., 2020].

Light is not only essential for vision: it also has profound impacts on human physiology, health and behaviour [Münch et al., 2017]. Indeed, light information reaching the retina is conveyed through so-called non-visual pathways to the "core biological clock" in the brain [Berson et al., 2002]. This internal key pacemaker governs the timed physiological responses of most body and brain functions and synchronizes them with each other and with the solar light/dark cycle [Buijs et al., 2006; Honma et al., 2012; Weaver & Emery, 2013]. Examples of such physiological functions are the sleep/wake cycle, core body temperature, heart rate and hormonal secretion. All these functions exhibit a "circadian" rhythm (from the Latin words *circa* and *dies*, i.e., "approximately" and "day"). Besides influencing the circadian rhythms, exposure to light has also acute effects, such as increasing alertness and improving cognitive performance and mood. In general, light responses which are not primarily related to visual functions are called "non-visual effects" of light. The entity of non-visual effects depends on many features of light exposure, for instance the quantity (irradiance, brightness) and quality (spectrum) of the luminous flux, but also the timing, as well as prior exposure history, etc. (see Chapter 3 and [Prayag et al., 2019] for a review).

A well-known example for circadian rhythms is the diurnal modulation of hormonal secretions, such as melatonin and cortisol. Melatonin is secreted by the pineal gland of the brain during the night. It provides an internal biological signal of darkness, in preparation for sleep in humans. Its concentrations are normally very low during daytime and start rising in the evening: the onset of melatonin secretion is defined as the time when melatonin concentrations (measured in blood or in saliva) exceed a certain threshold, which occurs approximately 2-3 hours before bedtime [Burgess et al., 2003]. After reaching the peak in the early morning hours, melatonin concentration drops (*offset*). Because light suppresses melatonin secretion in the pineal gland [Lewy et al., 1980], assessments need to be performed in dim light. The time of the dim light melatonin onset (DLMO) and the dim light melatonin offset (DLMOff) are the two most common *circadian phase markers* [Lewy & Sack, 1989].

On the other hand, cortisol, usually known as "stress hormone", follows a different circadian pattern: its plasma concentrations peak around wake-up time and decrease during the day, reaching the lowest level around habitual bedtime [Weitzman et al., 1971; Stewart, 1999].

Light exposure influences these phase markers. For example, bright light exposure in the evening

causes acute suppression of melatonin concentrations in the blood or saliva [Gronfier et al., 2004; Lewy et al., 1980], and delays the phase of the circadian clock [Khalsa et al., 2003]. It was also shown that bright light in the early morning hours or at midday increases the melatonin peak during the night and advances the onset of melatonin, suggesting that exposure to bright light earlier in the day has a potential to advance the phase of the circadian clock [Hashimoto et al., 1997; Mishima et al., 2001; Khalsa et al., 2003; Takasu et al., 2006].

Core body temperature (CBT) also exhibits a circadian rhythm, typically reaching its maximum in the late afternoon and a minimum (*nadir*) during the night, shortly before wake-up time [Czeisler et al., 1980]. Such a decline of CBT in the evening is facilitated by peripheral heat loss through the skin and it is interconnected with the rise of melatonin concentrations, and is physiologically linked to sleep in humans [Van Someren, 2000]. Bright light in the evening also diminishes the natural decline in CBT before and around sleep time [Dijk et al., 1991]. Several studies found a link between melatonin and CBT levels, suggesting that melatonin additionally induces sleep through a thermoregulatory process [Kräuchi et al., 2006].

As previously mentioned, the circadian timing of the core pacemaker and peripheral oscillators (i.e., peripheral clocks of cells, tissues and organs) lasts approximately, but not exactly 24 hours. Hence, these internal clocks need to be synchronized with each other and entrained to the external 24-hour solar day. Therefore, external time cues (or “Zeitgebers” [Aschoff, 1960]), such as light, meals, sleep, physical activity, are necessary to keep the circadian pacemaker (and in turn the circadian rhythms) synchronized to the precise 24-hour environmental time. Among these different Zeitgebers, light is the strongest one [Aschoff & Wever, 1981; Lockley, 2009].

To all of us, it is crucial to be exposed to natural light, or, when this is not possible, to electric light (at the right time), for good entrainment of the endogenous circadian rhythms to the external 24-hour day. If that is not the case, internal clocks become misaligned with the 24-hour day and can cause circadian rhythm disorders when such misalignment becomes chronic, as it is frequently occurring in blind individuals without light perception [Emens & Lewy, 2005; Lockley et al., 2007]. In modern societies, many people spend the majority of their time inside of buildings, where they very likely receive an insufficient amount of light during daytime and too much light in the evening (receive light at the wrong time). In 2009 the CIE (*Commission Internationale de l’Éclairage*) concluded that daily light exposure in modern, industrialized societies could be too low for good mental health [Veitch, 2011; Commission Internationale de l’Éclairage (CIE), 2009]. As stated above, chronically inappropriate light exposure can lead to circadian rhythm misalignment, and in turn, can increase the risk for more severe health issues such as cardio-vascular disease, diabetes and cancer [Baron & Reid, 2014].

There are many open questions regarding the impact of daylight on humans [Münch et al., 2020], for instance: how much light do we need? The answer is still not clear. Peter R. Boyce suggested that “until a full understanding of the role of light exposure on human health is available, the best

*approach to lighting for human health is to replicate the conditions under which mankind evolved: daylight by day and little light at night”* [Boyce, 2013]. According to the existing literature, the answer remains to be elucidated, some recent recommendations are underway [Brown et al., 2020].

### 1.2 Problem statement

An optimal controller of daylighting in buildings must face several challenges: the use of daylighting should be maximized because of the clear advantages for energy savings and human factors (as stated above). On the other hand, there are also possible issues which need to be mitigated, for instance discomfort glare. Most importantly, the design and control of lighting in indoor working environments has so far not sufficiently considered non-visual effects of light, mainly due to the lack of knowledge, and lack of recommendations and guidelines for its translation into practice. Therefore, taking non-visual effects into account in the design of dynamic lighting systems can be essential to contribute to well-being, high productivity and performance of office occupants.

An optimal automated lighting control should integrate the following needs: good vision, sound visual comfort, optimal non-visual functions as well as low energy consumption (Figure 1.1).

It is worth mentioning that another issue often brought with high daylight influx is overheating of the indoor space, resulting in thermal discomfort for the occupants. Adding optimization strategies for thermal comfort to the automated control system goes beyond the main scope of this doctoral thesis. Nevertheless, room temperature and subjective thermal perception were monitored and possible influences on the occupants' overall comfort as well as on their non-visual functions were reported and discussed.

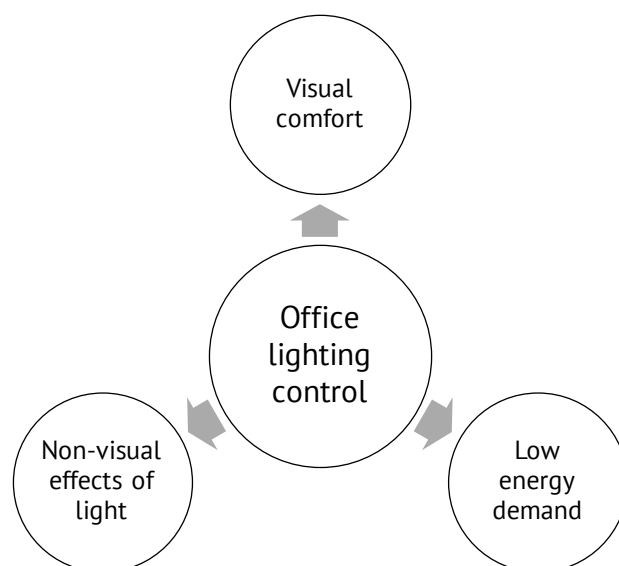


**Figure 1.1** – Conceptual scheme: important aspects which need to be integrated for an optimal office lighting.



### 1.3 Research questions

There is to date no automated control system for daylighting available which simultaneously includes aspects of visual comfort and non-visual functions in humans. This thesis tackles this problem and is developed around two main research questions, each of them with several more specific questions:

- A. Is it possible to provide high quality dynamic lighting in an office by means of a strategy that includes an advanced daylighting room design and a daylight-responsive automated controller for blinds and electric lighting?
  - a. Can such a strategy prevent the user from discomfort glare at the desk during working hours?
  - b. Can such a strategy help to mitigate the energy demand for electric lighting?
- B. Does the mentioned strategy have an effect on non-visual functions?
  - a. Does it advance the circadian phase of melatonin and cortisol secretions?
  - b. Does it affect the modulation of peripheral skin temperatures?
  - c. Can it improve cognitive performance during daytime?
  - d. Can it enhance subjective alertness and mood during daytime?

More specific hypothesis for each of the two main research topics will be formulated in detail in Chapters 2 and 3.

### 1.4 Thesis objectives

The overall objectives of this thesis are:

- To implement an automated control system that integrates daylighting and electric lighting dynamically. Such a control system should maintain objective visual comfort at the work space in a defined range and keep energy demands low.
- To test the effects of the automated office lighting control, combined with an advanced daylighting room design, on non-visual functions and visual comfort in young volunteers.

To achieve the overall objectives, the thesis work aimed at developing a specific algorithm for the automated control of venetian blinds and electric lighting in an office at the LESO experimental building at EPFL campus (Lausanne, Switzerland, 46°32' N latitude, 410 meters above sea level). The automated controller, in combination with an advanced daylighting room design, was designed to support visual and non-visual functions such as alertness, mood and cognitive performance in office occupants. It was also tuned in a way to continuously provide sound visual comfort and keep a low electricity demand by prioritizing daylighting over artificial lighting. In the experimental setup, the automated control system was implemented in one office room and compared with a

non-automated office room (serving as reference room, where also the daylight influx was additionally reduced in order to make it more comparable to a 'standard' office room) in the framework of a semi-realistic study. In a cross-over within-subject design, 34 young and healthy women and men were enrolled to spend five consecutive days (during daytime work hours) in the office room with the automated control system and five consecutive days in the reference room. During this time, participants performed cognitive tests, subjective sleepiness and comfort ratings, produced regularly saliva samples for the assessment of melatonin and cortisol concentrations; their light exposure at the eye and their skin temperatures were continuously recorded.

In addition, the automated control system was recently adapted for implementation in an open plan office, in the framework of an ongoing research project ("Safe and smart blind and lighting control"; led by the Swiss Laboratory for Material Science and Technology - Empa). The project and some preliminary results are briefly presented in this thesis.

This interdisciplinary thesis is linking three research areas: building automation engineering, daylighting research and human chronobiology (Figure 1.2).

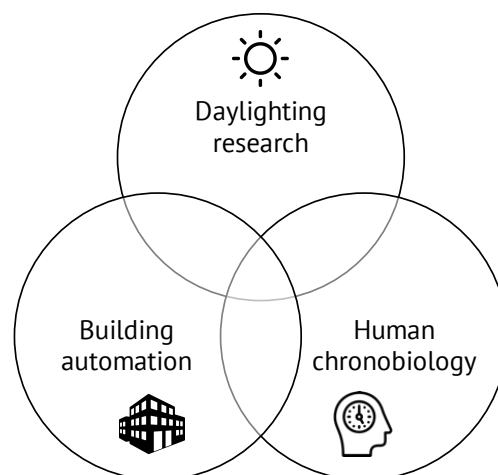


**Figure 1.2** – Conceptual figure: the three research areas of this interdisciplinary doctoral thesis.

### 1.5 Significance of the thesis

The findings of this thesis will contribute to a better understanding of the role of optimized mixed daylight/electric light exposure during daytime on circadian rhythms and non-visual functions in young adults. The results of this thesis will generate new insights for better designs of daylighting control in buildings, supporting individual needs and tailored lighting solutions which ultimately also repercuss on health and well-being. The results will bring new scientific and practical insights to building automation for "Human Centric Lighting" (HCL) at workspaces, in which both visual and non-visual effects of light are considered [Boyce, 2016; Houser et al., 2020]. Lastly, the findings will also provide new means for energy savings by smart control of daylighting indoor work places, which

can contribute to current strategies to help mitigating global warming ("Energy Strategy 2050" [Swiss Federal Office of Energy, 2012]).

## 1.6 Thesis overview

Chapter 1 (this introduction) outlined the thesis work. Because of the interdisciplinary nature of this thesis, the two aspects of focus are split into the following two Chapters:

Chapter 2 is focused on the engineering aspects of the new automated control system:

The first part (section 2.1) reports the state of the art of daylighting use and lighting control in buildings, including recent technologies and studies in the field. The second part of Chapter 2 (2.2) explains and describes the design of the automated controller for venetian blinds and electric lighting, which was carried out by the author. The results of the controller's performance in terms of objective lighting conditions, glare and energy consumption are reported and discussed at the end of the chapter (sections 2.3 and 2.4).

Chapter 3 is focused on non-visual aspects of daylighting in humans:

The background knowledge of non-visual effects of light is described in the first section, (3.1) before getting to the design and procedure of the intervention study with human participants in the LESO experimental building (section 3.2). The results of the study are reported and discussed in sections 3.3 and 3.4.

Chapter 4 introduces a first practical implementation of the automated control system in an open-plan office at the SolAce unit at the Empa NEST building in Dübendorf (Zürich, Switzerland) in an ongoing project.

Chapter 5 critically discusses the results of Chapters 2 and 3, states the achievements and some limitations and highlights the general significance of the work. The thesis ends with a summary and outlines future research.



# 2

## Daylighting control in buildings

---

Chapter 2 is about the use and control of daylight in buildings and is divided into 4 main sections. Section 2.1 presents the background knowledge and explores the existing technologies used for the assessment of lighting conditions inside of buildings and the control of daylighting. Section 2.2 describes the automated venetian blinds and electric lighting controller developed by the author in the context of this doctoral thesis. Results of the controller's performance related to lighting conditions, protection from discomfort glare and energy consumption are reported in section 2.3 and discussed in section 2.4.

### 2.1 Background

#### 2.1.1 Photometric measurements

Light sources have many properties and their characteristics can be assessed by different metrics. Firstly, a radiative flux transports radiant energy and can be characterized using two different types of metrics, reflecting its radiometric and photometric properties. Radiometric units define the properties of the flux in terms of quantities of absolute emitted electromagnetic radiation (from the entire electromagnetic spectrum between 0.01 and 1000 micrometers). Photometric units define measures in the visible range of light, i.e., from 380 to 780 nanometres (nm). A photometric unit is computed by weighing the correspondent radiometric unit with the photopic efficiency function  $V(\lambda)$ , the sensitivity curve of the photoreceptors in the human eye which mediate colour vision (i.e., cones [Commission Internationale de l'Éclairage (CIE), 1926]; see also Chapter 3). Both radiometric and photometric quantities include four basic variables, summarised in Table 2.1. These metrics are used to characterize properties of light emitting sources.<sup>a</sup>

Radiant power or luminous flux refers to the total output flux (radiant or luminous) from a light source. Radiant intensity is the flux emitted in a direction per unit solid angle. As the flux travels outward from a source, it ultimately impinges on surfaces (where it is reflected, transmitted, and/or absorbed). The irradiance or illuminance of a surface is the density of the radiant power or luminous flux incident on that surface. Finally, radiance or luminance is the amount of light emitted by an

---

<sup>a</sup>a light source can also be a surface which reflects light.

## Chapter 2. Daylighting control in buildings

element of area of a light source in a given direction per solid angle [McCluney, 2003; Choudhury, 2014].

Another characteristic of a light source is the Correlated Colour Temperature (CCT), defined as "*the temperature of an ideal black-body radiator that radiates light of comparable hue to that of the light source*" [Choudhury, 2014; Commission Internationale de l'Éclairage (CIE), 1987]. The CCT is expressed in Kelvin (K) and gives information about the tone or colour of the emitted light: for conventional light sources, it typically ranges from 2700-3500 K for warm-white light sources to 4500-7500 K for cool-white (i.e., with more 'blue' light).

Radiometry [Unit]		Photometry [Unit]	
Radiant power	[W]	Luminous flux	[lm]
Radiant Intensity	[W/sr]	Luminous Intensity	[cd]=[lm/sr]
Irradiance	[W/m <sup>2</sup> ]	Illuminance	[lux] = [lm/m <sup>2</sup> ] = [cd sr/m <sup>2</sup> ]
Radiance	[W/(m <sup>2</sup> sr)]	Luminance	[cd/m <sup>2</sup> ]=[lm/m <sup>2</sup> sr]

**Table 2.1** – Principal radiometric and photometric quantities; table adapted from [Goodman, 2009]. Abbreviations for international standard (SI) units: W = Watt; sr = steradian; lm = lumen; cd = candela; m = meter.

The International Committee of Illumination (*Commission Internationale de l'Eclairage* - CIE) defined so-called "standard illuminants", i.e., theoretical light sources (both electric and natural) with a spectral power distribution (SPD) published in [Commission Internationale de l'Éclairage (CIE), 2004]. Standard illuminants serve as reference spectra in applications for colorimetry. For instance, the standard illuminant D65, which was defined in 1964, represents daylight (average noon daylight from the northern sky, with a CCT of  $\sim 6500$  K). It is described and referenced in the standards [ASTM International, 2016; DIN 6173-2, 1983].

### New metrics based on human photoreceptor sensitivities

In the last two decades, there has been increasing awareness and new scientific findings on the impact of light on humans. It is well known that light exposures acutely impact on human physiology and modulate circadian rhythms: these are so called non-visual effects of light which will be described in more detail in Chapter 3. There is growing evidence that non-visual responses to light are not adequately predicted by photopic illuminance alone [Brown, 2020; Nowozin et al., 2017; Giménez et al., 2016; Münch et al., 2017; Prayag et al., 2019], which is primarily based on mixed inputs from sensitivity functions of rods and cones.

A third class of photoreceptors has been discovered more than 20 years ago first in rodents [Berson et al., 2002; Hattar, 2002; Ruby et al., 2002], but also in non-human primates [Dacey et al., 2005] and was also described in humans [Zaidi et al., 2007]. This new class of photoreceptors is called intrinsically photosensitive retinal ganglion cells (ipRGCs). The ipRGCs contain the photopigment *melanopsin* and have a maximum (unfiltered) peak sensitivity at 480 nm [Commission Internationale

de l'Éclairage (CIE), 2018] (see also Chapter 3).

A new metric to quantify the spectral power distribution of a light source for different photoreceptor sensitivities was first proposed by Lucas and colleagues [Lucas et al., 2014]. The metric was called  $\alpha$ -opic illuminance, where the  $\alpha$  is a place holder for one of the 5 human photoreceptors: rods, and the 3 different cones i.e., long (L-cone), middle (M-cone) and short (S-cone) wavelengths cones as well as ipRGCs (Mel). More recently, the CIE has officially released a revised version [Commission Internationale de l'Éclairage (CIE), 2018], which defines the spectral sensitivity functions of all photoreceptor classes in the human eye, including ipRGCs, and related quantities and metrics. It is important to note that for non-visual responses, light perception from all photoreceptor classes is integrated [Lucas et al., 2014] and there is no single action spectra accountable alone for non-visual light effects [Commission Internationale de l'Éclairage (CIE), 2018]. In order to estimate the potential for non-visual effects of a light source, it is crucial that the absolute (or relative) light intensity is measured in a vertical plane at the level of the human eye [Spitschan et al., 2019]. The *melanopic* action spectrum  $s_{mel}$ , for example, is used to weigh absolute irradiance to define the melanopic irradiance  $E_{e,mel}$  [ $W/m^2$ ] (equation 2.1):

$$E_{e,mel} = \int E_{e,\lambda}(\lambda) \cdot s_{mel}(\lambda) d\lambda \quad (2.1)$$

The CIE standard S026/E:2018 also defines the melanopic Equivalent Daylight Illuminance (EDI or  $E_{v,mel}^{D65}$  [lux]), as *"illuminance produced by radiation conforming to standard daylight (D65), producing an equal melanopic irradiance as the test source"* (equation 2.2).

$$E_{v,mel}^{D65} = \frac{E_{e,mel}}{K_{mel,v}^{D65}} \quad (2.2)$$

where  $K_{mel,v}^{D65}$  is the melanopic Efficacy of Luminous Radiation (ELR) for the standard illuminant D65, which is equal to 1.326 mW/lm. In support of the aforementioned international standard, in 2020 the CIE finally made the " $\alpha$ -opic Toolbox" freely available, which enables calculations and conversions of light quantities weighted for the different photoreceptor sensitivities [Commission Internationale de l'Éclairage (CIE), 2020]. Among all available metrics, the melanopic EDI (lux) was chosen as the most suitable one to predict non-visual responses to different environmental illumination conditions [Brown, 2020].

### 2.1.2 Visual comfort and glare risk assessment

Visual comfort at the workplace is a well-known and important factor which can influence work quality and performance in office workers [Richter et al., 2019]. In order to provide appropriate visual comfort in office rooms, the illuminance on the work plane must be sufficiently high to perform work tasks, the light should be properly distributed and discomfort glare (e.g. from luminaires or

through windows) must be avoided [Linhart, 2010]. There is no universally accepted definition of visual comfort, but it is often simply defined as "the absence of visual discomfort" [Iacomussi et al., 2015]. Glare is the most common source of visual discomfort and derives from excessive luminance contrast within the field of view.<sup>b</sup> As mentioned in paragraph 2.1.4, daylighting can cause discomfort glare due to direct or indirect daylight from windows or skylights creating high luminance contrasts.

Discomfort glare can be quantified by monitoring luminance contrasts and calculating glare indexes [Osterhaus, 2005; Commission Internationale de l'Éclairage (CIE), 1995]. There are several indices available to assess discomfort glare. The analytical expressions of such metrics were derived from experiments including human observers and glare sources from daylight and electric light. Generally, equations of these indices are based on factors such as the luminance of the glare source(s), the solid angle subtended by the glare source, the angular displacement of the source from the user's line of sight, and the background luminance. Among these different glare indices, the Daylight Glare Index (DGI) was introduced by the Cornell University (Ithaca, NY, USA) and the Building Research Establishment (BRE) [Robinson et al., 1962]. Its equation derives from the British Glare Index, established in 1950 [Petherbridge & Hopkinson, 1950] and was adapted for the use with large sources such as windows. The DGI was recommended for daylighting conditions [Hopkinson, 1972]. However, the DGI has been criticized for being not fully reliable because it overestimates discomfort glare under daylighting conditions (i.e., glare from windows), which is generally better tolerated than glare from electric light sources [Chauvel et al., 1982; Boubekri & Boyer, 1992]. Other common glare indices are for example the the CIE Glare Index (CGI) proposed by Einhorn [Einhorn, 1969] and adopted by the CIE in 1969, and the Unified Glare Rating (UGR), recommended by CIE for use with electric lighting conditions. More recently, a robust index to evaluate visual comfort related to daylight was defined by Wienold & Christoffersen [2006]: the Daylight Glare Probability (DGP, see below).

### Daylight Glare Probability

This DGP index is based on High Dynamic Range (HDR) images of a scene and it quantifies the probability of experiencing discomfort glare for the image captured by the sensor [Wienold & Christoffersen, 2006]. The DGP was proven to have a reasonable correlation to what a person actually perceives [Hirning et al., 2013]. The use of this index is recommended by the European Standard EN 17037:2018 for intensive protection against glare [Technical Committee CEN/TC 169 "Light and Lighting", 2018]. The DGP is a function of vertical eye illuminance, glare source luminance, its solid angle and position index. It is given by the equation 2.3:

$$DGP = 5.87 \cdot 10^{-5} E_v + 9.18 \cdot 10^{-2} \cdot \log \left( 1 + \sum \frac{L_{s,i}^2 \omega_{s,i}}{E_v^{1.87} P_i^2} \right) + 0.16 \quad (2.3)$$

---

<sup>b</sup>The field of view (FoV) is defined as *the angular extent of the field which can be observed with an optical instrument or the eye* [Paschotta, Paschotta].



where:

$E_v$  [lux] is the vertical illuminance (i.e., illuminance on a vertical plane);

$L_{s,i}$  [ $\text{cd m}^{-2}$ ] is the luminance of the glare source (i);

$\Omega_{s,i}$  [sr] is the solid angle subtended by the glare source (i);

$P_i$  [–] is the Guth position index of the glare source (i);

Table 2.2 (from EN17037:2018, Table E.1) indicates the categorization of DGP values based on the degree of perceived glare.

Criterion	Daylight Glare Probability
Glare is mostly not-perceived	$DGP \leq 0.35$
Glare is perceived but mostly not disturbing	$0.35 < DGP \leq 0.40$
Glare is perceived and often disturbing	$0.40 < DGP \leq 0.45$
Glare is perceived and mostly intolerable	$DGP > 0.45$

**Table 2.2** – Categorization of DGP values [Technical Committee CEN/TC 169 “Light and Lighting”, 2018].

### 2.1.3 High Dynamic Range (HDR) sensors

At the Solar Energy and Building Physics Laboratory (LESO-PB, EPFL, Switzerland), several research projects have been carried out in the last decade using High Dynamic Range (HDR) imaging technology to assess indoor lighting conditions and visual comfort. For this purpose, three generations of HDR vision sensors were developed and calibrated in the course of an ongoing collaboration between LESO-PB (EPFL) and the Swiss Center for Electronics and Microtechnology (CSEM, Neuchâtel, Switzerland).

The HDR vision sensor is equipped with a fish-eye lens and several filters, which were calibrated to match photometric ( $V(\lambda)$ ) and non-visual sensitivity ( $C(\lambda)^c$ ) functions. The device can generate real-time luminance maps and allows to assess quantities of a given light environment weighted for different photoreceptor action spectra over time, as well as discomfort glare indices.

For her doctoral thesis, Dr. A. Borisuit had calibrated the first generation of the camera-like-sensor (the "IcyCam", see Figure 2.1a, on the right side [Borisuit et al., 2011, 2012]). The device was then validated in an experimental cross-sectional study with young participants by using the HDR vision sensor to assess luminance distributions of office spaces under different lighting conditions. The aim of that study was to investigate the effects of office lighting including different sky conditions and time-of-day changes on visual comfort and non-visual functions (e.g., subjective alertness, mood and well-being [Borisuit et al., 2011, 2015]). The results showed significant correlations between objective and subjective visual comfort assessments, and correlations of visual comfort with subjective well-being ratings and other non-visual effects of light [Borisuit et al., 2011]. Motamed et al. [2016]

<sup>c</sup>a "circadian sensitivity function" defined by [Gall, 2002] with a sensitivity peak at 460 nm.

adopted the same HDR vision sensor in the framework of an integrated control platform for shadings and electric lighting with the goal of reducing lighting electricity demand while maintaining the user's visual comfort in offices.



**Figure 2.1** – (a) The two HDR vision sensors: VIP (left) and IcyCam (right); (b) The new Glare Meter.

A more recent and compact version of the IcyCam, the Vision In-Package (VIP) sensor, was calibrated by Dr. A. Motamed for his doctoral thesis [Motamed, 2017] with the support of the author. The VIP sensor is much smaller than its predecessor (see Figure 2.1a on the left side). Similar to the IcyCam, it is equipped with a fish-eye lens and filters (in this case, made of organic material instead of glass) that allow to adapt its spectral sensitivity to the  $V(\lambda)$  function; it was calibrated photometrically (to convert the generated greyscale images in luminance maps) and geometrically (to account for vignetting effect, i.e., the drop of response at the image's corners). The VIP sensor's field of view is  $132^\circ$  vertical and  $178^\circ$  horizontal [Motamed, 2017]. From the luminance maps recorded by the device it is possible to extract different information about the lighting conditions through the embedded software (developed by CSEM in collaboration with LESO-PB): for instance, vertical illuminance (perceived by the sensor) and DGP can be computed. The two mentioned HDR vision sensors (first and second generation) are shown in Figure 2.1a. Typically in the aforementioned studies (by Dr. A. Borisuit and Dr. A. Motamed) the sensor was installed on a support (e.g. a tripod) next to the desk and the window, at the approximate eye level of a user sitting on the chair, and oriented vertically in order to capture a field of view as similar as possible to the user sitting (as shown in the sketch in Figure 2.2). An example of the luminance map captured by the VIP sensor placed in such position is shown in Figure 2.3.

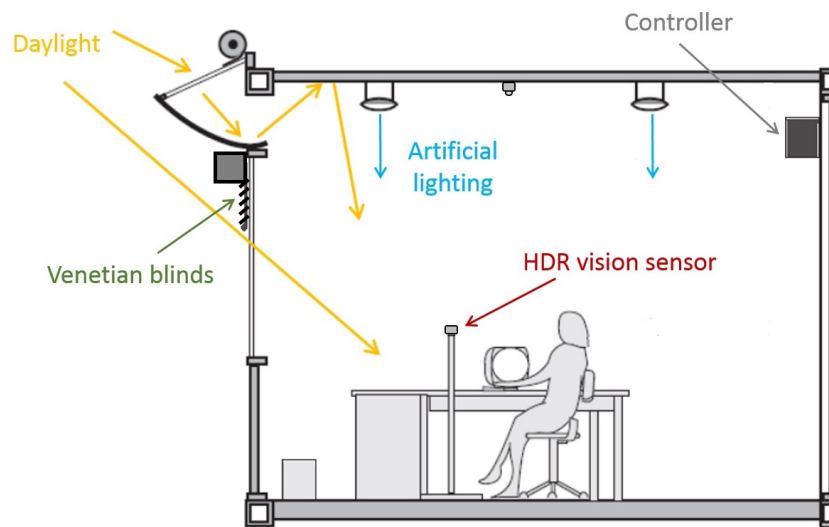


**Figure 2.2** – Simplified schematic overview of an office at the LESO experimental building. Here, the HDR vision sensor is installed on a support next to the desk, at the eye level of a user sitting, and oriented in a horizontal direction (parallel to the floor). The coloured arrows show the daylight propagation via windows and the anidolic daylighting system, the HDR vision sensor and the electric lighting.

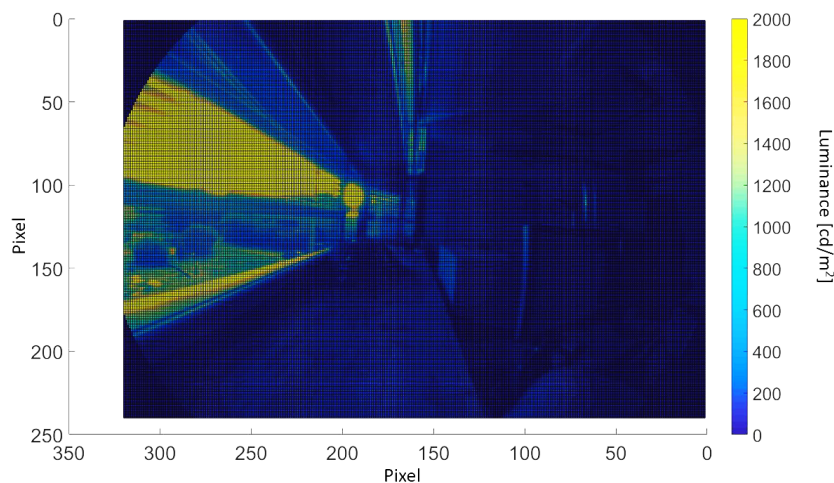


**Figure 2.3** – Luminance map captured by the VIP sensor placed close to the user sitting at the desk (at the approximate eye level on a vertical plane). The image is false-colour enhanced and the colour bar on the right side depicts the computed luminance ( $\text{cd/m}^2$ ).

### Glare Meter

Recently, the VIP sensor was embedded in the new “Glare Meters” edition (Figure 2.1b), resulting from the collaboration between LESO-PB and CSEM Neuchâtel and manufactured at LESO-PB. The new Glare Meter includes an HDR vision sensor and an Intel® Compute Stick; it is able to capture images continuously at a frequency of 5 s, and it transmits data (e.g. incident and work plane illuminance, glare indexes) in real time via Wi-Fi connection. Figure 2.4 shows the Glare Meter software interface. Between 2019-2020 the device has been tested in the LESO experimental building to validate its performance. Later, it has been adopted in a recent project with anti-glare

blinds and lighting control in an office at the LESO building as well as in an open-plan office in the experimental NEST building in Dübendorf (Switzerland), as described in Chapter 4.

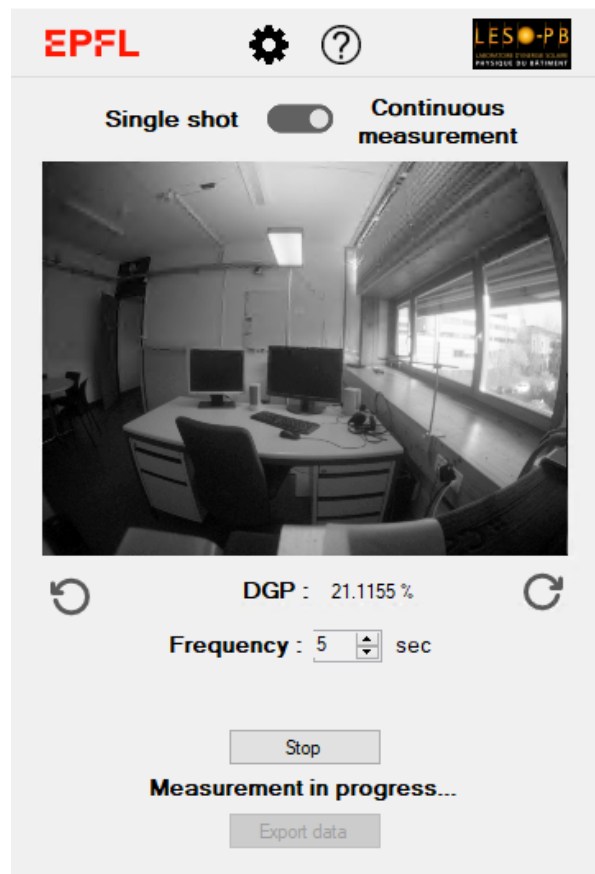


**Figure 2.4** – The new Glare Meter interface with the real image in greyscale. The sensor is placed on the wall behind the desk in an office room at the LESO experimental building. The software allows to choose between single and continuous measurement (in the latter case, the frequency can be changed; the DGP is shown in percentage below the image).

### 2.1.4 Daylight in offices

#### Impact on office occupants

A good lighting environment in offices has many beneficial effects on the occupants. Several studies showed that access to daylight and view to the outside favours the users' satisfaction and mood [Butler & Biner, 1989; Galasiu & Veitch, 2006]. A study including nearly 500 office workers in 1983 in England and New Zealand showed that 99% of them preferred offices with windows [Cuttle, 1983]. According to a recent review, satisfaction with lighting is strongly associated with the access to windows [Leder et al., 2016] and daylight can also have salutogenic effects (reviewed in [Beute & de Kort, 2014]). In addition, daylight at the workplace enhanced occupants' cognitive performance and well-being [Veitch, 2006; Jamrozik et al., 2019] and reduced sick leaves at work [Sundaram & Croxton, 1998; Markussen & Røed, 2015].

On the other hand, lack of daylight exposure at work is associated with several physiological problems such as headache and eyestrain, sleep disorders [Franta & Anstead, 1994; Léger et al., 2011; Harb et al., 2015], but also depressive symptoms and greater risks for seasonal affective disorder (SAD), which has also been associated with insufficient lighting levels, especially during fall/winter [Edwards & Torcellini, 2002]. There is some indication that chronically lower light levels negatively impact on concentration, well-being and performance [Aries, 2005].

### **Impact on energy demand**

Another important beneficial effect of daylighting is its potential for reduced energy consumption. In 2002, Bodart and De Herde performed a study based on daylighting and thermal simulations on different façade configurations for an office building in Belgium. They found that daylighting can reduce energy consumption for electric lighting by 50% to 80% [Bodart & De Herde, 2002]. Furthermore, daylight has a higher luminous efficacy (ratio of luminous flux to power [lm/W]) than traditional electric light sources such as incandescent lamps, which means that less heat is dissipated for the same amount of light, which also reduces the energy demand for cooling and air conditioning [Li & Lam, 2001; Yu & Su, 2015].

In the last decades, significantly higher luminous efficacies have been reached first with compact fluorescent lamps (CFLs) and then with solid-state lighting (SSL) including light emitting diodes (LEDs), which promise considerable energy savings with respect to traditional sources [Jenkins & Newborough, 2007; Khan & Abas, 2011]. However, approximately 70% of the input electrical energy is still converted to heat in LED products [Luo et al., 2016], which requires additional technologies for thermal management. Furthermore, the increased light usage following the reduced energy costs of LED might oppose the energy savings over time, according to a recent study [Hicks et al., 2015].

### **Main issues from daylighting**

The two most common negative side effects of maximising the use of daylight in buildings are the discomfort glare of occupants and overheating of rooms. Solar protections such as shading devices are key elements for the control of daylighting, but they have to be used in a proper way to exploit and balance the aforementioned benefits for thermal management, energy efficiency and user's comfort and well-being.

As mentioned in Chapter 1, the manual control of blinds by the building occupants does often lead to sub-optimal use of daylight. Foster & Oreszczyn [2001] monitored three offices in central London (UK) and found that on average 40% of the window surfaces were obscured by blinds, reducing the daylight penetration and likely resulting in an increased use of electric light. Moreover, the use of blinds in that study was not linked to sunlight availability.

Properly designed automated control systems for blinds are likely to positively contribute to the

daylight exploitation in buildings, and consequently to energy savings, while ensuring occupants visual comfort, as shown in past studies, for instance [Motamed, 2017; Wu et al., 2019].

### Standard recommendations for office lighting

Generally, recommendations for office lighting have been based on horizontal work plane illuminance as the main design variable (those standards are based on traditional offices where paperwork is the most common activity). For example, the standard EN 12464-1 (*Light and lighting. Lighting of workplaces. Indoor workplaces*) recommends a horizontal illuminance of 500 lux for normal office work like writing, typing and reading. Studies on behaviour and preferences of office workers during daytime showed that they tended to prefer higher and dynamic illuminance levels, instead of static (electric) light levels [Begemann et al., 1997; Smolders & de Kort, 2009].

The first European standard dealing exclusively on design and use of daylight in buildings is the EN 17037:2018 [Technical Committee CEN/TC 169 “Light and Lighting”, 2018]. The criteria for a sound daylighting design include protection from glare, view to the outside and sunlight exposure duration.

On the basis of the newest and state-of-the-art scientific knowledge, the first recommendations for healthy indoor light exposure targeting non-visual responses were published by [Brown et al., 2020]. The recommendations are based on the melanopic Equivalent Daylight Illuminance (EDI). During daytime, a minimum EDI of 250 lux on the vertical plane at the eye level (at 1.2 m height) is recommended. This light level should be provided, whenever possible, by daylight, or by polychromatic white electric light with a spectrum in the visible range as close as possible to daylight.

### Daylighting control systems

There are several types of lighting control systems in buildings. The most common ones are based on occupancy sensors, timers, or simple manual control at the user level. Electric lighting can be controlled either by simple on/off switches, or through dimmable ballasts, e.g. Digital Addressable Lighting Interface (DALI) systems, which allow to regulate the brightness of the light source. Advanced building automation systems offer the possibility to apply programmed controllers for lighting.

A review on lighting control technologies in commercial buildings was published recently by [ul Haq et al., 2014]. Among the different technologies, one of the most promising in terms of energy savings is certainly the Daylight-linked Control (DLC, also called Daylight-responsive Control), which can be implemented in daylight spaces. Recently Gentile et al. [2015] published recommendations for such systems from design to commissioning and installation. The goal of a DLC is to provide lighting levels at the work plane equal to the target design level by minimum use of electric lighting, either by switching it on and off, or through dimming. In 1988 Rubinstein proposed one of the

first daylight-linked control (DLC) algorithms. The aim was to maintain constant illuminance level on a task surface by using a photo-electrical lighting system and a dimming unit to regulate the electric lighting power [Rubinstein et al., 1989]. Since then, several daylighting control systems have been proposed by researchers and practitioners. A field study on an automated daylighting control was implemented in a mockup of a commercial building, the New York Times Headquarters [Lee & Selkowitz, 2006]. The authors evaluated the performance of an open-loop and a closed-loop controller for roller shadings and dimmable electric lighting in an open-plan office, with the goal of maintaining a design work plane illuminance and blocking direct sunlight. Both control systems led to significant lighting energy savings, which depended on the distance of the considered area from the windows.

Despite the obvious benefits, DLCs are not widely spread due to different reasons: according to a recent review by Bellia et al. [2016], the main difficulties are related to the DLC design, installation and calibration, as well as low user acceptance and the lack of appropriate technologies. Usually, the DLC for blinds and electric lighting are based on work plane illuminance measured by sensors installed at the ceiling. The problem with this approach is that it does not guarantee any protection from glare, or an optimal and efficient management of blinds and electric lighting.

In order to ensure the user's visual comfort, automated controls should not only regulate electric lighting, but also shadings. Shading devices substantially vary by their transmission properties of light. Venetian blinds for example, offer a better control of the daylight flux entering the room due to the possibility to manage the tilt angle of slats. Indeed, the view to the outside can be maintained while direct sunlight is blocked. Koo et al. [2010] proposed an automated controller of venetian blinds to optimise daylight usage and at the same time protect the occupants from glare.

Goovaerts et al. [2017] developed a controller based on a low-resolution camera assessing DGP, aimed at optimizing visual comfort and reducing energy demand for heating, cooling and lighting. Although the low-cost camera was found to underestimate the glare sources, their controller was able to keep visual comfort and lighting sufficiency in the office room.

Wu et al. [2019] recently validated an automated shading control system based on real-time simulations of indoor lighting, based on sky luminance distributions captured by a photometric device embedded in the venetian blinds. The system can provide optimal daylighting control by preventing glare, maximising outside view, mitigating excessive solar gains and significantly reducing cooling loads.

An important innovation, also very relevant to this thesis, was developed by Dr. A. Motamed Motamed et al. [2017]; Motamed [2017] (PhD thesis). He designed an "advanced" automated controller for electric lighting and shadings based on the HDR vision sensors presented in section 2.1.3. The system was implemented in an office room at the LESO building and was compared against a "best practice" controller in an adjacent identical office room during an 8-month long experimentation. The advanced controller could significantly reduce the energy demand compared

to the best practice and to a manual control scenario (considering a "standard occupant" behaviour) during the heating season. Since the advanced controller leaves a larger window area uncovered with respect to the standard manual control, the higher solar heat gains during winter can mitigate the back-up space heating demand. At the same time, indoor lighting conditions were kept in the comfortable range for 88% of the time. The controller was also tested in a 15-days field study, in which 30 young participants evaluated their visual acuity, thermal comfort and glare sensation in the afternoon in the office rooms [Motamed et al., 2017]. Overall, thanks to the real-time assessment of glare, presence detection and work plane illuminance by the HDR sensors, the advanced controller achieved significant energy savings with minimal number of shading and lighting adjustment, while keeping occupants' visual comfort. Later, a self-commissioning controller based on the same principles, including a learning module, was successfully validated, which allows to overcome the issue of time-consuming design and programming [Motamed et al., 2020].

Among the commercial 'smart' control systems for lighting, the most installed worldwide are the ones by Somfy (Cluses, France) and Warema (Marktheidenfeld, Germany), covering more than 50% of the European market. These systems surely offer great advantages in terms of building automation and energy savings, however they are not designed to provide specific (pre-set) lighting conditions or to prevent discomfort glare, as they are not designed to rely on indoor sensors for those specific purposes.

### 2.1.5 Hypotheses

Since (day-)light exposure is crucial for human health, it is desirable to provide "healthy" lighting in indoor working environments in the absence of discomfort glare. In addition, daylight influx supports reduced energy costs from electric lighting.

The hypotheses at the basis of this work are that a specifically designed automated controller for venetian blinds and electric lighting in an office, implemented in an office room with an advanced daylighting design, can:

- provide dynamic lighting patterns which follow preset illuminance levels;
- maintain a high visual comfort for the occupants;
- maintain a low energy demand for electric lighting.

The next section is dedicated to the description of the design of this novel automated controller.



## 2.2 Automated controller for venetian blinds and electric lighting

At the LESO experimental building, a novel automated control system for venetian blinds and electric lighting for office rooms was designed and developed in the framework of this thesis. This section describes the experimental setup and validation steps as well as the automated controller operation in detail.

### 2.2.1 Experimental setup

The LESO solar experimental building (Figure 2.5) is located on the EPFL campus in Lausanne, Switzerland ( $46^{\circ}31'13''\text{N}$   $6^{\circ}33'56''\text{E}$ , altitude of 410 m above sea level). The building's main axis is east-west oriented; the main façade, where most offices are located, is facing south. A detailed description and information about the building is reported in other publications and PhD theses [Scartezzini et al., 1987; Altherr & Gay, 2002; Linhart, 2010; Zarkadis, 2015].



**Figure 2.5** – Outdoor view of the southern façade of the LESO building on EPFL campus. The red circles indicate the two office rooms at the second floor which were used during the experiments (left: *Reference* room, right: *Test* room).

The experiments took place in two south-facing adjacent office rooms at the second floor of the building, which are usually occupied by a single user. Figure 2.6 shows an indoor view of the two rooms: the novel automated control system was applied in one of the rooms, while the adjacent room served as a reference room (i.e., without an automated controller). During the colder season the rooms are heated by electric heaters, while there is no active cooling or ventilation system in spring/summer except for effective passive ventilation in the entire building.

Each office room is set-up with two windows on the southern façade: at the lower part there is a conventional window with double insulated glazing with e-coating; on the upper part there is an Anidolic Daylighting System (ADS) made of plain insulated glazing [Scartezzini & Courret, 2002],

including a light shelf<sup>d</sup>. The ADS favors a considerable daylight flux to enter and lighten the room, while the bottom window allows the view to the outside. The floor area of the rooms is identical and equal to 17.15 m<sup>2</sup> (i.e., 4.90 m depth, 3.50 m width) and the height is 2.80 m. The glazed area of the bottom window is 2.1 m<sup>2</sup> while the upper (anidolic) window occupies 1.80 m<sup>2</sup> of the façade and is inclined at 45° [Lindelöf, 2007]. The window-to-wall ratio (or WWR) is calculated as the fraction of glazed area on the total façade area, as in 2.4:

$$WWR = \frac{\text{Total glazed area}}{\text{Total façade area}} \approx 41\% \quad (2.4)$$

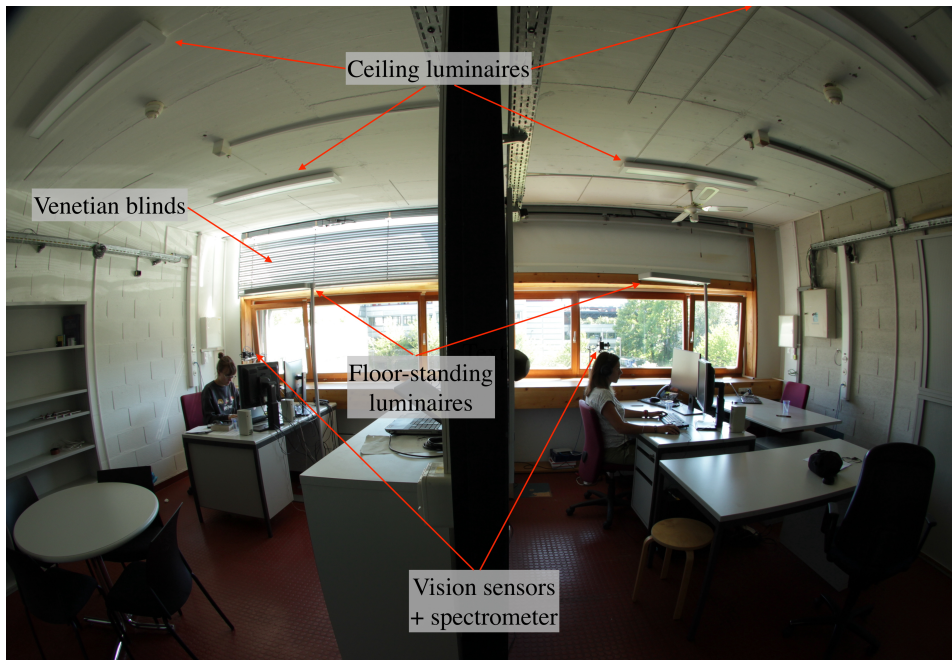


**Figure 2.6** – Indoor view of the two office rooms (LE 2 201 and LE 2 202) at the second floor of the LESO building used for the experiments. The left room was used as the "Test room" with the automated control system and the room on the right was used as "Reference room" (see section 2.2.4).

### Venetian blinds and electric lighting

The windows in both rooms are equipped with motorized venetian blinds (Lamisol<sup>®</sup> and Grinotex<sup>®</sup> metal blinds, Griesser AG, Aadorf, Switzerland). For practical reasons, the top blind was installed indoor, while the bottom blind is outdoor.

The artificial lighting fixtures in each room were identical and consist of a floor-standing lamp post providing both direct and indirect light fluxes (Tweak Essential CLD LED, Regent Lighting, Basel, Switzerland), and two ceiling-mounted luminaires (Item LED, Regent Lighting, Basel, Switzerland), all hosting dimmable LED lamps of a correlated colour temperature (CCT) of 4000 K. The total

<sup>d</sup>A light shelf is a daylighting system which consists in a horizontal baffle installed on the window façade, designed to shade and reflect light on its top surface and to protect from glare [Ruck et al., 2000].

## 2.2. Automated controller for venetian blinds and electric lighting

connected power in each room is 114 W (68 W for the floor-standing lamp post and 23 W for each of the two ceiling-mounted luminaires). The main characteristics of the lighting fixtures are summarized in Table 2.3. Their luminous intensity (or candle power) distributions and the spectral power distribution are illustrated in Figure 2.7. and Figure 2.8, respectively. Both venetian blinds and electric lighting can be controlled manually via switchers or automated (see section 2.2.3).

	Ceiling-mounted luminaire	Floor-standing luminaire
Light source	LED	LED
Maximum light flux	2400 lm	9400 lm
Correlated Colour Temperature	4000 K	4000 K
Light emission	direct	direct-indirect
System power	23 W	68 W

**Table 2.3** – Main characteristics of the installed electric lighting fixtures (identical in both rooms); lm = lumen, K = Kelvin, W = Watt.

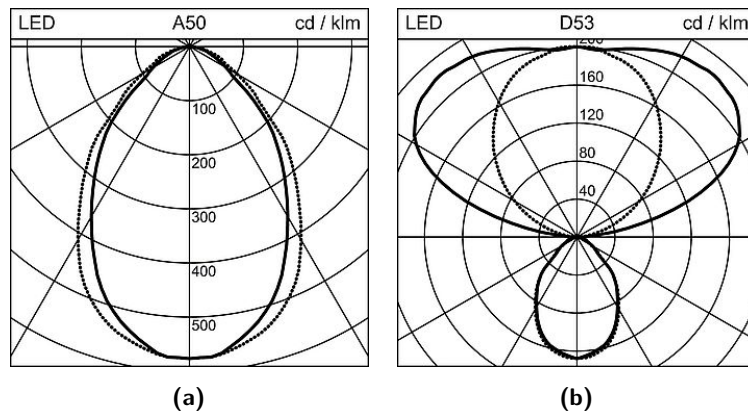


**Figure 2.7** – Candle power distribution of (a) ceiling-mounted luminaire and (b) floor-standing luminaire.

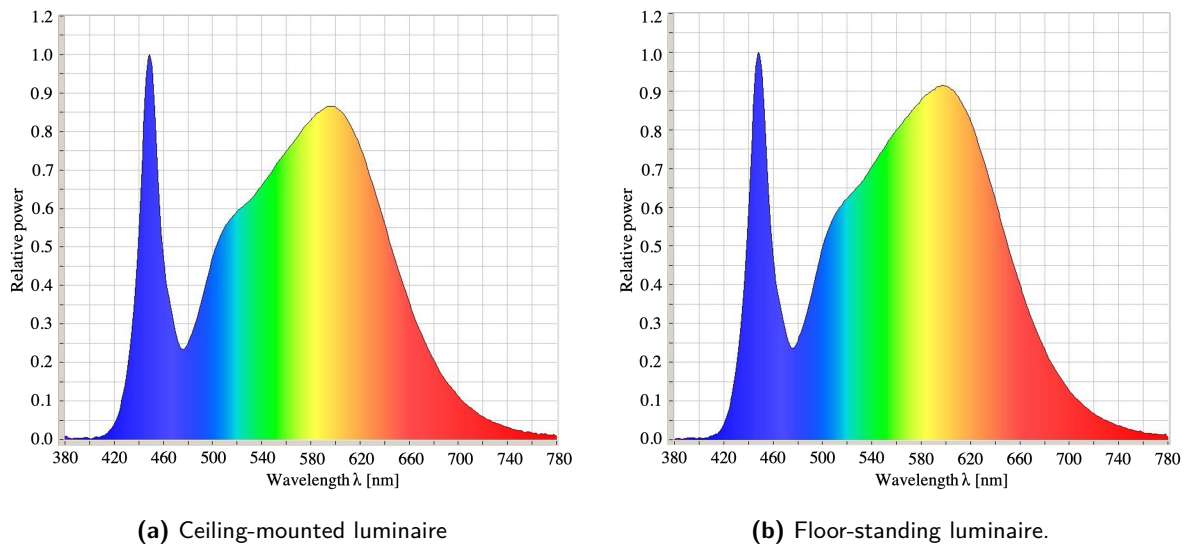


**Figure 2.8** – Spectral power distribution (SPD) of the electric lighting fixtures, in approximately matching colours of the visible spectrum. The SPD was measured with the spectrometer Jeti Specbos 1201 and the plots were generated with the software Jeti LiVal (JETI, Jena, Germany) and are shown with relative radiant power (-) on the y-axis and wavelength ( $\lambda$ ) on the x-axis.

Quantity		Luminaire	
		Ceiling-mounted	Floor-standing
Irradiance [ $\text{W}/\text{m}^2$ ]		0.55	1.67
Photopic illuminance [lux]		180.9	546.8
$\alpha$ -opic Irradiance [ $\text{W}/\text{m}^2$ ]	S-cone-opic	0.09	0.25
	M-cone-opic	0.23	0.70
	L-cone-opic	0.29	0.89
	Rhodopic	0.18	0.54
	Melanopic	0.15	0.44
$\alpha$ -opic Equivalent Daylight (D65) Illuminance [lux]	S-cone-opic	106.3	307.8
	M-cone-opic	159.1	479.1
	L-cone-opic	180.5	545.8
	Rhodopic	124.1	370.8
	Melanopic	111.6	331.7

**Table 2.4** – Photometric and  $\alpha$ -opic quantities calculated from the two spectral power distributions of the luminaires (Figure 2.8), using the CIE toolbox [Commission Internationale de l'Éclairage (CIE), 2018]. The spectral measurements were taken when either only the ceiling-mounted or the standing luminaire was on (without daylight), on a vertical plane at the approximate eye level of a person sitting at the desk (see Figure 2.6 for room overview and position of sensors).

### Dimming function of electric lighting

With the automated controller described later in this chapter, electric lighting was only switched on when daylight was not sufficient to reach the target illuminance (according to the preset levels described in section 2.2). Depending on the light flux necessary to fill the gap and reach this target, artificial lighting could be dimmed, i.e., it was possible to switch lights on at a fraction of their full power, which allows to avoid excess energy consumption. For the dimming function, it was necessary to determine the (linear) relationship between the power absorbed by the lighting fixtures and the illuminance provided by them (vertically and horizontally). In order to find this relationship, several measurements were carried out in which the relative lighting power (or dimming level) was varied progressively from 0 to 100% and illuminance was measured at each step. This procedure was carried-out in the evening with blinds closed to ensure the absence of daylight. Illuminance was measured twofold: 1) by using a digital illuminance meter (LMT Lichtmesstechnik GmbH, Berlin, Germany) placed on the desk (at the center of the work plane, to measure horizontal work plane illuminance  $E_h$ ) and 2) with the device positioned on a vertical plane at the approximate eye level next to the user (to measure vertical illuminance  $E_v$ ). Simultaneously, the power absorbed by the lighting system was monitored using a three-phase energy meter (TE360 and TE332, Hager Group, Blieskastel, Germany) connected to the luminaire's plug. This procedure was repeated firstly by using the standing luminaire alone, and secondly in combination with the ceiling-mounted luminaires. Table 2.5 summarises the measurements results, and the two plots in Figure 2.9 show the dimming curves of both luminaires (i.e., illuminance vs. relative power) for both  $E_h$  and  $E_v$ . Since the floor-standing luminaire provides a considerably higher illuminance compared to the ceiling-mounted luminaires, the former was selected as primary electric lighting source, where the latter were used as a secondary aid to provide even higher illuminance values if/when it was required.

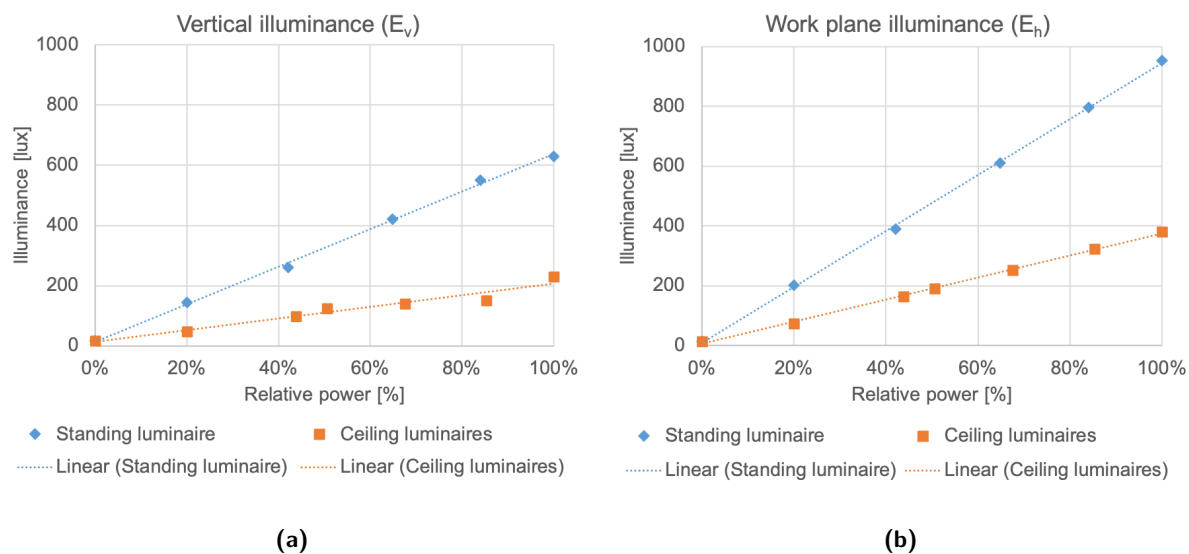


**Figure 2.9** – Dimming curves: vertical (a) and work plane (b) illuminance vs. relative power. Orange symbols = ceiling-mounted luminaires; blue symbols = floor-standing luminaire; dashed lines = trendlines (linear fit). The measurements were taken by progressively increasing the dimming power of each luminaire (one at a time, with the other one switched off) and reading the absorbed power (W) and the illuminance (lux) at each measurement step.

Relative power [0% – 100%]		$E_v$ [lux]	$E_h$ [lux]
Ceiling luminaire	Standing luminaire		
0%	0%	17	13
20%	0%	47	74
43.8%	0%	98	164
50.6%	0%	125	190
67.6%	0%	140	252
85.3%	0%	150	323
100%	0%	230	380
0%	20%	143	202
0%	42.1%	260	389
0%	64.9%	420	610
0%	84.1%	550	796
0%	100%	630	954
100%	100%	750	1260

**Table 2.5** – Relative power (RP) of ceiling-mounted and standing luminaire and corresponding measured vertical illuminance ( $E_v$ ) and horizontal illuminance on the work plane ( $E_h$ ). All the reported values are means of at least 3 measurements per each dimming step.



### 2.2.2 Continuous monitoring of indoor lighting conditions

For continuous evaluation of lighting conditions in the rooms, the two HDR vision sensors introduced in section 2.1.3 were implemented as follows: the VIP sensor equipped with  $V(\lambda)$  filters was used to assess the vertical illuminance  $E_v$  (lux) as well as DGP (%) on a vertical plane at the eye level of a user sitting at the desk (see schematic overview in Figure 2.11).<sup>e</sup> The spectral power distribution (SPD) was monitored over time by using a spectrometer (Jeti Specbos 1201, JETI, Jena, Germany), placed next to the HDR vision sensor. Based on SPD in the visible range (i.e., between 380 nm and 780 nm), several metrics, e.g. melanopic irradiance  $E_{mel}$  and melanopic Equivalent Daylight Illuminance (EDI) were derived according to the recent International CIE Standard [Commission Internationale de l'Éclairage (CIE), 2018] and the toolbox [Commission Internationale de l'Éclairage (CIE), 2020]. These two metrics and their general importance for assessing non-visual functions are presented in more details in Chapter 3. Since there was only one spectrometer device available, continuous SPD could only be derived in one office room at a time and not in two rooms simultaneously. The calibration of all three devices (VIP, IcyCam and spectrometer) was accurately double-checked prior the start of the experiment. They were installed on a metallic support that was placed at the desk and next to the window (Figure 2.10), at the eye level of the user sitting at the desk - i.e., at a height of 1.20 m approximately.

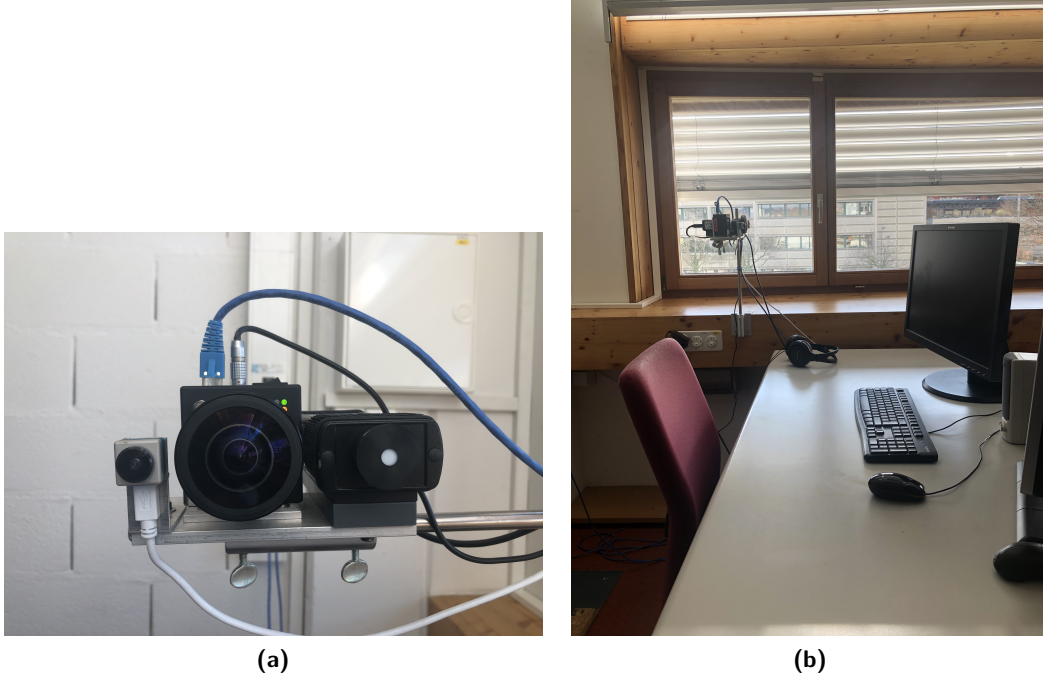


**Figure 2.10** – a) Photograph of the VIP (left) and IcyCAM (middle) vision sensors and spectrometer (right) mounted on the support next to the office desk; b) Exemplary photograph of the work space set-up of the two office rooms.

<sup>e</sup>The IcyCam equipped with  $C(\lambda)$  filters [Borisuit et al., 2013] was initially adopted to assess circadian-weighted irradiance  $E_{e,c}(W/m^2)$ . For technical reasons, results for  $E_{e,c}(W/m^2)$  are not reported in this thesis.

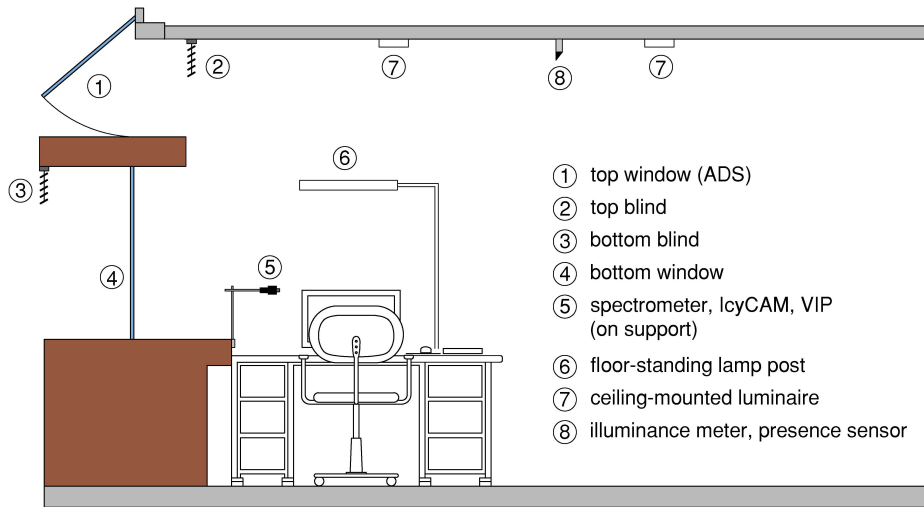


**Figure 2.11** – Schematic overview of the *Test* room. The *Reference* room was identical except that the ADS was covered (see section 2.2.6).

Figure 2.12 shows typical spectral power distributions (SPD) measured vertically next to the desk at the approximate eye level (see position 5 in Figure 2.11). The first graph (a) represents the SPD measured with daylight only (intermediate sky), while electric lighting was off; the second one (b) results from the mix of daylight and electric lighting (specifically, with floor-standing lamp post switched on and dimmed to approximately 50% of the full power).

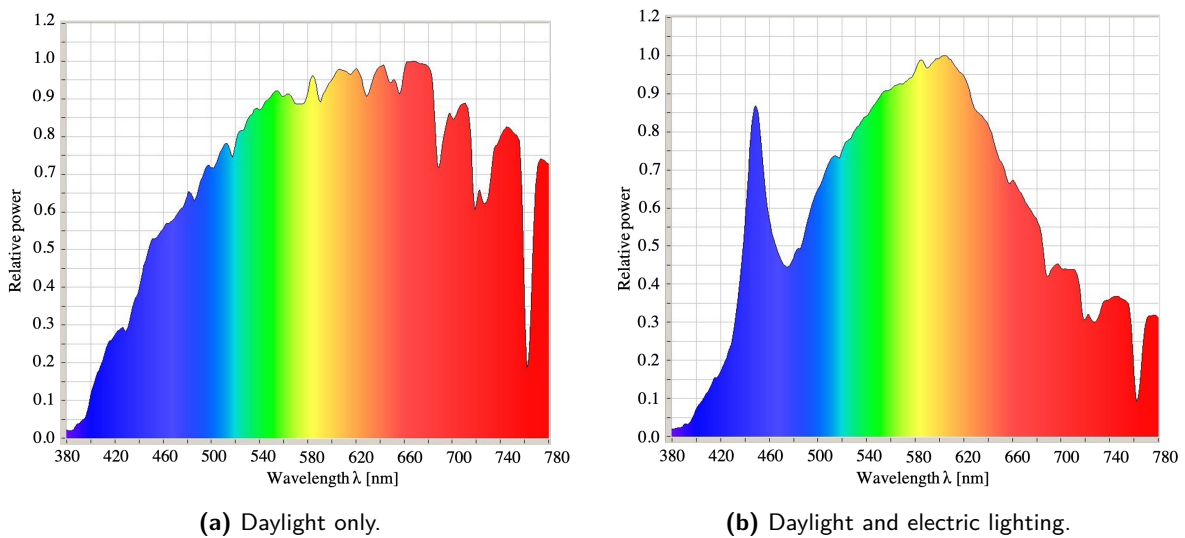


**Figure 2.12** – SPD (between 380 and 780nm, coloured with the approximate colours in the visible spectrum) measured at the desk on a vertical plane at the approximate eye level, at 1.20m height above the floor: a) daylight only, electric lighting switched off; b) mix of daylight and electric lighting.



### 2.2.3 Sensors, actuators and control platform

The LESO building features more than 200 sensors and actuators that control or generate information on air temperature, occupant presence, photometric variables, shading, heating, electric lighting and occupant interactions with switches [Motamed, 2017; Zarkadis et al., 2014; Lindelöf, 2007]. This is carried-out through a KNX<sup>f</sup> network communication protocol, which was first installed in the building in 1999.

In the course of this doctoral thesis, the author (with support of the IT team at LESO-PB) programmed and set up an ad-hoc control platform to guarantee the flawless and appropriate data acquisition and logging, as well as actuators commanding for venetian blinds and electric lighting. The schematic overview in Figure D.1 in the Appendix D shows the system's hierarchical structure. In each of the two office rooms used for this thesis, an IcyCam is connected to a laptop that reads the data sent by the camera and saves it continuously on a shared folder which is password protected on a LESO-PB internal server. The spectrometer is connected via an USB cable to the local laptop (in one room at a time) and the VIP vision sensors (one in each of the two rooms) are connected to a "DIGI Anywhere USB", a device used to connect USB peripheral devices on a Local Area Network (LAN) to the virtual machine (VM). The VM performs the scheduled data acquisition, hosts the controller, sends the commands to the monitoring systems and logs the data continuously. The data transfer between the local laptops in both rooms and the control platform on the VM is carried out through the "mapped drive" technique provided by MS Windows.

### 2.2.4 The control algorithm

An automated control system was developed and implemented in one of the two rooms used in this thesis, which is named "*Test room*" and is illustrated on the left side in Figure 2.6. The other room is used for the sake of comparison and is named "*Reference room*". The automated control system described in this section is implemented only in the *Test room*. The control algorithm was developed for this doctoral thesis using MATLAB<sup>®</sup> (version R2016b, MathWorks, MA, USA), installed on the virtual machine. The system's basic template is similar to the one originally developed by Dr. A. Motamed (see chapter 3 of his PhD thesis [Motamed, 2017]). From this first version, several essential adaptations and changes for the purposes of the present work were necessary and performed during the doctoral thesis by the author, and were implemented in the physical systems in collaboration with the IT group at LESO-PB.

---

<sup>f</sup>KNX is an open standard for building automation.

### Main principles of the controller

The aim of the automated controller for blinds and lighting was to prevent discomfort glare from direct sunlight for a user sitting at the desk in the *Test* room. Discomfort glare, determined by the Daylight Glare Probability (DGP), was monitored by the VIP vision sensor. When the DGP exceeded the value of 35% (which is defined as the threshold of "perceptible glare sensation" [Wienold & Christoffersen, 2006]), the controller intervenes by adjusting the blinds to protect the user from potential visual discomfort.

### Target vertical illuminance curve

Simultaneously, the automated controller also ensures an appropriate illuminance by adjusting the electric lighting when natural light is not sufficiently bright, based on an a preset target illuminance curve at the vertical eye level ( $E_{v,target}$ ) across a working day. The target curve indicates the required minimum level of  $E_v$  at the work place at different times of the day. The shape and values of the curve were set by the author, based on the dynamics of daylight and on results from the literature (Figure 2.13). It was for example shown that illuminance levels which induce circadian phase delays in humans (under controlled laboratory conditions) saturate at approximately 1000 lux (when prior light exposure was around 15 lux [St Hilaire et al., 2012; Zeitzer, 2000; Duffy & Czeisler, 2009]; see also Chapter 3). The curve is dynamic and varies throughout the day following a pattern similar to daylight. In the morning of a working day in the office, a minimum  $E_{v,target}$  of photopic 500 lux was required, which increases to 1000 photopic lux around noon, and decreases again in the afternoon. Minimum illuminance in the later afternoon was set to 200 photopic lux (see the next subsection for threshold values and set points).

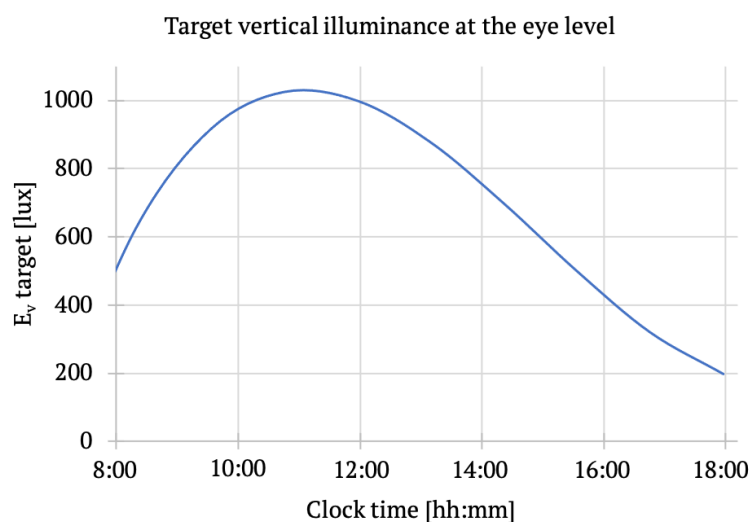


**Figure 2.13** – Preset dynamic target vertical illuminance curve at the eye level ( $E_{v,target}$ ) throughout the working day, from 8:00 to 18:00.

## 2.2. Automated controller for venetian blinds and electric lighting

A third-degree polynomial function (equation 2.5) was fitted to the curve:

$$E_{v,target} = a \cdot t^3 + b \cdot t^2 + c \cdot t + d \quad (2.5)$$

where  $a = 51000$ ,  $b = -95630$ ,  $c = 55770$ ,  $d = -9354$ , and  $t$  is the clock time expressed in decimals as a fraction of the 24-hour day (i.e. 8:00 = 0.3, 12:00 = 0.5, 18:00 = 0.75).

A conceptual scheme of the automated control system is illustrated in Figure 2.14. The clock time is used to sample the curve of  $E_{v,target}$  and also to determine the sun profile angle. Real-time data acquired by the VIP vision sensor is continuously processed and used as an input to the controller. The difference (or "error") between the lighting set points and the monitored data is used to determine the controller's actions on the blinds or electric lighting.

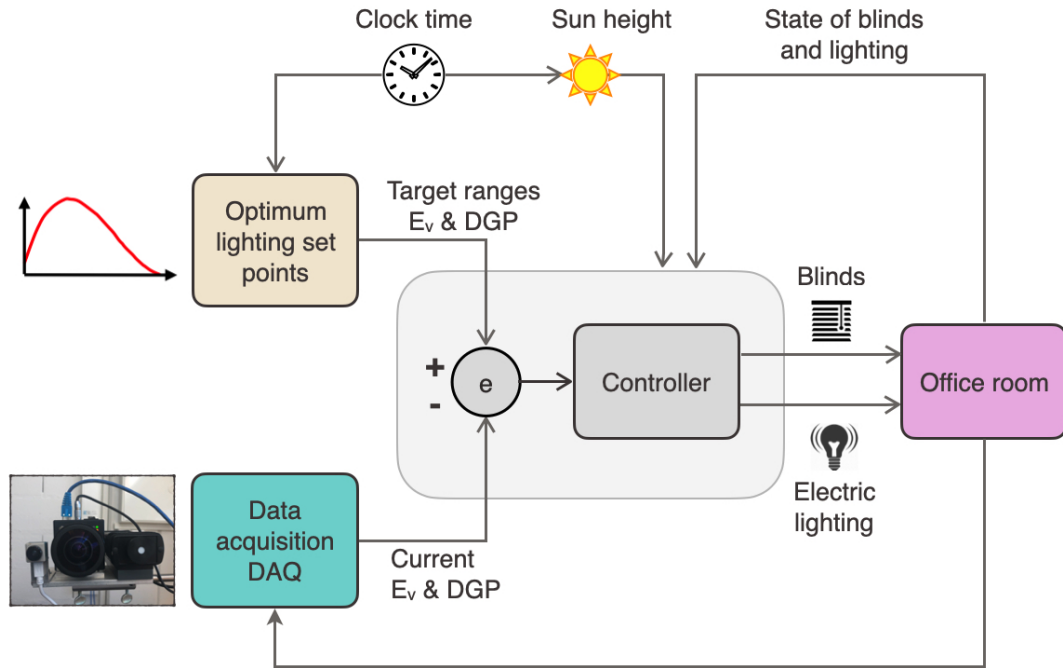


**Figure 2.14** – Scheme of the information flow and decision making of the automated control platform. The optimum lighting set points are based on  $E_{v,target}$  (according to the time of day) and DGP threshold values; the "e" in the grey circle is the "error" between measured (current) values and target values of  $E_v$  ( $eE_v$ ) and DGP ( $eDGP$ ). The controller sends commands to the venetian blinds and the electric lighting, and the data acquisition loop (DAQ) runs continuously.

### Venetian blinds controller

As explained in section 2.2.1, the *Test* room is equipped with two venetian blinds, one for each window. When adjusting the blinds, the automated controller regulates firstly their position, secondly the tilting angle of the slats. The two blinds are not moved at the same time, but priority is given to one of them depending on the sun's position. Indeed, the top window (ADS) allows a considerable amount of daylight flux to enter and lighten the room, while the bottom window allows the view

to the outside: both daylight use and view to the outside are important aspects that have to be considered. Since it is assumed that any discomfort glare sensation mainly derives from direct sunlight, it is necessary to consider through which window the direct sunlight enters, depending on the sun height, i.e., the angle between the horizon and the center of the sun's disc. An accurate assessment the room geometry revealed that when the sun was more than  $35^\circ$  above the horizon, direct sunlight passing through the top window is very likely to hit the work plane and cause visual discomfort to the user. In this case, the controller prioritized the top blind adjustment. In other words, if the DGP exceeded the 35% threshold while the sun height was higher than  $35^\circ$ , the top blind was regulated first, whereas if the sun was less than  $35^\circ$  above the horizon, discomfort glare was more likely due to direct sunlight entering through the bottom window, thus the bottom blind control had the priority.

### Bottom blind: geometry-based controller

The control of the bottom blind position is based on a simple analytical equation that considers the room geometry and sun altitude with the aim of protecting the work plane (and thus the user) from direct sunlight. Figure 2.15 shows the geometrical section of the *Test* room: for a hypothetical sun height  $\theta$ ,  $x_b$  (the unknown variable) is the opening fraction of the bottom blind required to protect the work plane from direct sunlight; since the height of the window  $L_b$  - which is also the height of the blind - is equal to 1 m,  $x_b$  can be expressed equally in meters or in relative fraction of blind opening;  $y_b$  is the horizontal distance from the edge of the work plane to the blind and is equal to 1.15 m. Based on these measurements we can assume (equation 2.6):

$$\tan\theta = \frac{x_b}{y_b} \quad (2.6)$$

Therefore, the opening fraction of the blind can be calculated according to equation 2.7:

$$x_b = \tan\theta \cdot y_b \quad (2.7)$$

As  $\theta$  increases,  $x_b$  will reach its maximum value of 1 (or 100%, bottom blind completely open). For further increase of  $\theta$ , the bottom blind is lowered in case of a high DGP: in that case, the top blind is activated (its control will be addressed in the next paragraph). According to some preliminary calculations carried-out on the basis of the room geometry, the highest value of  $\theta$  above which the bottom blind does not need to be lowered is equal to  $\theta' = 41^\circ$ . This means that the bottom blind is only activated when  $\theta < 41^\circ$  (equation 2.8):

$$0 < \theta < 41^\circ \quad (2.8)$$

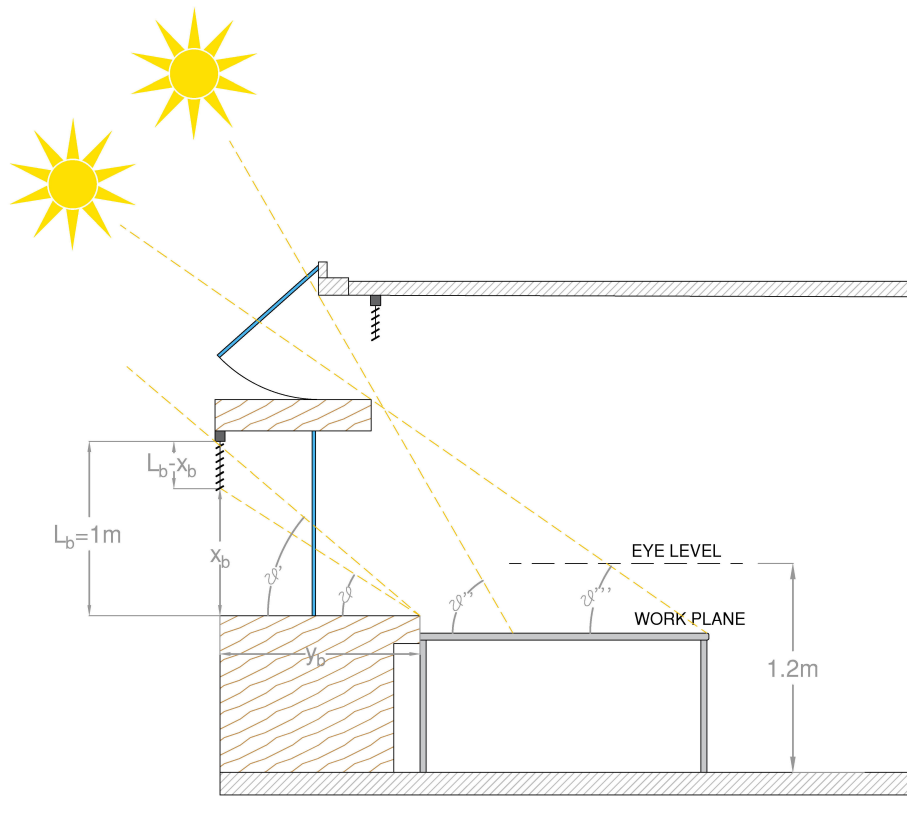


**Figure 2.15** – Geometry of the *Test* room (LE2201) for the computation of the blind positions.

## Top blind: Fuzzy Logic Controller

Due to the presence of the ADS in the upper window part, a more complex approach was used to set-up the upper blind controller, using fuzzy logic. The Fuzzy Logic Controller (FLC) involves a logic that is based on human experience, such that the variables (i.e., rules and membership functions) are empirically defined [Lee, 1990]. The FLC is based on "if-then" logical arguments (rules) applied to fuzzy sets (fuzzy = not exact) and used to formulate conditional statements [Jang & Gulley, 1997]. The Fuzzy Logic Toolbox™ in MATLAB was used. All variables and rules used are summarised in Appendix A, and the scheme in Figure 2.16 shows the input and output variables of the FLC.

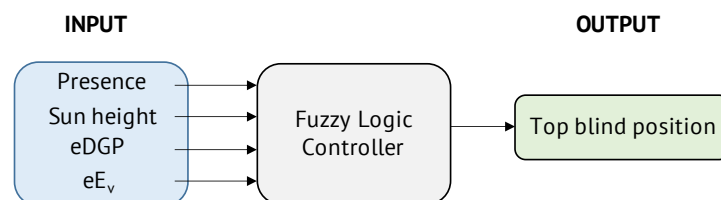


**Figure 2.16** – Scheme of input and output variables of the FLC for the top blind. The variables eDGP and eE<sub>v</sub> are the "errors" between the target values and the measured values of DGP and E<sub>v</sub> respectively (more details in Appendix A).

## Input variables

Among the input variables, the user presence is recorded by the passive infrared (PIR) sensor installed

## Chapter 2. Daylighting control in buildings

on the ceiling of the room (see n. 8 in Figure 2.11). Normally, the controller does not act if there is nobody in the room. For simplicity, in the framework of the field study described in the next chapter, presence was set as a fixed value "1" (i.e., someone is present in the room) from 8:00 to 18:00, and "0" (nobody is present) otherwise.

As mentioned in the previous paragraph, the sun height is defined as the angle between the horizon and the center of the sun's disk and it is expressed in degrees ( $^{\circ}$ ). It is also calculated as:  $90^{\circ} - \text{zenith}$ , where *zenith* is the angle between the zenith and the sun. In the FLC presented here, sun height can take the following values: "low", "mid", "high" (see Appendix A).

The "error" of DGP ( $eDGP$ ) is defined as the difference between the "current" measured DGP and the maximum threshold (35%), calculated as in equation 2.9:

$$eDGP = DGP_{measure} - DGP_{max} \quad (2.9)$$

where  $DGP_{max} = 35\%$  and  $DGP_{measure}$  is the maximum value of DGP registered either in the last 15 minutes, or since the latest actuation.

Similarly, the error  $eE_v$  indicates how far the current  $E_v$  is from the target value at that time of the day. The following threshold values were defined:

- $E_{v,max} = 2500$  lux: above this value, the room is considered "too bright";
- $E_{v,ref} = E_{v,target}(\text{clocktime})$  is the target illuminance which depends on the time of day (see curve in Figure 2.13);
- $E_{v,min} = E_{v,ref} - 200$  lux, is the minimum accepted  $E_v$  below which the room is considered "too dark";
- $E_{v,measure}$  is the lowest  $E_v$  recorded since the last controller actuation or in the last 15 minutes.

The fuzzy input variable  $eE_v$  is defined in such a way that:

- The closer  $E_{v,measure}$  is to  $E_{v,ref}$ , the closer  $eE_v$  will be to 0.
- When  $E_{v,measure}$  is in the range  $\{E_{v,min}, E_{v,max}\}$ , then  $eE_v$  is included between -1 and 1.
- Outside of the range  $\{E_{v,min}, E_{v,max}\}$ ,  $eE_v$  decreases or increases more rapidly, following a linear function with an arbitrary slope equal to  $\tan(0.1)$ .

This results in the definition of  $eE_v$  as in system of equations 2.10. The diagram in Figure 2.17 shows  $eE_v$  as a function of  $E_{v,measure}$ .

$$\begin{cases} eE_v = \tan(0.1) \cdot (E_{v,measure} - E_{v,min}) - 1 & \text{if } E_{v,measure} < E_{v,min} \\ eE_v = \frac{E_{v,measure} - E_{v,min}}{E_{v,ref} - E_{v,min}} - 1 & \text{if } E_{v,min} \leq E_{v,measure} < E_{v,ref} \\ eE_v = \frac{E_{v,measure} - E_{v,ref}}{E_{v,max} - E_{v,ref}} & \text{if } E_{v,ref} \leq E_{v,measure} < E_{v,max} \\ eE_v = \tan(0.1) \cdot (E_{v,measure} - E_{v,max}) + 1 & \text{if } E_{v,measure} \geq E_{v,max} \end{cases} \quad (2.10)$$

## 2.2. Automated controller for venetian blinds and electric lighting

Since the FLC accepts only a limited range of input values, which is set to  $\{-4, 4\}$ , the computed value of  $eE_v$  would be trimmed to fit in the acceptable range if needed.

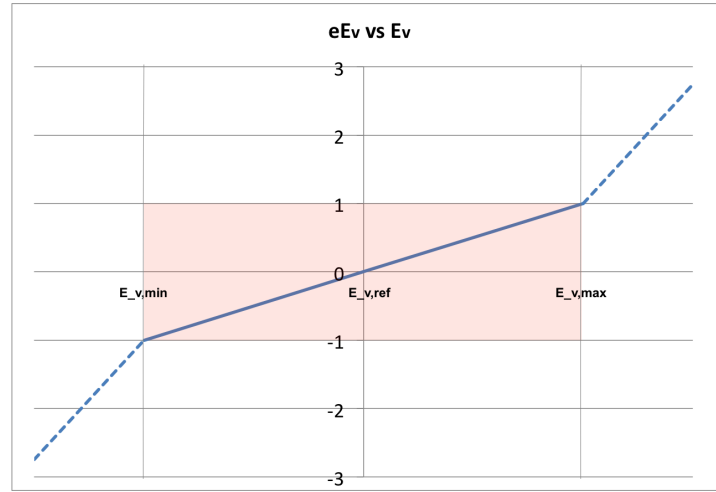


**Figure 2.17** – The "error"  $eE_v$  (y-axis) as a function of  $E_{v,measure}$  (x-axis). The red rectangle delimits the range between  $E_{v,min}$  and  $E_{v,max}$  and  $eE_v$  between -1 and 1.

### Output variable

The only output of the FLC is the top blind position, expressed as "opening fraction" in decimal values between 0 and 1 as in Table 2.6.

Blind position	FLC output
Open	1
Closed	0

**Table 2.6** – The output variable of the FLC: the top blind position. The variable could take decimal values between 0 (for completely closed) to 1 (completely open).

### Logic for control rules

According to Figure 2.15, two additional critical sun heights  $\theta''$  and  $\theta'''$  were defined to analyse three possible scenarios and deduce some preliminary control rules, as shown in Table 2.7.

Scenario	Condition	Description	Desired top blind opening [%]
1	$\theta > \theta''$	The sun is high on the horizon	100%
2	$\theta''' < \theta < \theta''$	Direct sunlight is likely to hit work plane	0%
3	$\theta < \theta'''$	The sun is low on the horizon, bottom blind should rather be adjusted	100%

**Table 2.7** – Possible scenarios for top blind control, where  $\theta$  is the actual sun height and  $\theta''$  and  $\theta'''$  are critical angles shown in Figure 2.15. The calculated values of these critical angles are:  $\theta'' = 60^\circ$ ,  $\theta''' = 35^\circ$ .

In the first scenario the sun height exceeds  $\theta''$ : in this case the direct sunlight does not reach the work plane due to the geometrical layout of the room and the lightshelf located on the southern

facade of the building. Since there is no need of protecting the user and the work plane in this scenario, the top blind remains open to allow the daylight flux entering the room. When  $\theta$  is between  $\theta'''$  and  $\theta''$ , the direct sunlight hits the work plane (and likely the eyes of the user), therefore the top blind must be lowered. In the third scenario, the direct sunlight does not reach the work plane. Instead, it hits the ADS and is redirected on the ceiling, and occasionally it might cause discomfort glare. In this case, the top blind would normally stay open, but it must be closed if the DGP and/or high  $E_v$  is high. The corresponding values of the critical angles are:  $\theta'' = 60^\circ$  and  $\theta''' = 35^\circ$ .

### Calculation of the slat angle

The angle of the slats can be adjusted after each translational movement of the blinds. The slats regulation is performed in a way to completely cut the direct solar radiation. By assuming the slats

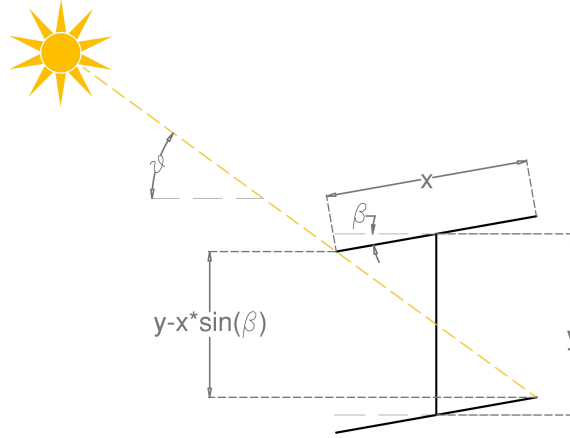


**Figure 2.18** – Geometry of the blinds for calculation of the slat angle.  $\theta$  = sun height;  $\beta$  = slat angle;  $x$  = slats width,  $y$  = distance between slats;

being flat (for simplicity), Equation 2.11 was defined based on the geometry of the slats (see Figure 2.18):

$$\beta_c = \sin^{(-1)} \left( \frac{y}{x} - \frac{\tan(\theta)}{\cos(a)} \right) \quad (2.11)$$

where  $\beta_c$  is the critical slat angle,  $y$  the distance between the slats,  $x$  the slat width,  $\theta$  the sun altitude,  $a$  the relative azimuth, i.e., the angle between the perpendicular to the façade and the direction of the sun projected on a horizontal plane, positive towards the east direction.

### Electric lighting controller

The aim of the lighting controller in the *Test* room is to provide a sufficient vertical illuminance at the eye level ( $E_v$ ) at the desk, i.e. equal to or above the target, which is defined by the dynamic  $E_{v,target}$  curve in Figure 2.13 and equation 2.5. The electric lighting is activated only when the daylight availability is not sufficient to reach the required level of  $E_{v,target}$ . The lighting controller is



## 2.2. Automated controller for venetian blinds and electric lighting

executed after the blinds controller. The amount of "lacking"  $E_v$  is calculated as:

$$\Delta E_v = E_{v,now} - E_{v,target} \quad (2.12)$$

where  $E_{v,now}$  is the most recent  $E_v$  recorded by the VIP. Depending on  $\Delta E_v$  the command sent to the electric lighting varies, as shown in Table 2.8. For  $\Delta E_v$  between -350 and 0 lux, the combination of lighting setting (including both ceiling and floor-standing luminaire) is computed by means of the MATLAB function *fmincon*, a nonlinear programming solver, starting from the measured values in Table 2.5. As mentioned in section 2.2.1, the floor-standing luminaire is prioritised over the ceiling luminaires because of its larger contribution to increase the illuminance levels.

Scenario	Command to electric lighting
$\Delta E_v < -600$	ON
$-350 \leq \Delta E_v \leq 0$	Optimization through <i>fmincon</i>
$0 \leq \Delta E_v \leq 350$	Dead zone (no command)
$\Delta E_v > 350$	OFF

**Table 2.8** – Commands to electric lighting according to the "lacking" vertical illuminance  $E_v$ .

### 2.2.5 Summary of the controller steps

The detailed operation of the controller is illustrated in the execution block diagram in Figure 2.19. The loop starts with data acquisition (DAQ), which consists in reading and saving the real-time data, including  $E_v$  and DGP, position and slat angle of the blinds, electric lighting status, energy consumption, and other monitored variables such as the work plane illuminance  $E_h$  (measured by a sensor on the ceiling, see Figure 2.11), indoor and outdoor temperature, global and diffuse irradiance, etc.

The DAQ is followed by the evaluation of whether there is an "event" or not (as in Motamed [2017], chapter 5). The occurrence of an "event" takes place when one of the following options is true:

- it is the first loop of the day;
- the presence parameter has changed, i.e., the occupant has left or has arrived in the room;
- $E_v$  or  $E_h$  have changed by more than 30 lux with respect to the recent data previously recorded;
- DGP has varied by more than 3% with respect to previous recent data.

If the current situation applies to one of these options, the control loop begins. As mentioned before, the controller starts from the venetian blinds and passes to the electric lighting afterwards. Depending on the sun height, one of the two blinds will be activated first. Note that in Figure 2.19 the bottom blind control is in the first place for sake of illustration, but the position of the blocks "bottom blind" and "top blind" may be swapped according to the sun height.

The first step in a control block is preparing the inputs to the controller, which are defined as  $eDGP$  and  $eE_v$ . The controller processes the inputs and returns as an output the new position and the slat angle of the blinds.

The next important step is the "command filter", which filters the commands by comparing the controller output with the current settings: more specifically, commands that would result in small amendments (less than 20% for the position and less than  $5^\circ$  for the slat angle, or less than 20% of dimming level for electric lighting) are not considered. The command filter also avoids too frequent adjustments of the blinds and electric lighting which could be disturbing the occupant: each adjustment can be executed at earliest 15 minutes after the previous one. If the command generated by the controller passes through the filter, it is sent to the actuators. At this point, a new DAQ is carried-out to assess the new lighting conditions, and the loop continues and is concluded with the lighting controller.

### 2.2.6 The *Reference* room

The "*Reference* room" setup is almost identical to the one of the *Test* room. However, in order to make *Reference* room more similar to a standard office space in terms of window-to-wall ratio, the WWR was reduced from the original 41% value of the façade to approximately 21% by keeping the upper window covered throughout the experimental monitoring. The two main differences with respect to the *Test* room are the following:

- The top window (i.e., the anidolic daylighting system, ADS) is covered by means of an opaque blind that remained closed for the entire duration of the experiments. The choice of covering the ADS was made because the purpose was to compare the advanced daylighting and the control system with an office room that is as much as possible similar to a standard office in terms of WWR (and therefore daylight influx).
- There is no automatic control. The user is free to adjust the blind and the electric lighting according to his/her needs and preferences.

## 2.2. Automated controller for venetian blinds and electric lighting

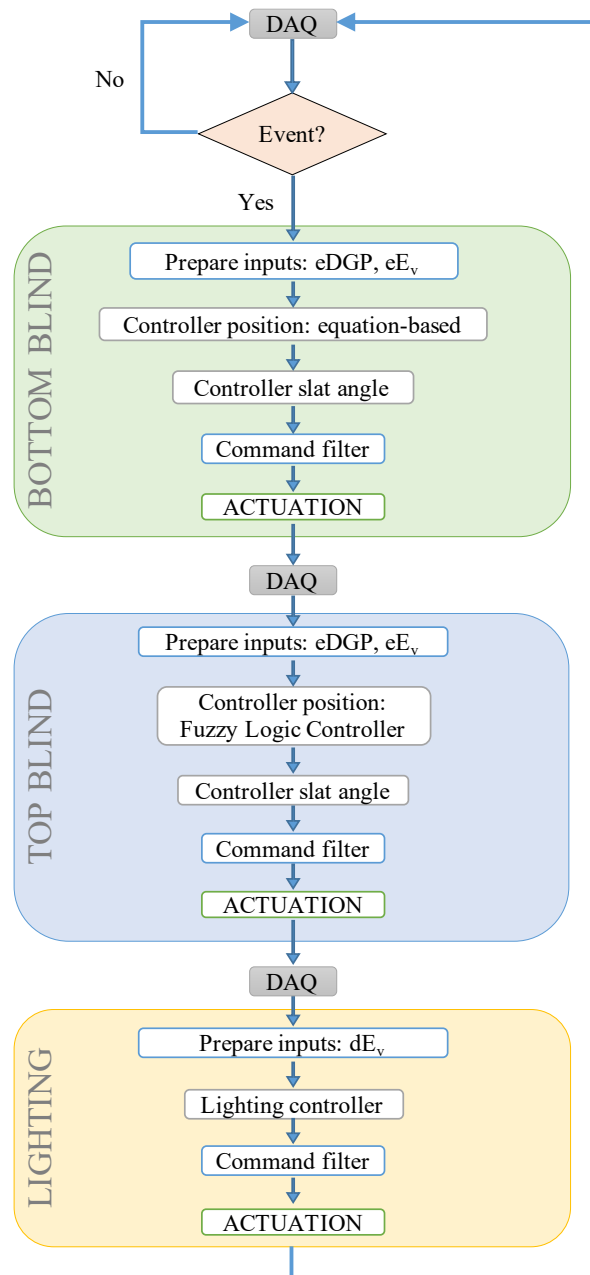


**Figure 2.19** – Execution block diagram of the controller. DAQ = data acquisition (reading and saving data);  $eDGP$  and  $eE_v$  = input variables to the blinds controller;  $dE_v$  = input to the electric lighting controller.

### 2.2.7 Data collection and analysis

The automated controller described in the previous section was tested during 160 days between September 2018 and December 2019 in the framework of a field study including human participants (the details of the study procedure are reported in Chapter 3). In the next section, a summary of the results of the controller performance and comparison of the two office rooms, i.e., the *Test* and the *Reference* room, is presented. The following outcome variables were assessed:

- Objective characteristics of the lighting conditions in the two office rooms, assessed by the VIP vision sensor and the spectrometer, both placed on a support next to the desk at a height of 1.20 m (as described in section 2.1.3, see also Figure 2.11):
  - Vertical illuminance ( $E_v$ )
  - Melanopic Equivalent (D65) Daylight Illuminance (EDI)
  - Daylight Glare Probability (DGP)
- Electric energy consumption for artificial lighting.

Furthermore, data of monitored room temperature and power consumption for space heating were extracted from the data collection and included in the analysis. It must be noted however, that the automated controller was not designed to consider the room temperature or to act on the space heating. As reported by Zarkadis [2015], the electric radiators are managed by an on/off controller which uses a pulse width modulation for implementing a proportional controller. The switch in each room allows to set manually the temperature set point within a range of 5 points, from colder to warmer (see Figure 2.20). The error of measurement of the sensor is estimated to be  $0.5^{\circ}\text{C}$  [Lindelöf, 2007]. Since the analysis of the room temperature, space heating and thermal comfort goes beyond the main scope of the work presented in this thesis, the use of such a control box during the on-site experimentation was not included, and no instructions were given to office occupants about such a regulation. During the experimentation,  $E_v$ , EDI, DGP and room temperature were collected



**Figure 2.20** – Control box for electric lighting and temperature set point (Siemens UP 231/2). The left switch (+/-) is used to select the desired temperature set point, indicated at the bottom of the switch.

## 2.2. Automated controller for venetian blinds and electric lighting

---

continuously from 8:00 to 19:00 and monitored data were collapsed into 30-minute bins. Only the days when the rooms were occupied by the study participants were considered in the analysis. Due to technical issues with the automated controller during the summer (July and August), data collected during 15 days in the *Test* room had to be excluded from the analysis, and there were 8 more days of data missing in the *Test* room and 10 missing days in the *Reference* room due to technical monitoring issues. Furthermore, the two office rooms were not always occupied at the same time, even though the control system and the data collection were active. The final analysis was performed only for days when a study participant was present in (at least) one room, i.e., during a total of 147 days in the *Test* room and 160 days in the *Reference* room.

Electrical energy consumption was derived from the instantaneous power measured by the power meters (separately for heating and lighting), on a time-step basis. Instantaneous power was measured at each power variation, which made the frequency of measurements vary between a few seconds to several minutes. The accuracy of power meters is not specified: in his doctoral thesis, Lindelöf [2007] estimated conservatively an uncertainty of 8% on the energy consumption measurement for space heating, and 2% for lighting. For the analysis of energy consumption, the same procedure as described below was applied. Here, a total of 155 days in each condition was included in the analysis.<sup>g</sup>

The results presented in this section reflect the average of days monitored during office hours in both rooms (i.e., *Test* and *Reference*) between 8:00 and 18:00, and expressed in absolute clock time. This is a slightly different representation than in Chapter 3, where the timing is adjusted to actual presence time in the office (which varies between individuals), and expressed as elapsed time since midsleep (see Chapter 3).

Weather conditions (cloudiness and outdoor temperatures) were also monitored and reported. The amount of daily sunshine hours was used to classify the sky for each day of the field study into three categories (clear, intermediate, overcast sky) as below. The meteorological data was available from the local weather station (Meteosuisse, Pully, VD, Switzerland) [Meteosuisse, Meteosuisse]. The ratio between the sunshine duration and the total day length (i.e., time between sunrise and sunset) was used for the classification of the sky type (according to the Swiss Norm 150 911 [Association Suisse de l'Eclairage (SLG/ASE), 1989]):

- > 75%: clear sky
- between 25% and 75%: intermediate sky
- < 25%: overcast sky

The outdoor temperature was recorded by a sensor located on the rooftop of the LESO building and connected to the overall sensing platform. Data was retrospectively downloaded from the database.

---

<sup>g</sup>This number differs from the sample size for the lighting variables because energy meters were not linked to the control platform, which resulted in less data missing (while missing data of  $E_v$  and DGP was due for example to temporary failure of the MATLAB software).

### Statistical analysis

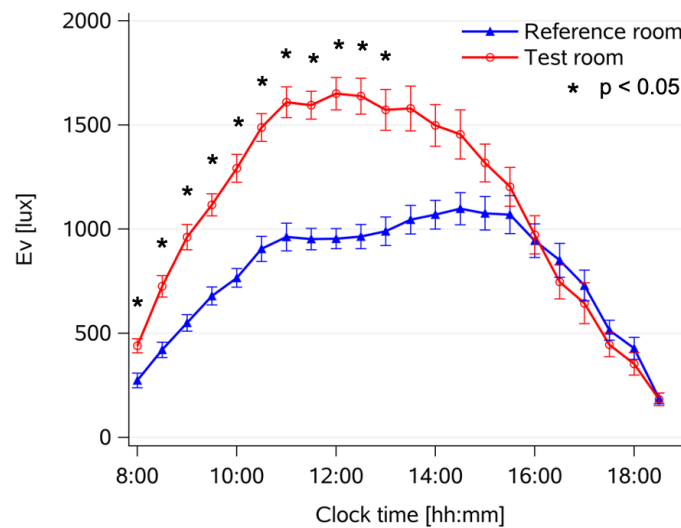
Statistical analysis was performed with the collected environmental data, similar to the procedures presented in more details in Chapter 3 (section 3.2). Using the software SAS (SAS Institute Inc., Cary, NC, USA; version 9.4), a generalized linear model (PROC GLIMMIX) was applied. The fixed factors "condition" (i.e., *Test room* vs. *Reference room*) and "time" (30-minute bins from 8:00 to 18:30), as well as their interactions, were used in the model. Degrees of freedom were determined with the Satterthwaite approximation and a post-hoc analysis was performed by using the Tukey-Kramer test with p-values adjusted for multiple comparisons. To assess statistical significance, an alpha level of 0.05 was used. In this thesis, F-values and p-values are reported in the Results sections (in this Chapter and in Chapter 3). Average results are reported in the text as mean  $\pm$  standard deviation (SD).

Even though the study was not designed to test for seasonal differences, potential effects from different seasons due to differences in photoperiod length were also explored by including the factor "season" as covariate to the generalized linear model (only significant differences are reported). The distribution of monitored days between the four seasons was: 45% in fall, 32% in spring, 12% in summer, 11% in winter.

## 2.3 Results

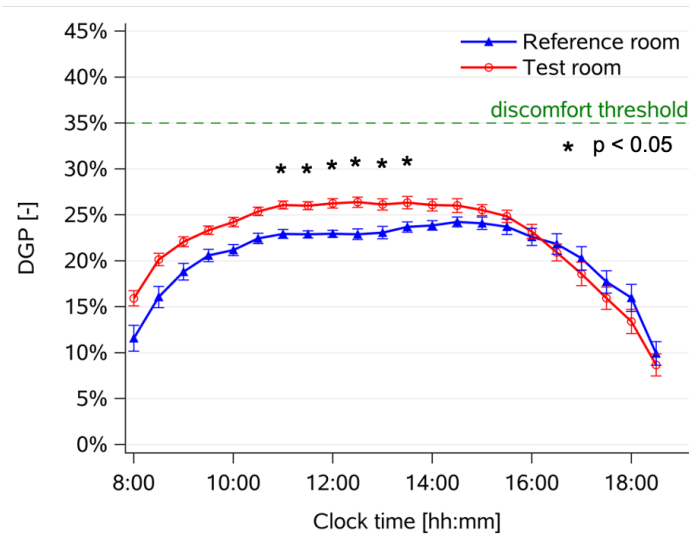
### 2.3.1 Lighting conditions in the office rooms

Figure 2.21 shows the time course of the photopic illuminance  $E_v$  in the two office rooms during normal working hours, averaged across all days. A high variability throughout the day is evident in both rooms (main effect of *time*:  $F_{21,1308}=101.2$ ,  $p<0.0001$ ). Vertical illuminance was significantly higher in the *Test* room ( $1114 \pm 633$  lux, mean  $\pm$  SD) than in the *Reference* room ( $792 \pm 443$  lux; main effect of *condition*:  $F_{1,1325}=150$ ,  $p<0.0001$ ). The interaction between the factors *condition\*time* was statistically significant ( $F_{21,1308}=5.6$ ,  $p<0.0001$ ), and adjusted p-values indicated a significant higher  $E_v$  in the *Test* than in the *Reference* room from 8:00 until 13:00.



**Figure 2.21** – Average time course of vertical illuminance  $E_v$  during the day (mean  $\pm$  standard error, SEM), recorded by the VIP sensor fixed next to the office desk at a height of 1.20 m above the floor. Number of days:  $n=147$  in the *Test* room and  $n=160$  in the *Reference* room. \* = statistically significant difference between the two conditions (after adjusting for multiple comparisons;  $p<0.05$ ).

The glare index DGP also varied during the day (Figure 2.22; main effect of *time*:  $F_{21,1308}=73.8$ ,  $p<0.0001$ ) and was slightly, but significantly higher in the *Test* than in the *Reference* room (main effect of *condition*:  $F_{1,1320}=115.9$ ,  $p<0.0001$ ). The average DGP was  $22\% \pm 6\%$  in the *Test* room and  $21\% \pm 6\%$  in the *Reference* room. Such levels are, on average, far below the discomfort threshold of 35%, also indicated by the green dashed line in Figure 2.22. An interaction between the factors *condition\*time* was also found ( $F_{21,1308}=5.6$ ,  $p<0.0001$ ). Post-hoc tests (with adjusted p-values) showed a significantly higher DGP in the *Test* than in the *Reference* room from 11:00 to 13:30.



**Figure 2.22** – Average time course of Daylight Glare Probability (DGP, in %) during the day (mean  $\pm$  standard error, SEM), recorded by the VIP sensor fixed next to the office desk at a height of 1.20 m from the floor;  $n=147$  in the *Test* room and  $n=160$  in the *Reference* room; the discomfort glare threshold of 35% is indicated by the dashed green line. \* = statistically significant difference between the two conditions (adjusted for multiple comparisons,  $p<0.05$ ).

The melanopic EDI was calculated for less monitored days with respect to the other measurements presented in this section, due to the availability of only one spectrometer (90 days in each room were included in the analysis, see also section 2.2.2). Thus, all spectral measurements in the two rooms were not taken simultaneously and might vary also because of different weather conditions. The time course of melanopic EDI dynamically changed across the day (main effect of *time*:  $F_{21,622}=26.2$ ,  $p<0.0001$ ; Figure 2.23) and was significantly higher in the *Test* room ( $987 \pm 558$  lux) than in the *Reference* room ( $732 \pm 429$  lux; main effect of *condition*:  $F_{1,622}=35.8$ ,  $p<0.0001$ ). The interaction between both factors was significant ( $p<0.0001$ ), however adjusted  $p$ -values did not reveal any statistically significant differences in EDI between the two conditions at any time point. From visual inspection it appears that the difference between both conditions is mainly during the first half of the day, similar to  $E_v$  (Figure 2.21).



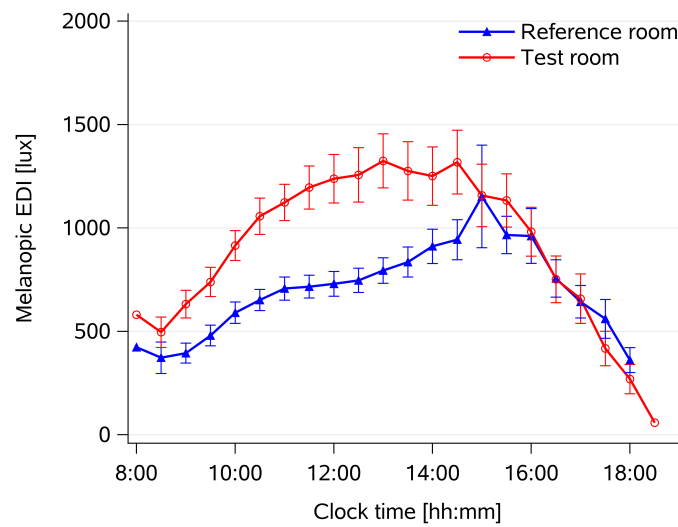


**Figure 2.23** – Time course of melanopic Equivalent Daylight Illuminance (EDI), averaged across days for each condition (mean  $\pm$  SEM);  $n=80$  for both conditions.

### 2.3.2 Room temperature

Room temperature (Figure 2.24) was on average  $23.1 \pm 1.7^\circ\text{C}$  in the *Test* room and  $23.9 \pm 1.7^\circ\text{C}$  in the *Reference* room. The *Reference* room was on average  $0.8^\circ\text{C}$  warmer, and this difference was statistically significant (main effect of *condition*:  $F_{1,1309}=285.3$   $p<0.0001$ ). Room temperature was lowest in the morning and continuously increased in the course of the day (main effect of *time*:  $F_{1,1306}=33.15$ ,  $p<0.0001$ ).

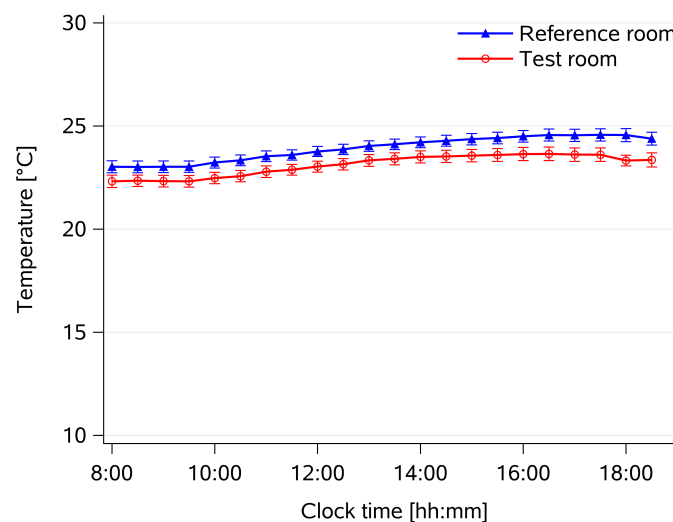


**Figure 2.24** – Time course of room temperature ( $^\circ$ ) averaged across days (mean  $\pm$  SEM);  $n=147$  in the *Test* room and  $n=160$  in the *Reference* room.

### 2.3.3 Electric energy consumption

The average daily electricity consumption (including both electric lighting and space heating) was significantly higher in the *Reference* room than in the *Test* room (i.e.,  $2.18 \pm 5.31$  kWh/day vs.  $1.97 \pm 2.99$  kWh/day, mean  $\pm$  SD, respectively; main effect of *condition*:  $F_{1,302}=7.9$ ,  $p=0.005$ , Figure 2.25a). There was also a significant difference between seasons, with a higher electricity demand in fall than in the rest of the year. The interaction between the factors *condition* and *season* was additionally tested and indicated a significant difference between the two rooms only in winter, with a higher energy demand in the *Test* room than in the *Reference* room ( $p=0.012$ ; Figure 2.25b).

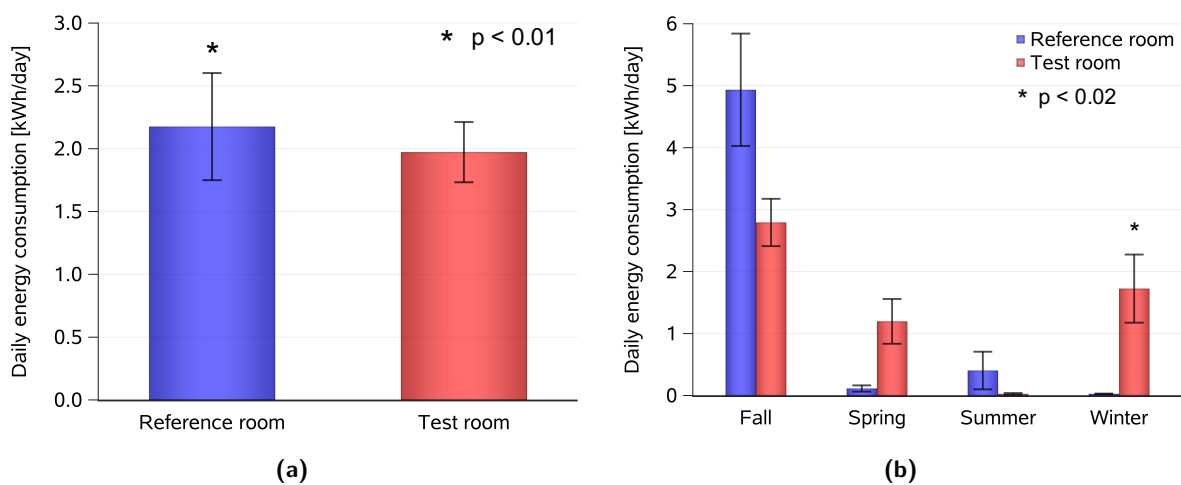


**Figure 2.25** – Bar charts of total energy demand (including space heating and electric lighting), averaged across days, mean  $\pm$  SEM: a) grouped by condition ( $n=155$  days in each condition); b) grouped by season and condition. Number of days in fall:  $n=76$  in the *Test* room and  $n=65$  in the *Reference* room; winter:  $n=20$  in *Test* room and  $n=15$  in *Reference* room; spring:  $n=49$  in the *Test* room and  $n=49$  in the *Reference* room; summer:  $n=10$  in the *Test* room and  $n=26$  in the *Reference* room. \* = statistically significant difference between the two conditions (after p-values adjustments).

#### Electric lighting

The electricity consumption for artificial lighting was on average higher in the *Test* room ( $0.20 \pm 0.20$  kWh/day) than in the *Reference* room ( $0.12 \pm 0.18$  kWh/day; main effect of *condition*:  $F_{1,302}=12$ ,  $p=0.005$ , Figure 2.26a). The electric lighting energy demand was higher in fall, followed in the order by winter, spring, summer (main effect of *season*:  $F_{1,302}=42.1$ ,  $p<0.0001$ ). There was also an interaction effect of *condition\*season* such that energy consumption from electric lighting was significantly higher in fall in the *Test* than in the *Reference* room ( $p<0.0001$ ; Figure 2.26b), whereas in the other seasons the difference was not statistically significant.

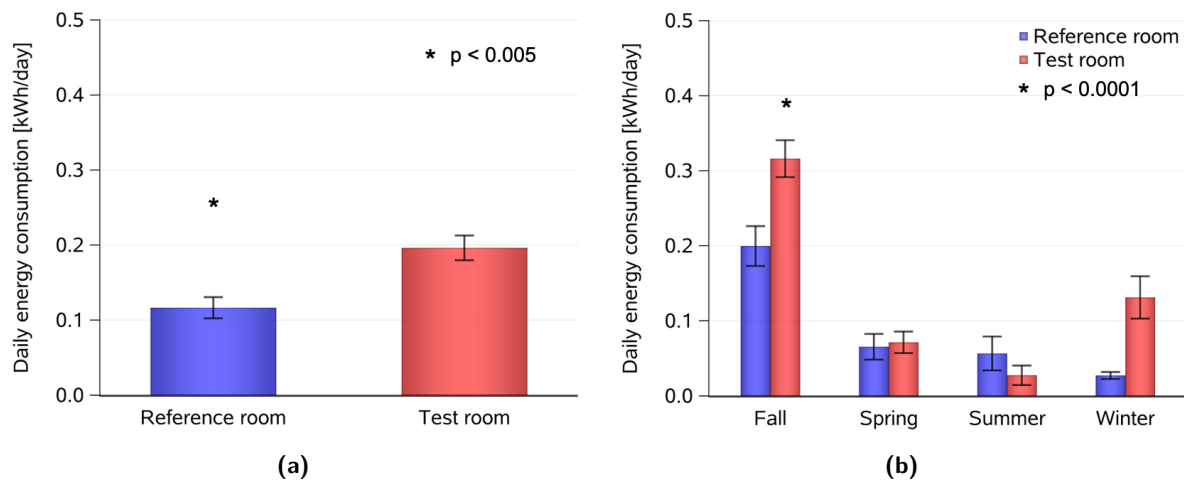


**Figure 2.26** – Bar charts of electric lighting energy demand, averaged across days, mean  $\pm$  SEM: a) grouped by condition ( $n=155$ ); b) grouped by season and condition. Number of days for each season: fall  $n=76$  in the *Test* room and  $n=65$  in the *Reference* room; winter  $n=20$  in *Test* room and  $n=15$  in *Reference* room; spring  $n=49$  in the *Test* room and  $n=49$  in the *Reference* room; summer  $n=10$  in the *Test* room and  $n=26$  in the *Reference* room.

### Space heating

The total energy consumption for space heating was higher in the *Reference* than in the *Test* room ( $2.06 \pm 5.29$  kWh/day in the *Reference* room and  $1.78 \pm 2.94$  kWh/day in the *Test* room, respectively; main effect of *condition*:  $F_{1,302}=5.9$ ,  $p=0.01$ ; Figure 2.27a). Regarding seasonal differences, the heating energy demand was significantly higher in fall than in the other seasons, without significantly different energy demands across seasons between both rooms (Figure 2.27b).

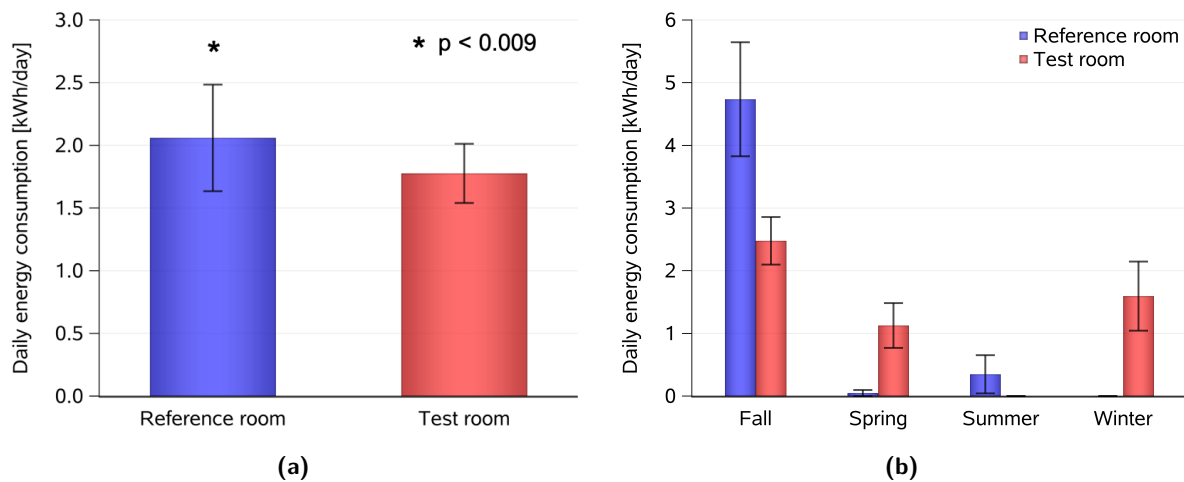


**Figure 2.27** – Bar charts of electric energy demand for space heating, averaged across days, mean  $\pm$  SEM: a) grouped by condition ( $n=155$ ); b) grouped by season and condition. Number of days in fall:  $n=76$  in the *Test* room and  $n=65$  in the *Reference* room; winter:  $n=20$  in the *Test* room and  $n=15$  in the *Reference* room; spring:  $n=49$  in the *Test* room and  $n=49$  in the *Reference* room; summer:  $n=10$  in the *Test* room and  $n=26$  in the *Reference* room.

### Weather conditions

The weather conditions during the study were analysed retrospectively, in the attempt to better interpret the lighting and energy consumption results.

Figure 2.28a shows the number of days for each sky type in both conditions. In the *Test* room, the sky was clear in 30% of the overall number of days, intermediate for 24%, and overcast for 46% of the days. In the *Reference* room, the sky was clear for 35% of the time, intermediate for 29% and overcast for 36% of the days. There was no significant difference in sunshine duration between the two conditions ( $p=0.7$ ).

Figure 2.28b shows the average outdoor temperatures in each of the four seasons. The outdoor temperature differed significantly between seasons, however there was no difference for days when the *Test* or the *Reference* room were occupied.

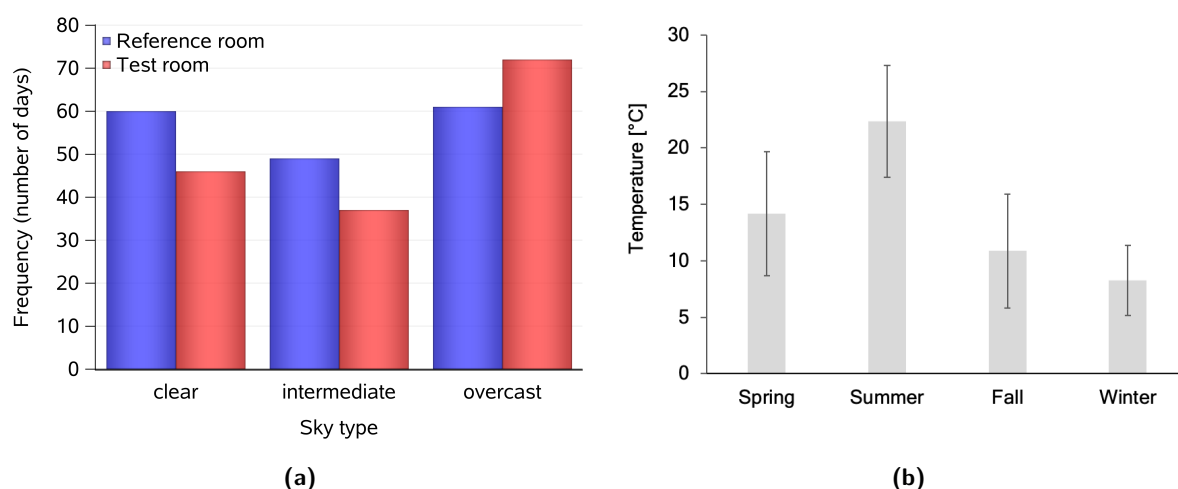


**Figure 2.28** – Bar charts of a) sky type during the study (total number of days for each sky type for both conditions) and b) outside temperature (mean  $\pm$  SD in each season).

## 2.4 Summary and discussion

The use of daylighting in non-residential buildings should be optimally controlled in order to ensure general comfort of the occupants, with sufficient lighting levels and low glare risks. Furthermore, a good daylighting control system should also guarantee a low electric energy demand.

In this Chapter, a novel automated controller for venetian blinds and electric lighting was presented. The automated controller was aimed at providing dynamic lighting levels at optimized target illuminance and sound visual comfort in a *Test* office room, and compared to a standard *Reference* room (where also the WWR was reduced). The results included vertical photopic illuminance, DGP, melanopic EDI, room temperature, and electric energy consumption for electric lighting and space heating.

Overall, the results showed that in the *Test* room (with the daylight-responsive automated controller combined to an anidolic daylighting system) vertical illuminance was higher compared to the *Reference* room in the first half of the day. The DGP values were well below any discomfort probability in both rooms. Despite higher electricity consumption for electric lighting in the *Test* room, the total energy demand was overall higher in the *Reference* than in the *Test* room, most likely due to higher space heating consumption than in the *Test* room. Potential reasons will be further discussed below.

### 2.4.1 Lighting conditions and DGP monitoring

The two office rooms benefit from a large daylight flux. Indeed, photopic illuminance on a vertical plane at the eye level was higher than 500 lux during most of the office hours. The continuously monitored vertical illuminance  $E_v$  and melanopic EDI at the approximate eye level showed a dynamic pattern during the day, which is due to the orientation of the rooms (south-oriented) and the lighting sensors in the rooms (i.e., VIP and spectrometer, facing towards west parallel to the windows). Indeed, in both rooms lighting variables ( $E_v$  and melanopic EDI) were higher around midday, which is when the sunlight penetration was larger. Overall, higher  $E_v$  levels were recorded in the *Test* room until the early afternoon, compared to the *Reference* room. This difference is explained by a combined effect of the automated controller, which was designed to provide dynamic lighting levels that varied according to the time of day, and the anidolic daylighting system (ADS), that allows a considerable amount of daylight flux to enter the room (please note that the ADS was covered in the *Reference* room, which resulted in an obvious reduction of the daylight influx as described earlier). The  $E_v$  levels in the *Test* room were based on the preset target curve, which often caused the activation of electric lighting by the automated controller (when daylight was not sufficient).

Concomitant with the higher  $E_v$ , also DGP values were  $\sim 2\%$  higher in the *Test* room than in the *Reference* room. However, it is important to state that the DGP index was always kept considerably below the discomfort threshold (in both rooms), indicating that visual comfort was on average maintained throughout the day.

Also, melanopic EDI was higher in the *Test* room mostly in the first part of the day, which indicates a higher impact of the lighting for non-visual effects (see Chapter 3). Overall, these results showed a successful performance of the advanced daylight-responsive automated controller in keeping  $E_v$  and visual comfort in the *Test* room sufficiently high while fostering the potential non-visual effects of daylight, as determined by the melanopic EDI. Both the preset threshold levels of  $E_v$  (Figure 2.13) and the absence of perceived glare were always provided. It should also be stated that  $E_v$  and melanopic EDI were high in both rooms and potential differences on the impact of physiological functions and performance will be presented in Chapter 3.

### 2.4.2 Considerations on room temperature

As stated before, the room temperature was not managed by the automated controller described in the previous section of this Chapter. The increase of room temperature throughout the day is a natural consequence of the solar radiation penetrating through the windows. The temperature difference between the two rooms was constant during the entire day all over the monitored period, although it appears from the plot that the slope of the curve in the late afternoon (around 16:00) is steeper in the *Reference* room, while it gets more flattened in the *Test* room. This might be a result of the activation of the venetian blinds by the automated controller in the afternoon, which favoured a better control of the passive solar gains. As a result, the automated control system offers more reasonable conditions of thermal comfort in the office room by maintaining the room temperature in a lower range.

The room temperature was on average  $0.8^{\circ}\text{C}$  higher in the *Reference* room than in the *Test* room. This difference is not trivial to explain. For instance, it can be possibly a consequence of the coverage of the ADS in the *Reference* room, which prevented heat loss to the outside; another interpretation would be the location of the rooms in the layout of the building, the *Reference* room being in direct communication with the corridor and surrounded by heated spaces, differently from the *Test* room which communicates only with the *Reference* room) and thus, it may be that the door remained open at some rare occasions, exchanging heat with the back part of the building, while the *Test* room was more isolated (having also the eastern façade connected to the outdoor). Moreover, the temperature set point for the heating system, that can be regulated via the manual switch (see Figure 2.20), might have been different between the two rooms during some study weeks, and also the users behaviour, for example with regard to opening/closing the windows. The room temperature set points for the heating system were analysed retrospectively. They varied in time in both rooms, spanning from  $16^{\circ}\text{C}$  to  $24^{\circ}\text{C}$  during the study; the set point in the *Reference* room was generally not higher than in the *Test* room, thus the indoor temperature difference is apparently not due to the temperature setting of the heaters.

It must be mentioned that the room temperature was measured in the control boxes located on the wall. Adopting an additional sensor for a more accurate measurement of the indoor temperature closer to the user in the room would have been out of the scope of this thesis. In order to check the reliability of the room temperature sensors and compare them between each other, a post-hoc verification was made using a portable digital instrument for precise indoor air quality monitoring (Testo 480, Testo Inc.). The device was placed on a tripod, next to the wall, for 2-3 hours in each of the two office rooms, and its measurements of mean radiant temperature were compared to those from the two room sensors. The radiant temperature measured by the Testo 480 device was on average  $1.5^{\circ}\text{C}$  higher than the temperature from both room sensors. Importantly, the offset between the measurements by the portable device and the room sensors was equal in the two office rooms. This confirmed that the temperature sensors were calibrated and there were no intrinsic temperature

monitoring differences between the sensors in the two rooms.

### 2.4.3 Electric energy demand

On the total electricity demand over the duration of the on-site monitoring, an energy saving of 9.6% was obtained by the automated control system, which is reached by an optimisation of passive solar gains in the *Test* room. The reasons are to a certain extent due to the difference of indoor temperatures in the two rooms, however the differences in energy consumption between the two rooms are close to what was expected.

The electricity demand for lighting remained very low throughout the on-site experimentation in both conditions, reflecting the intensive use of daylight achieved in both rooms due to the architectural design of the southern façade of the LESO building. In spite of this, the automated control system led to a higher energy consumption from electric lighting in the *Test* than the *Reference* room (where the occupants were free to adjust the lighting according to their preferences). Such higher electricity consumption is mainly due to the (high) pre-set levels of  $E_v$ , which caused the automated controller to switch on the electric lighting (especially at the beginning of the day and during the winter period). Importantly however, the electricity consumption for electric lighting represents a very small fraction (between 5% and 10%) of the total electricity demand (e.g. including space heating), and is in both rooms very low.

Finally, the energy demand for space heating was on average significantly lower in the *Test* room (especially in the fall season). As previously mentioned, the controller was not specifically designed to optimize the passive solar gains; nevertheless, such optimization was still reached in comparison to the *Reference* room. It is worth noting that the consumption for space heating in the two office rooms is significantly larger than that of the electric lighting: as a result, the total energy demand including both heating and lighting remains significantly lower in the *Test* room. The higher energy demand for space heating in the *Reference* room can be due to a higher room temperature. Indeed, it is possible that differences in energy consumption for space heating were due to different temperature set points (which could be modified by the users via the manual switch): as already mentioned, the participants were not instructed on the use of these switches but we can not exclude that a temperature set point was changed during the study, also accidentally or by mistake, for example when regulating the electric lighting (as the buttons are placed next to each other on the same control box). Moreover, the users were allowed to open the windows and there were no restrictions on their behaviour in this sense. However, based on knowledge from previous studies in Lausanne area, increasing the temperature set point by 1°C leads to approximately 3 to 6% increase in energy demand (see for example [Coccolo et al., 2015]). Based on our results, the temperature was on average 0.8°C higher in the *Reference* room, thus the temperature difference could explain about 2.4 to 4.8% of the extra demand. Besides, differences in space heating energy demand between the two rooms can not be explained by differences in weather conditions: as seen, there was no

significant difference in sunshine duration and there were even more sunny days and less cloudy days in the *Reference* room compared to the *Test* room.

Based on our initial hypotheses, we could confirm that the lighting strategy with the automated controller for venetian blinds and electric lighting allowed to obtain high quality lighting and visual comfort at the work place, while also obtaining encouraging results in terms of energy savings and thus supporting reduced greenhouse gas (GHG) emissions.



# 3

## Impact of light on humans

---

Chapter 3 is divided into four parts: section 3.1 summarizes the relevant background knowledge on the impact of light on health, physiology and cognition, and the following section 3.2 describes the experimental study where the automated controller for blinds and lighting (Chapter 2) was implemented and tested with office workers; the study results are reported in section 3.3 and discussed in section 3.4.

### 3.1 Background

The effects of light on humans are usually associated with vision. However, light profoundly impacts our health in different ways. As light reaches the eye, neuronal signals are conveyed not only to the primary visual cortex of the brain, but also to many other brain areas, responsible for regulation of physiology and behaviour. This phenomenon is explained in this first section, firstly introducing the process of vision and then the so called "non-visual system" by which our physiology is also influenced.

#### 3.1.1 The visual system

Vision begins when light is entering the eye and reaching the retina, a thin membrane lining the inner part of the eyeball. The retina contains various layers of light-sensitive cells, named photoreceptors, that are directly connected to the brain by the optic nerve.

Visual effects are mediated by two different types of photoreceptor cells: the roughly 120 million rods, which are activated with dim light and are responsible for night vision (*scotopic* vision), and the approximately 6 million cones, which are capable to perceive colours, brightness, contrast and responsible for daytime vision (*photopic* vision). The names "cones" and "rods" derive from their peculiar shape (Figure 3.1).

The photoreceptors capture the light information (electromagnetic radiation), which is then converted into electrochemical signals (by a process called phototransduction). These biochemical and electrical neuronal impulses are sent via the optic nerve to the primary visual cortex in the occipital part of the brain, where they are interpreted to construct physical images (Figure 3.1), and

finally, to other association cortices [Prasad & Galetta, 2011]. Each class of photoreceptor contains a specific type of photopigment molecule (rods have *rhodopsin* and cones have *photopsins*) which determines how the photoreceptor responds to light.

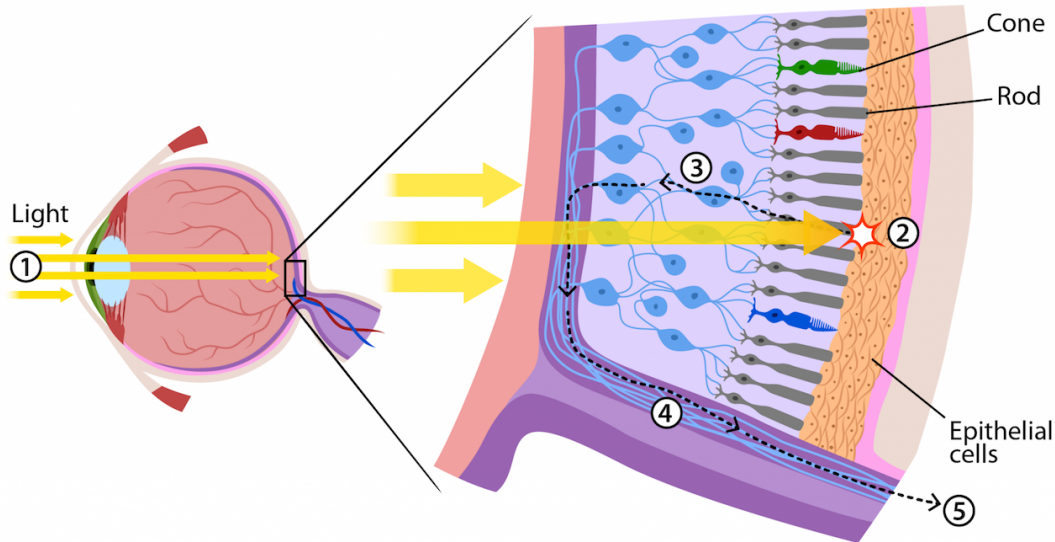


**Figure 3.1** – Simplified scheme of light detection in the retina for vision [Kazilek & Cooper, 2010]. Light entering the eye (1) reaches the photoreceptor cells layers in the retina (2), where it is transformed to electrochemical signals conveyed through specialized neurons (3) to the optic nerve (4); the optic nerve conveys the signals to the primary visual cortex in the occipital brain region through the dorsal lateral geniculate nuclei of the thalamus (5). Used with permission of ©Arizona Board of Regents [Kazilek & Cooper, 2010].

Photoreceptors differ in their sensitivity to photons (electromagnetic radiation) of different wavelengths, and the ability of a photoreceptor to respond to light depends on the type of photopigment that it contains. The spectral sensitivity function describes the relative response of photoreceptors to light as a function of wavelength. The overall spectral sensitivity of human cones,  $V(\lambda)$ , peaks at 555 nm, whereas the scotopic efficiency function  $V'(\lambda)$  is related to the rods response and peaks at 505 nm. The photopic sensitivity function (or photopic luminous efficiency)  $V(\lambda)$  is the bridge between radiometry, the measurement of radiant energy, and photometry, the measurement of light (luminous or visible energy). It was first published by the Commission Internationale de l'Eclairage (CIE) in 1926 [Commission Internationale de l'Éclairage (CIE), 1926]. The two luminous efficiency curves  $V(\lambda)$  and  $V'(\lambda)$  are illustrated in Figure 3.2. Cones can be distinguished into three categories, again depending on their specific photopigment properties: S-cones absorb light mostly at shorter wavelengths (blue part of the visible light spectrum, peaking at  $\sim 450$  nm), M-cones absorb more light in the middle wavelength range (green,  $\sim 540$  nm) and L-cones absorb longer wavelengths (red,  $\sim 570$  nm). Spectral sensitivity curves for each photoreceptor class are shown in Figure 3.3.

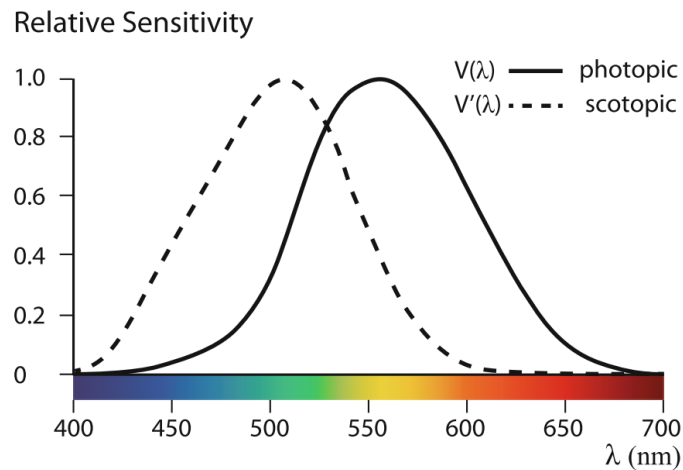


**Figure 3.2** – Standardized relative spectral sensitivity curves for photopic ( $V(\lambda)$ ) and scotopic vision ( $V'(\lambda)$ ). Used with permission: van Bommel [2019b].

### 3.1.2 The non-visual system

#### A third type of photoreceptor

Between 2001 and 2002 the presence of a novel non-rod, non-cone photoreceptor class in the mammalian retina was discovered [Berson et al., 2002; Hattar, 2002]. These photoreceptors are called "intrinsically photosensitive Retinal Ganglion Cells" (ipRGCs).

While cones and rods capture light information, process it and send it to the visual cortex via the optic nerve, the ipRGCs, which contain the photopigment *melanopsin* (a light-sensitive protein, first described in frog skin [Provencio et al., 1998], convey the light information to the *Suprachiasmatic Nucleus* (SCN), located in the hypothalamus [Gooley et al., 2003], and to many other brain regions, e.g. the olivary pretectal nuclei (OPN, pupillary light reflex) [Hattar et al., 2006]. The SCN is considered the main biological clock (see below) and is connected via neural and endocrine pathways also to brain areas responsible for hormonal secretion (such as melatonin and cortisol).

The ipRGCs have a different sensitivity to light with respect to cones and rods, as described before. The spectral sensitivity curve for ipRGCs was released by the International Lighting Committee (CIE), which defined the *melanopic* sensitivity function based on the absorption spectrum of the photopigment melanopsin [Commission Internationale de l'Éclairage (CIE), 2018]. The melanopic sensitivity curve peaks at approximately 480 nm and it is shown in Figure 3.3, together with the sensitivity curves of the other photoreceptor classes (rods and the three types of cones).

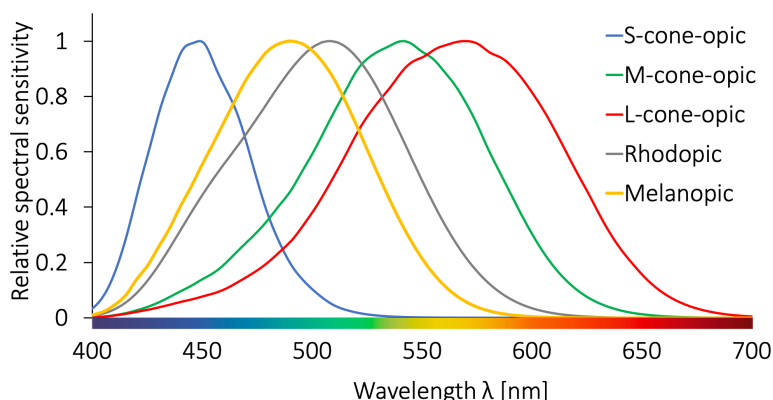


**Figure 3.3** – Relative spectral sensitivity functions of the human photoreceptors: ipRGCs (melanopic) in yellow, together with rods (rhodopic) and the three types of cones (S-cone-opic, M-cone-opic, L-cone-opic). Plotted by the author on the basis of the tabular data in the CIE publication [Commission Internationale de l'Éclairage (CIE), 2018].

### The circadian system

The ipRGCs play a fundamental role in mediating light effects on many physiological and psychological functions in humans. Figure 3.4 illustrates the two main pathways of the light signals from the eyes to different brain regions (e.g. primary visual cortex and SCN). Light signals conveyed via the retino-hypothalamic tract (in light blue), mediated by the ipRGCs, reach the SCN. Recent studies showed that the ipRGC are also receiving and integrating photic<sup>a</sup> information from rods and cones [Güler et al., 2008; Lee et al., 2019; Mure, 2021; Lucas et al., 2014].

As the core circadian pacemaker in the mammalian brain, the SCN regulates a series of endogenous biological rhythms, such as the sleep/wake cycle, core body temperature, heart rate, hormonal secretion, alertness and many other physiological functions (see e.g. [Boyce et al., 2006; Dijk & Archer, 2009]). Since these rhythms last approximately but not exactly 24 hours, they are called "circadian rhythms" (from Latin *circa*, "around" and *dies*, "day", meaning literally "approximately one day" [Halberg et al., 1959]). Circadian oscillators (or "peripheral clocks") exist in nearly all cells and tissues, e.g. in liver, muscle, kidneys, etc. These clocks need to be synchronized with each other and receive time-of-day information from the core pacemaker in the SCN [Buijs et al., 2006].

In particular, the SCN is connected via a multi-synaptic pathway to the pineal gland, responsible for the secretion of melatonin, and has efferent neuronal projections to many other regions in the brain and body, e.g. with the adrenal cortex, located on top of the kidneys, which produces cortisol. Both melatonin and cortisol secretion profiles follow a circadian rhythm.

### Circadian markers

The endogenous pacemaker, located in the SCN of the human brain, governs daily circadian rhythms throughout the body [Stephan & Zucker, 1972]. Here, the most relevant markers to indirectly

<sup>a</sup>Photic = related to light.

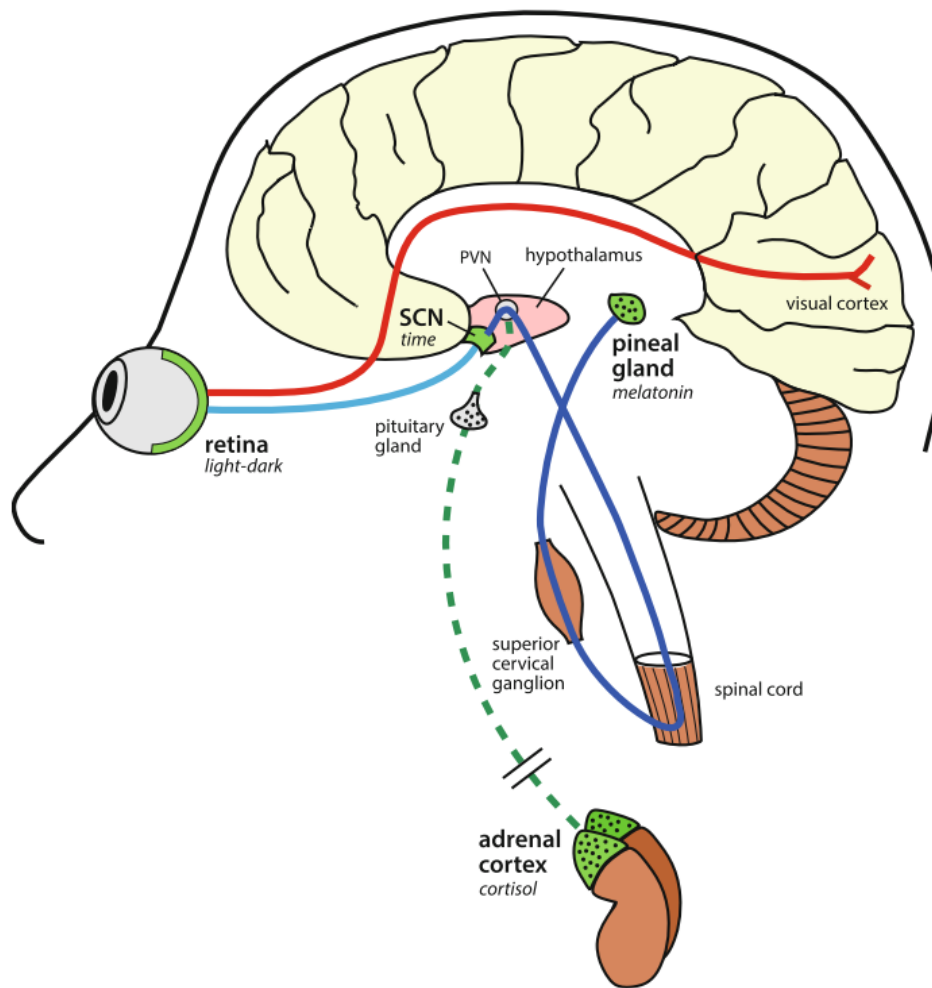


**Figure 3.4** – Two main neuronal pathways in response to light which are signalled to different brain areas: 'visual' path (red) and 'non-visual' path (cyan) to the SCN. The SCN has a multisynaptic connection to the pineal gland, responsible for the secretion of melatonin (blue), and via paraventricular nucleus (PVN) it also communicates with the adrenal cortex (dashed green line) where cortisol is produced. Reproduced from van Bommel [2019b].

measure the circadian phase are described.

### Melatonin

Melatonin is colloquially called "the hormone of darkness", because its secretion in mammals typically occurs during nighttime. In humans, this hormone tells the body that it is time to rest by facilitating sleep. Melatonin is released by the pineal gland during the night and provides the body's internal biological signal of darkness. Melatonin concentrations decrease in the morning after waking up and typically stay low during daytime. The "dim light melatonin onset" (DLMO) is defined as the time at which melatonin concentrations, measured in saliva or blood samples, reach a threshold that can be measured (e.g. 3 pg/ml [Benloucif et al., 2008]). The DLMO is considered as one of the most reliable markers of the circadian phase [Lewy & Sack, 1989; Benloucif et al., 2005]. It typically occurs 2-3 hours before the onset of sleep. In the early morning, melatonin concentration decreases,

and the time when it gets below the concentration threshold is referred to as melatonin secretion *offset* (DLMO<sub>off</sub>). The onset and the offset of melatonin secretion represent the beginning and the end of the biological night, respectively [Wehr et al., 2001].

### Cortisol

Cortisol is secreted in the adrenal cortex, located on top of both kidneys. In general, its function is to mediate stress responses in the body and some metabolic and inflammatory responses as well as immune functions [Oakley & Cidlowski, 2013]. Endogenous cortisol concentrations peak in the morning around wake time, generating the Cortisol Awakening Response (CAR). In the course of the day, cortisol concentrations decrease to reach a minimum shortly before bedtime. Compared to melatonin, cortisol is more sensitive to external factors (e.g. physical and physiological activity, stress), thus it is usually considered a less strong or stable circadian phase marker when compared to the DLMO, even though both hormones can be suppressed by light exposure (see section 3.1.4).

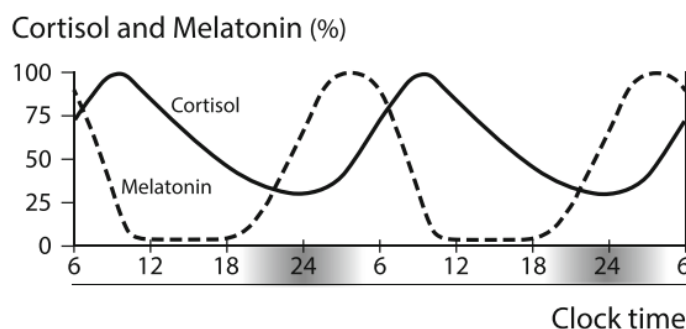


**Figure 3.5** – Qualitative representation of daily rhythms of melatonin and cortisol secretion in humans, shown on a 2-day scale. Reproduced from van Bommel [2019a].

### Core Body Temperature

The regulation of Core Body Temperature (CBT) is also modulated by the endogenous circadian clock [Aschoff, 1982; Moore & Danchenko, 2002]. The circadian rhythm of CBT exhibits a peak in the late afternoon and a minimum (nadir) during the biological night, 2-3 hours before habitual wake time [Refinetti, 2010; Aschoff, 1982; Aschoff & Heise, 1972], as shown schematically in Figure 3.6. There is a strong interconnection between melatonin secretion in the evening and peripheral heat loss via hands and feet which precedes the CBT decline in preparation for nocturnal sleep [Kräuchi, 2002]. Such thermoregulatory modulation can be determined by the distal-proximal skin temperature gradient (DPG) [Kräuchi et al., 2000]. The DPG is the difference between skin temperatures at distal (or peripheral) regions (e.g. hands and feet) and skin temperature at proximal regions (e.g. the chest). Kräuchi et al. [2000] showed that the DPG is a strong predictor of sleep-onset latency, and in particular a rapid sleep onset is favoured by peripheral vasodilatation (hence heat loss) in distal skin regions like hands and feet.

The melatonin secretion onset in the evening has a crucial role in thermoregulatory processes in

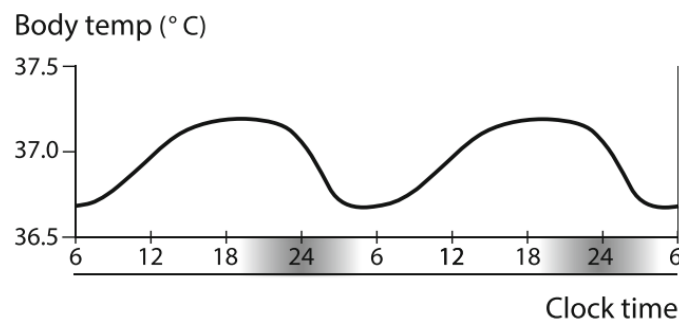


**Figure 3.6** – Daily circadian rhythm of core body temperature shown on a double-plotted (2-day) scale. Reproduced from van Bommel [2019a].

humans, by enabling peripheral heat loss and a decrease of core body temperature, which results in a rise of DPG [Cajochen et al., 2003; Kräuchi et al., 2000]. This process altogether has sleep promoting effects. In other words, sleep onset is promoted by melatonin secretion because the CBT decrease in the evening is facilitated by peripheral heat loss [Kräuchi et al., 1997; Van Someren, 2000].

### Alertness and cognitive performance

Another physiological function which exhibits a circadian oscillation and depends on the circadian pacemaker is alertness. Since alertness is linked to the sleep/wake cycle, its oscillations have always been related to the time of day. But sleepiness (the 'opposite' of alertness) directly derives from the build-up of sleep propensity, which increases with elapsed time awake and is therefore also homeostatically regulated [Borbély, 1982; Cajochen et al., 2004]. Circadian modulation of alertness, cognitive performance and core body temperature show a minimum around the same time of day which is 1-2 hours before habitual waketime [Wright et al., 2003].

Subjective evaluation of the level of sleepiness/alertness is generally done by applying validated scales, such as the Karolinska Sleepiness Scale (KSS) [Åkerstedt & Gillberg, 1990] or the Visual Analogue Scale (VAS) for sleepiness [Monk, 1989]. These subjective assessment methods have been shown to give reliable results and are correlated with objective measures of sleepiness such as slower frequencies of neuronal oscillations in the Electroencephalogram (EEG) or Slow Eye Movements (SEMs) during extended wakefulness. Studies showed that higher sleepiness is paralleled by an increase in SEMs activity [Cajochen et al., 2000; Finelli et al., 2001; Marzano et al., 2007].

In field studies, a widely used assessment method as a proxy for objective alertness or sustained attention is also the Psychomotor Vigilance Task (PVT) [Dinges & Powell, 1985], a simple computer-based reaction time test in which the user has to respond to visual or auditory stimuli as fast as possible. It is named "psycho-motor" because it involves both brain and movement. This test is used also in the study presented in this thesis (see section 3.2). The other cognitive test method used here is the *N-Back* task [Kirchner, 1958]. This is a test for short-term working memory capacity,

which implies a higher load on cognitive functions. During the test, a series of visual or auditory stimuli (letters) are presented, and the user is asked to indicate for each letter whether it matches a letter  $n$  trials before or not. For example, in the 2-back task, the user must decide whether the current letter is the same as the second-last letter he/she heard. The detailed test procedure is explained in section 3.2.

### 3.1.3 Circadian entrainment

During evolution, mammals - including humans - developed circadian clocks as an adaptive response to environmental 24-h light dark cycles that results from the Earth's rotation around its axis and around the sun.

Without any external stimuli, the intrinsic period of the endogenous circadian pacemaker is slightly longer than 24 hours. In the early 1960s the first experiments were carried-out to get to know the behaviour of the internal clock in the absence of external stimuli such as the light/dark cycle [Aschoff, 1965] and without knowledge of external clock time. It was found that humans, as other animals, still show regular patterns of sleep and wakefulness, body temperature and other functions; however, without any time cue, these "free-running circadian rhythms" in humans had a period length closer to 25 hours [Aschoff & Wever, 1962; Wever, 1979]. Later, Czeisler and colleagues applied a forced desynchrony protocol (a 28-hour sleep/wake cycle) on human subjects and found that the intrinsic period of the human circadian pacemaker was on average 24.2 hours [Czeisler et al., 1999].

External time cues (or *Zeitgebers* in German) are necessary to entrain the circadian pacemaker (and in turn the circadian rhythms) to the exact 24 hours of the environmental time. Indeed, thanks to these time cues, the biological clocks can reset every day by synchronizing the endogenous period length with the solar 24-h day. For mammals, one of the strongest Zeitgeber is the natural light-dark cycle [Lockley, 2009; Roenneberg et al., 2013], and especially bright light in the morning [Rosenthal et al., 1990]. Other examples of time cues for the human circadian system are exercise, social activity, alarm clocks, and food intake [Stephan, 2002; Tahara et al., 2017; Lewis et al., 2018].

The relationship between internal (biological) time and environmental time is called *phase angle of entrainment*. It can be defined as the time range between a marker of the internal biological time (i.e., the onset of melatonin secretion in dim light - the DLMO - in the evening) and for example sleep onset time. A stable phase angle of entrainment denotes an appropriate synchronisation of the circadian clock to the 24-hour dark/light cycle [Duffy & Wright Jr., 2005; Wright et al., 2005].

### Circadian misalignment

Desynchronization of the circadian clock – also called "circadian misalignment" or "circadian disruption" - occurs when the endogenous pacemaker is not in sync with the 24-hour environmental



time and/or with the human behaviour (i.e., activities and sleep). This mismatch occurs for example in night-shift workers, or when bed- and wake time strongly vary between work days and free days (typically named also "social jet-lag" [Wittmann et al., 2006]).

In the modern society, we spend most of our time indoors, where lighting levels are significantly reduced with respect to those experienced by pre-industrialized societies, when daytime was mostly spent outdoors under natural light conditions (see Figure 3.7, reproduced from Skeldon et al. [2017]). In addition, it is very common to extend light exposure time in the evening by using electric light.

In a recent publication, Skeldon et al. [2017] analysed the phenomenon of social jet-lag. The authors illustrate the circadian sleep-wake cycle which is regulated by two main processes (this 2-process model was introduced for the first time by Borbély [1982]): the rhythms of circadian wake propensity (C-WP) and the homeostatic sleep propensity (H-SP). Normally, wake propensity is high during the day and low during the night, whereas sleep propensity increases during wakefulness and dissipates during sleep. In Figure 3.7, these two processes are shown in the absence/presence of evening light in black/red respectively. The graph clearly shows that the typical modern light exposure (with electric light in the evening) causes a phase-delay in the circadian sleep/wake timing, which results in a later sleep onset. Social constraints (e.g. work or school) force us to wake up early, when sleep propensity is still high and wake propensity is low. On free days (e.g. during the weekend), we tend to sleep longer in the morning to recover the 'sleep debt', but the following week the pattern is very likely repeated.

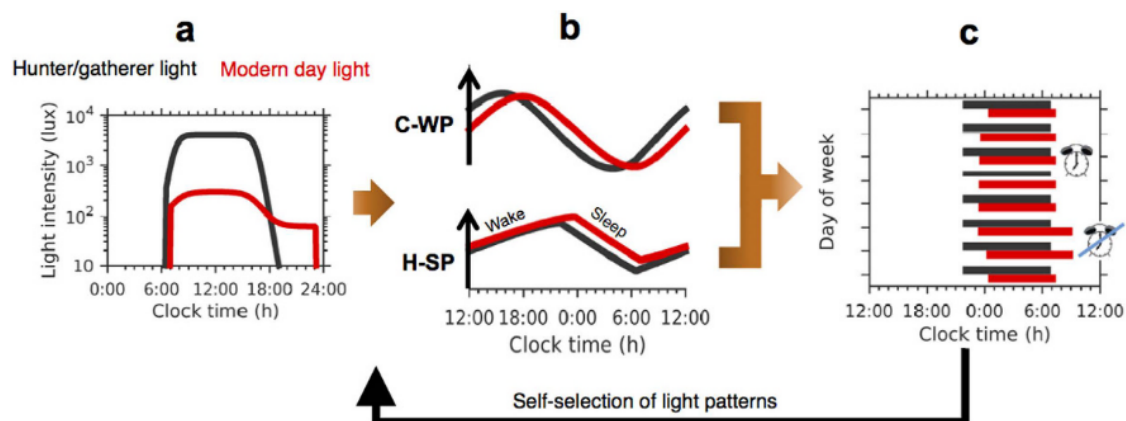


**Figure 3.7** – Reproduced from [Skeldon et al., 2017] (schematic diagram of the impact of ancestral versus modern day light exposure and social constraints on sleep patterns). A) typical light exposure pattern in pre-industrialized societies (black) and in modern societies; b) circadian wake-propensity (C-WP) and homeostatic sleep propensity (H-SP) in the absence/presence of electric light in the evening, shown in black/red respectively; c) sleep patterns in the two situations: in modern society, sleep timing is irregular, and in the absence of social constraints (indicated by alarm clock), wake-up times are shifted later.

The same study, by applying a mathematical model, found that the phase-delaying effect of evening light is reduced when daytime light exposure levels are higher, and that teenagers tend to be particularly sensitive to the impact of evening light. Several recent studies found that the common use of bright screens and other light sources in the evening, which has become a diffuse habit among

teenagers and adults, leads to circadian phase delays and late sleep timing [Tähhämö et al., 2019; Chang et al., 2015; Chellappa et al., 2013; Green et al., 2017; Cajochen et al., 2011]. This may reinforce existing circadian rhythm disorders, or even trigger their manifestation. Moreover, low lighting levels during the day exacerbate non-visual responses to light in the evening, e.g. on circadian phase shift, melatonin suppression and alertness [Hébert et al., 2002; Chang et al., 2011, 2013; Smith et al., 2004; Münch et al., 2017], even though these evening light levels are not necessarily very bright.

Circadian misalignment has negative consequences on brain and body functions, such as sleep disorders, depression, heart diseases, and cancer [Stevens & Rea, 2001; Wirz-Justice et al., 2009; Boyce, 2010; Abbott et al., 2020; Walker et al., 2020]. Circadian misalignment often occurs in night-shift workers, whose habitual schedules and lifestyles are out of phase with the normal day-night rhythm of wakefulness and sleep. Negative health effects and medical consequences are often evident in these individuals, who have an increased risk for: gastrointestinal disorders, cardiovascular disease, chronic sleep deprivation, cancer (e.g. breast cancer) and depression [Moore-Ede et al., 1982; Hansen & Stevens, 2011; Morris et al., 2016; Chellappa et al., 2019; Lee et al., 2017].

#### Light exposure for circadian entrainment

Despite recent recommendations for lighting [Brown et al., 2020; Stefani & Cajochen, 2021; Vetter et al., 2019], it still remains to be elucidated, how much light is needed for optimal synchronization and stable entrainment of the circadian clock(s) with the 24-hour day, especially at the individual level and under daily life conditions.

Rather few studies were done in naturalistic, real-life settings [Wright et al., 2013; Wams et al., 2017; Christensen et al., 2020; Kozaki et al., 2012; Vetter et al., 2011]. Among those, Wright and colleagues conducted a study with only daylight exposure and lighting from fireplaces while camping [Wright et al., 2013]. They compared the results of melatonin secretion patterns and sleep timing of the same study participants when they were living and working in their habitual indoor environments, with less light during the day and additional electric light in the evening (Figure 3.8 shows the average light exposure pattern in the two conditions during their study) [Wright et al., 2013].

The authors found that exposure to natural light during the day led to a circadian phase-advance of the onset of melatonin secretion in the evening of about 2 hours, which was more pronounced in later than earlier chronotypes<sup>b</sup>. Living under natural light conditions also prolonged the phase angle of entrainment by 49 minutes [Wright et al., 2013] (see supplement). This suggests that exposure to the natural light/dark cycle, i.e., with more sunlight and no (or limited) electric light in the evening, may support proper entrainment of the circadian clock and reduce the negative health consequences of circadian disruption. For instance, it can help to advance the sleep timing for persons with delayed sleep phase syndrome.

---

<sup>b</sup>The chronotype is an indication of an individual's preferred timing of sleep and activity [Roenneberg et al., 2003]

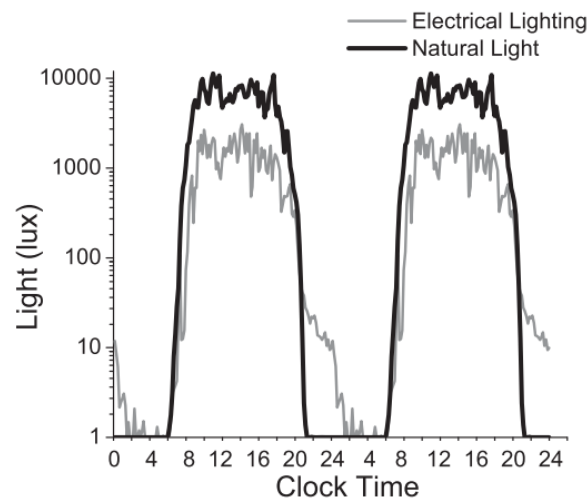


**Figure 3.8** – Reproduced from [Wright et al., 2013]: averaged light exposure (on a log-scale) for study participants during the week of natural light/dark exposure while camping (black line) and during the week in the built environment with electric lighting (grey line).

### 3.1.4 Non-visual effects of light

Light elicits a series of non-visual effects in both humans and animals, by influencing brain and body processes in different ways. For instance, in healthy humans, exposure to light during the night causes alerting effects (non-visual responses) which also correlate with the degree of melatonin suppression [Cajochen et al., 2000], but these effects are present also when melatonin levels are low, i.e., during daytime [Vandewalle et al., 2006; Phipps-Nelson et al., 2003; Rüger et al., 2006; Cajochen et al., 2019]. Exposure to light in the evening/night both shifts the timing of the circadian rhythm of melatonin secretion and acutely suppresses melatonin secretion [Lewy et al., 1980; Czeisler et al., 1986].

#### Properties of light influencing non-visual responses

The entity of the non-visual effects of light on humans depends on several properties of light exposure, such as illuminance, timing, spectrum, prior light history and duration, as explained in the next paragraphs. All of these factors contribute to the acute light effects as well as to the phase resetting effects of light on the circadian clock, although their interactions have not been fully revealed and understood [Prayag et al., 2019; Münch et al., 2017; Aarts et al., 2017; Münch et al., 2020].

#### Illuminance

Bright light exposure has a major effect in term of non-visual responses as compared with dim light. In the last decades, several studies attempted to establish the relationship between illuminance and non-visual responses (such as melatonin suppression and phase shift, objective and subjective assessments of alertness). In particular, Zeitzer [2000], Cajochen et al. [2000] and McIntyre &

Norman [1989] demonstrated that there is a non-linear relationship between photopic illuminance (in lux) and the percentage of melatonin suppression. Daytime bright light was found to increase the nocturnal melatonin peak [Mishima et al., 2001; Takasu et al., 2006]. Many other studies found beneficial effects of bright light on alertness and cognition when compared to dim light, both during day and night time [Phipps-Nelson et al., 2003; Rüger & Gordijn, 2005; Smolders et al., 2012; Cajochen et al., 2014]. Furthermore, higher lighting levels during the day can improve sleep: some recent studies found a positive correlation between light exposure levels during daytime and sleep duration and quality, assessed both objectively and subjectively [Hubalek et al., 2010; Wams et al., 2017; Boubekri et al., 2020] and also objectively deeper sleep after brighter daytime light [Cajochen et al., 2019].

Regarding the impact of bright light on acute suppression and circadian phase resetting of cortisol, Jung and colleagues showed that a prolonged bright light exposure in the morning (i.e., when cortisol levels are high) *reduced* cortisol concentrations compared to dim light exposure [Jung et al., 2010]. The results were obtained when exposing subjects to polychromatic white light at ~10'000 photopic lux for 6.7 hours, during the night before habitual wake-up time (i.e., on the rising portion of the cortisol secretion curve) and immediately after wake-up time (descending portion). Other studies found that one hour of exposure to 800 lux in the early morning increased the cortisol peak [Scheer & Buijs, 1999], and that the transition from dim to bright light in the morning acutely elevates cortisol levels by 50% [Leproult et al., 2001].

#### Timing of light exposure

Timing of light exposure is certainly one of the most important factors in resetting the circadian clock. Depending on the time of day (relative to the endogenous circadian phase) at which light is administered, exposure to light can cause a phase-shift of the circadian system. In simple words, a circadian phase shift means that the timing of circadian phase markers, (used as proxy for the endogenous circadian pacemaker in the SCN), such as melatonin secretion, sleep/wake cycles, CBT, etc. will move to an earlier time (= *phase-advance*) or to a later time (= *phase-delay*) depending on the timing of light exposure. Ocular exposure to light stimuli in the early night can phase-delay the circadian clock, whereas in the early morning, light exposure causes a phase-advance. The relationship between the timing of a light stimulus and the direction and magnitude of the resultant phase shift is described in the phase-response curve (PRC, Figure 3.9, [Khalsa et al., 2003]). Specifically, the PRC refers to a light stimulus of 10'000 lux (for 6.7 hours), and phase advances (= positive values) and delays (= negative values) are plotted relative to the core body temperature minimum, that normally occurs in the early biological morning. This shows that exposure to bright light shifts the phase of CBT in a circadian phase-dependent manner.

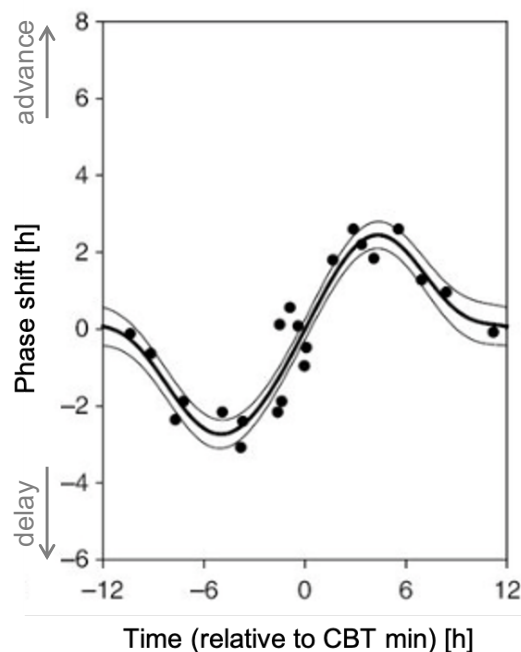


**Figure 3.9** – Reproduced from Beersma et al. [2009] (adapted from original: [Khalsa et al., 2003]): Phase-Response Curve (PRC) to a bright light stimulus of 10000 lux. Phase advances (positive values) and delays (negative values) are plotted relative to the core body temperature minimum (the 0 of the x-axis), which normally occurs in the early morning. The thicker solid line represents the best fitting function to the data, and the other two lines represent an additional shift of  $3 \times 0.18$  h starting from the main curve, to make it compatible with other findings (for example [Czeisler et al., 1999], see [Beersma et al., 2009]).

In humans, light has always a phase shifting effect: it was shown for example that exposure to bright light (5'000 photopic lux) at midday for three consecutive days led to a phase advance of the melatonin secretion onset [Hashimoto et al., 1997]. On the other hand, bright light in the evening delays the phase of the circadian clock [Gronfier et al., 2004; Lewy et al., 1980; Brainard et al., 1988]. Also the circadian phase of cortisol was found to be advanced by bright light in the morning [Rea et al., 2012; Dijk et al., 2012].

### Spectral composition

The maximum spectral sensitivity of the ipRGCs is in the shorter wavelength portion of the visible light spectrum (see section 3.1.2), which suggests that exposure to light with high melanopic illuminance is more likely to causes stronger non-visual responses such as melatonin suppression, circadian phase shifting, alertness, emotions, cognitive performance and sleep [Brainard et al., 2001; Thapan et al., 2001; Lockley et al., 2003; Cajochen et al., 2005; Santhi et al., 2012; Münch et al., 2006; Nowozin et al., 2017; de Zeeuw et al., 2019; Blume et al., 2019].

Lockley et al. [2003] found a greater circadian phase-shifting effect and melatonin suppression with monochromatic blue light at 460 nm than with green light in the medium wavelengths (555 nm) in humans, which was confirmed by Revell et al. [2005] who obtained similar results when comparing short wavelengths monochromatic light pulses with long wavelength (600 nm). Exposure

to such wavelengths at the same photon density resulted in greater effects on subjective alertness, thermoregulation, heart rate and sleep with blue than with green light [Lockley, 2009; Cajochen et al., 2005; Münch et al., 2006].

#### **Exposure duration/pattern**

Light exposure can be very short or discontinuous to elicit non-visual responses. Experimental studies have demonstrated that shorter but more frequent light exposure over time impact the non-visual system even more effectively than a continuous stimulus, indicating that brief episodes of light exposure (even ultra-short light stimuli) may be a cost- and time-effective way of resetting the circadian timing system in humans [Gronfier et al., 2004; Zeitzer et al., 2014]. Chang et al. [2012] demonstrated that there is a non-linear relationship between the duration of light exposure and the human non-visual response (duration-response curve, DRC). Both melatonin suppression and phase delay increased with light exposure duration, but not linearly: the curve was steeper at the beginning of light exposure, but after a certain duration the curve tended to flatten indicating that the response did not change significantly anymore. Also Dewan et al. [2011] studied the impact of different light exposure durations on the melatonin rhythm and found that increasing the duration from 1 h to 3 h, at a fixed illuminance between 2'000 and 8'000 lux, increased the magnitude of phase delays, while increasing the light intensity (within the mentioned range) did not have such impact.

#### **Prior light history**

Since non-visual photoreceptors seem to integrate the light information over time, prior photic history is important in determining the magnitude of any upcoming response to light. Experimental findings showed that prior exposure to dim light amplifies the suppression of melatonin with respect to brighter light history [Hébert et al., 2002; Smith et al., 2004; Chang et al., 2011]. The acute and circadian response to light also depends on prior light exposure qualities. Other studies suggest that cone photoreceptors contribute substantially to non-visual responses at the onset of a light exposure and at low irradiances, whereas ipRGCs may be the primary photoreceptors mediating the response to long-duration light exposure and at high irradiances [Gooley et al., 2010]. Münch et al. [2012] compared two realistic office lighting conditions in the afternoon and tested hormonal concentrations and performance in the evening. They found significant improvements in both alertness and cognitive performance (in N-Back tasks) after spending the afternoon in brighter light (including daylight) than illuminance provided by 'normal' electric room light. One last aspect contributes to all of the aforementioned effects which is inter-individual differences in light sensitivity (see e.g. [Chellappa, 2021] for a recent review).

#### Effects of light on alertness, cognition and mood during daytime

The alerting effect of light during nighttime is linked to the suppression of melatonin. However, during daytime, when melatonin levels are negligible, it was found that light exposure can still enhance alertness [Phipps-Nelson et al., 2003; Rüger et al., 2006; de Zeeuw et al., 2019; Cajochen et al., 2019], suggesting that the alerting effect of light is not necessarily linked to melatonin suppression, even though this was not shown in all studies (see review by [Lok et al., 2018; Souman et al., 2018]). Effects of light on alertness and performance during daytime occur through two processes: a "circadian" process (i.e., by influencing the circadian rhythms, sleep/wake regulation and body temperature on the next day), and a "direct" or "acute" process (which is a short term effect, e.g. acute melatonin suppression, pupillary reflex (reviewed in [Cajochen, 2007; Lockley, 2009; Chellappa et al., 2011])).

Phipps-Nelson et al. [2003] showed that exposure to 1000 lux from 12:00 to 17:00, compared to dim light ( $< 5$  lux) significantly decreased sleepiness (assessed both subjectively and objectively by measuring slow eye movements in the waking EEG) and improved performance in the PVT. Similarly, Rüger & Gordijn [2005] showed that a bright light stimulus ( $\sim 5000$  lux) from 12:00 to 16:00 reduced subjective sleepiness without causing any change in melatonin level (while the same stimulus given in the night time contributed to suppress melatonin).

Smolders et al. [2012] carried-out a laboratory study simulating an office environment, comparing two different lighting conditions: 1000 lux vs. 200 lux at the eye level, with a fixed CCT of 4000 K, either in the morning or in the afternoon. They found that the higher illuminance significantly improves subjective alertness in both morning and afternoon. Performance in PVT was improved by brighter light only in the morning, but not in the afternoon.

A recent literature review by Souman et al. [2018] stated that many (but not all) studies failed to find a significant effect of bright polychromatic light on alertness and cognitive performance during daytime.

Huiberts et al. [2015] examined the effects of illuminance levels on working memory assessed with n-Back tests of different difficulty levels, and found that higher lighting levels improved performance more significantly on the easier than the more difficult tasks. Besides, the time of day plays a role: this study, together with others mentioned previously, suggests that bright light effects on cognitive performance are stronger in the morning than in the afternoon.

The spectrum of light also plays a role in its impact on alertness such that light exposure to light with high melanopic irradiance induced objectively greater levels of alertness as assessed in the waking EEG [de Zeeuw et al., 2019]. The impact of the light spectrum on performance was found after a 2-hours exposure to a light source with high CCT (2500 K) led to better sustained attention (assessed with PVT and GO/NoGo task) [Chellappa et al., 2011].

Light also has positive effects on mood. In a field study with office employees, bright light helped to alleviate distress and improve mood, especially in winter when natural light levels are lower

[Partonen & Lönnqvist, 2000]. Furthermore, bright light has beneficial effects on emotions and helps to improve the quality of life in people affected by dementia [Burns et al., 2009; Münch et al., 2017; Sekiguchi et al., 2017]. Light therapy (even greater daylight exposures [Wirz-Justice et al., 1996]) has been shown to be an effective treatment for depression and other psychiatric disorders [Wirz-Justice et al., 2009] [Rosenthal et al., 1984; Wirz-Justice et al., 2005; Terman & Terman, 2005; Pail et al., 2011].

### 3.1.5 Experimental studies with dynamic office lighting

Early studies tried to improve office lighting in the field by providing greater portions of shorter wavelengths of light (blue-enriched lighting) during daytime to increase non-visual effects in office workers. Viola et al. for example showed that 4 weeks of blue-enriched office lighting (17'000 K) significantly improved subjective alertness, mood, performance and sleep quality [Viola et al., 2008].

The current standard legislation does not express any exact requirement for office lighting protocols aimed at optimising non-visual effects of light (e.g. to improve cognitive performance, alertness, mood, etc.). In other words, non-visual effects have not been considered yet by standard regulations for lighting in offices.

In 2003 the Light and Health Committee of the Dutch Lighting Society (NSVV) defined for the first time lighting recommendations that consider both visual and non-visual requirements, as reported by Aries [2005]. Regarding non-visual demands, the Committee recommended an illuminance of 1000-1500 lux on the vertical plane, but not all day. A dynamic lighting pattern was proposed, where both illuminance and CCT vary throughout the day. A "dynamic light dosage" means a high level of illuminance and CCT in the morning to support wake-up, then a decrease to the standard level, and again a high level to prevent or compensate the post-lunch-dip [Van den Beld, 2003; NSVV, 2003]. In winter, it is suggested to increase the lighting level again after 15:00 to prevent tiredness.

A similar protocol was proposed some years later by de Kort & Smolders [2010], based on the preferences of office workers for overcast days in winter [Begemann et al., 1997] and aimed at stimulating workers' productivity, helping to reduce tiredness and facilitate relaxation around lunch time and towards the evening. Similar to the protocol reported by Aries, this one offers a higher illuminance and higher CCT in the morning and after lunchtime (700 lux, 4700 K measured horizontally at the desk), and lower illuminance and 'warmer' (i.e., lower CCT) white light during the late morning and afternoon (500 lux, 3000 K). The results of this study reported no statistically significant beneficial effect on alertness and performance with respect to a static lighting system, but subjects were more satisfied with the dynamic lighting condition.

Recently, Zhang et al. [2020] carried-out a study in office rooms, where they compared static lighting with dynamic lighting conditions (i.e., both illuminance and CCT) aiming at investigating their impact on well-being, mood and productivity. They found that the dynamic lighting scenario



could significantly enhance afternoon sleepiness and also mood. Their findings suggest that dynamic lighting can be effective in reducing the feelings of sleepiness in the second half of the working day.

In another recent study, Stefani and colleagues compared a dynamic LED lighting scenario (iboth illuminance and CCT) with static lighting across a 16-hour waking day in healthy men in a laboratory setting, with the aim of investigating rhythms of melatonin and sleep, sleepiness and cognitive performance [Cajochen et al., 2019; Stefani et al., 2021]. After the day under dynamic lighting conditions, the participants reported lower vigilance in the evening, had an earlier and faster rise in melatonin concentrations, and their sleep latency was shorter, with respect to the evening after exposure to the static polychromatic white light.

### 3.1.6 Hypotheses

Daily exposure to light is crucial for the entrainment of the circadian clock to the 24-hour light/dark cycle. The timing, quantity and quality of light exposure have altogether the potential to influence our health, physiology, well-being and cognitive performance in several ways. For office workers, better health and well-being translates to higher productivity and performance at work.

The strategy with the advanced daylighting room design and a daylight-responsive automated controller for blinds and electric lighting (see Chapter 2) was aimed at providing optimized lighting conditions during office hours. In the experimental study with human participants, we wanted to test this strategy and compare it to a *Reference* room with no automated control and lower daylight influx.

The first aim was to investigate the effects of this strategy during daytime working hours over several days on the circadian phase of salivary melatonin onset, body temperature and cortisol concentrations in healthy young participants.

The second aim was to examine the impact of such automated office lighting control on cognitive performance, mental effort and subjective assessments of sleepiness and mood, as well as subjective comfort (specifically visual and thermal comfort).

Compared to a reference condition with manual control of blinds and electric lighting and lower daylight influx (*Reference* room), the advanced daylighting room design and daylight-responsive controller in the *Test* room was expected to:

- enable high daytime illuminance (at all weather conditions) with phase advancing effects, e.g. on melatonin secretion, cortisol and skin temperature when working for 5 days in the experimental laboratory and otherwise living under habitual home lighting conditions;
- improve or maintain a good cognitive performance, prevent subjective sleepiness and maintain a high mood, as well as good visual and thermal comfort during the days in the office.

### 3.2 Experimental study with young participants

This section describes the semi-naturalistic experimental study with 34 young and healthy participants which took place in two rooms at the LESO experimental building (EPFL) between September 2018 and December 2019. One of the two rooms was provided with the automated control system for venetian blinds and electric lighting (see Chapter 2).

#### 3.2.1 Screening procedure and participants

Potential participants were recruited by flyers at EPFL and UNIL and via online platforms for students (job offer websites). The applicants had to complete a general entry questionnaire and four screening questionnaires (in French): the Munich ChronoType Questionnaire (MCTQ, Roenneberg et al. [2003]) and the Horne-Östberg questionnaire (HO, Horne & Ostberg [1976]) to assess morning-evening types; the Epworth Sleepiness Scale (ESS, Johns [1991]) to score for daytime sleepiness; the Pittsburgh Sleep Quality Index (PSQI, Buysse et al. [1989]) to assess habitual sleep quality. Inclusion criteria were:

- intermediate chronotypes (MCTQ  $> 2.9$  and  $< 5$ ; HO  $> 30$  and  $< 70$ )
- no excessive daytime sleepiness (ESS score  $\leq 10$ )
- normal sleep quality (PSQI  $\leq 5$ )
- age between 19 and 30 years
- non-smokers
- being in good health, not suffering of any psychiatric or medical disease and not using any medications or drugs except for oral contraceptives
- no shift work and no travel across time-zones in the three months prior to the study

The target was to include 34 participants (based on precedent sample size estimation). Out of 138 completed screening questionnaires, the selected 34 participants were 18 females and 16 males, aged  $23.4 \pm 2.7$  years (mean  $\pm$  standard deviation, SD). Table 3.1 summarises the mean scores of the four screening questionnaires. Most of the participants (26) were students. A remuneration of 400 Swiss Francs was attributed to each participant who completed the entire study.

Due to technical issues with the control system during 5 sessions, the data for 3 participants in the *Test* room had to be excluded from analysis, and 2 participants repeated the session in the *Test* room. Hence, data of 31 participants for the *Test* room and 34 participants for the *Reference* room were included in the final analysis.

### 3.2. Experimental study with young participants

	AGE	MCTQ	PSQI	HO	ESS
<b>Mean</b>	23.4	4.51	3.62	53.85	5.74
<b>SD</b>	3.2	0.72	1.30	6.79	2.64

**Table 3.1** – Scores of the screening questionnaires ( $n = 34$ ; mean and standard deviation, SD). Age is shown in years; for the MCTQ the MSFsc (corrected for sleep duration on free days) was used.

#### 3.2.2 Study protocol

Before the study, each eligible participant took part in a first face-to-face meeting with the investigator (MB), where the protocol was thoroughly explained and detailed instructions were provided. All participants gave written informed consent and the study was approved by the local ethical review board *Commission Cantonale d'éthique de la recherche sur l'être humain* (CER-VD, Lausanne; project n. 2018-00642).

The 4-weeks study protocol is illustrated in Figure 3.10. Seven days prior to starting the study in the laboratory, participants were asked to maintain regular habitual bed- and wake times at home (within a self-selected target time and a range of  $\pm 30$  minutes) and do keep these times for the entire duration of the study (i.e., 4 weeks). Compliance was controlled by activity monitors (see below) and sleep logs. Participants were asked to consume alcohol, caffeine and chocolate with moderation and not to take any medication. The protocol is summarized on Figure 3.10:

- **Week 1**

The participant was at home and followed his/her habitual daily life routines. He/she had to keep regular bed- and wake times, but the daily schedules were otherwise free.

- **Week 2**

The participant spent 5 consecutive days (generally from Monday to Friday) for 8 hours in one of the two experimental office rooms (*Test room* or *Reference room*);

- **Week 3**

Week 3 was identical to week 1 in terms of study procedures. For some participants, the time span between the weeks spent in one of the two rooms (i.e., week 2 and 4) was longer than one week (on average 17 days);

- **Week 4**

Week 4 was identical to week 2 in terms of study procedures, except that participants were in the *Test* or the *Reference* room in a counter-balanced order which was randomized prior the study for each participant.

For the entire study duration, participants were asked to wear an activity monitor *ActTrust* (Condor Instruments, São Paulo, Brasil) which had to be worn on the wrist of the non-dominant hand (Figure 3.13). In addition, they had to daily note their bed- and wake times (sleep log) by means of an application on the smartphone (QuestionPro Inc, OR, USA) or on paper.

During weeks 2 and 4 participants spent five consecutive days, 8 hours per day, in one of the office rooms in the LESO building. The protocol of a typical day in the office is illustrated in Figure 3.10. Participants arrived at LESO in the morning approximately one hour after their habitual wake time. Time of arrival in the office ranged from 8:00 to 9:30, depending on the habitual wake times. Subjective assessments and cognitive tests were repeated several times during the day (see more details in the next sections). The lunch break was required to be one hour long, starting 4 hours after arrival in the office. During the break participants were allowed to leave the building. A short mid-morning and mid-afternoon break inside the building were also scheduled, and some snacks were provided. Nine hours after arrival, the participants left the office.

### 3.2.3 Study measures

#### Lighting conditions in the two office rooms

The assessment of vertical illuminance ( $E_v$ , photopic lux) as well as spectral measurements (needed to calculate melanopic Equivalent Daylight Illuminance) was carried out throughout the study during scheduled office hours in weeks 2 and 4. These lighting measurements were performed with the HDR vision sensor (VIP) and spectrometer, which were installed next to the desk at the approximate eye level of a sitting person, as already described in section 2.2.2.

#### Individual light exposure (illuminance) at the eye

During weeks 2 and 4, participants were required to wear a photometric sensor mounted on glasses, in order to have a continuous assessment of their individual light exposures during their wake phases in the laboratory and at home. The light sensor 'Luxblick' was used, provided by Prof. C. Schierz, TU Ilmenau, Germany and validated by Hubalek [2007] (for specifications of the device see also Wolf [2009]). Participants were asked to wear the light sensor during the entire day, from the time when they woke up to bedtime (i.e., approximately 16 hours), except during sport activities, shower, etc. The device records photopic illuminance (in lux) at a resolution of 1 Hz. After the recordings, data was downloaded to a PC and was averaged into hourly bins per condition. The device has an upper detection limit around 45000 photopic lux (confirmed by Dr. S. Wolf, TU Ilmenau, Germany, by written communication). Data above such threshold and data collected when the device was removed (e.g., for shower or sport activities) and during the night were manually excluded prior to the analysis.

In order to determine the amount and the timing of the total "light dose" received, the accumulated individual  $E_v$  across the waking period was computed for each participant (from the average of 5 days) and for both conditions separately. A non-linear curve fitting was applied. The time at which the accumulation curve reached its half maximum (EC50) was calculated on the individual profiles

### 3.2. Experimental study with young participants

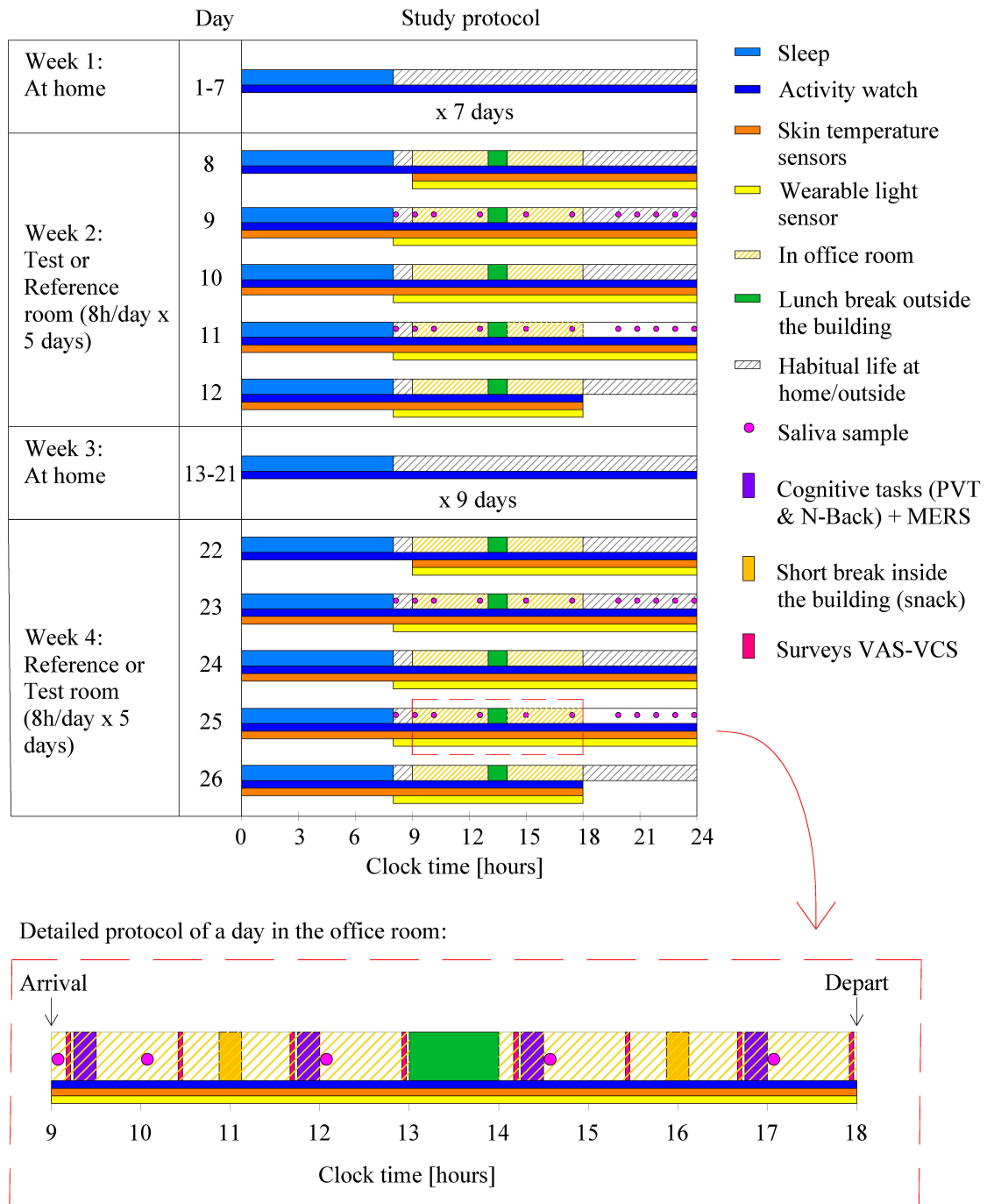


**Figure 3.10** – Overview of the 4-week study protocol: example for a participant with habitual wake time at 8:00. In the dashed red rectangle below: protocol of a typical day in the laboratory. The indicated clock time is indicative. Participants arrived in the office between 8:00 and 9:30 depending on individual wake times. Light-blue filled rectangles = sleep episodes; grey stripes = time when the participant could carry on his habitual life at home, at work or outside; yellow stripes = time spent in the office rooms (weeks 2 and 4) with 1-hour lunch break (outside the office; green fill) and 15-min breaks inside the building (orange fill); purple fill = cognitive performance tasks (5-min auditory Psychomotor Vigilance Task + 9-min auditory N-Back) and self-rated effort on MERS; red fill = surveys on subjective comfort (VAS = Visual Analogue Scale, VCS = Visual Comfort Scale); pink circles = saliva samples for melatonin and cortisol (on two days/week during weeks 2 and 4).

### Chapter 3. Impact of light on humans

---

by using a non-linear logistic regression function following the procedure for parametrization with the software SAS (see below) showed by Dmitienko et al. [2007].

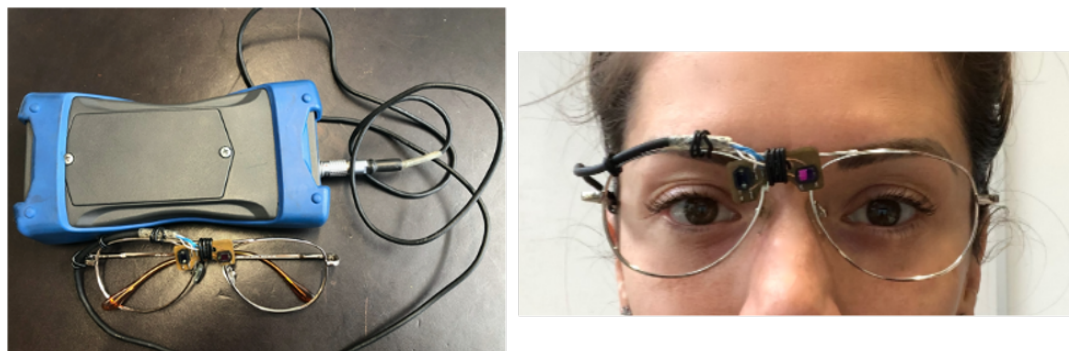


**Figure 3.11** – Wearable light sensor device "Luxblick" mounted on glasses frames with a recording box (worn separately in a case), used to record individual light exposure (illuminance) at the eye. Participants were required to wear the light sensor every day during the weeks spent in the laboratory (weeks 2 and 4), from get-up time to bedtime. Photograph: M. Benedetti.

#### Salivary hormones

Saliva samples were collected by each participant in order to assess the onset and offset of melatonin secretion as well as cortisol concentration on certain days throughout the study. During the weeks spent in the office rooms (weeks 2 and 4) participants were asked to produce saliva samples on two days in each condition (day 2 and 4), at 11 occasions per day (from habitual wake time to bedtime). Samples were taken every 60-120 min (see also Figure 3.10); the first 1-2 and the last 5 samples were taken at home and stored in the fridge until the next day and then frozen at  $-20^{\circ}\text{C}$ . Samples collected in the laboratory were immediately frozen at  $-20^{\circ}\text{C}$ .

After the study completion, all samples were sent for radio-immuno assay to an external laboratory. For cortisol assays (ELISA, American Laboratory Products Company - ALPCO, NH, USA) the inter-assay coefficient of variance (CV) for high and low cortisol concentrations was 8.8% and 11.27% respectively; for high cortisol concentrations, the intra-assay CV was 10.03%. Detection threshold was 4 ng/ml. For melatonin assays (Direct Saliva Melatonin RIA, order code: RK-DSM2, NovoLytiX GmbH, Witterswil, Switzerland), the inter-assay coefficient was 16.7% for low melatonin concentrations and 7.5% for high concentrations, while the intra-assay CV was 20.1% for low melatonin concentrations and 3.8% for high concentrations. The limit of detection was 0.9 pg/ml.

Prior to the analysis, melatonin concentrations per participant were averaged per condition (i.e., across two days). Melatonin secretion onset and offset times were calculated by linear interpolation by determining the time of a threshold concentration of 3 pg/ml [Benloucif et al., 2008] using the software tool for threshold detection developed by Danilenko et al. [2014].

### Skin temperature

Small wireless temperature sensors with integrated batteries, called i-Buttons (Maxim Integrated, USA), were adopted to continuously monitor different skin temperatures. The i-Buttons are a reliable tool to continuously measure wireless skin temperatures [van Marken Lichtenbelt et al., 2006]. In order to assess distal and proximal skin temperatures, the sensors were taped (with medical tape Mefix<sup>®</sup>) on the skin at 5 different body locations: on the back of the two hands, on the insteps of both feet, and one below the left clavicle, as shown in Figure 3.12. Participants continuously wore the temperature sensors (24h/day) during the laboratory part of the study (i.e., during weeks 2 and 4); skin temperatures were recorded at 5 minutes intervals.



**Figure 3.12** – Wireless skin temperature sensors (i-Buttons, Maxim Integrated, USA). During weeks 2 and 4 of the study, participants wore five i-Buttons (just below the left clavicle, on the back of the hands and on the insteps of the feet). The sensors were directly taped on the skin by means of a hypoallergenic medical tape (Mefix<sup>®</sup>). Photograph: M. Benedetti.

After the study, the data was downloaded and visually inspected. Very high temperature data ( $>42^{\circ}\text{C}$ ) and very low temperature data ( $<22^{\circ}\text{C}$ ) were removed (using a PYTHON<sup>®</sup> algorithm). For analysis, all data was collapsed into hourly bins (over 24 hours) per participant and condition. The distal-proximal skin temperature gradient (DPG) was calculated as the difference between the average temperature of hands and feet (distal) and the temperature at the clavicle (proximal) [Rubinstein & Sessler, 1990; Kräuchi et al., 1999].

The DPG rise time in the evening was determined from the 5-hour time window ranging from 4 hours before sleep onset until 1 hour after sleep onset by using individually assessed temperature data (averaged per participant and condition and collapsed into 30 min bins). The DPG rise time was defined as the time when the DPG was one standard deviation (SD) higher than the lowest DPG within the 5-hour time window. Therefore, one SD was added to the lowest DPG and the exact time was determined by linear interpolation. For the morning decline, a time window ranging from 1 hour before wake time until 4 hours after wake time was considered. The DPG decline time was defined as the time when the DPG became 1 SD lower than the highest DPG within the 5-hour time window. Therefore, 1 SD was subtracted from the highest DPG, and the DPG decline time was determined by linear interpolation.

### Cognitive performance tests

During the 2 × 5 study days in the office (weeks 2 and 4), participants were required to perform computer-based cognitive task sessions, 4 times per day (Figure 3.10). Each session had a total duration of about 15 min and consisted of two different consecutive cognitive tasks:

- auditory Psychomotor Vigilance Task (PVT)
- auditory N-Back

#### Auditory Psychomotor Vigilance Task (PVT)

The Psychomotor Vigilance Task is widely used to assess sustained attention, which is a proxy of vigilance and objectively assessed alertness [Dinges & Powell, 1985]. A laptop-based version was used which was programmed in MATLAB (v. R2013b with Cogent toolbox) [Schmidt et al., 2009]. The participant must respond to an auditory stimulus (a tone) delivered at random inter-stimulus intervals (usually between 2 and 10 seconds [Khitrov et al., 2014]). The participant's task is to press a key (space bar) as soon as he/she hears the tone. Despite the original version of PVT has a 10-15 minutes duration, the 5-minute version of PVT was used in this study, as it was proved that *"the 5 min PVT may provide a reasonable substitute for the 10 min PVT in circumstances where a test shorter than 10 min is required"* [Roach et al., 2006]. A study performed by Killgore [2010] confirms that the 5-minutes PVT is sufficient *"to elicit significant effects of sleep deprivation and is sensitive to the effects of stimulant countermeasures"*. Each PVT test consisted of 45-50 stimuli and a total of 20 PVT tests were performed in each room condition (i.e., 4 tests per day in the *Test* and in the *Reference* room respectively).

After each study day, the data was downloaded and any anticipatory responses (reaction times  $RT < 100$  ms) and lapses ( $RT > 500$  ms) were removed from the data using a MATLAB algorithm. For each test, the fastest 10% RTs, slowest 10% RTs and median of the RTs were calculated. The outcome variable presented in this thesis is the mean of the 10% fastest RTs, which better represents performance capability according to Drummond et al. [2005].

For quality assessment, the computers used in the *Test* and *Reference* room were also compared in order to exclude technical issues due to differences in the hardware (keyboard, PC, screen), signal transmittance, etc., which could have caused differences in response times. Identical and proper functioning of the hardware in both rooms was tested and confirmed by the IT team at LESO, and empirical validation of both computer devices (performed by the author) revealed a negligible difference in RT below 3 ms.

#### Auditory N-Back

In cognitive neuroscience, the N-Back test is widely used to test short-term working memory. The user hears different letters at 2-seconds intervals. For each spoken letter (in French) in a sequence, the user must then judge whether it matches the letter presented  $n$  items ago by pressing the key X



### 3.2. Experimental study with young participants

for "yes" and key "N" for "no". There are three task levels, distinguished by task difficulty:

- *0-back*

This is the easiest level, used as a control for task adherence; the user must press X when he/she hears the letter K, and N for all the other letters.

- *2-back*

The user must press X when the letter that he/she has just heard is the same as the second-last letter. Otherwise, he/she should press N.

- *3-back*

The user must press X when the letter is the same as the third-last heard letter. Otherwise he/she should press N.

In each N-Back session, each of the three versions (i.e., 0-, 2-, and 3-back) was performed three times with a random sequence of letters. Each session contained a total of 30 letters presented, the duration of one N-Back session was 9 minutes and a total of 20 sessions were completed per condition (4 tests per day, as for PVT). After each study day, the data was downloaded and the accuracy score was calculated separately for each of the three N-back versions in each session as the fraction of correct responses according to the formula 3.1:

$$Score = \frac{N_{correct\ responses} - N_{false\ alarms}}{Total} \quad (3.1)$$

#### Subjective mental effort

Perceived mental effort or cognitive load was subjectively assessed by participants after each cognitive test session (i.e., four times per day in each condition). These evaluations were performed by using the Mental Effort Rating Scale [Paas et al., 1994] on paper. Participants were required to estimate their perceived effort in the preceding tasks on a scale from 0 (no effort) to 150 (extremely demanding). The scale is reported in Figure B.2 in the Appendix B. After the study, all the answers were digitised from the paper-based scale to a computer file for each participant and each condition.

#### Subjective assessments

While in the office, participants were asked to perform self-evaluations of their sleepiness, mood, visual and thermal comfort on visual analogue scales (VAS) as well as visual comfort scales (VCS) [Borisuit et al., 2015; Eklund & Boyce, 1996; Maierova et al., 2016]. The VAS presents two extremes between a horizontal line for each item, and the participant indicated his/her answer graphically by posting a marker on the line between these extremes. The following example shows the VAS scale for the assessment of subjective sleepiness:

*How do you feel in this moment?*

*extremely alert* \_\_\_\_\_ *extremely sleepy*

The VAS and VCS were generated as online survey (created with the help of the IT team at LESO-PB on the internal server). Each survey was repeated eight times per day, i.e., approximately every 75 min (see protocol in Figure 3.10). The survey popped-up automatically on the computer screen in the office at the scheduled times. The 18 questions included in the survey are listed in Appendix B. Three examples of how questions were visualized on the screen are shown in Figure B.1 in the same Appendix. For analysis, the answers were averaged per participant, day and condition.

#### **Activity monitoring and assessment of midsleep**

The rest/activity data from the activity watches (Figure 3.13) was downloaded at the beginning and at the end of each week in the laboratory. For each participant, the data was inspected on the first day of each week to determine the average wake time of the 7 preceding days for the starting time of the protocol for the week in the laboratory. The time of arrival in the office was scheduled to be approximately one hour after wake time (or maximum two hours, depending on the participant's commute to LESO-PB).



**Figure 3.13** – Actigraphy watch "ActTrust" by Condor Instruments ([www.condorinst.com.br](http://www.condorinst.com.br)).

In order to align the data to individual 'internal circadian phase', habitual midsleep was used as proxy [Roenneberg et al., 2003] for each participant. All outcome variables were aligned accordingly. Midsleep was derived from rest-activity recordings and calculated as the midpoint between habitual sleep times (i.e., between sleep onset and wake time) during the seven days prior to the respective laboratory condition (i.e., week 1 and week 3). It was on average  $4:07 \pm 0:40$  (h:mm, mean  $\pm$  SD) for both conditions (without a significant difference between both weeks, see Table 3.3 for more details).

The time of arrival in the office was on average  $8:43 \pm 0:20$ , which is 4:36 after the average midsleep time. Sleep- and wake times were also monitored during the weeks in the office in order to

verify compliance with the protocol.

### 3.2.4 Statistical analysis

For statistical analysis, all data was averaged into hourly bins (if not otherwise stated) and expressed relative to the individual midsleep time. The software SAS University Edition (SAS Institute Inc., Cary, NC, USA; version 9.4) was used to perform the statistical analysis. Generalized linear models (GLIMMIX) were used to fit the data, with log-normal distribution when the data was not normally distributed. When data was right-skewed, it was linearly transformed to left-skewed according to [Wicklin, 2016]. Degrees of freedom were determined with the Satterthwaite approximation and post-hoc analysis was performed by using the Tukey-Kramer test with p-values adjusted for multiple comparisons or by using least square mean comparisons (with p-values adjustments by using the false-discovery rate, FDR). The fixed factors were: *condition* (*Test room* vs. *Reference room*) and *season* (winter, mid-season, summer, see classification below). Elapsed time after midsleep (in hours, referred to as *time*, for simplicity) was added as repeated factor.

The interaction effects of *condition\*time* were also assessed in all data sets, whereas the interaction effects between the factors *season\*condition* and *season\*time* (as well as the three-way interaction *condition\*season\*time*) were performed in a separate analysis and only reported if there were significant main effects of *season* and/or interactions, which was the case for some but not all variables (e.g. individual  $E_v$  from wearable sensors, cognitive performance, subjective ratings). To assess statistical significance, an alpha level of 0.05 was used.

The allocation of laboratory sessions to different seasons was performed retrospectively and the classification of seasons is based on the photoperiod length (i.e., time from sunrise to sunset) which resulted in three "seasons" (i.e., approximately  $\pm 45$  days around spring and fall equinoxes as well as winter and summer solstices): 'Winter' (short days, November 6th - February 3rd), 'Mid-seasons' (spring and autumn, February 4th - May 5th and August 9th to November 5th) and 'Summer' (long days, May 6th to August 8th). As a result, the number of participants in each of the 3 "seasons" was as follows: in winter  $n=10$  (*Test room*) and  $n=6$  (*Reference room*); in mid seasons  $n=16$  (*Test room*) and  $n=20$  (*Reference room*); in summer  $n=5$  (*Test room*) and  $n=8$  (*Reference room*).

Potential sex differences were also explored in the physiological and cognitive performance output variables, by adding the main factor *sex* to the generalized linear model in a separate analysis. Statistically significant sex differences are reported.

### Missing data

Because of some data communication issues on the control platform, data of  $E_v$  and DGP could not be used for a total of 8 days in the *Test room* and 10 days in the *Reference room* (not consecutive, see also section 2.2.7). Due to technical problems, light sensors data from wearable devices could

not be used for one participant in the *Test* room and one in the *Reference* room condition, thus data from  $n=30$  and  $n=33$  participants respectively were included in the final analysis of individual  $E_v$ . The activity watch data was not recorded (technical failure) for one participant in the week before the *Test* room session, thus the sleep/wake times from the sleep log were used to assess midsleep for that week. Out of all scheduled salivary samples, 18 and 27 samples were missing in the *Test* room and in the *Reference* room, respectively (either because the sample was not taken, or the analysis was not possible because there was not enough saliva). For one participant, the offset time of melatonin secretion in the morning (*Test* room) could not be assessed, likely because it occurred before wake time. Due to the technical failure of two i-Buttons (including the one for proximal skin temperature), the DPG could not be calculated for one participant in the *Test* room because of missing data from i-Buttons: therefore, data from  $n=30$  participants in the *Test* room were included in the analysis of DPG.

### 3.3 Results

#### 3.3.1 Lighting conditions in the office rooms

Results of photopic vertical illuminance and melanopic Equivalent Daylight Illuminance assessed in the office rooms were already reported in Chapter 2 (section 2.3.1). For comparison and interpretation of the physiological measures presented in this section, the lighting data was additionally aligned to midsleep time for each participant and analysed accordingly. For the sake of clarity, average clock time was also added in the graphic representations.

Photopic vertical illuminance ( $E_v$ , lux) was continuously monitored by the fixed HDR vision sensor (VIP, see section 2.2.2) during scheduled office hours. It showed a dynamic pattern over time, with lower  $E_v$  in the mornings and later afternoons (Figure 3.14a, main effect of *time*:  $F_{12,564}=36.2$ ,  $p<0.0001$ ).  $E_v$  was overall significantly higher in the *Test* room than in the *Reference* room:  $1177 \pm 562$  lux vs.  $858 \pm 478$  lux (mean per hour  $\pm$  SD; main effect of *condition*:  $F_{1,599}=54.9$ ,  $p<0.0001$ ). An interaction between the factors *condition\*time* was also observed ( $F_{11,563}=8.65$ ,  $p<0.0001$ ) and post-hoc comparisons revealed significantly higher  $E_v$  levels in the *Test* than in the *Reference* room from 5 to 10 hours after midsleep (indicated with \* in Figure 3.14a), which corresponds to clock times between 9:00 and 14:00 ( $p<0.05$ ).

Similarly to  $E_v$ , melanopic Equivalent Daylight Illuminance (EDI, lux, calculated from SPDs), significantly varied during scheduled office hours for 18 participants (Figure 3.14b, main effect of *time*:  $F_{9,291}=19.6$ ,  $p<0.0001$ ). The EDI was higher in the *Test* room ( $931 \pm 484$ ) than in the *Reference* room ( $730 \pm 390$ ; main effect of *condition*:  $F_{1,311}=16.6$ ,  $p<0.0001$ ) and there was also a significant interaction between the factors *condition\*time* ( $F_{9,291}=5.2$ ,  $p<0.0001$ ). Post-hoc tests (p-values adjusted using false discovery rate, FDR) revealed significantly higher melanopic EDI in the *Test* room in the morning between 5-10 hours after midsleep, and higher EDI in the *Reference* room in the evening (14 h after midsleep, around 18:00). For both  $E_v$  and melanopic EDI there were no statistically significant differences between seasons ( $p>0.05$ ).

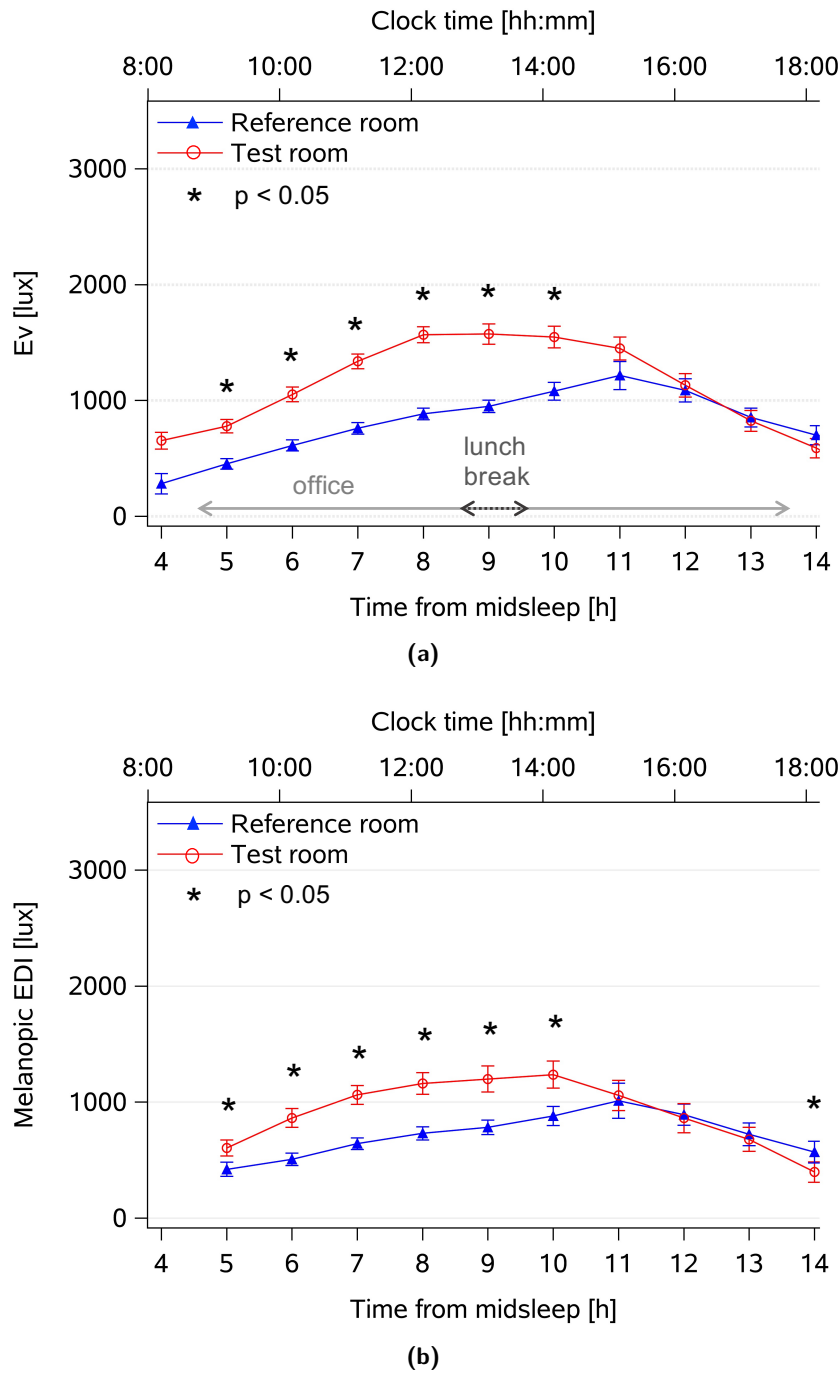


**Figure 3.14** – a) Time course of photopic vertical illuminance ( $E_v$ ) assessed by the HDR vision sensor (VIP, see section 2.2.2) next to the desk, at 1.2 m height from the floor on a vertical plane at the approximate eye level of a sitting person (as shown in Figure 2.6), averaged across 5 days during office hours. *Test room* = red circles and lines; *Reference room* = blue lines and triangles (mean  $\pm$  standard error, SEM;  $n=31$  in the *Test room* and  $n=34$  in the *Reference room*). Data is aligned to individual midsleep time and averaged across participants (the lower x-axis indicates elapsed hours after midsleep). Corresponding clock time is shown on the upper x-axis (though it was not the exact time for every participant but only an average time across all participants). b) Averaged time course of melanopic Equivalent Daylight (EDI) Illuminance (lux) at the desk for 53% of all sessions ( $n=18$ , mean values  $\pm$  SEM). Midsleep time for  $n=18$  is at  $4:08 \pm 0:40$ , similar as for all participants ( $n=34$ ). The lunch break and time spent in office are indicated by the grey arrows.

### 3.3.2 Individual light exposure at the eye

The time course of individual illuminance at the eye (recorded during the entire waking period by the wearable light sensor 'Luxblick', see section 3.2.3) varied over time in both conditions and was highest around midday (main effect of *time*:  $F_{16,998}=173.4$ ,  $p<0.0001$ ; Figure 3.15). In contrast to  $E_v$  assessed by the fixed sensors in the office rooms, individually measured  $E_v$  across the entire waking period revealed no statistically significant differences between the two conditions ( $p>0.5$ , mean  $\pm$  SD per hour was  $650 \pm 1132$  lux for the *Test* room and  $675 \pm 1351$  lux for the *Reference* room). From visual inspection it appeared that there might be illuminance differences between the two conditions only in the first half of the day. Thus, a separate analysis was carried out on individual  $E_v$  in the first half of the waking period, between 5 and 9 hours after midsleep (i.e., between the time of arrival in the office and lunch time). The results showed significantly higher individual  $E_v$  in the *Test* ( $1231 \pm 1665$  lux) than in the *Reference* room ( $973 \pm 1300$  lux during these 4 hours; main effect of *condition*:  $F_{1,289}=10.1$ ,  $p=0.002$ ), with significant variations over time (with highest  $E_v$  around midday;  $F_{4,267}=38.2$ ,  $p<0.0001$ ) but no significant interaction between both factors ( $p>0.1$ ). When the same analysis was carried-out in the second part of the day (i.e., starting 10 hours after midsleep until bedtime), there was no significant difference between the two conditions ( $p>0.1$ ).

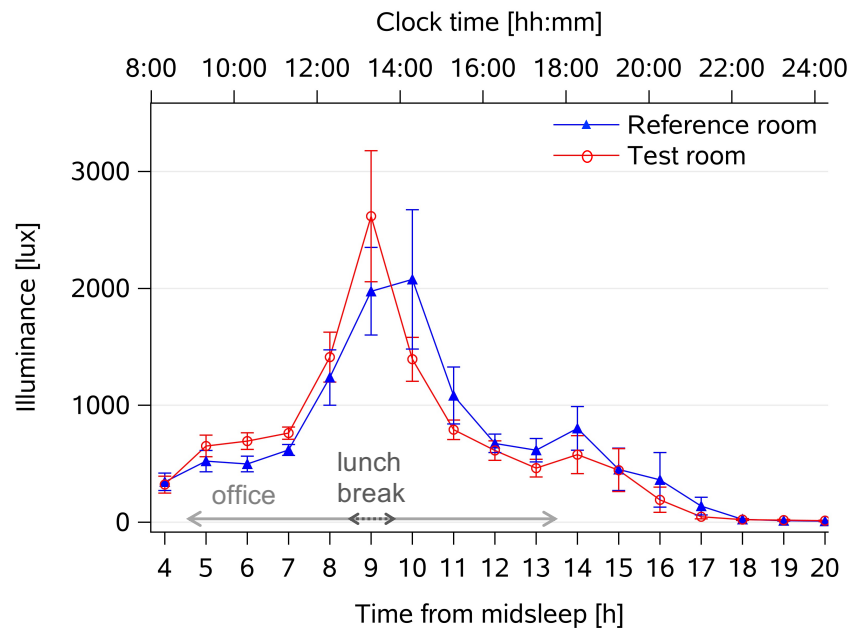


**Figure 3.15** – Time course of averaged individual photopic illuminance ( $E_v$ ) measured by wearable devices across the entire waking period, averaged across 5 days and aligned relative to midsleep (mean values  $\pm$  SEM,  $n=30$  in *Test* room and  $n=33$  in the *Reference* room). The lunch break and time spent in the office are indicated by the grey arrows.

Table 3.2 summarizes the mean values (averaged per hour in the office for  $E_v$  and melanopic EDI and also across the entire waking period for the wearable light sensor) and SD of lighting data in each condition, as well as p-values for differences between conditions.

		<i>Reference room</i> mean $\pm$ SD	<i>Test room</i> mean $\pm$ SD	p-value
<b><math>E_v</math> [lux]</b>	office hours	857.6 $\pm$ 477.8 (n=34)	1177.3 $\pm$ 562.0 (n=31)	<0.0001*
<b>Melanopic EDI [lux]</b>	office hours	730.4 $\pm$ 389.8 (n=18)	931.4 $\pm$ 484.4 (n=18)	<0.0001*
<b>Individual <math>E_v</math> (wearable sensor) [lux]</b>	office hours	674.6 $\pm$ 1350.5 (n=34)	649.5 $\pm$ 1132.1 (n=31)	>0.5
	all day (from wake- to bedtime)	1035.5 $\pm$ 1517.7 (n=33)	1018.2 $\pm$ 1245.9 (n=30)	>0.5

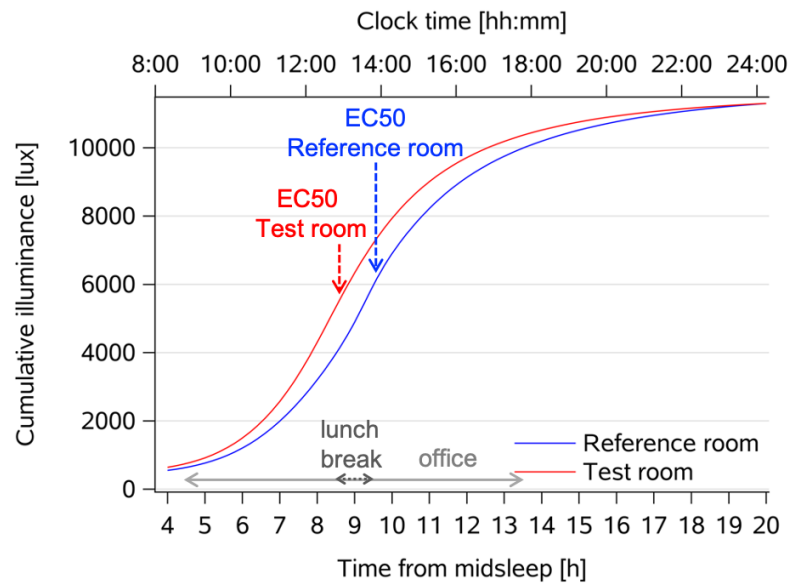
**Table 3.2** – Results for light recordings:  $E_v$  = photopic illuminance, EDI = equivalent (D65) daylight illuminance (lux, SPD derived from the SPD assessed by the spectrometer), both assessed on a vertical plane at the approximate eye level during office hours; individual  $E_v$  from wearable light sensor devices during the entire waking period including office hours (mean  $\pm$  SD across days and participants). P-value: main effect of *condition*.

#### Accumulated individual illuminance

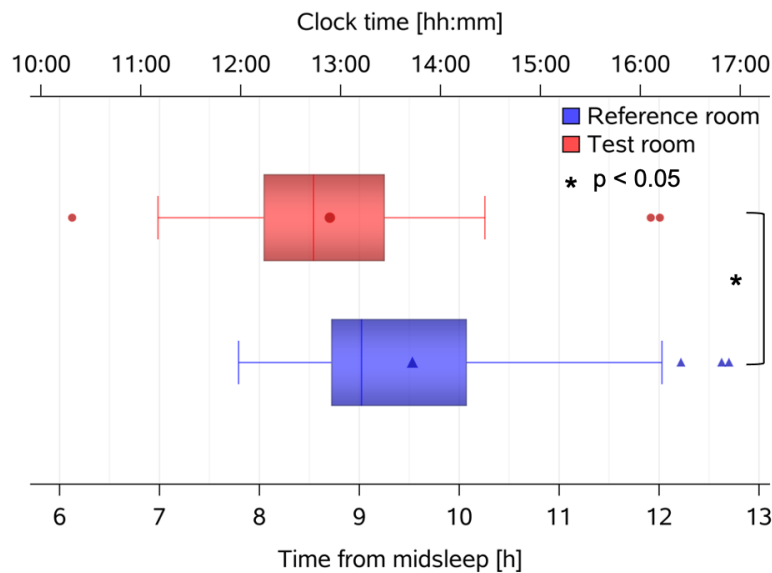
In a next step, the accumulated individual  $E_v$  across the waking period was computed for each participant in each condition (see section 3.2.3). The results from the individually fitted curves showed that individual  $E_v$  was significantly higher in the *Test* room than in the *Reference* room (Figure 3.16a shows the average fitted curve of accumulated  $E_v$  in each condition); main effect of *condition*:  $F_{1,1026}=4.7$ ,  $p=0.031$ ). Importantly, the half-maximum response (EC50) of the accumulated  $E_v$  (i.e., the time at which 50% of the total accumulated illuminance is reached) occurred significantly earlier in the *Test* room than in the *Reference* room: EC50 was reached on average 8:42  $\pm$  1:16 (h:mm) after midsleep time in the *Test* room and 9:32  $\pm$  1:22 after midsleep in the *Reference* room, which corresponds to average clock times 12:57 and 13:35, respectively (main effect of *condition*:  $F_{1,33}=5.4$ ,  $p=0.026$ ; Figure 3.16b). The accumulated  $E_v$  at EC50 was on average 5950 lux in the *Test* room, which corresponds to EDI of  $\approx$  4800 melanopic lux.

Please note that average midsleep was 12 minutes later in the *Test* than in the *Reference* room (see Table 3.3). Therefore, the difference in clock times is smaller than difference in "time after midsleep" between the two conditions; this is true also for the other results presented in this section.





(a)



(b)

**Figure 3.16** – a) Dose-response curves for accumulated individual  $E_v$  from wearable devices (fitted sigmoidal curves), aligned to midsleep time; the times for half-maximum response are indicated for the two conditions: 8.7 hours after midsleep in the *Test* room and 9.5 hours after midsleep in the *Reference* room (red line for *Test* and blue line for *Reference* room); b) Box plot of half-maximum response (EC50) of accumulated  $E_v$ . The box plot shows mean values (symbol inside the box), median (vertical line), minimum and maximum values (horizontal bars) and outliers (symbols outside the boxes). Red symbols = *Test* room, blue symbols = *Reference* room.

#### Seasonal differences in individual light exposure

Analysis for seasonal differences on individual  $E_v$  revealed overall lower light exposures in winter ( $395 \pm 622$  lux) than both summer ( $842 \pm 1406$  lux) and mid-seasons ( $720 \pm 1384$  lux; main effect of *season*,  $F_{2,95}=6.3$ ,  $p=0.003$ , Figure 3.17a), but without significant interactions of *season\*condition* ( $p>0.1$ , Figure 3.17b). There was an interaction effect with *time\*season*, with significantly higher  $E_v$  in summer between 12 and 17 hours after midsleep (which corresponds to clock times between 16:00-21:00) than in mid seasons and winter. As shown in Figure 3.18, recorded  $E_v$  levels were highest in summer and lowest in winter.

The analysis also showed a significantly earlier EC50 times in winter (i.e.,  $7:54 \pm 0:44$  after midsleep; main effect of *season*,  $F_{2,46}=15.6$ ,  $p<0.0001$ ) than in mid seasons ( $9:16 \pm 1:03$  after midsleep) and summer ( $10:20 \pm 1:33$  after midsleep). To summarize, individual  $E_v$  was on average lowest and EC50 was earliest in winter, compared to mid-seasons and summer, without further differences between room conditions.

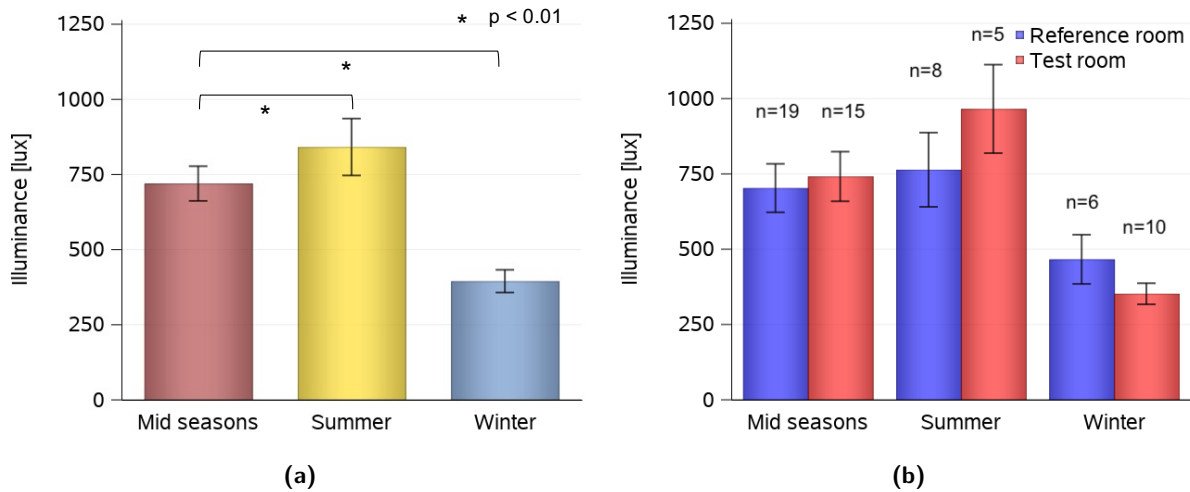


**Figure 3.17** – Bar charts of individual  $E_v$  from wearable devices (mean  $\pm$  SEM) grouped by season (a) and by season and condition (b); n = number of participants for each group; \* = statistically significant differences ( $p<0.05$ ).

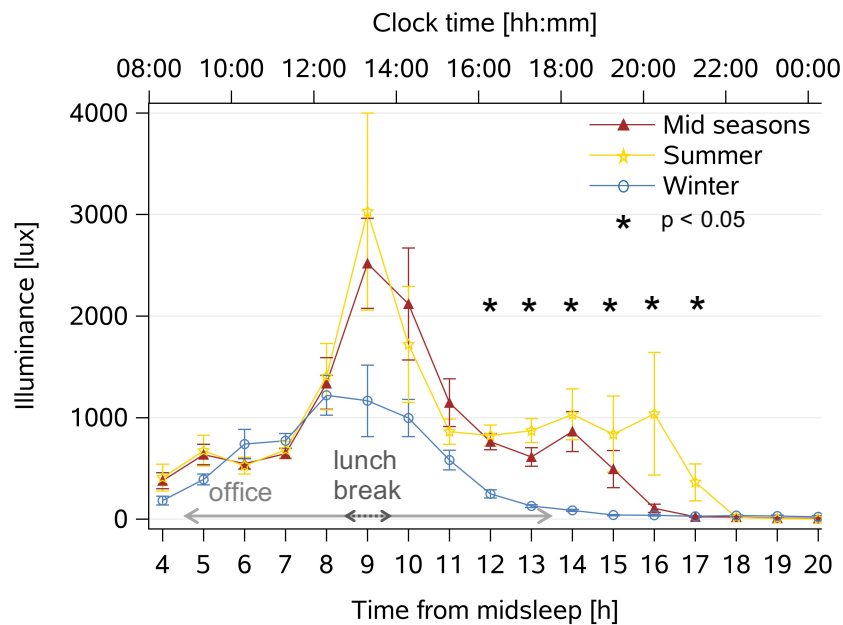


**Figure 3.18** – Time course of averaged individual illuminance ( $E_v$ ) from wearable light sensor devices across the entire waking period, averaged per season (mean values  $\pm$  SEM; winter: blue circles and lines; mid seasons: red triangles and lines; summer: yellow stars and lines; for the number of participants in each season, see Figure 3.17b or section 3.2.4). The x-axis at the bottom shows elapsed time from midsleep, and the upper x-axis shows corresponding clock time (hh:mm). The horizontal arrows show the time in the offices and the lunch break (spent outside the office).

### 3.3.3 Salivary hormones

#### Melatonin

Salivary melatonin secretion exhibited a typical diurnal profile (main effect of *time*,  $F_{10,565}=123.2$ ,  $p<0.0001$ ; Figure 3.19), where concentrations decreased significantly after get-up time, stayed close to zero during the day and increased again in the evening.

Overall, no significant concentration differences between both conditions and seasons were observed ( $p>0.1$ ). When the data in the evening was tested separately (i.e., the last 5 samples of the day, from 16 to 20 hours after midsleep), there were significantly higher melatonin concentrations in the *Test* than in the *Reference* room (main effect of *condition*:  $F_{1,266}=8.6$ ,  $p=0.004$ ), also suggesting an earlier onset of melatonin secretion in the evening.

Indeed, melatonin onset times (see section 3.2.3) occurred significantly earlier during the week in the *Test* than in the *Reference* room, i.e., at  $16:40 \pm 1:18$  after midsleep in the *Test* room vs.  $17:05 \pm 1:29$  after midsleep in *Reference* room, which corresponds to clock times  $20:54 \pm 1:18$  vs.  $21:07 \pm 1:31$ , respectively (main effect of *condition*:  $F_{1,31}=4.2$ ,  $p=0.048$ ; Figure 3.20a).

For the melatonin secretion offset there were no significant differences between the two conditions: the offset occurred  $4:56 \pm 0:54$  after midsleep in the *Test* room and  $5:02 \pm 0:56$  after midsleep in the *Reference* room, corresponding to clock times  $9:11 \pm 1:00$  and  $9:04 \pm 1:01$ , respectively; Figure 3.20b); overall, there was no main effect of *season* or interaction between the factors *condition\*season*

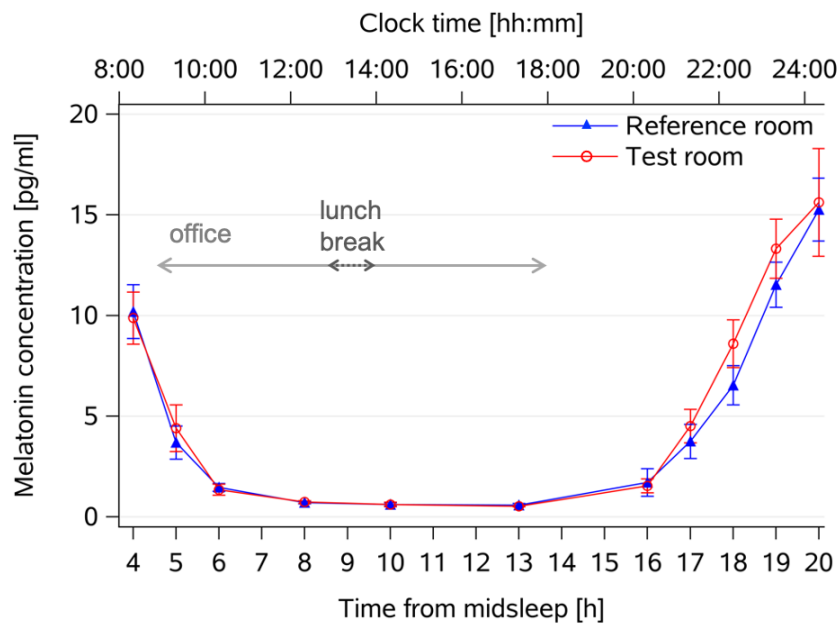
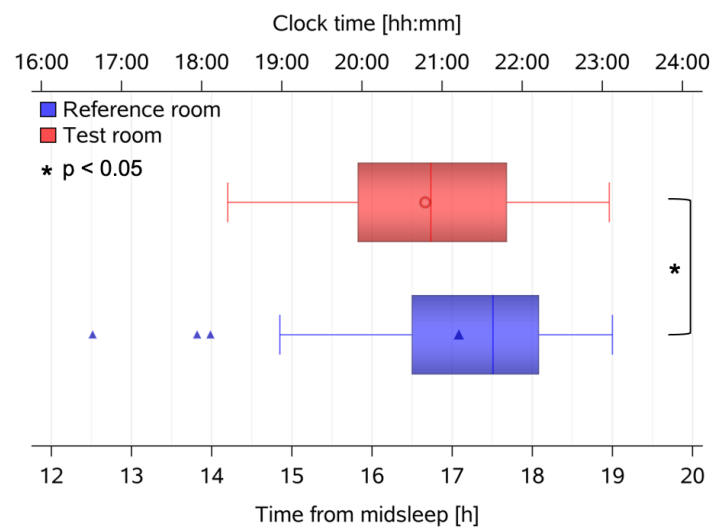


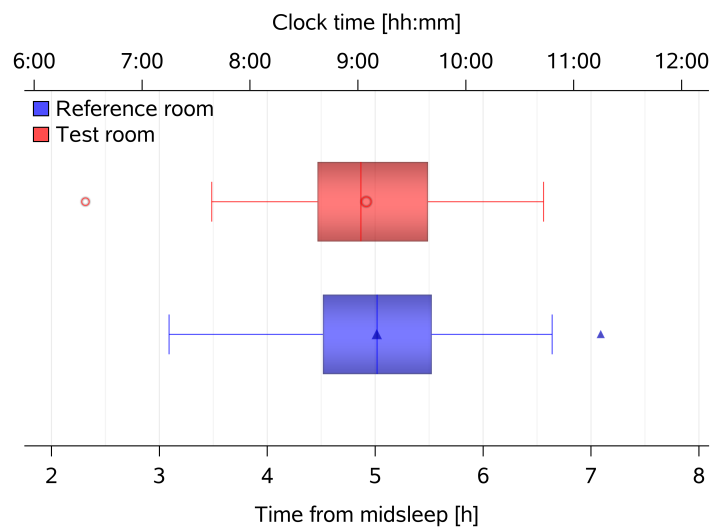
**Figure 3.19** – Diurnal profile of melatonin concentrations (pg/ml, mean ± SEM) in both conditions, averaged across two days per condition.

for melatonin profiles, nor for onset and offset times ( $p>0.1$ ).

Phase angles of entrainment between melatonin secretion onset and sleep onset times became 31 minutes longer in the *Test* room when compared to the *Reference* room (main effect of *condition*:  $F_{1,32}=7.7$ ,  $p=0.009$ ) while sleep timing was not significantly different between the two conditions, as was designed for this study (see Table 3.3).



(a) Melatonin onset



(b) Melatonin offset

**Figure 3.20** – Box plots for melatonin secretion onset (a) and offset (b) times aligned relative to midsleep. Melatonin onset occurred significantly earlier in the *Test* room (red symbols) than in the *Reference* room (blue symbols; \*:  $p < 0.05$ ). There was no significant difference between the two conditions for melatonin offset time. The boxplots show mean (red and blue symbols inside the boxes), median (red and blue vertical lines), minimum and maximum values (red and blue horizontal bars), outliers (symbols outside the boxes).

Cortisol

As expected, cortisol concentrations varied diurnally, with a peak after wake-up time and progressively lower values during the day (main effect of *time*,  $F_{10,593}=85.6$ ,  $p<0.0001$ ; Figure 3.21). There were no statistically significant differences between conditions (or seasons), even when analysing the first 4 data points separately (morning values;  $p>0.5$ ). The interaction effect between *condition\*season* was significant, with higher cortisol concentrations in the *Test* room than in the *Reference* room in winter, whereas in mid seasons the concentrations were lower in the *Test* room (see Figure 3.22).

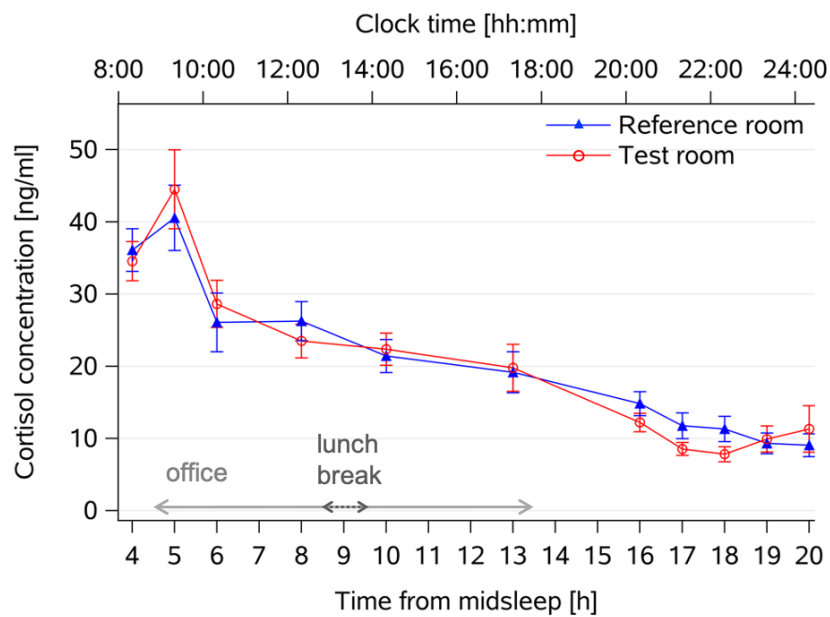


Figure 3.21 – Diurnal profile of cortisol concentrations (ng/ml) averaged across 2 days per condition (mean ± SEM).

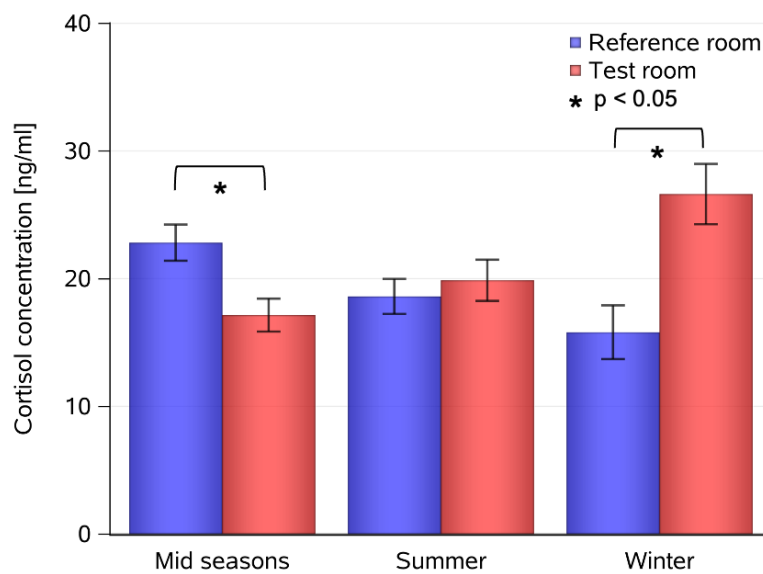
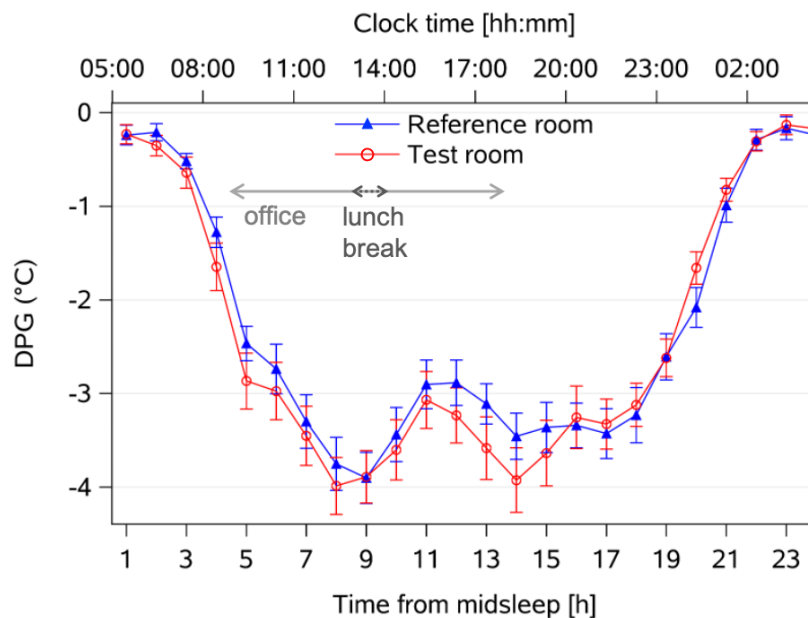


Figure 3.22 – Bar chart of all cortisol concentration grouped by season and condition (mean ± SEM).

### 3.3.4 Distal-proximal skin temperature gradient

The 24-hour time course of the distal-proximal skin temperature gradient (DPG; Figure 3.23) showed a significant circadian profile (main effect of *time*:  $F_{23,1454}=36$ ,  $p<0.0001$ ). The DPG was overall significantly higher for the week in the *Reference* room than in the *Test* room (main effect of *condition*:  $F_{1,1466}=4.1$ ,  $p=0.04$ ), but there was no interaction between the factors *condition\*time*. Performing the same analysis only in the evening/night data points (i.e., from 16 to 24 hours after midsleep) did not show significant differences in the DPG between the two conditions ( $p>0.5$ ). However, when analysing the first part of the day (between 0 and 12 hours after midsleep), the DPG was significantly lower in the *Test* room (main effect of *condition*:  $F_{1,742}=4.3$ ,  $p=0.04$ ), suggesting a circadian phase-shift (advance) of the DPG decline in the morning.



**Figure 3.23** – 24-hour time course of the DPG (mean  $\pm$  SEM) in the *Test* room ( $n=30$ , red symbols and line) and in the *Reference* room ( $n=34$ , blue symbols and line). The x-axis at the bottom depicts elapsed time since midsleep (hours) and the upper x-axis shows clock time averaged across participants. The lunch break and time in office are indicated by the grey arrows.

In a next step the exact DPG "rise time" in the evening and DPG "decline time" were computed per condition (see procedure in section 3.2.3). The evening rise of the DPG tended to occur earlier in the *Test* than in the *Reference* room (difference = 20 minutes,  $p=0.10$ ; Figure 3.24, Table 3.3). Besides, the rise occurred significantly earlier in the mid seasons than in winter and summer (main effect of *season*:  $F_{2,46}=4.1$ ,  $p=0.02$ ). The phase angle of entrainment, calculated as difference between the habitual sleep onset time (derived from rest-activity recordings) and the time of the DPG rise became significantly longer in the *Test* room than in the *Reference* room (difference = 27 min; main effect of *condition*:  $F_{1,34}=4.5$ ,  $p=0.041$ ; Figure 3.26a). The phase angle was longer in mid seasons ( $1:38 \pm 0:57$ , h:mm, mean  $\pm$  SD) than winter ( $1:10 \pm 0:48$ ) and summer ( $0:39 \pm$

1:05).

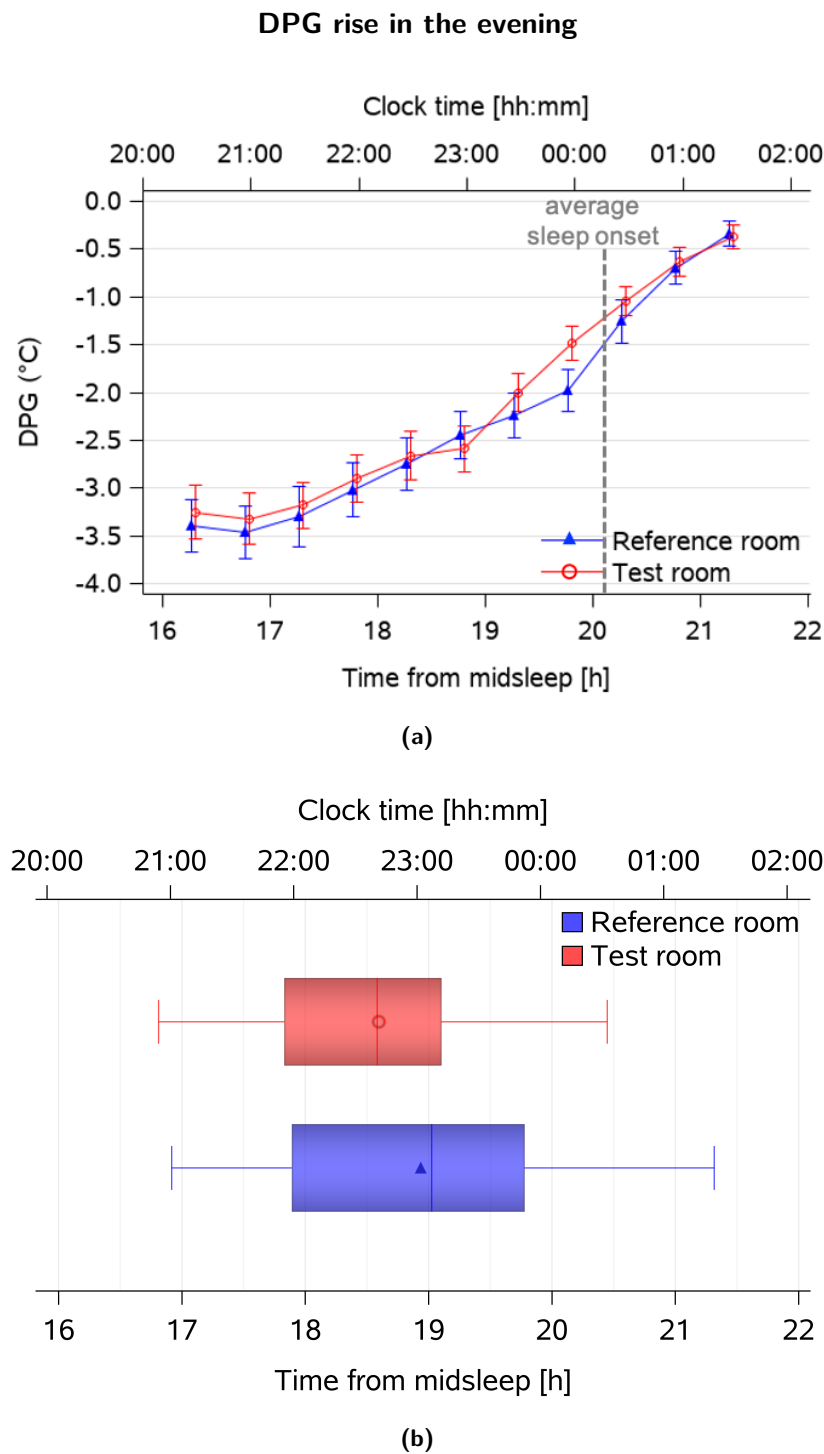


**Figure 3.24** – DPG evening rise: a) averaged time course of DPG between 4 hours before bedtime and 1 hour after bedtime (mean  $\pm$  SEM), aligned relative to midsleep; average sleep onset is indicated by dashed grey line; b) The box plot shows mean values (symbol inside the box), median (vertical line), minimum and maximum values (horizontal bars).



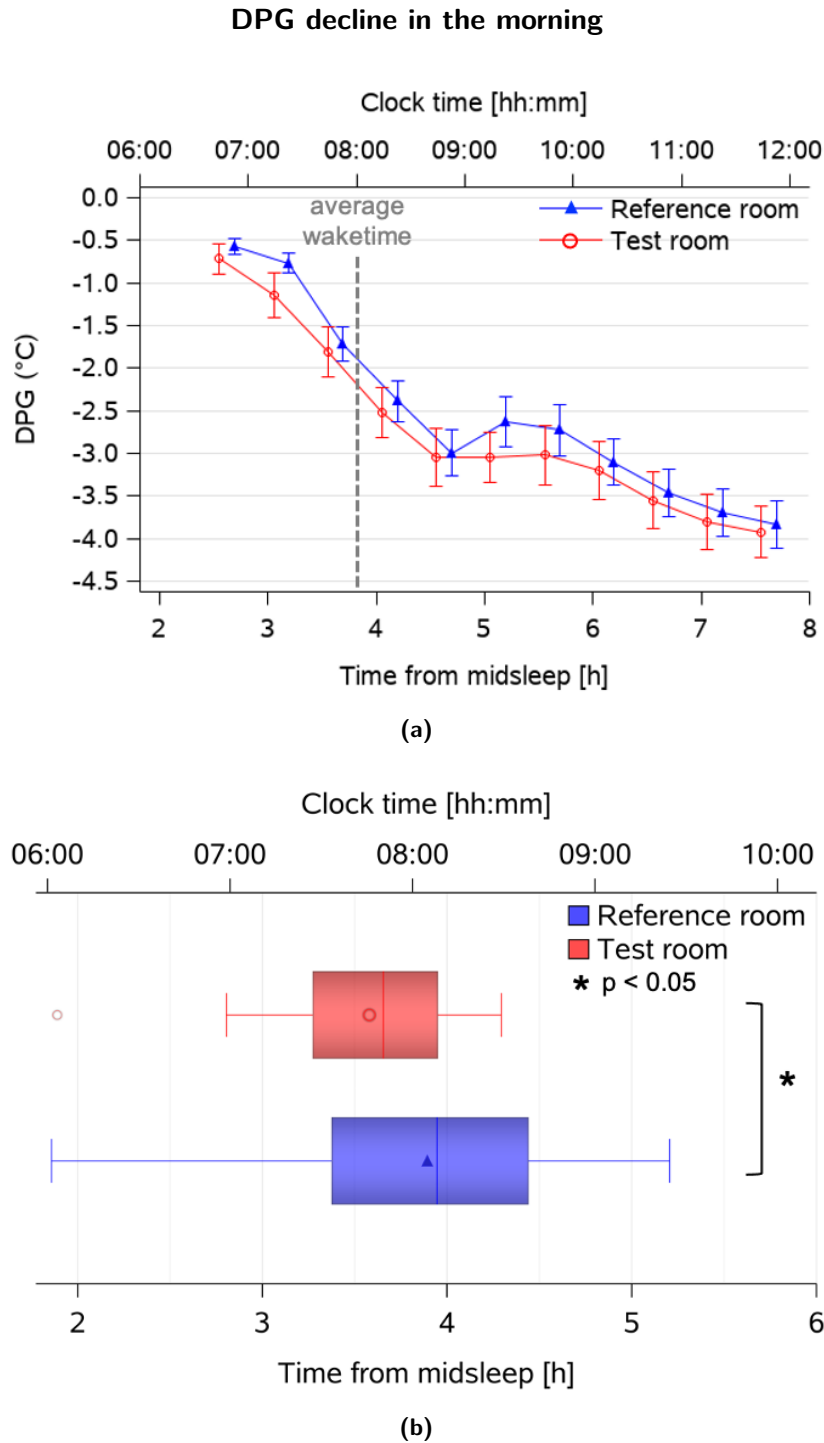


**Figure 3.25** – DPG morning decline: a) averaged time course of DPG from 4 hours before bedtime to 1 hour after bedtime (mean  $\pm$  SEM), aligned relative to midsleep; average wake time is indicated by dashed grey line; b) The box plot shows mean values (symbol inside the box), median (vertical line), minimum and maximum values (horizontal bars). \* = statistically significant difference ( $p < 0.05$ ).

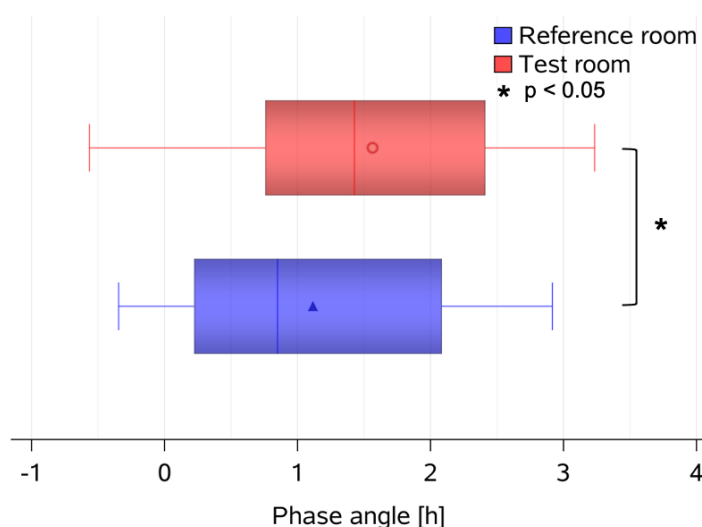
The DPG decline in the morning occurred on average 19 minutes earlier in the *Test* room than in the *Reference* room (main effect of *condition*:  $F_{1,32}=7.2$ ,  $p=0.011$ ; Figure 3.25, Table 3.3), and the phase angle of entrainment calculated as the time difference between habitual wake time

### Chapter 3. Impact of light on humans

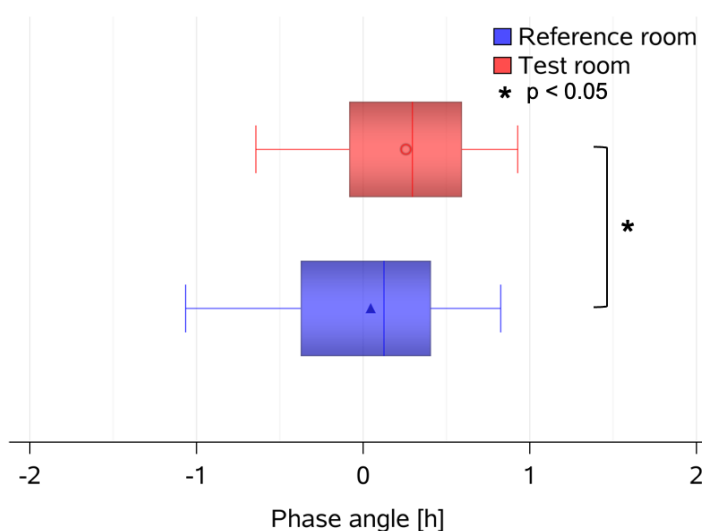
and DPG decline was on average 13 min longer in the *Test* room than in the *Reference* room ( $F_{1,32}=4.2$ ,  $p=0.049$ ; Figure 3.26b, Table 3.3). Both the DPG decline and the phase angle did not differ significantly between seasons.

The DPG decline occurred 31 minutes earlier in males than in females with respect to individual midsleep time (main effect of sex:  $F_{1,33}=6.2$ ,  $p=0.018$ , data not shown), and there was a trend for larger skin temperature gradients (i.e., a "more negative" DPG) on average in females ( $p=0.09$ ). There were no main effects of season for any of the DPG data ( $p>0.1$ ).

#### Phase angles of entrainment



(a)



(b)

**Figure 3.26** – a) Phase angle of entrainment between DPG rise and sleep onset (calculated as sleep onset – DPG rise time); b) Phase angle between DPG decline and wake time (calculated as wake time – DPG decline). The box plots show means (red and blue symbol inside the box), median (vertical red and blue lines), minimum and maximum values (horizontal red and blue bars). \*:  $p < 0.05$ .

### 3.3. Results

	<i>Reference room</i>	<i>Test room</i>	<i>p-value</i>
<b>Clock time [hh:mm, mean <math>\pm</math> SD]</b>			
Wake time	07:58 $\pm$ 00:36	08:05 $\pm$ 00:50	0.86
Sleep onset	00:05 $\pm$ 00:56	00:23 $\pm$ 00:46	0.66
Midsleep	04:02 $\pm$ 00:39	04:14 $\pm$ 00:40	0.23
<b>Elapsed time since midsleep [hh:mm, mean <math>\pm</math> SD]</b>			
<b>(Clock time [hh:mm, mean <math>\pm</math> SD]) *</b>			
Half-maximum response of accumulated $E_v$ (EC50)	09:32 $\pm$ 01:22 (13:35 $\pm$ 01:01)	08:42 $\pm$ 01:16 (12:57 $\pm$ 01:03)	0.026*
Melatonin secretion onset	17:05 $\pm$ 01:29 (21:07 $\pm$ 01:31)	16:40 $\pm$ 01:18 (20:54 $\pm$ 01:18)	0.048*
Melatonin secretion offset	05:02 $\pm$ 00:56 (09:04 $\pm$ 01:01)	04:56 $\pm$ 00:54 (09:11 $\pm$ 01:00)	0.62
DPG rise	18:56 $\pm$ 01:08 (22:55 $\pm$ 01:04)	18:35 $\pm$ 00:55 (22:45 $\pm$ 00:54)	0.10
DPG decline	03:53 $\pm$ 00:44 (07:55 $\pm$ 00:50)	03:34 $\pm$ 00:32 (07:47 $\pm$ 00:46)	0.011*
<b>Phase angles</b>			
<b>Duration [hh:mm, mean <math>\pm</math> SD]</b>			
melatonin onset - sleep onset	02:58 $\pm$ 01:41	03:29 $\pm$ 01:22	0.009*
DPG rise - sleep onset	01:07 $\pm$ 01:00	01:34 $\pm$ 01:00	0.042*
DPG decline - wake time	00:02 $\pm$ 00:28	00:15 $\pm$ 00:26	0.049*

**Table 3.3** – Summary of sleep times and melatonin and DPG results from study measures in the two conditions: wake- and sleep- time, midsleep, EC50, melatonin secretion onset and offset, DPG rise and decline, phase angles of entrainment. Times are indicated as time after midsleep and corresponding clock time (in brackets; hh:mm; mean  $\pm$  SD). \* = significant differences between the two conditions ( $p < 0.05$ ).

### 3.3.5 Cognitive performance

During the time spent in the office rooms (during weeks 2 and 4), participants performed auditory PVT and N-back tasks four times per day at regular intervals (see protocol in Figure 3.10). The mean and SD of the results of cognitive performance tests in each condition are summarized in Table 3.4.

#### Auditory Psychomotor Vigilance Task (PVT)

##### 10% fastest reaction times

The 10% fastest RTs were significantly higher (i.e., slower response) in the *Test* room than in the *Reference* room (main effect of *condition*,  $F_{1,232}=26.7$ ,  $p<0.0001$ , Figure 3.27a). The analysis revealed also an interaction between the factors *condition\*season* ( $F_{2,216}=6$ ,  $p=0.003$ , Figure 3.27b). Post-hoc tests showed faster RT in the *Reference* than in the *Test* room in mid-seasons and summer ( $p<0.0001$ ), but not in winter ( $p>0.5$ ). In the course of the 5 days, mean RT significantly decreased in both conditions from day 1 to day 3 and remained then at a constant level (Figure 3.27c). There was a statistical trend for slower mean RT in the course of the day ( $p=0.06$ , Figure 3.27d). In addition to the 10% fastest RT, also the median RT and the 10% slowest RT were analysed and the result was very similar for all of them. The mean values and SD in each condition, as well as p-values, are summarised in Table 3.4.

## PVT: 10% fastest Reaction Times (RT)

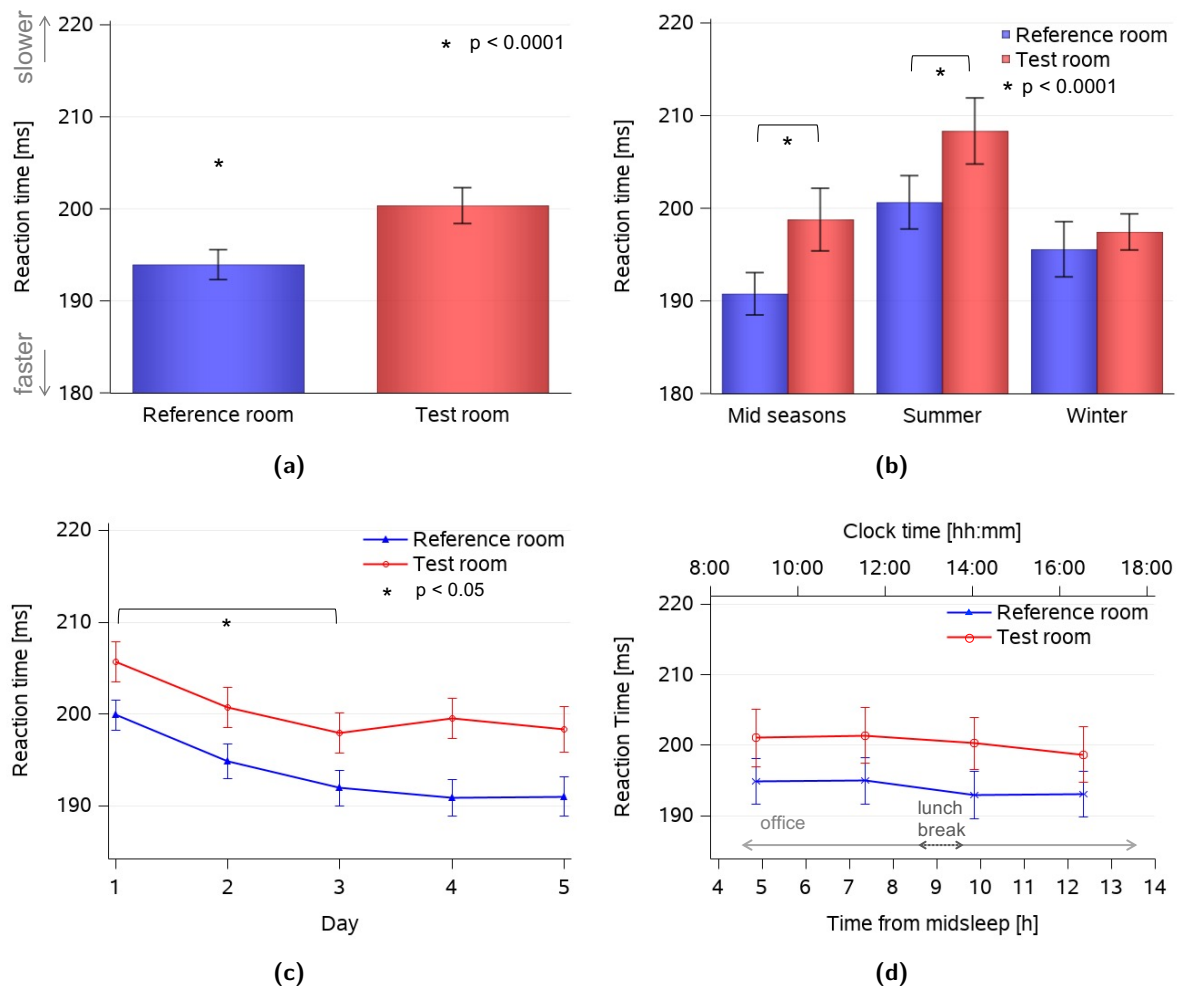


**Figure 3.27** – Bar charts of fastest 10% reaction times (RT) in the PVT, corrected for lapses and anticipations (see section 3.2.3; mean  $\pm$  SEM), grouped by condition (a), by season and condition (b); line plot showing mean of 10% RT averaged per day (c) and time course averaged across days, aligned to midsleep time (d). The y-axis shows RT in milliseconds (ms). \* = significant differences between conditions.

## Auditory N-Back test

## 3-back.

In the most difficult of the cognitive performance tasks, accuracy differed significantly among seasons (main effect of *season*:  $F_{2,230}=13.2$ ,  $p<0.0001$ , Figure 3.28a) with better scores in winter ( $0.86 \pm 0.09$ , mean  $\pm$  SD) than summer ( $0.83 \pm 0.10$ ) and mid seasons ( $0.76 \pm 0.12$ ) for both conditions. An interaction effect between the factors *condition\*season* resulted in significantly better accuracy in the *Reference* than in the *Test* room only in summer ( $F_{2,209}=13.9$ ,  $p<0.0001$ , Figure 3.28b). There was also a learning effect such that accuracy significantly improved between day 1 and 3 in both conditions ( $p<0.0001$ , Figure 3.28c), without a significant change in the course of the days ( $p>0.5$ , Figure 3.28d).

## 3-back

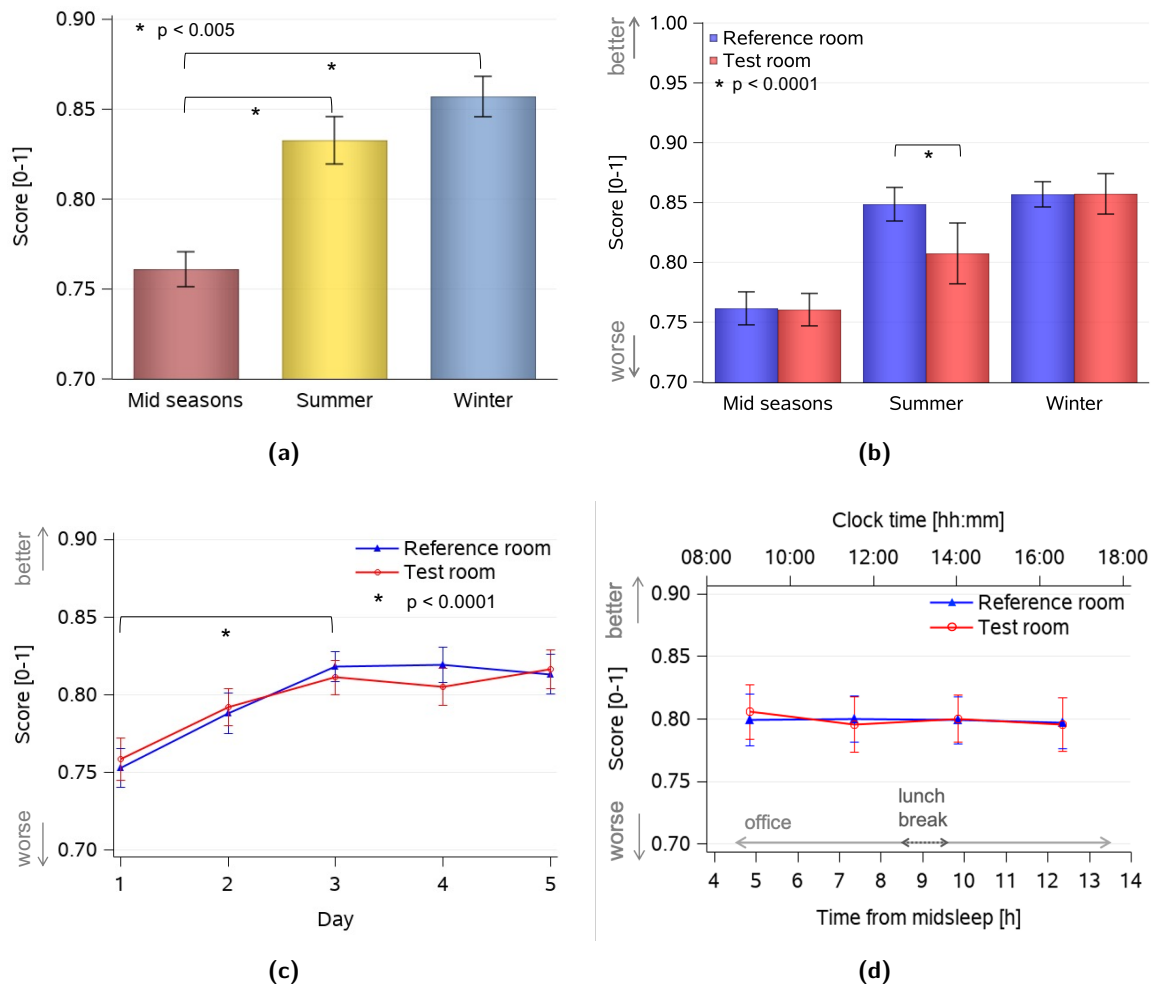


**Figure 3.28** – Bar charts and line plots for 3-back accuracy scores (mean  $\pm$  SEM across participants) grouped by season (a), by condition and season (b), by day (c) and across office hours, aligned as time after midsleep (d). The accuracy score is reported on the y-axis. Number of participants in winter:  $n=10$  in *Test* room,  $n=6$  in *Reference* room; mid seasons:  $n=16$  in *Test* room,  $n=20$  in *Reference* room; summer:  $n=5$  in *Test* room,  $n=8$  in *Reference* room. \* = statistically significant differences ( $p < 0.05$ ).

## 2-back.

Accuracy in 2-back was significantly higher in the *Reference* than in the *Test* room (main effect of *condition*,  $F_{1,210}=7$ ,  $p=0.009$ , Figure 3.29a). Similarly to the 3-back results, participants performed better in the *Reference* room than in the *Test* room in summer (interaction effect *condition\*season*:  $F_{2,208}=6$ ,  $p=0.003$ , Figure 3.29b). In both conditions, performance varied significantly during the day, with better scores in the morning and worse in the afternoon (main effect of *time*,  $p < 0.0001$ , Figure 3.29d). Also in the 2-back test, a significant improvement was observed between day 1 and the following days ( $p < 0.001$ , Figure 3.29c).

## 2-back

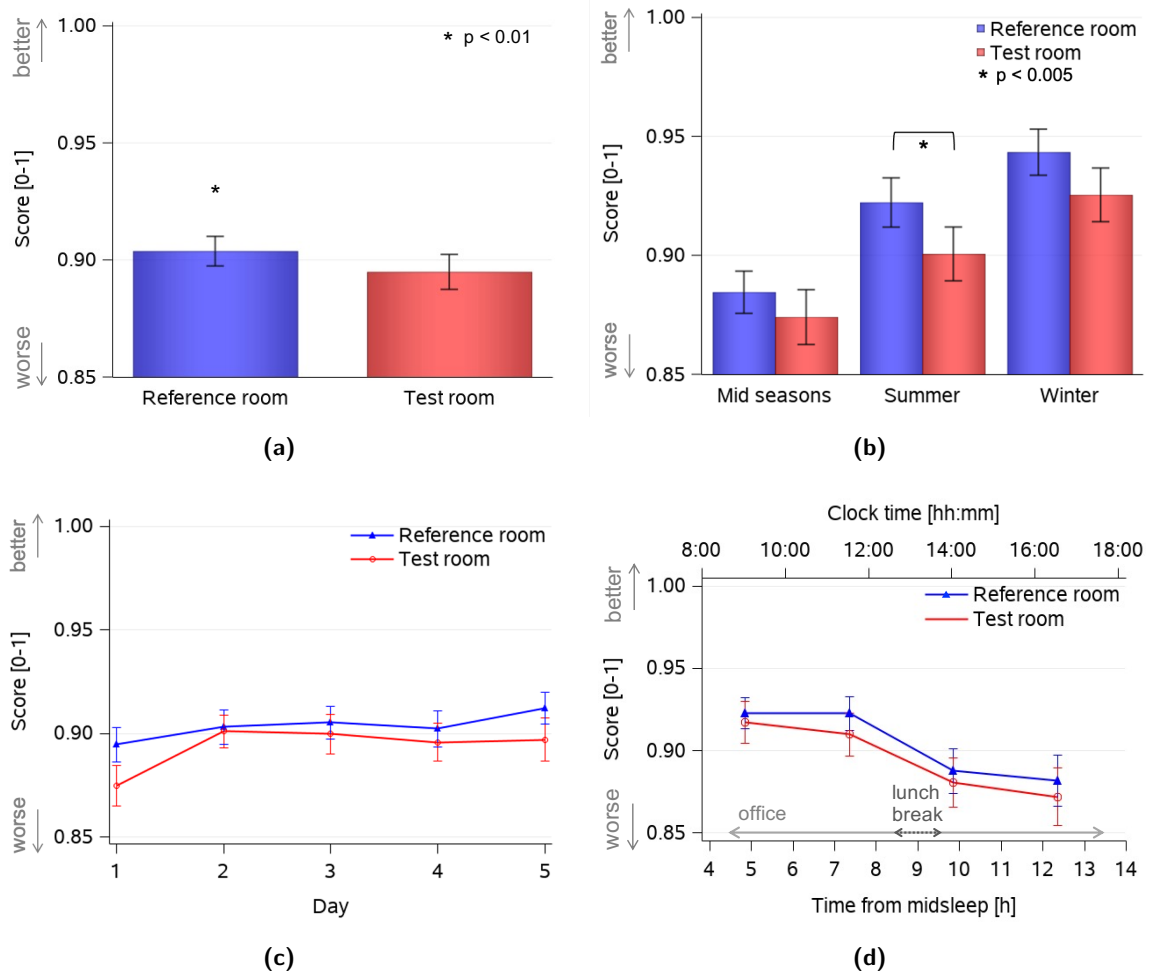


**Figure 3.29** – Bar charts and line plots for 2-back accuracy scores (mean  $\pm$  SEM across participants) grouped by condition (a), by condition and season (b), by day (c) and across office hours (d). The accuracy score is reported on the y-axis. Number of participants in winter:  $n=10$  in *Test* room,  $n=6$  in *Reference* room; mid seasons:  $n=16$  in *Test* room,  $n=20$  in *Reference* room; summer:  $n=5$  in *Test* room,  $n=8$  in *Reference* room. \* = statistically significant differences ( $p < 0.05$ ).

## 0-back.

In the easiest of the  $n$ -back tasks, which serves as a control task, accuracy was similar in both conditions, across seasons and between days.

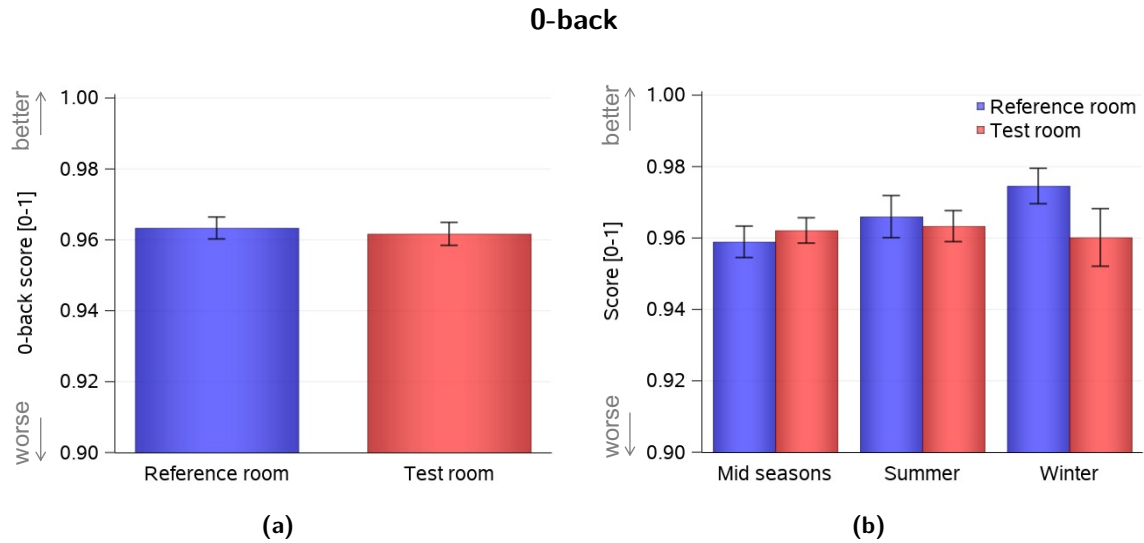


**Figure 3.30** – Bar charts for 0-back accuracy scores: by condition (a) and by condition and season (b). Number of participants in winter:  $n=10$  in *Test* room,  $n=6$  in *Reference* room; mid seasons:  $n=16$  in *Test* room,  $n=20$  in *Reference* room; summer:  $n=5$  in *Test* room,  $n=8$  in *Reference* room.

<i>Test</i>	Measure [unit]	<i>Reference</i> room	<i>Test</i> room	p-value
PVT	10% fastest RT [ms]	193.9 ± 18.9	200.4 ± 22.8	<0.0001
	median RT [ms]	238.2 ± 26.8	242.4 ± 27.9	0.003
	10% slowest RT [ms]	348.6 ± 43.1	356.1 ± 44.1	0.03
N-Back	3-back score [-]	0.799 ± 0.113	0.799 ± 0.116	ns
	2-back score [-]	0.900 ± 0.070	0.890 ± 0.080	0.01
	0-back score [-]	0.963 ± 0.036	0.962 ± 0.036	ns

**Table 3.4** – Summary of results of cognitive performance tasks (mean values ± SD). RT are shown in ms and accuracy is shown as score (see section 3.2.3); ns = not significant ( $p>0.05$ ).

## Mental Effort

Self-estimated mental effort results (MERS, see section 3.2.3) showed no differences between both conditions ( $p>0.05$ ). In the morning, mental effort was lowest after the first cognitive task, then progressively increased during the day in both conditions (main effect of *time*:  $F_{3,200}=4.4$ ,  $p=0.005$ ): the effort was lowest after the first cognitive task in the morning and progressively increased during the day in both conditions. There was a significant interaction effect with the factors *condition\*season* ( $F_{2,206}=7.3$ ,  $p=0.001$ ), however after p-value adjustment with the Tukey-Kramer test, there were no significant differences between conditions in any of the three seasons.

The analysis also showed a significant three-way interaction *condition\*time\*season* ( $F_{6,200}=2.6$ ,  $p=0.018$ ) and the analysis was done for each season separately (Figures 3.31c-d-e). Only in winter and in the first test in the morning the perceived effort in the *Test* room was significantly lower than in the *Reference* room ( $p=0.011$ , Figure 3.31c).



## Mental Effort

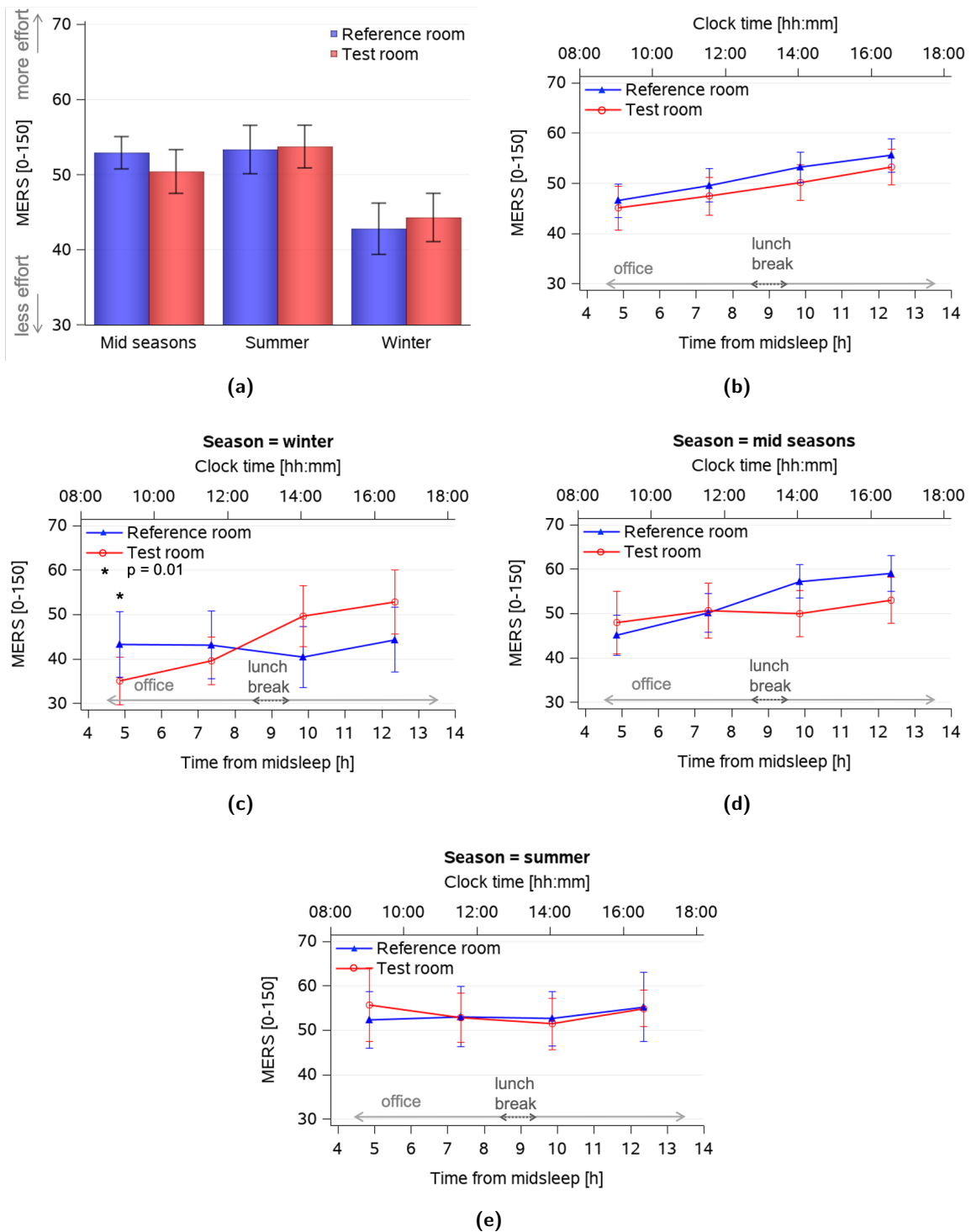


**Figure 3.31** – Plots of Mental Effort Rating Scale (MERS, mean  $\pm$  SEM): a) bar chart grouped by condition and season; b) time course in each condition aligned as time after midsleep, averaged across days; c) time course in winter; d) time course in mid seasons; e) time course in summer.

### 3.3.6 Subjective assessments (VAS/VCS)

#### Sleepiness

As mentioned in section 3.2.3, the assessment of subjective sleepiness during the time spent in the office rooms was done on the VAS scale (question n. 15 in the online survey, see Appendix B), where the rating ranged from 0 ("extremely alert") to 100 ("extremely sleepy").

Overall, subjective sleepiness ratings were low, suggesting that participants were quite alert. The average was always around 30 on a scale between 0 and 100 in both conditions. No significant differences were observed between the two conditions ( $p > 0.1$ , Figure 3.32a), however sleepiness ratings varied significantly among seasons ( $F_{2,320}=4.2$ ,  $p=0.01$ , Figure 3.32b), with highest sleepiness in winter ( $37.4 \pm 15.1$ , mean  $\pm$  SD), followed by mid-seasons ( $30.8 \pm 17.1$ ) and summer ( $26.4 \pm 16.4$ ). Significant variations were observed also during the day (main effect of *time*,  $F_{7,440}=3.4$ ,  $p=0.002$ ), with higher sleepiness ratings just after the arrival in the office in the morning, then decreasing until lunch time and increasing progressively in the afternoon, which was similar in both conditions, and there was no interaction with the factor *condition* (Figure 3.32c).

#### Mood

Mood was evaluated during office hours with question n.17 of the online survey (Appendix B). Mood ratings were overall high, on average around 70 on a scale between 0 and 100 (0 = "in a bad mood"; 100 = in a good mood) in both conditions. There was a significant difference between the two conditions ( $F_{1,447}=5.3$ ,  $p=0.022$ , Figure 3.33) with better mood ratings in the *Reference* room ( $70.9 \pm 13.9$ , mean $\pm$ SD) than in the *Test* room ( $68.8 \pm 13.7$ ). No significant differences between seasons or interaction effects were found, and mood ratings did not significantly vary across or between days.

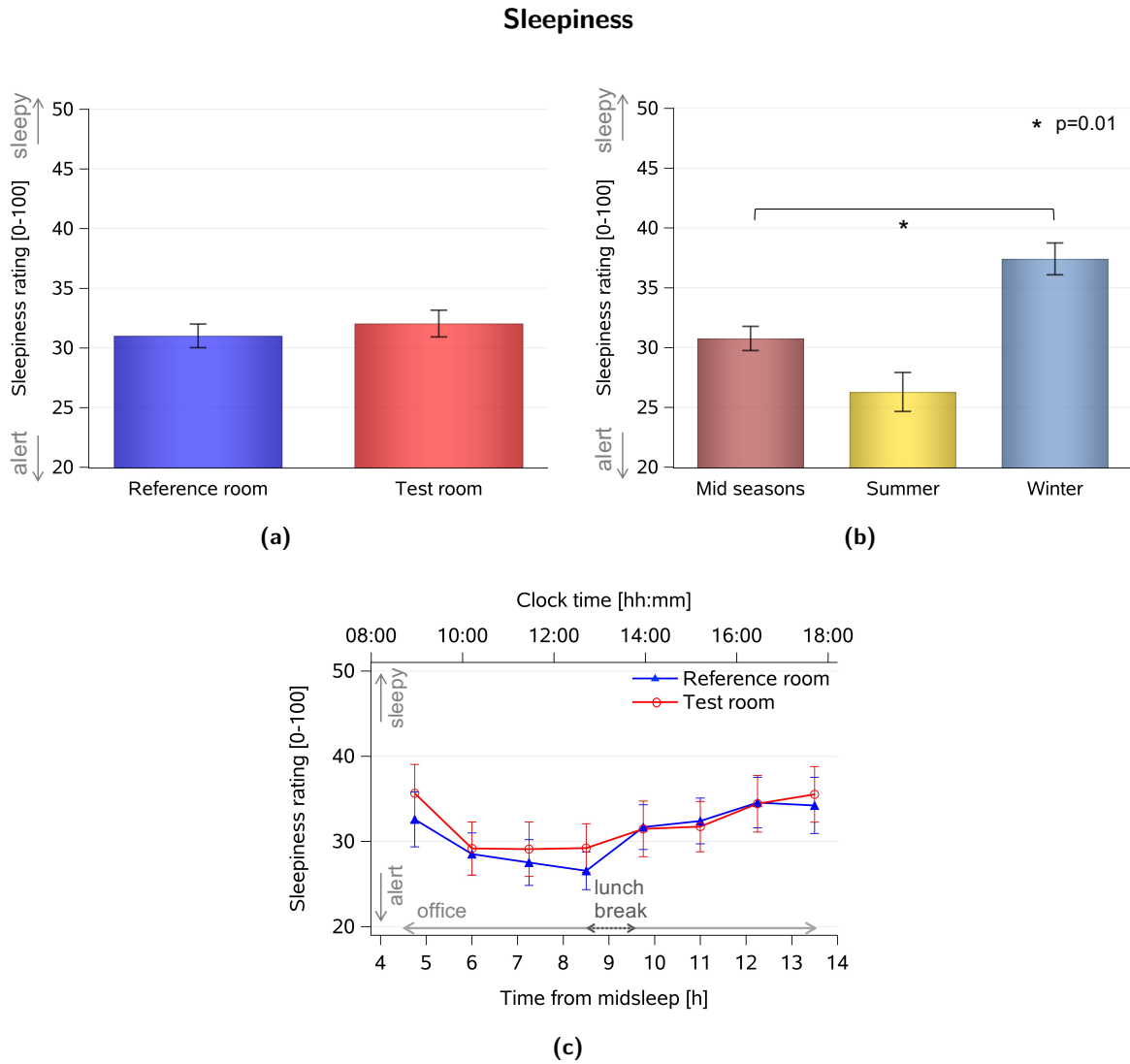


**Figure 3.32** – Plots of subjective sleepiness (mean  $\pm$  SEM): bar charts grouped by condition (a) and by season (b); c) time course in both conditions, averaged across days and aligned relative to midsleep; red symbols and lines = *Test* room, blue symbols and lines = *Reference* room. \* = statistically significant difference ( $p < 0.05$ ).

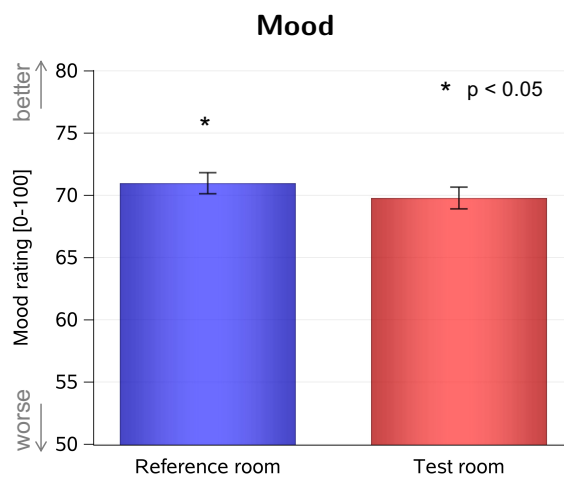


**Figure 3.33** – Bar chart of mood rating (mean  $\pm$  SEM) grouped by condition. \* = statistically significant difference.

### 3.3.7 Thermal comfort

#### Room temperature

Room temperature was significantly higher in the *Reference* room (main effect of *condition*:  $F_{1,543}=101$ ,  $p<0.0001$ ). Significant variations were also observed between seasons (main effect of *season*:  $F_{2,545}=9.6$ ,  $p<0.0001$ ), with higher temperatures in summer ( $25.4 \pm 1.95^{\circ}\text{C}$ , mean  $\pm$  SEM) than mid seasons ( $23.5 \pm 1.25^{\circ}\text{C}$ ) and winter ( $22.2 \pm 0.9^{\circ}\text{C}$ ). Room temperature increased progressively from morning to evening (as shown in Chapter 2, Figure 2.24; main effect of *time*:  $F_{9,816}=29.5$ ,  $p<0.0001$ ). An interaction effect between the factors *condition\*season* was found for all the three seasons ( $F_{2,821}=18$ ,  $p<0.0001$ ), with higher room temperatures in the *Reference* than in the *Test* room.

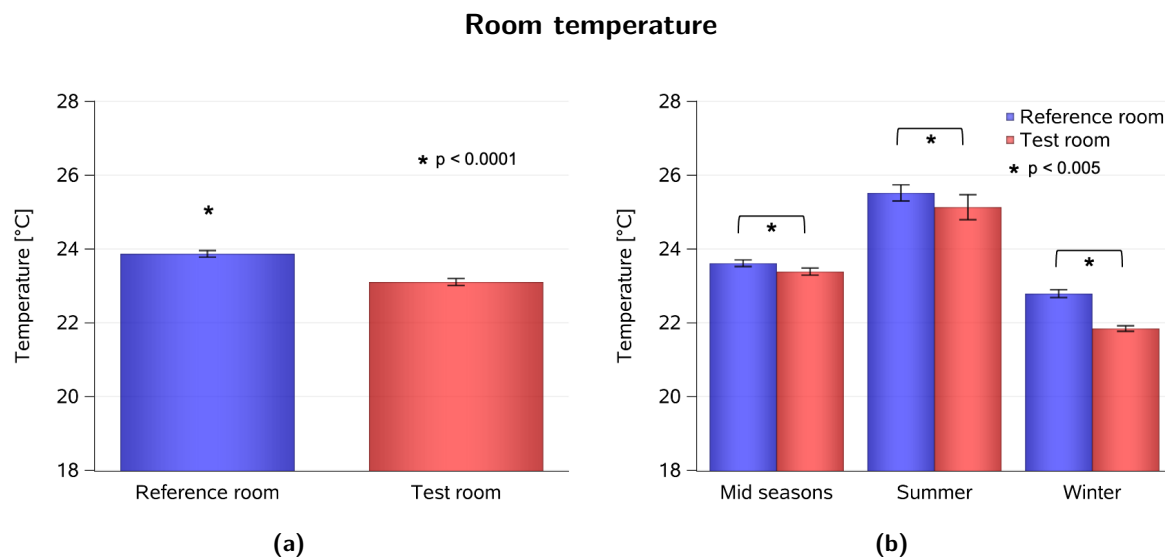


**Figure 3.34** – Bar charts of room temperature (mean  $\pm$  SEM) in  $^{\circ}\text{C}$  (see section 2.2.7 for details on the sensor) grouped by condition (a) and by condition and season (b). \*  $p<0.05$ .

#### Subjective thermal comfort

Subjective thermal comfort (or thermal perception) was evaluated with question n.18 in the VAS questionnaire (Appendix B), with the scale ranging from 0 ("extremely warm") to 100 ("extremely cold"). For the sake of comparison with room temperature, the scale was later inverted by subtracting the answer from 100 (which is equivalent to reversing the scale direction), which resulted in lower values for colder temperature perception and higher for warmer. Thermal perception did not change between conditions ( $p>0.1$ ) but it varied during the day (main effect of *time*:  $F_{7,433}=12.7$ ,  $p<0.0001$ ) with generally perceived warmer temperatures in the afternoon than in the morning hours. Seasonal differences were not significant, but there was an interaction effect between the factors *condition\*season* with significantly warmer temperature perception in the *Reference* room in mid-seasons ( $p=0.031$ , Figure 3.35a).

Figure 3.36 shows the averaged time courses of room temperatures and subjective thermal comfort

## Subjective thermal perception

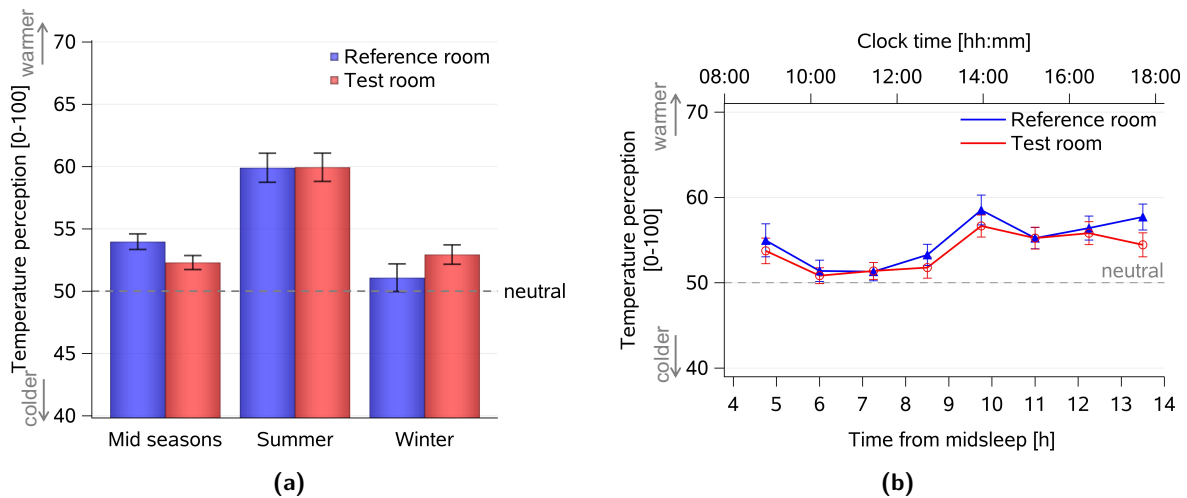


**Figure 3.35** – a) Bar chart of subjective thermal comfort (or thermal perception, mean  $\pm$  SEM) grouped by condition and season; b) time course of thermal perception in each condition (mean  $\pm$  SEM) aligned relative to midsleep. The dashed green line indicates the optimal (or neutral) thermal comfort, on a scale from 0 (extremely cold) to 100 (extremely warm).

together for the two conditions. In both rooms, temperature increased throughout the day, and was overall higher in the *Reference* room. Participants generally felt rather warm than cold, as the average rating of thermal perception was above 50 in both conditions. Not surprisingly, the perception of warmer temperatures is higher at the arrival in the office in the morning (first data point) and after the lunch break (5th data point). Except from these two higher points, which are likely due to the fact that participants had just entered the building from outside and felt immediately warmer when they sat down. The thermal perception also seems to follow the time course of room temperature, slightly increasing throughout the day.

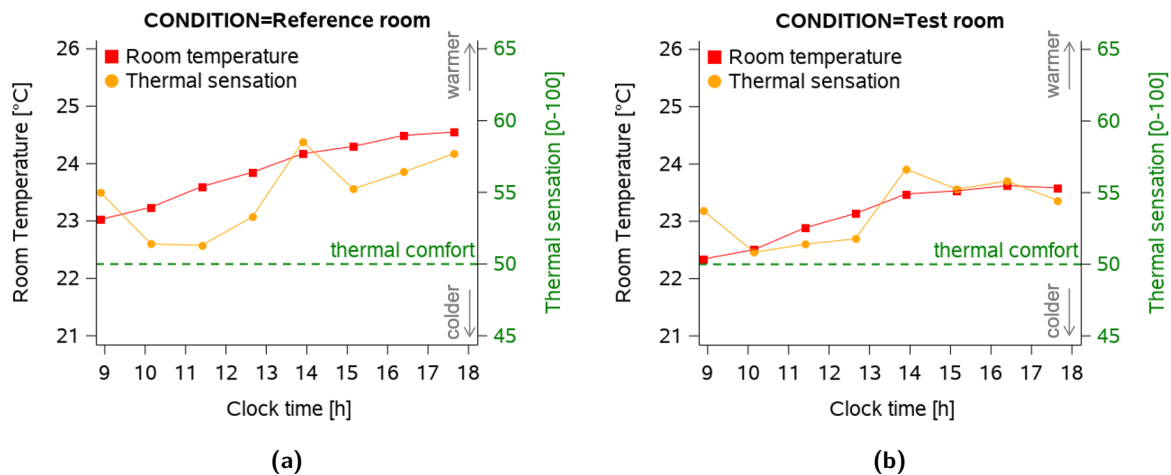


**Figure 3.36** – Time courses for room temperature (red symbols, left y-axis; averaged per week) and subjective thermal comfort (orange symbols, secondary y-axis) for the *Reference* room (a) and for the *Test* room (b) during the time spent in the office (in absolute clock times). The dashed green line indicates the optimal (or neutral) subjective thermal comfort, on a scale from 0 (extremely cold) to 100 (extremely warm).

To additionally illustrate the trend of room temperature and subjective thermal comfort, the heat maps in Figure C.2 in the Appendix C show the distribution of both variables in both conditions and for all seasons. An alternative representation is shown by the 3D plots in Figure C.3 in the same Appendix, which represent the trend of thermal comfort during the day in the office averaged for each season and condition. For the heat maps (Figure C.2) all values for each participant were averaged across days. The heat maps show that for only a few participants thermal comfort became worse with higher temperature perceptions around noon or in the second half of the office day, and one or two participants felt cold in the morning.

### 3.3.8 Visual comfort

#### Objective measure: Daylight Glare Probability (DGP).

The Daylight Glare Probability (DGP) is derived from a probabilistic glare model based on subjective assessments: it is used as an objective variable to directly assess visual discomfort from glare risks. As presented in Chapter 2 (section 2.3.1, Figure 2.22), the DGP was always maintained in a comfortable range in the *Test* room by means of the automated controller. Analysis revealed significantly higher DGP levels in the *Test* room than in the *Reference* room (main effect of *condition*:  $F_{1,603}=21$ ,  $p<0.0001$ ). Nevertheless, the DGP values always remained considerably below the visual discomfort threshold of 35%. For seasonal differences there was an interaction between the factors *condition\*season* suggesting higher DGPs in mid seasons and in summer in the *Test* room than in the *Reference* room (Figure 3.37).

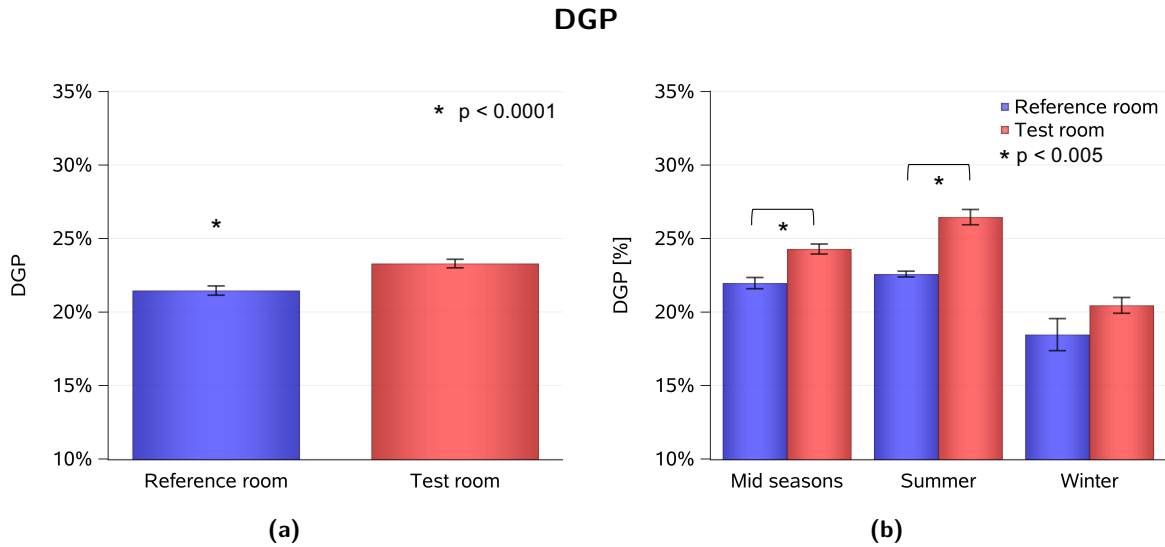


**Figure 3.37** – Bar charts of DGP (mean  $\pm$  SEM) grouped by condition (a) and by condition and season (b). Number of participants in winter:  $n=10$  in the *Test* room,  $n=6$  in the *Reference* room; mid seasons:  $n=16$  in the *Test* room,  $n=20$  in the *Reference* room; summer:  $n=5$  in the *Test* room,  $n=8$  in the *Reference* room.

#### Subjective measure: perceived discomfort glare.

Subjective glare was assessed by the question n. 6 of the survey (Appendix B), Ratings ranged on a scale of discrete values from 1 ("imperceptible") to 9 ("intolerable"). No significant differences between conditions were found ( $p > 0.5$ ) and the ratings were within the comfortable range (i.e., between imperceptible and acceptable). Visual comfort varied significantly during the day (main effect of *time*:  $F_{7,439}=3.4$ ,  $p=0.002$ ) with higher glare ratings in the afternoon than in the morning. As in DGP, there was an interaction effect of *condition\*season* ( $F_{2,443}=15$ ,  $p<0.0001$ ) with significant differences between the two conditions in mid-seasons (higher glare ratings in the *Reference* room); and summer (higher glare ratings in the *Test* room); but there were no differences in subjective glare assessments between both conditions in winter (Figure 3.38b).

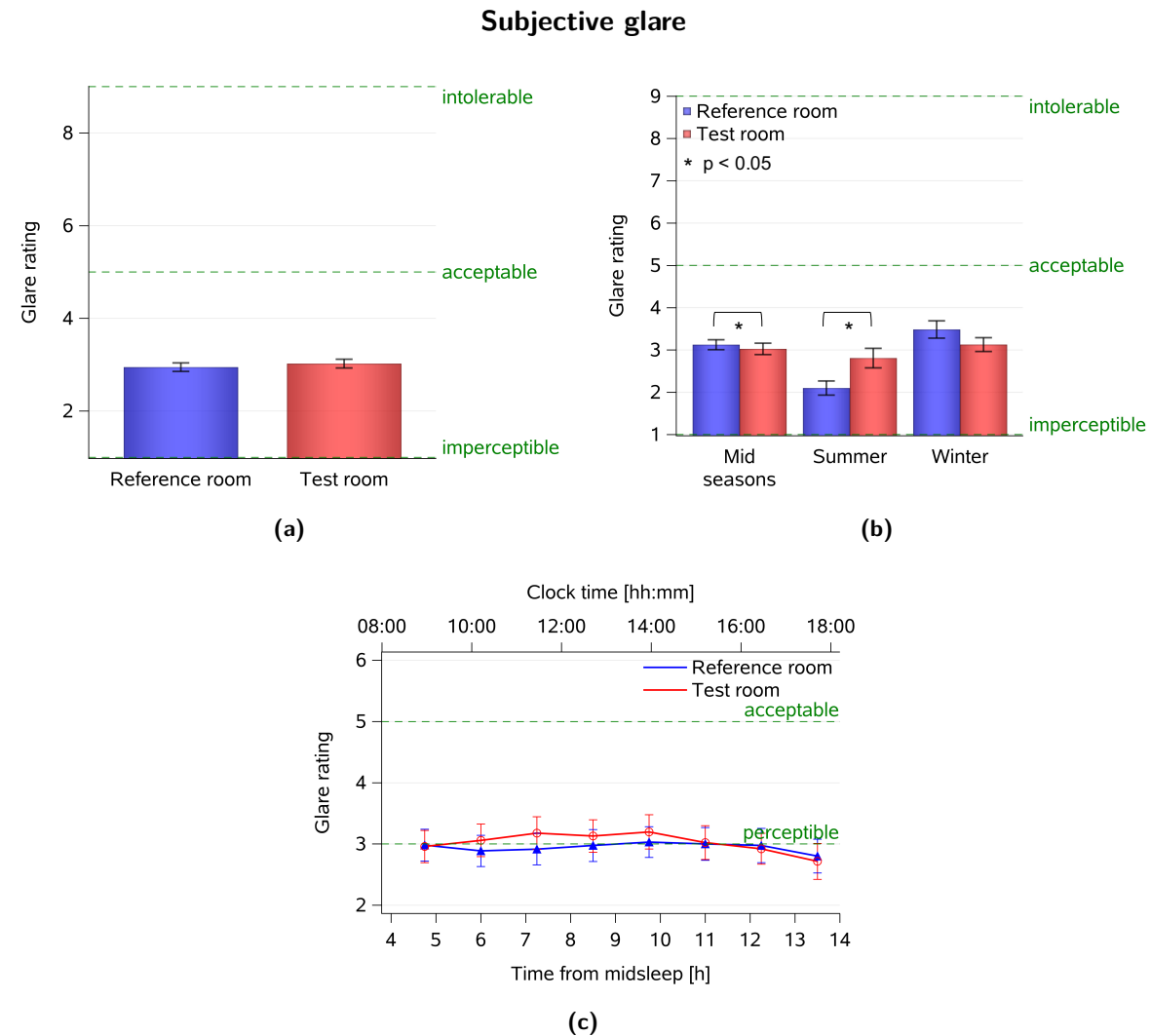


**Figure 3.38** – Plots of subjective glare (mean ± SEM) grouped by condition (a), by season and condition (b); c) time course averaged across 5 days and aligned relative to midsleep.

Figure 3.39 shows the time course of DGP together with subjective glare rating in both conditions, averaged across days and participants. The heat maps in Figure C.4 in the Appendix C show DGP and subjective glare for all participants, averaged across days, in all seasons and conditions, similarly to the plots seen for thermal comfort. The result shows that for all participants, subjective perception of glare was below the discomfort threshold in all seasons and in both conditions.



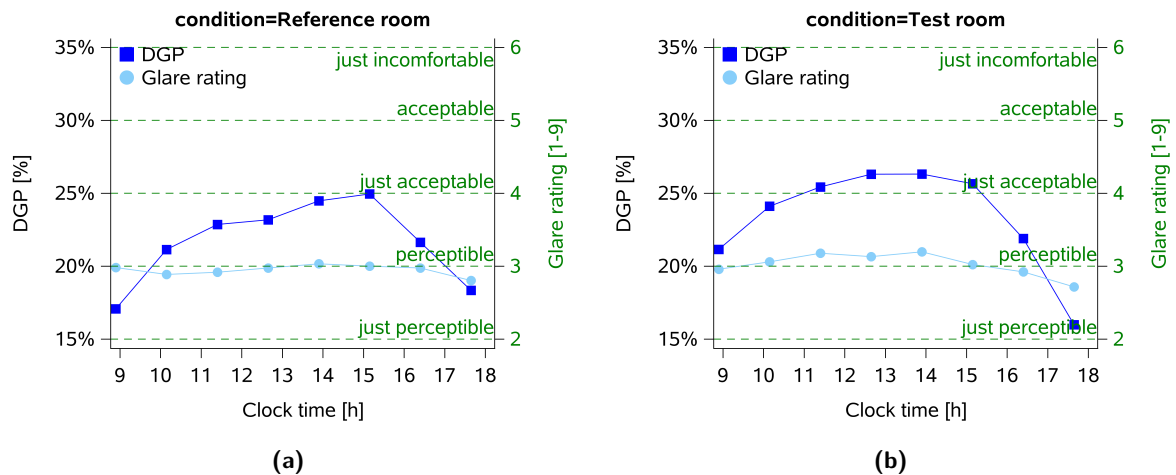


**Figure 3.39** – Time course of the Daylight Glare Probability (DGP) index (dark blue, left y-axis) and subjective visual comfort ratings (light blue, right y-axis) in the *Reference* room (a) and in the *Test* room (b), averaged across participants during the time in the office and aligned to clock time.

Table 3.5 summarizes the results of subjective assessments in the two conditions.

Variable	Range [min-max]	<i>Reference</i> room mean $\pm$ SD	<i>Test</i> room mean $\pm$ SD	p-value
Sleepiness	[0-100]	31.0 $\pm$ 16.3	32.0 $\pm$ 17.6	0.99
Mood	[0-100]	70.9 $\pm$ 13.9	69.8 $\pm$ 13.7	0.02*
Thermal comfort	[0-100]	54.9 $\pm$ 8.7	53.3 $\pm$ 7.2	0.25
Subjective glare (visual comfort)	[1-9]	2.9 $\pm$ 1.5	3.0 $\pm$ 1.5	0.8

**Table 3.5** – Summary of results (mean  $\pm$  SD) of subjective sleepiness (0 = extremely alert, 100 = extremely sleepy), mood (0 = very bad mood, 100 = very good mood), thermal comfort (0 = extremely cold, 100 = extremely warm), perceived glare (from 1 = imperceptible to 9 = intolerable). \* = significant difference between the two conditions.

### 3.3.9 Correlation analysis

An exploratory correlation analysis was carried-out to find any associations among the main variables presented in this Chapter (i.e., lighting variables, physiological measures, cognitive performance, sleepiness, mood, room temperature, thermal comfort). This analysis was performed using one averaged value per participant and condition, for each of the included variables. The correlation matrix is shown in Figure C.1, in the Appendix C. The significant correlations and the respective p-values are highlighted, where the colour indicates the Spearman's correlation coefficient (i.e., the direction: red for negative correlations, blue for positive correlations). On the other hand, blank cells indicate no statistically significant correlations. The most relevant correlations are included in the discussion in the next section.

### 3.4 Summary and discussion

The study presented in this Chapter was aimed at exploring the effects of a lighting strategy involving an automated daylight-responsive controller together with an intensive use of daylighting (presented in Chapter 2) on circadian markers (melatonin, cortisol and DPG), as well as on cognitive performance, mental effort, sleepiness, mood, visual and thermal comfort on young participants during normal office hours.

As already noted in section 2.4, both rooms used for the study already benefited from a considerable daylight flux thanks to the large windows on the south-oriented façade of the building. During the study, objective monitoring of lighting conditions via the sensors fixed in the two office rooms revealed overall higher vertical illuminance and melanopic EDI (at the eye level) in the *Test* room when compared to the *Reference* room, especially during morning hours. The light pattern during the day was dynamic in both rooms with highest  $E_v$  values around noon and lower at the end of the working day (inverted U-shape). The obtained averaged time course in the *Test* room corresponded to the pattern desired when designing the controller algorithm. On the other hand, in the *Reference* room, with no automated controller,  $E_v$  was significantly lower until the early afternoon and similar, or slightly higher than in the *Test* room, after 15:00.

Interestingly, individual measurements of illuminance at the eye by means of the wearable devices did not confirm such large differences of light exposure between the two conditions, likely due to a substantial impact of the angle of gaze and head movements, confirming findings of previous studies [Sarey Khanie et al., 2013; Broszio et al., 2018; Adamsson et al., 2019; Peeters et al., 2020]. This suggests that individual behavioural aspects, such as head movements and gaze direction, need to be considered when assessing individual light exposure. One factor might also be that the steady state light sensor in the office was located between the window and the participant, which might slightly overestimate the  $E_v$  at the user's place, or also underestimate it when the sensor was 'protected' from direct sunlight by a light shelf.

The individually accumulated  $E_v$  at the end of the day was very similar in both conditions. But the accumulation of  $E_v$  was faster in the *Test* room, such that 50% of the accumulated  $E_v$  was reached 50 minutes earlier due to the higher  $E_v$  in the morning hours, when compared to the *Reference* room.

Concomitant with the earlier 'light dose' accumulation, a significantly earlier melatonin onset and an earlier rise of peripheral heat loss (DPG) were observed in the *Test* room. Also, the decline of DPG in the morning, which has been shown to facilitate sleep pressure dissipation [Kräuchi et al., 2004], occurred earlier during the week in the *Test* room, confirming the phase-advance in the circadian system. Consequently, phase angles of entrainment became significantly longer for both melatonin and DPG in the *Test* compared to the *Reference* room, because sleep times were scheduled to remain constant.

On the other hand, such shift could not be observed in the melatonin offset, nor in the cortisol peak. This could be due to the lack of a 24-hour sampling period, as in some of the participants both melatonin secretion offset and cortisol peak might have occurred before the first salivary sample was taken in the morning.

Overall, these physiological results suggest that the use of an automated controller together with an optimized lighting system during the day has the potential to advance circadian phase markers, even under semi-naturalistic conditions which included exposure to electric light in the evening.

Although the analysis of seasonal and gender differences was beyond the main scope of this thesis, their effects were also explored, even though participants were not equally balanced between the three "seasons" (the majority of them came in the mid-seasons). The only seasonal differences were found with the wearable light sensor, with lower  $E_v$  and earlier half-maximum responses occurring in winter compared to the other seasons. One interpretation could be that in winter the total accumulated light dose at the end of the day was lower, and thus the half-maximum dose was reached earlier. In summer, the accumulated light dose was higher than in the other seasons, likely because participants were exposed to daylight for a longer time outside of the office hours: as a result, the half-maximum growth occurred later.

These seasonal differences in individual light exposure do not seem to be reflected in the circadian markers, where generally no seasonal effects were observed. An exception was found in the rise of the DPG in the evening, which occurred earlier in mid seasons and later in summer ( $p < 0.05$ ); also the phase angle between DPG rise and sleep onset was longer in mid seasons and shortest in summer.

Generally, none of the variables showed significant sex differences, except for an earlier DPG decline in the morning in males than in females. The slight and not statistically significant trend for a larger skin temperature gradient (i.e., a "more negative" DPG) in females might be due to variations of CBT across the menstrual cycle, which is lower during the follicular phase and higher during the luteal phase [Kräuchi et al., 2014], which we did not monitor in our study.

The positive effects of the lighting strategy including an automated daylight-responsive controller for blinds and electric light on the circadian markers did not extend to better cognitive performance. In contrast to our hypotheses, reaction times in PVT were significantly slower in the *Test* than in the *Reference* room. Since we could exclude potential technical differences between the two office rooms (see section 3.2) other explanations are warranted. It seems that beyond a certain threshold, higher  $E_v$  and melanopic EDI may not be as effective at improving sustained attention as it is for advancing circadian rhythms. This is in accordance with some other studies which did not find a beneficial effect of bright light on cognitive performance either [Souman et al., 2018; Leichtfried et al., 2015; Huiberts et al., 2016].

The results of the 2-back and 3-back tasks are in the same line, with better accuracy scores in the *Reference* than in the *Test* room only during summer, while 0-back, used as a control task for compliance, did not show significant differences between the two conditions. Self-estimated perceived

mental effort did not differ between the two conditions (except for one time point in the morning in winter), which suggests that the different lighting conditions and the differences in cognitive performance (see below) were not reflected by differences due to the perceived mental load.

Also, subjective sleepiness did not vary between the *Test* and the *Reference* room but was overall higher in winter than in the two other seasons. The observed time course goes along with the expected homeostatic and circadian diurnal variation of sleepiness: with increasing time awake, homeostatic sleep pressure increases and thus sleepiness. Averaged individual  $E_v$  during office hours and accumulated  $E_v$  were associated with lower subjective daytime sleepiness (see correlation table in Appendix C), confirming the positive link between brighter lighting levels and greater alertness confirmed by many controlled laboratory studies [Cajochen, 2007; de Kort & Smolders, 2010; Smolders & de Kort, 2014]. Higher sleepiness was also associated with lower DGP and worse mood. Mood ratings showed that participants seemed to be in a slightly better mood in the *Reference* room, however the difference between the two conditions was very small, and most importantly, on a scale from 0 to 100 the average mood rating in both rooms was  $\sim 70$ , which is definitely on the "happier" side. Interestingly, a better mood was associated with higher scores in 0-back and 2-back, but also with higher reaction times in PVT (which means slower responses).

Thermal comfort was very similar in the two conditions, with slightly warmer subjective temperature perceptions in the *Reference* room only in mid-seasons, which most likely also reflect the warmer room temperatures, even though room temperatures were higher in the *Reference* room across all seasons.

The objective measure of visual comfort, Daylight Glare Probability (DGP), was in a comfortable range and overall slightly higher in the *Test* room, mostly in summer and mid-seasons, as a consequence of the higher illuminance levels from both daylight and electric lighting. Subjectively though, glare was perceived as higher in the *Test* room only in summer, while in the mid seasons, participants perceived higher glare in the *Reference* room. Objective and subjective assessments of glare do not seem to follow the same curve during the day. Indeed, the mechanisms behind discomfort glare perception are not well understood: glare sensation indeed is influenced by several different factors such as time of day, age, season, chronotype, room temperature, and many others [Pierson et al., 2017]. Also the rating scale used for subjective assessments plays a role in the outcome [Fotios, 2015].

Except for the circadian markers, cognitive performance, sleepiness and thermal comfort showed some interactions with seasons, as it was observed for both individual illuminance and thermal comfort. About the possible reasons for the worse performance in the *Test* room in summer (and in part in mid seasons) can only be speculated.

Firstly, it is possible that the lighting conditions were too bright in summer in the *Test* room for sustained attention and working memory, whereas in winter, when the contribution from daylight was generally lower, this was not the case, and there were no statistically significant differences

in the cognitive tests either. Maybe in the *Reference* room the illuminance levels were already sufficient to elicit maximum cognitive performance, and increasing  $E_v$  and melanopic EDI further would not lead to any improvement. This might suggest that there is a saturation point for some non-visual responses to light (in terms of neurobehavioural performance), or even that the functional relationship between light and response has an inverted U-shape: this would suggest that increasing illuminance beyond a maximum would result in performance decrements. Indeed, in winter, when light exposure was significantly lower, cognitive performance was overall better in both conditions.

A second explanation for the neurobehavioural decrements in the *Test* room in summer could be room temperature, such that it was too hot to maximally perform. This argument can be rejected since it was on average warmer in the *Reference* than in the *Test* room in all seasons, and these warmer room temperatures were also accompanied by warmer subjective thermal perceptions in the *Reference* room during mid seasons.

A third interpretation might be that the higher objective glare (DGP) in the *Test* room was compromising directly or indirectly cognitive performance, especially in summer. This factor cannot be excluded a priori because there is no mechanistic evidence possible from our data. At least subjectively, the higher DGP was not perceived as higher, since subjective visual comfort was only during mid seasons lower in the *Test* than in the *Reference* room, but not in summer. As already stated, despite a significantly higher glare probabilities in the *Test* room, the averaged values were still below visual discomfort threshold.

However, this aspect is also not trivial, since DGP and subjective glare ratings did not follow the same time course, meaning that an "objectively" glaring situations might not be perceived as glare, as it is known for daylight conditions [Chauvel et al., 1982; Osterhaus, 2001; Pierson et al., 2017]. Interestingly indeed, mental effort showed a positive correlation with DGP (objective glare) but a negative one with subjective glare (see correlation table in Appendix C): in other words, a high mental effort was associated with high (objective) DGP but also with low subjective glare. Besides, it must be noted here that the tasks involved auditory stimuli exclusively, and not visual ones, thus the luminous contrast between computer screen and surrounding does not seem to be an explanation for differences in performance due to mitigated vision.

To conclude, we found that an automated daylight-responsive controller implemented in a room with advanced daylighting design and applied in a balanced cross-over study with young participants led, as hypothesized, to higher  $E_v$  (measured by wearable sensors) and earlier accumulation of  $E_v$  in the first half of the days spent in the office, when compared to a *Reference* room ('standard' office). Concomitant with these higher lighting variables in the *Test* room, there was a circadian phase advance of melatonin onset and the DPG of skin temperatures. In contrast to our hypotheses, the effects on reaction time and accuracy in cognitive performance tests revealed better results in the *Reference* room especially during summer, which might be indirectly linked to higher room temperature in the *Reference* room and/or to saturation effects of  $E_v$  (with higher objective but not

subjective glare levels) in the *Test* room which was also highest in summer. It might be that the combined factors, higher  $E_v$  and DGP in the *Test* room in summer and lower room temperatures led to lower cognitive performance in the *Test* but not in the *Reference* room.

The correlation matrix in the Appendix C shows that room temperature, in fact, was positively correlated with mental effort (MERS), which suggests that a warmer environment increases the perception of mental effort. High temperature was also associated with high individual illuminance and DGP, which shows once again the impact of seasons. Interestingly, there was also an association with the skin temperature gradient DPG. As seen, room temperature differed between the two conditions, averaging at 23.1°C in the *Test* room and at 23.9°C in the *Reference* room. The mean DPG, averaged per hour, was -2.35°C during the week in the *Test* room and -2.24°C during the week in the *Reference* room. Here, a smaller gradient indicates higher peripheral skin temperature and thus higher heat loss. The correlation table indicates that warmer room temperature is associated with a higher (i.e., more positive) DPG, which is what happened in this case in the *Reference* room. This indicates that there was a response in the body's thermal regulation to the increase in room temperature.

# 4

## Practical implementation in an open-plan office

---

This Chapter presents a first practical implementation of an automated controller for blinds and electric lighting in a different set up. The test bed here is an open plan office in the NEST infrastructure, a new experimental building at the Swiss Federal Laboratories for Material Science and Technology (EMPA) in Dübendorf (Zürich, Switzerland). The aim of this work is to adapt the automated blinds and lighting controller to an open-plan working space. This study started a year ago and is still ongoing.

### 4.1 Motivation

An extensive survey in office workers revealed that employees working in open-plan offices reported lower health status and job satisfaction compared to people working in cell offices<sup>a</sup> [Danielsson, 2008]. Moreover, employee's satisfaction and motivation significantly decreased after they moved from a conventional office to an open-plan office containing no walls or partitions between workstations [Oldham & Brass, 1979].

The main issue in open plan offices is that people are sitting in different positions and orientations with respect to the windows, being exposed to different lighting conditions and perceiving different degrees of discomfort glare. This phenomenon can often lead to situations in which a lighting scenario is optimal for one user but inappropriate for the other, causing visual discomfort and low task performance. An optimized automated control solution for shadings and lighting can preserve the visual comfort of most of the users simultaneously, without compromising light sufficiency. Among other advantages of such an automated controller on biological functions and cognition, preserving visual comfort would also allow to increase motivation and task performance.

Luminous conditions that cause visual discomfort or distraction from tasks affect visual acuity and comfort, which have a direct effect on task performance and motivation perform a task [Eklund et al., 2000; Veitch et al., 2008]. Lighting conditions also influence appraisal and consequently on mood, that in turns affects the motivation to carry-out a task [Baron et al., 1992]. Regarding existing lighting control systems, a wireless-networked lighting control integrating daylight harvesting, occupancy monitoring and task lighting was developed and tested by Wen & Agogino [2011]. The

---

<sup>a</sup>cell office = single room office.

system showed more than 60% energy savings compared to conventional practice without any control. According to the online platform "Advanced Lighting Guidelines" [New Buildings Institute, Inc. (NBI), 2003], for open-plan offices the user's control of task lighting induces higher worker satisfaction, and controls should be designed to minimize visual distraction. For this purpose, state-of-the-art HDR vision sensors can be adopted to evaluate the indoor lighting conditions in the framework of customized lighting control systems.

### 4.2 The SolAce unit at NEST

The NEST building was set up by different collaborative teams at the EMPA in Dübendorf (Zürich, Switzerland,  $47^{\circ}23'54''\text{N}$   $8^{\circ}37'10''\text{E}$ , at 440 m above sea level). The main objective of the NEST building is testing, tweaking and demonstrating new sustainable building technologies under realistic conditions. The NEST building (in Figure 4.1) has a modular structure and is housing several units featuring the latest research, development and innovation in the field of the construction industry.



**Figure 4.1** – Outdoor view of the NEST building in Dübendorf. The SolAce unit at the second floor of the building is indicated by the red rectangle.

The SolAce-REcomfort Unit has been designed and realized by the Solar Energy and Building Physics Laboratory (LESO-PB) together with the Laboratory of Integrated Performance in Design (LIPID, EPFL). Built in collaboration with Lutz Architects and EMPA, the unit is an Energy-Plus and Low Carbon combined working/living space. Since the finalization of its construction in 2018, the unit has been used to showcase and test multi-functional façade technologies developed by EPFL in partnership with industrial companies. The unit is characterized by a multifunctional façade, which results in a combined living and working environment with a low CO<sub>2</sub> footprint. Both solar photovoltaic and thermal collector systems are installed on the SolAce façade. These systems allow to cover the hot water demand on the one hand and the electrical energy demand on the other,



thus leading to an overall positive energy balance. Furthermore, innovative, micro-structured glazing ensures optimal utilization of daylight and solar heat gain.

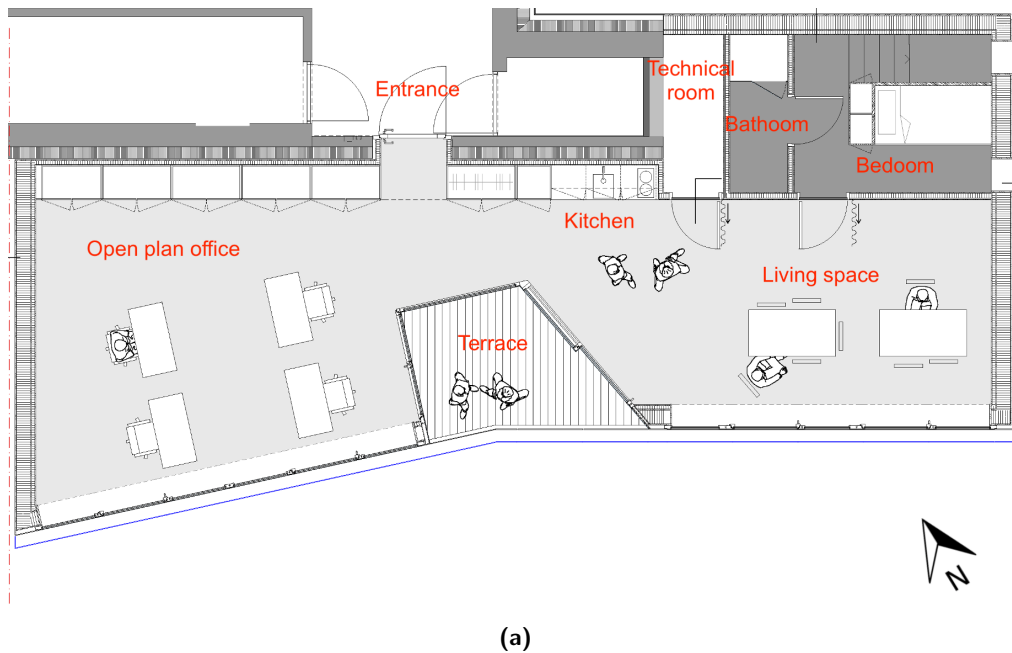


**Figure 4.2** – a) Plan of SolAce (made by LUTZ Architectes Sàrl, Givisiez, Switzerland); b) indoor view of the working space (open plan office); c) the living space. Photographs: G. Vaitl.

The unit is a combined working/living space of 94 m<sup>2</sup> floor area (Figures 4.2 and 4.3). It includes an open-plan office (on the left side) and a living room (on the right side), which can be converted into single spaces by closing the specific partition curtains. The main façade of the unit is South-West oriented.

The lighting system for the entire unit was designed and supplied by Regent Lighting (Basel, Switzerland). The open plan office area is equipped with 12 luminaires hosting dimmable LED lamps (model: Solo Slim LED), suspended at 2.3 m from the floor, providing both direct and indirect light flux (as can be seen in Figure 4.2a). The installation provides up to 1000 photopic lux at the eye level on a vertical plane, and the correlated colour temperature (CCT) is tunable within the range

## Chapter 4. Practical implementation in an open-plan office

2700-6500 K. The luminaires are connected through a DALI bus connection and can be controlled manually or automated.

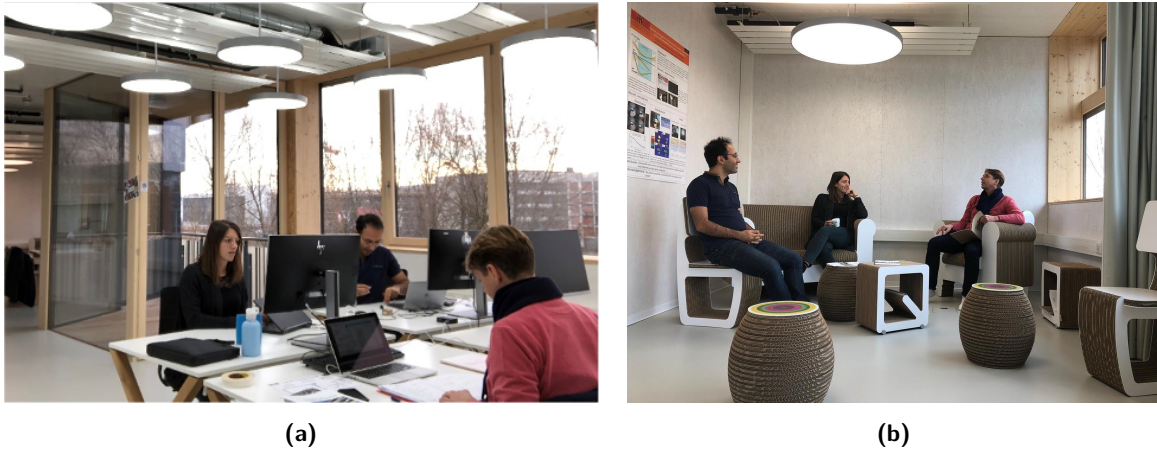


Figure 4.3 – Working (a) and chilling (b) in SolAce. Picture: A. Motamed.

The windows in the open plan office are equipped with two motorized venetian blinds manufactured by Griesser AG (Aadorf, Switzerland), as shown in Figure 4.4.



Figure 4.4 – Motorized venetian blinds in the open plan office.

### 4.3 Experimental setup

State-of-the-art Glare Meters (described in section 2.1.3) are installed in different positions inside the open plan office space. One of them is installed on the ceiling facing downwards (Figure 4.5a), and is used to estimate the work plane illuminance  $E_h$  starting from the average luminance of the pixels within the red rectangle (see Figure 4.5b). The calculation of illuminance from luminance is based on the assumption that all surfaces included in the rectangle are *Lambertian*, i.e., the surfaces luminance

is isotropic (the apparent brightness is constant in any angle of view of the observer). Given this assumption, the work plane illuminance  $E_h$  is directly proportional to the observed luminance from the ceiling [Motamed et al., 2017]. To find the coefficient of proportionality, a validation procedure needs to be done by using an illuminance meter, as described for instance in [Motamed et al., 2017]. Vertical illuminance and DGP are assessed by the Glare Meters installed on the back side of the



**Figure 4.5** – a) Glare Meter installed on the ceiling; b) greyscale image captured by the sensor: the average work plane illuminance is estimated starting from the average luminance of the pixels within the red rectangle (which can be adjusted via software according to the requirements).

computer screens, facing in different view directions. One example is shown in Figure 4.6a. The idea is to have several Glare Meters monitoring DGP and illuminance in different directions.

The devices are integrated into a data communication platform at NEST (see Figure D.2 in the Appendix D) and send data to the server via Wi-fi. The platform includes also the algorithm for the control of blinds and electric lighting, which is currently being developed and tested.

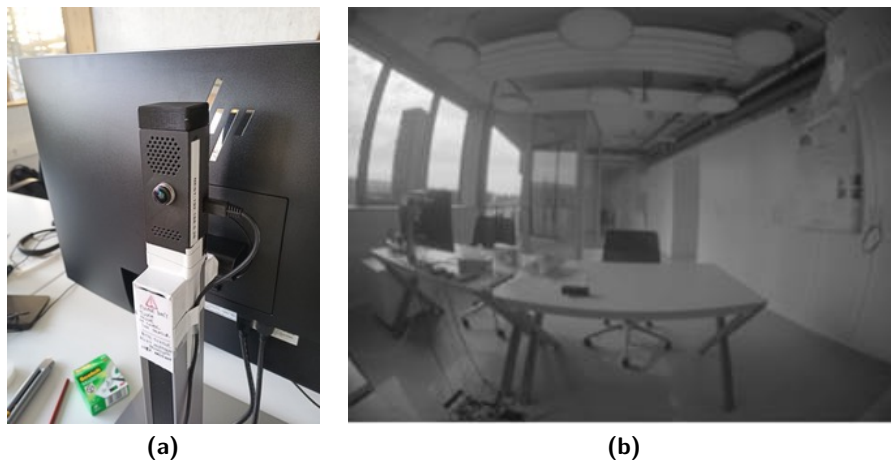


**Figure 4.6** – a) Glare Meter installed on the computer screen, used to assess vertical illuminance and Daylight Glare Probability at the eye level (here, the sensor is oriented towards south-east); b) greyscale image captured by the sensor.

### 4.4 First monitoring results

The data communication platform has been tested for several weeks starting in spring 2021, and so far has worked reliably. As an example of some of the outcome variables, Figure 4.7 shows the continuous time course of vertical illuminance ( $E_v$ ), Daylight Glare Probability (DGP) and work plane luminance during 5 days in May 2021. The vertical illuminance and DGP reported here were monitored by the Glare Meter fixed on the back side of the computer screen, at the approximate eye level of a user sitting at the desk, as shown in Figure 4.6a. On the other hand, the average work plane luminance (in  $\text{cd}/\text{m}^2$ ), used to estimate  $E_h$  as described in the previous section, was recorded by the Glare Meter installed on the ceiling facing downwards, as shown in Figure 4.5a. The preliminary results in Figure 4.7 show the dynamic variations of lighting conditions (i.e.,  $E_v$ , DGP and  $E_h$ ) across several days, also reflecting changes in weather conditions and/or by the automated/manual regulation of blinds and electric lighting by the occupants who occasionally are in the unit.

### 4.5 The control algorithm

As mentioned at the beginning of this Chapter, the automated control system is currently in the testing phase of this ongoing project. A first, simple algorithm has been designed to automatically control the two venetian blinds and the electric lighting in the open-plan office. The algorithm, programmed by the author and the student Haoyuan Sun, integrates  $E_v$ , DGP and  $E_h$ , room temperature, blinds position and slat angle, electric lighting status (dimming power and CCT). The execution diagram in Figure 4.8 represents the main steps on which the algorithm is based.

### 4.6 Aims and future directions

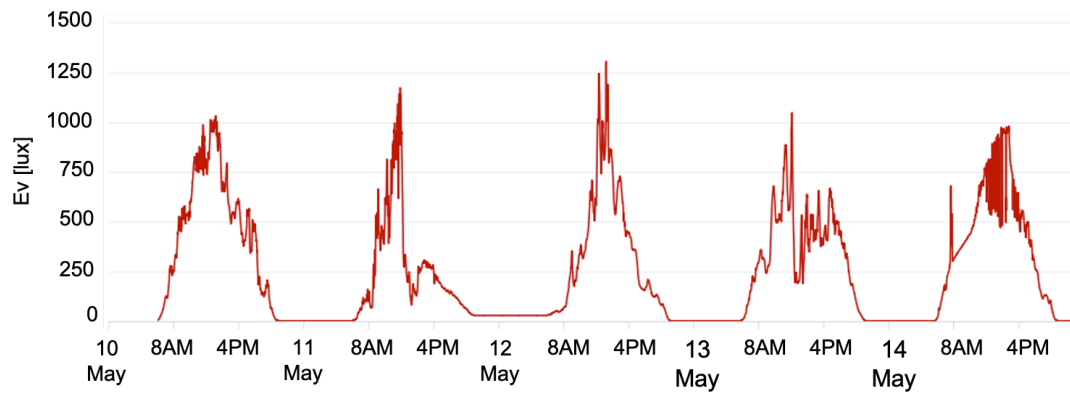
Currently, the data recorded by Glare Meters in different relative positions in the office space is continuously being monitored. Further work is needed to fine-tune the control parameters and validate the system also across different seasons of the year. For instance, the variations in dimming power and CCT of the electric lighting during the day are still to be integrated. Further work is needed to fine-tune the control parameters and validate the system also across different seasons of the year. In addition, fast lighting changes due to weather variations during the day need to be integrated by adjusting the dimming power and CCT of the electric lighting. The idea is to pre-set different lighting levels and CCTs (based for instance on melanopic EDI) according to the time of day, in order to support optimal non-visual functions and well-being, (see Chapter 3).

The main objectives of this project are:

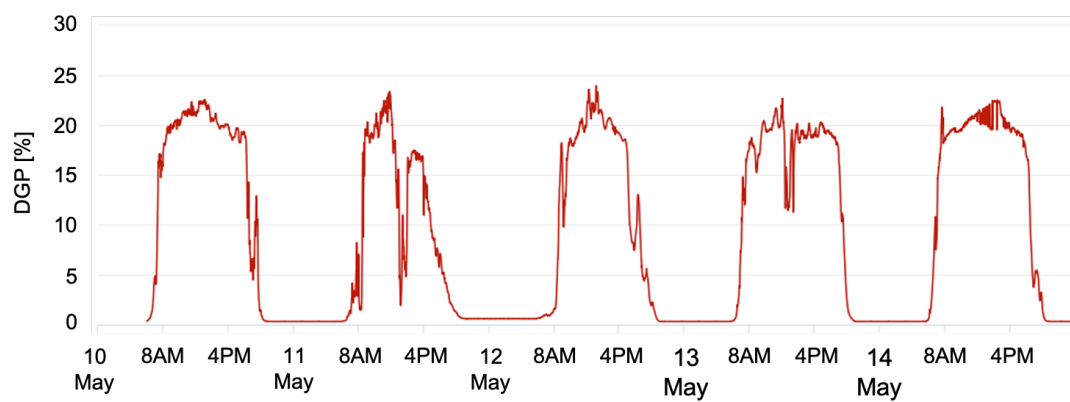
- to provide sound visual comfort and lighting sufficiency for office occupants sitting at different locations and orientations in the open plan office;

- to adequately support non-visual functions (e.g., alertness, circadian entrainment);
- to mitigate the energy demand for both electric lighting (by prioritizing daylight over electric light), and heating/cooling (by means of a proper management of solar heat gains).

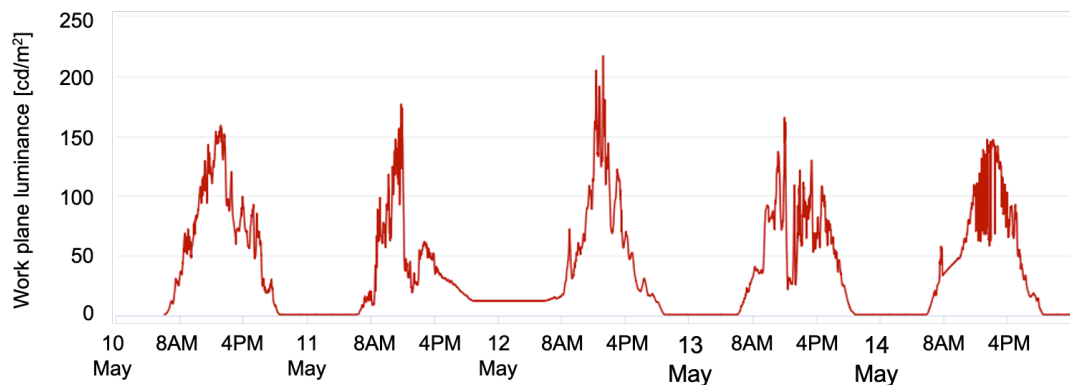
These three aims also need to be tested and validated with users working in the open plan office space and using the living space regularly.



(a) Time course of vertical illuminance  $E_v$  at the eye level over 5 days, monitored in the open office space of SolAce



(b) Daylight Glare Probability at the approximate eye level over 5 days, monitored in the open office space of SolAce.



(c) Average horizontal work plane luminance over 5 days, monitored in the open office space of SolAce.

**Figure 4.7** – First monitoring results in SolAce: vertical illuminance (a), Daylight Glare Probability (b) and average luminance of the work plane (c), all measured by the Glare Meters during 5 days starting from May 10, 2021. The vertical illuminance and DGP were monitored by the Glare Meter fixed on the computer screen, at the approximate eye level of a user sitting at the desk as shown in Figure 4.6a, and oriented towards south-east. The work plane luminance (in  $\text{cd}/\text{m}^2$ ) was recorded by the Glare Meter installed on the ceiling and facing downwards, as shown in Figure 4.5a.

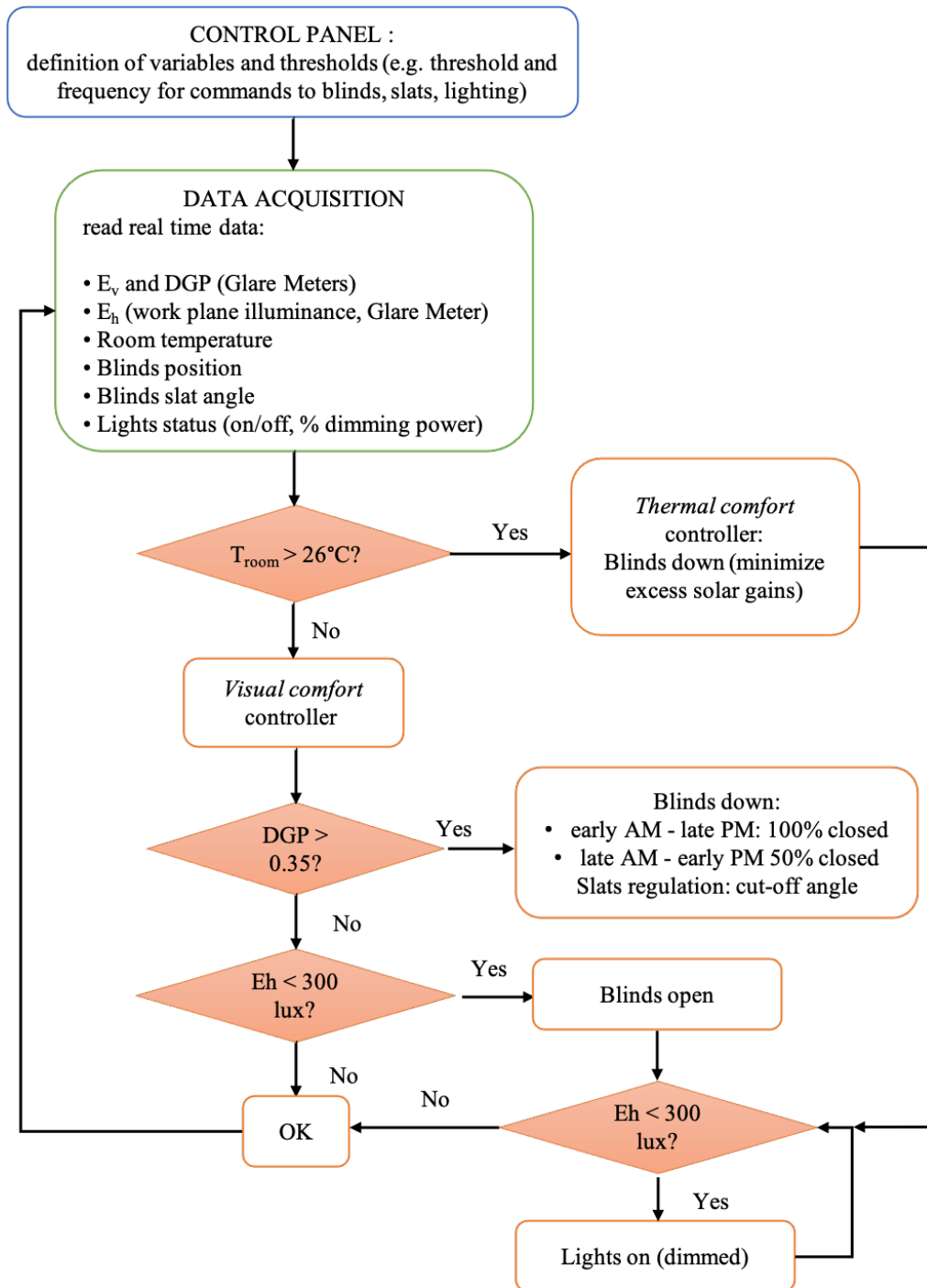


**Figure 4.8** – Execution diagram of the first version of the control system for blinds and electric lighting in the SolAce unit.  $E_v$  = vertical illuminance; DGP = Daylight Glare Probability;  $E_h$  = work plane (horizontal) illuminance.





# 5

## General discussion and conclusion

---

The main objectives of this thesis, as stated in Chapter 1, were the following:

- To adopt and implement a lighting strategy that includes an advanced daylighting room design and a daylight-responsive automated controller, integrating daylighting and electric lighting dynamically, in order to maintain visual comfort at the desk in a defined range and optimize non-visual functions and circadian entrainment (Chapter 2).
- To test the effects of the strategy on non-visual functions and visual comfort of young volunteers in real office rooms in a within-subject cross-sectional study (Chapter 3).
- To implement the automated controller in an open plan office in an experimental building (Chapter 4).

After the design and thorough validation process of its algorithm, the control system was implemented in the framework of a field study including 34 participants over a time span of approximately one year. The controller was applied in one room at the LESO solar experimental building and was compared with an adjacent room with no automated control, representative of a standard office room. The study participants spent five days in each of the room; data collected during the study included lighting conditions, room temperature, energy consumption for electric lighting and space heating, physiological variables (i.e., salivary melatonin and cortisol concentration, skin temperature), cognitive performance and subjective comfort assessments. The main achievements of this work are summarized in the next section.

### 5.1 Achievements and discussion

The automated controller for blinds and electric lighting demonstrated to function in a stable and effective way. Thanks to the ad-hoc design of the control rules, the system was able to always maintain illuminance levels above the pre-set minimum, in all weather conditions and during the whole year. At the same time, it could prevent the occurrence of discomfort glare at the office desk, ensuring a sound visual comfort throughout the day in the office.

In addition, the automated control system was implemented for the first time also in a larger open plan office, and preliminary assessments of the monitored lighting conditions were presented a

the end of the thesis (Chapter 4).

The comparison between the two rooms in terms of lighting conditions (both vertical illuminance,  $E_v$ , and melanopic Equivalent Daylight Illuminance, EDI) confirmed that the lighting strategy provided significantly higher  $E_v$  and melanopic EDI at the eye in the *Test* room, when compared to the *Reference* room. More importantly, the time course during the day in the *Test* room followed the desired pre-set dynamic curve similar to the daylight pattern.

Illuminance measured at the eye by wearable devices did not show such large differences between the two rooms, but importantly, participants were exposed to higher illuminance levels in the morning during the week in the *Test* room compared to the *Reference* room.

Such different timing of the light exposure occurred concomitantly with earlier accumulation of the vertical illuminance (or 'light dose') during the week in the *Test* room, such that half of the response was reached 50 minutes earlier than in the *Reference* room. For the physiological measures we found, as hypothesised, a significant circadian phase advance in melatonin secretion and the skin temperature gradients (DPG). The association between higher lighting levels in the office and circadian phase advance is confirmed by a negative correlation between  $E_v$  (measured by the fixed HDR vision sensor) and the rise time of DPG (see correlation matrix in Figure C.1), which means that higher  $E_v$  in the office was associated to an earlier rise of the DPG. Also a longer phase angle of entrainment of the DPG rise was associated with higher  $E_v$ . In addition, lower subjective sleepiness during the day at the office was associated with higher individual illuminance.

The results give evidence that such an office lighting, regulated by an automated control system, can advance the circadian phase of melatonin and DPG without changing the sleep timing. The observed substantial circadian phase advance of melatonin onset and distal-proximal skin temperature gradient (DPG) rise under semi-realistic office conditions with young participants could be a useful tool in clinical settings, for example in patients with delayed sleep phase syndrome (DSPS) [Weitzman et al., 1981]. Our results corroborate findings from the literature, where it was shown that brighter morning light exposures can advance circadian phase (including sleep/wake timing) [Duffy & Wright Jr., 2005] and is an effective treatment for such disorders [Rosenthal et al., 1990; Wilson et al., 2018]. Thus, translation of our findings into practice by using smart 'phase advancing' office lighting, enabled by automated controllers, could be an asset at workplaces in the future.

Late chronotypes and patients suffering from DSPS could benefit from the presented optimized office lighting control, as it favours an earlier circadian phase and prevents further delays. Another application would be in schools and universities. It was shown that daylight or morning light with greater portions of short-wavelengths lighting can be used as a countermeasure to mitigate such negative phase delaying effects of light in the evening, since it reduces the magnitude of phase shifts [Münch et al., 2017; Smith et al., 2009; Geerdink et al., 2016; Moderie et al., 2017], probably by desensitisation effects to evening light exposure. Therefore, late chronotypes and persons suffering from DSPS could benefit from the presented optimized office lighting, as it favors a stable circadian

phase and prevents further delays. This beneficial effect would be even more effective if combined with limited exposure to short-wavelength or bright light (emitted also from screens) in the evening [Esaki et al., 2016].

In contrast to our hypotheses, cognitive performance was higher in the *Reference* room, predominantly in summer. The lower cognitive performance in the *Test* room could be linked to illuminance saturation concomitant with higher DGP but rather not too high room temperature, since the latter was lower than in the *Reference* room (see discussion in section 3.4). It will be interesting to define lighting levels for all purposes, based on inter-individual differences which supports high cognitive performance. A model with an inverted U shape for lighting and cognitive performance is possible as is known for productivity and stress [Wilke et al., 1985]. Since none of the cognitive performance results were significantly correlated with any of the lighting data, we may speculate that the effect was rather indirect, and may be even accumulated and induced by other factors than or office lighting conditions. Interestingly, with less daylight in winter, there were no significant differences in cognitive performance between both conditions, for example in sustained attention. The results were even significantly better (i.e., faster RT) than in summer. Since we can exclude substantial differences due to interindividual differences in this within-subject study design, it is rather something like motivation, which we did not assess but could have had an effect. From visual inspection of the MERS, mental efforts were at least 10% lower in winter, than for example in summer (though not statistically significant), indicating that it probably was easier for participants to stay focused at lower efforts in winter than summer. In winter, usual individual light exposure is lower [Thorne et al., 2009], as we also found in our data, which makes a bright office even brighter, and therefore, the threshold of the automated controller is perfectly appropriate in winter but maybe needs adjustment in summer and perhaps adaptation of room temperature should also be included. Therefore, based on the seasonal differences in cognitive performance in this study, further fine tunings of the automated controller could be made, in order to adapt  $E_v$  especially in summer to inter-individual needs and also in the NEST for open space offices.

## 5.2 Limitations

There are some limitations related to this work which will be discussed.

Firstly, it was not possible for the controller to take into account multidimensional optimizations, for example for thermal comfort, and adaptation to user wishes with self-learning algorithms. The latter was done already in previous work, e.g. [Lindelöf, 2007; Motamed, 2017].

As already stated, the control of the room temperature was not included in the automated controller, because the focus was mainly on lighting and visual comfort. It is well known that excessive solar gains in summer have been a recurring issue in the LESO building in the last years (as the average air temperatures increase) in absence of a sound blinds' management by users and/or an

automated control system. The building does not have any cooling system and relies only on natural ventilation and night cooling, which is sometimes not sufficient to keep a comfortable temperature in the offices. For a sound thermal comfort during mid seasons and summer, when the heating system in the LESO building is normally switched off, it is crucial to control the indoor comfort by using the external textile blinds (which block part of the incoming solar radiant flux) and opening the window during nighttime and in the morning. The building has a heavy thermal mass: as a result, if the indoor space is heated up by excessive solar gains already at the beginning of the working day, it will likely take a long time to cool down the room. In other words, high room temperatures likely derive from the high efficiency of the building in terms of thermal isolation, glazing, passive solar gains, etc., which makes it more challenging for a controller to maintain comfortable conditions. On the other hand, in winter the control of both indoor temperature (usually around 21-22°C on average) and passive solar gains is easier, and the automated controller was more efficient in providing comfortable conditions. We must emphasize the fact that the controller was not designed to optimally manage solar gains and overheating as a first priority, and therefore prevent thermal discomfort: such optimization was beyond the main scope of the presented study.

Participants were not instructed on the use of such switches to regulate the temperature set points, so it is supposed that they did not intervene, however this was not monitored during the study. It is possible that for some study weeks the set points were different between the two rooms, which could partially explain the differences in room temperature and in space heating energy demand. However, the temperature differences can not be justified by a systematic difference in temperature set point for the heaters, but it is most probably due to the different location of the rooms in the building (walls in communication to indoor heated spaces or to the outdoor). Furthermore, participants were free to open/close the windows and there might have been inter-individual behavioural differences in this sense.

Other limitations of the study are certainly linked to the semi-realistic approach: there were no constraints on light exposures out of the office, for instance in the evening hours, or during the lunch break outside the building. Furthermore, there were no instructions for physical activity or meal timing, which may have contributed to individual variability of hormonal and light exposure data between conditions and participants. In addition, during the week in the *Reference* room, participants could use the blinds and electric lighting according to their individual needs, and there was no control regarding their behaviour in this sense.

### 5.3 Summary

Summarising, the presented lighting strategy, consisting of a daylight-responsive automated controller for blinds and electric lighting implemented in an office room with advanced daylighting design, showed its capabilities in providing "healthy" lighting levels and sound visual comfort, while maintaining a

low energy demand overall (despite greater electricity use for lighting).

Importantly, the lighting strategy has been found to have significant circadian phase-resetting potential on healthy young office occupants, without compromising cognitive performance. For a future use, the controller would need to be evaluated and probably fine-tuned to different seasons of the year, defining which preset threshold is best for: 1) physiological measures, and 2) neurobehavioural performance, work productivity and mood.

Most of the existing studies on non-visual effects measuring physiological variables (e.g. salivary hormones) and/or cognitive performance have been conducted in strictly controlled laboratory conditions, and not under realistic daylight conditions. On the other hand, daylight studies on non-visual effects typically evaluate only the lighting environment before it is perceived by the users, and subjective measures of non-visual effects, not considering the objective physiological measures. Therefore, this study is among the first ones using realistic daylight conditions to evaluate the body related non-visual effects.

## 5.4 Outlook

The work presented in this thesis can be considered as a first step towards an automated control strategy of integrated daylighting and electric lighting to support circadian rhythms and high visual comfort at the workplace. Future work should consider refining lighting conditions according to seasons of the year, room temperature thresholds and individual needs and work schedules. In addition, the effects of such an automated controller could be explored in different age groups, for example in older adults.



**Figure 5.1** – Indoor view of the open plan office in the SolAce unit, described in Chapter 4.

Moreover, implementation of such a lighting strategy should be adapted to other indoor working environments such as open plan offices, where the challenge is to provide optimal lighting conditions without compromising visual comfort to occupants sitting in different orientations and positions within the same room. Such an adaptation approach has been addressed in the ongoing project in the SolAce unit in the NEST experimental building (Figure 5.1), presented in Chapter 4.



## References

---

- Aarts, M. P. J., Brown, S. A., Bueno, B., Gjedde, A., Mersch, D., Münch, M., Scartezzini, J.-L., Volf, C., Wienold, J., Wirz-Justice, A., Bodart, M., & Kaempf, J. (2017). Chapter 5. Reinventing daylight. In *Changing perspectives on Daylight: Science, Technology, and Culture* (pp. 33–37). Science/AAAS, Washington, DC.
- Abbott, S. M., Malkani, R. G., & Zee, P. C. (2020). Circadian disruption and human health: a bidirectional relationship. *European Journal of Neuroscience*, 51(1), 567–583.
- Adamsson, M., Laike, T., & Morita, T. (2019). Comparison of static and ambulatory measurements of illuminance and spectral composition that can be used for assessing light exposure in real working environments. *LEUKOS - Journal of Illuminating Engineering Society of North America*, 15(2-3), 181–194.
- Åkerstedt, T. & Gillberg, M. (1990). Subjective and objective sleepiness in the active individual. *International Journal of Neuroscience*, 52(1-2), 29–37.
- Altherr, R. & Gay, J. B. (2002). A low environmental impact anidolic facade. *Building and Environment*, 37(12), 1409–1419.
- Aries, M. (2005). *Human Lighting Demands: Healthy Lighting in an Office Environment*. PhD thesis, Technische Universiteit Eindhoven, The Netherlands.
- Aschoff, J. (1960). Exogenous and endogenous components in circadian rhythms. *Cold Spring Harbor Symposia on Quantitative Biology*, 25, 11–28.
- Aschoff, J. (1965). Circadian rhythms in man. *Science (New York, N.Y.)*, 148(3676), 1427–1432.
- Aschoff, J. (1982). The circadian rhythm of body temperature as a function of body size. In R. Taylor & K. Johanson (Eds.), *A Companion to Animal Physiology* (pp. 173–188). Cambridge: Cambridge University Press.
- Aschoff, J. & Heise, A. (1972). *Thermal Conductance in Man: Its Dependence on Time of Day and on Ambient Temperature*, (pp. 334–348). Springer US.
- Aschoff, J. & Wever, R. (1962). Spontanperiodik des Menschen bei Ausschluß aller Zeitgeber. *Naturwissenschaften*, 49, 337–342.
- Aschoff, J. & Wever, R. (1981). The Circadian System of Man. In *Aschoff J. (eds) Biological Rhythms* (pp. 311–331). Springer, Boston, MA.
- Association Suisse de l'Eclairage (SLG/ASE) (1989). Éclairage intérieur par la lumière du jour. Schweizerische Normen-Vereinigung: Zürich.

## References

---

- ASTM International (2016). Standard practice for visual appraisal of colors and color differences of diffusely-illuminated opaque materials. Technical report, ASTM International, West Conshohocken, PA.
- Baron, K. G. & Reid, K. J. (2014). Circadian misalignment and health. *International Review of Psychiatry*, 26(2), 139–154.
- Baron, R. A., Rea, M. S., & Daniels, S. G. (1992). Effects of indoor lighting (illuminance and spectral distribution) on the performance of cognitive tasks and interpersonal behaviors: The potential mediating role of positive affect. *Motivation and Emotion*, 1(L), 1–33.
- Beersma, D., Comas, M., Hut, R., Gordijn, M., Rüger, M., & Daan, S. (2009). The progression of circadian phase during light exposure in animals and humans. *Journal of Biological Rhythms*, 24, 153–60.
- Begemann, S., van den Beld, G., & Tenner, A. (1997). Daylight, artificial light and people in an office environment, overview of visual and biological responses. *International Journal of Industrial Ergonomics*, 20(3), 231–239.
- Bellia, L., Fragliasso, F., & Stefanizzi, E. (2016). Why are daylight-linked controls (DLCs) not so spread? A literature review. *Building and Environment*, 106, 301–312.
- Benloucif, S., Burgess, H. J., Klerman, E., Lewy, A. J., Middleton, B., Murphy, P. J., Parry, B., & Revell, V. (2008). Measuring melatonin in humans. *Journal of Clinical Sleep Medicine*, 04(01), 66–69.
- Benloucif, S., Guico, M. J., Reid, K. J., Wolfe, L. F., L'Hermite-Balériaux, M., & Zee, P. C. (2005). Stability of melatonin and temperature as circadian phase markers and their relation to sleep times in humans. *Journal of Biological Rhythms*, 20(2), 178–188.
- Berson, D. M., Dunn, F. A., & Takao, M. (2002). Phototransduction by retinal ganglion cells that set the circadian clock. *Science*, 295(5557), 1070–1073.
- Beute, F. & de Kort, Y. A. (2014). Salutogenic effects of the environment: Review of health protective effects of nature and daylight. *Applied Psychology: Health and Well-Being*, 6(1), 67–95.
- Blume, C., Garbazza, C., & Spitschan, M. (2019). Effects of light on human circadian rhythms, sleep and mood. *Somnologie*, 23(3), 147–156.
- Bodart, M. & De Herde, A. (2002). Global energy savings in offices buildings by the use of daylighting. *Energy and Buildings*, 34(5), 421–429.
- Borbély, A. A. (1982). A two process model of sleep regulation. *Human Neurobiology*, 1(3), 195–204.
- Borisuit, A., Deschamps, L., Kämpf, J., Scartezzini, J.-L., & Münch, M. (2013). Assessment of circadian weighted radiance distribution using a camera-like light sensor. In *Proceedings of CISBAT 2013*, (pp. 305–310).
- Borisuit, A., Linhart, F., Kämpf, J., Scartezzini, J.-L., & Münch, M. (2011). Comparison of objective and subjective visual comfort and associations with non-visual functions in young subjects. In *Proceedings of CISBAT 2011 - CleanTech for Sustainable Buildings*, (pp. 361–366).



- Borisuit, A., Linhart, F., Scartezzini, J.-L., & Munch, M. (2015). Effects of realistic office daylighting and electric lighting conditions on visual comfort, alertness and mood. *Lighting Research & Technology*, 47(2), 192–209.
- Borisuit, A., Münch, M., Deschamps, L., Kämpf, J., & Scartezzini, J.-L. (2012). A new device for dynamic luminance mapping and glare risk assessment in buildings. *Proceedings of SPIE - The International Society for Optical Engineering*, 8485.
- Borisuit, A., Scartezzini, J.-L., & Thanachareonkit, A. (2011). Visual discomfort and glare rating assessment of integrated daylighting and electric lighting systems using HDR imaging techniques. *Architectural Science Review*, 53(4), 359–373.
- Boubekri, M. & Boyer, L. L. (1992). Effect of window size and sunlight presence on glare. *Lighting Research & Technology*, 24(2), 69–74.
- Boubekri, M., Lee, J., Macnaughton, P., Woo, M., Schuyler, L., Tinianov, B., & Satish, U. (2020). The impact of optimized daylight and views on the sleep duration and cognitive performance of office workers. *International Journal of Environmental Research and Public Health*, 17(9).
- Boyce, P. (2016). Editorial: Exploring human-centric lighting. *Lighting Research & Technology*, 48, 101–101.
- Boyce, P., Hunter, C., & Howlett, O. (2003). The benefits of daylight through windows. *Troy, NY: Lighting Research Center*.
- Boyce, P. R. (2010). Review: The impact of light in buildings on human health. *Indoor and Built Environment*, 19(1), 8–20.
- Boyce, P. R. (2013). Lemmings, light and health revisited. *LEUKOS: The Journal of the Illuminating Engineering Society of North America*, 8(2), 83–92.
- Boyce, P. R., Veitch, J. a., Newsham, G. R., Jones, C. C., Heerwagen, J., Myer, M., & Hunter, C. M. (2006). Lighting quality and office work: two field simulation experiments. *Lighting Research & Technology*, 38(3), 191–223.
- Brainard, G. C., Hanifin, J. P., Greeson, J. M., Byrne, B., Glickman, G., Gerner, E., & Rollag, M. D. (2001). Action spectrum for melatonin regulation in humans: evidence for a novel circadian photoreceptor. *The Journal of Neuroscience*, 21(16), 6405–6412.
- Brainard, G. C., Lewy, A. J., Menaker, M., Fredrickson, R. H., Miller, L. S., Weleber, R. G., Cassone, V., & Hudson, D. (1988). Dose-response relationship between light irradiance and the suppression of plasma melatonin in human volunteers. *Brain Research*, 454(1-2), 212–218.
- Broszio, K., Knoop, M., Niedling, M., & Völker, S. (2018). Effective radiant flux for non-image forming effects - is the illuminance and the melanopic irradiance at the eye really the right measure? *Light and Engineering*, 26(2), 68–74.
- Brown, T. M. (2020). Melanopic illuminance defines the magnitude of human circadian light responses under a wide range of conditions. *Journal of Pineal Research*, 69(1), e12655.

## References

---

- Brown, T. M., Brainard, G., Cajochen, C., Czeisler, C., Hanifin, J., Lockley, S., Lucas, R., Munch, M., O'Hagan, J., Peirson, S., Price, L., Roenneberg, T., Schlangen, L., Skene, D., Spitschan, M., Vetter, C., Zee, P., & Wright, K. (2020). Recommendations for healthy daytime, evening, and night-time indoor light exposure. *Preprints*, (December).
- Buijs, R. M., Scheer, F. A., Kreier, F., Yi, C., Bos, N., Goncharuk, V. D., & Kalsbeek, A. (2006). Organization of circadian functions: interaction with the body. In A. Kalsbeek, E. Fliers, M. Hofman, D. Swaab, E. van Someren, & R. Buijs (Eds.), *Hypothalamic Integration of Energy Metabolism*, volume 153 of *Progress in Brain Research* (pp. 341–360). Elsevier.
- Burgess, H. J., Savic, N., Sletten, T., Roach, G., Gilbert, S. S., & Dawson, D. (2003). The relationship between the dim light melatonin onset and sleep on a regular schedule in young healthy adults. *Behavioral Sleep Medicine*, 1(2), 102–114.
- Burns, A., Allen, H., Tomenson, B., Duignan, D., & Byrne, J. (2009). Bright light therapy for agitation in dementia: a randomized controlled trial. *International Psychogeriatrics*, 21(4), 711—721.
- Butler, D. L. & Biner, P. M. (1989). Effects of setting on window preferences and factors associated with those preferences. *Environment and Behavior*, 21(1), 17–31.
- Buysse, D. J., Reynolds, C. F., Monk, T. H., Berman, S. R., & Kupfer, D. J. (1989). The Pittsburgh Sleep Quality Index: a new instrument for psychiatric practice and research. *Psychiatry Research*, 28, 193–213.
- Cajochen, C. (2007). Alerting effects of light. *Sleep Medicine Reviews*, 11(6), 453–464.
- Cajochen, C., Blatter, K., & Wallach, D. (2004). Circadian and sleep-wake dependent impact on neurobehavioral function. *Psychologica Belgica*, 44(1-2), 59–80.
- Cajochen, C., Chellappa, S. L., & Schmidt, C. (2014). *Circadian and Light Effects on Human Sleepiness–Alertness*, (pp. 9–22). Springer, Milano.
- Cajochen, C., Frey, S., Anders, D., Späti, J., Bues, M., Pross, A., Mager, R., Wirz-Justice, A., & Stefani, O. (2011). Evening exposure to a light-emitting diodes (LED)-backlit computer screen affects circadian physiology and cognitive performance. *Journal of Applied Physiology*, 110(5), 1432–1438.
- Cajochen, C., Freyburger, M., Basishvili, T., Garbazza, C., Rudzik, F., Renz, C., Kobayashi, K., Shirakawa, Y., Stefani, O., & Weibel, J. (2019). Effect of daylight LED on visual comfort, melatonin, mood, waking performance and sleep. *Lighting Research & Technology*, 51(7), 1044–1062.
- Cajochen, C., Jewett, M. E., & Dijk, D. J. (2003). Human circadian melatonin rhythm phase delay during a fixed sleep-wake schedule interspersed with nights of sleep deprivation. *Journal of Pineal Research*, 35(3), 149–157.
- Cajochen, C., Münch, M., Kobińska, S., Kräuchi, K., Steiner, R., Oelhafen, P., Orgül, S., & Wirz-Justice, A. (2005). High sensitivity of human melatonin, alertness, thermoregulation, and heart rate to short wavelength light. *Journal of Clinical Endocrinology and Metabolism*, 90(3), 1311–1316.

- Cajochen, C., Zeitzer, J. M., Czeisler, C. a., & Dijk, D.-J. J. (2000). Dose-response relationship for light intensity and ocular and electroencephalographic correlates of human alertness. *Behavioural Brain Research*, 115(1), 75–83.
- Chang, A. M., Aeschbach, D., Duffy, J. F., & Czeisler, C. A. (2015). Evening use of light-emitting eReaders negatively affects sleep, circadian timing, and next-morning alertness. *Proceedings of the National Academy of Sciences of the United States of America*, 112(4), 1232–1237.
- Chang, A.-M., Santhi, N., St Hilaire, M., Gronfier, C., Bradstreet, D. S., Duffy, J. F., Lockley, S. W., Kronauer, R. E., & Czeisler, C. A. (2012). Human responses to bright light of different durations. *The Journal of Physiology*, 590(13), 3103–3112.
- Chang, A. M., Scheer, F. A., Czeisler, C. A., & Aeschbach, D. (2013). Direct effects of light on alertness, vigilance, and the waking electroencephalogram in humans depend on prior light history. *Sleep*, 36(8), 1239–1246.
- Chang, A.-M., Scheer, F. A. J. L., & Czeisler, C. A. (2011). The human circadian system adapts to prior photic history. *The Journal of Physiology*, 589(5), 1095–1102.
- Chauvel, P., Collins, J. B., Dogniaux, R., & Longmore, J. (1982). Glare from windows: current views of the problem. *Lighting Research & Technology*, 14(1), 31–46.
- Chellappa, S. L. (2021). Individual differences in light sensitivity affect sleep and circadian rhythms. *Sleep*, 44(2), zsaa214.
- Chellappa, S. L., Gordijn, M. C., & Cajochen, C. (2011). Chapter 7 - can light make us bright? effects of light on cognition and sleep. In H. P. Van Dongen & G. A. Kerkhof (Eds.), *Human Sleep and Cognition Part II*, volume 190 of *Progress in Brain Research* (pp. 119–133). Elsevier.
- Chellappa, S. L., Morris, C. J., & Scheer, F. A. (2019). Effects of circadian misalignment on cognition in chronic shift workers. *Scientific Reports*, 9(1), 1–9.
- Chellappa, S. L., Steiner, R., Blattner, P., Oelhafen, P., Götz, T., & Cajochen, C. (2011). Non-visual effects of light on melatonin, alertness and cognitive performance: can blue-enriched light keep us alert? *PLoS ONE*, 6(1), 1–11.
- Chellappa, S. L., Steiner, R., & Oelhafen, P. (2013). Acute exposure to evening blue-enriched light impacts on human sleep. *Journal of Sleep Research*, 22(5), 573–580.
- Choudhury, A. K. R. (2014). Chapter 1 - Characteristics of light sources. In A. K. R. Choudhury (Ed.), *Principles of Colour and Appearance Measurement* (pp. 1–52). Woodhead Publishing.
- Christensen, S., Huang, Y., Walch, O. J., & Forger, D. B. (2020). Optimal adjustment of the human circadian clock in the real world. *PLoS Computational Biology*, 16(12 December), 1–18.
- Coccolo, S., Kämpf, J., & Scartezzini, J.-L. (2015). The EPFL campus in Lausanne: new energy strategies for 2050. *Energy Procedia*, 78, 3174–3179.

## References

---

- Commission Internationale de l'Éclairage (CIE) (1926). Proceedings CIE 6th Session 1924, Geneva. Recueil des Travaux et Compte Rendu de Séances. Geneva.
- Commission Internationale de l'Éclairage (CIE) (1987). International Lighting Vocabulary (ILV. Technical report, CIE, Vienna. (updated most recent version: S017/E2020).
- Commission Internationale de l'Éclairage (CIE) (1995). 117:1995 Discomfort Glare in Interior Lighting. Technical report, CIE, Vienna.
- Commission Internationale de l'Éclairage (CIE) (2004). 15:2004 - Colorimetry. Technical report, CIE, Vienna.
- Commission Internationale de l'Éclairage (CIE) (2009). 158:2009 - Ocular Lighting Effects on Human Physiology and Behaviour. Technical report, CIE, Vienna.
- Commission Internationale de l'Éclairage (CIE) (2018). CIE System for Metrology of Optical Radiation for ipRGC-Influenced Responses to Light. Technical report, CIE, Vienna.
- Commission Internationale de l'Éclairage (CIE) (2020).  $\alpha$ -opic Toolbox for implementing CIE S 026. <https://doi.org/10.25039/S026.2018.TB>.
- Cuttle, C. (1983). People and windows in workplaces. In *Proceedings of the People and Physical Environment Research Conference, Wellington, New Zealand*, (pp. 203–212).
- Czeisler, C., Allan, J., Strogatz, S., Ronda, J., Sanchez, R., Rios, C., Freitag, W., Richardson, G., & Kronauer, R. (1986). Bright light resets the human circadian pacemaker independent of the timing of the sleep-wake cycle. *Science*, 233(4764), 667–671.
- Czeisler, C. A., Duffy, J. F., Shanahan, T. L., Brown, E. N., Mitchell, J. F., Rimmer, D. W., Ronda, J. M., Silva, E. J., Allan, J. S., Emens, J. S., Dijk, D.-J., & Kronauer, R. E. (1999). Stability, precision, and near-24-hour period of the human circadian pacemaker. *Science*, 284(5423), 2177–2181.
- Czeisler, C. A., Weitzman, E., Moore-Ede, M. C., Zimmerman, J. C., & Knauer, R. S. (1980). Human sleep: its duration and organization depend on its circadian phase. *Science*, 210(4475), 1264–1267.
- Dacey, D. M., Liao, H.-W., Peterson, B. B., Robinson, F. R., Smith, V. C., Pokorny, J., Yau, K.-W., & Gamlin, P. D. (2005). Melanopsin-expressing ganglion cells in primate retina signal colour and irradiance and project to the LGN. *Nature*, 433(7027), 749–754.
- Danielsson, C. B. (2008). Office type in relation to job satisfaction among employees. *Environment and Behavior*, 40(5), 636–668.
- Danilenko, K. V., Verevkin, E. G., Antyufeyev, V. S., Wirz-Justice, A., & Cajochen, C. (2014). The hockey-stick method to estimate evening dim light melatonin onset (DLMO) in humans. *Chronobiology International*, 31(3), 349–355.
- de Kort, Y. & Smolders, K. (2010). Effects of dynamic lighting on office workers: First results of a field study with monthly alternating settings. *Lighting Research & Technology*, 42(3), 345–360.

- de Zeeuw, J., Papakonstantinou, A., Nowozin, C., Stotz, S., Zaleska, M., Hädel, S., Bes, F., Münch, M., & Kunz, D. (2019). Living in biological darkness: Objective sleepiness and the pupillary light responses are affected by different metamer lighting conditions during daytime. *Journal of Biological Rhythms*, 34(4), 410–431.
- Dewan, K., Benloucif, S., Reid, K., Wolfe, L., & Zee, P. (2011). Light-induced changes of the circadian clock of humans: Increasing duration is more effective than increasing light intensity. *Sleep*, 34, 593–599.
- Dijk, D. J. & Archer, S. N. (2009). Light, sleep, and circadian rhythms: Together again. *PLoS Biology*, 7(6), 7–10.
- Dijk, D. J., Cajochen, C., & Borbély, A. A. (1991). Effect of a single 3-hour exposure to bright light on core body temperature and sleep in humans. *Neuroscience Letters*, 121(1-2), 59–62.
- Dijk, D. J., Duffy, J. F., Silva, E. J., Shanahan, T. L., Boivin, D. B., & Czeisler, C. A. (2012). Amplitude reduction and phase shifts of melatonin, cortisol and other circadian rhythms after a gradual advance of sleep and light exposure in humans. *PLoS ONE*, 7(2).
- DIN 6173-2 (1983). Farbabmusterung; Beleuchtungsbedingungen fuer kuenstliches mittleres Tageslicht (Colour matching; lighting conditions for average artificial daylight). Technical report, DIN.
- Dinges, D. F. & Powell, J. W. (1985). Microcomputer analyses of performance on a portable, simple visual RT task during sustained operations. *Behavior Research Methods, Instruments, and Computers*, 17(6), 652–655.
- Dmitienko, A., Chuang-Stein, C., & D'Agostino, B. (2007). *Pharmaceutical Statistics Using SAS: A Practical Guide*. SAS Publishing.
- Drummond, S. P. A., Bischoff-Grethe, A., Dinges, D. F., Ayalon, L., Mednick, S. C., & Meloy, M. J. (2005). The neural basis of the psychomotor vigilance task. *Sleep*, 28(9), 1059–1068.
- Duffy, J. F. & Czeisler, C. A. (2009). Effect of light on human circadian physiology. *Sleep Medicine Clinics*, 18(9), 1199–1216.
- Duffy, J. F. & Wright Jr., K. P. (2005). Entrainment of the human circadian system by light. *Journal of Biological Rhythms*, 20(4), 326–338.
- Edwards, L. & Torcellini, P. (2002). A literature review of the effects of natural light on building occupants. *National Renewable Energy Laboratory*, 55.
- Einhorn, H. D. (1969). A new method for the assessment of discomfort glare. *Lighting Research & Technology*, 1(4), 235–247.
- Eklund, N. H. & Boyce, P. R. (1996). The development of a reliable, valid, and simple office lighting survey. *Journal of the Illuminating Engineering Society*, 25(2), 25–40.
- Eklund, N. H., Boyce, P. R., & Simpson, S. N. (2000). Lighting and sustained performance. *Journal of the Illuminating Engineering Society*, 29(1), 116–130.

## References

---

- Emens, J. S. & Lewy, A. J. (2005). *Sleep and Circadian Rhythms in the Blind*, (pp. 311–323). Boston, MA: Springer US.
- Esaki, Y., Kitajima, T., Ito, Y., Koike, S., Nakao, Y., Tsuchiya, A., Hirose, M., & Iwata, N. (2016). Wearing blue light-blocking glasses in the evening advances circadian rhythms in the patients with delayed sleep phase disorder: An open-label trial. *Chronobiology International*, 33(8), 1037–1044.
- Figueiro, M. G., Steverson, B., Heerwagen, J., Kampschroer, K., Hunter, C. M., Gonzales, K., Plitnick, B., & Rea, M. S. (2017). The impact of daytime light exposures on sleep and mood in office workers. *Sleep Health*, 3(3), 204–215.
- Finelli, L. A., Achermann, P., & Borbély, A. A. (2001). Individual ‘fingerprints’ in human sleep eeg topography. *Neuropsychopharmacology*, 25(1), S57–S62.
- Foster, M. & Oreszczyn, T. (2001). Occupant control of passive systems: the use of venetian blinds. *Building and Environment*, 36(2), 149–155.
- Fotios, S. (2015). Research note: Uncertainty in subjective evaluation of discomfort glare. *Lighting Research & Technology*, 47(3), 379–383.
- Franta, G. & Anstead, K. (1994). Daylighting offers great opportunities. *Window & Door Specifier-Design Lab*, 40–43.
- Galasiu, A. D. & Veitch, J. A. (2006). Occupant preferences and satisfaction with the luminous environment and control systems in daylit offices: a literature review. *Energy and Buildings*, 38(7), 728–742.
- Gall, D. (2002). Circadiane Lichtgrößen und deren messtechnische Ermittlung. *Licht*, 54, 1292–1297.
- Geerdink, M., Beersma, D. J. M., Hommes, V., & Gordijn, M. C. M. (2016). Short blue light pulses (30 min.) in the morning are able to phase advance the rhythm of melatonin in a home setting. *Journal of Sleep Disorders & Therapy*, 5(2).
- Gentile, N., Dubois, M.-C., & Laike, T. (2015). Daylight harvesting control systems design recommendations based on a literature review. In *2015 IEEE 15th International Conference on Environment and Electrical Engineering, IEEEIC 2015 - Conference Proceedings*.
- Giménez, M., Schlangen, L., Lang, D., Beersma, D., Novotny, P., Plischke, H., Wulff, K., Linek, M., Cajochen, C., Löffler, J., et al. (2016). D3. 7 report on metric to quantify biological light exposure doses. *Accelerate SSL Innovation for Europe. SSL-erate Consortium*.
- Goodman, T. M. (2009). Measurement and specification of lighting: A look at the future. *Lighting Research & Technology*, 41(3), 229–243.
- Gooley, J. J., Lu, J., Fischer, D., & Saper, C. B. (2003). A broad role for melanopsin in nonvisual photoreception. *Journal of Neuroscience*, 23(18), 7093–7106.
- Gooley, J. J., Rajaratnam, S. M. W., Brainard, G. C., Kronauer, R. E., Czeisler, C. A., & Lockley, S. W. (2010). Spectral responses of the human circadian system depend on the irradiance and duration of exposure to light. *Science Translational Medicine*, 2(31), 31–33.

- Goovaerts, C., Descamps, F., & Jacobs, V. (2017). Shading control strategy to avoid visual discomfort by using a low-cost camera: A field study of two cases. *Building and Environment*, 125, 26–38.
- Green, A., Cohen-Zion, M., Haim, A., & Dagan, Y. (2017). Evening light exposure to computer screens disrupts human sleep, biological rhythms, and attention abilities. *Chronobiology International*, 34(7), 855–865.
- Gronfier, C., Wright, K. P., Kronauer, R. E., Jewett, M. E., & Czeisler, C. a. (2004). Efficacy of a single sequence of intermittent bright light pulses for delaying circadian phase in humans. *American Journal of Physiology, Endocrinology and Metabolism*, 287(1), E174–E181.
- Güler, A. D., Ecker, J. L., Lall, G. S., Haq, S., Altimus, C. M., Liao, H.-W., Barnard, A. R., Cahill, H., Badea, T. C., Zhao, H., et al. (2008). Melanopsin cells are the principal conduits for rod–cone input to non-image-forming vision. *Nature*, 453(7191), 102–105.
- Halberg, F., Halberg, E., Barnum, C. P., & Bittner, J. J. (1959). Physiologic 24-hour periodicity in human beings and mice, the lighting regimen and daily routine. In *Photoperiodism and Related Phenomena in Plants and Animals* (pp. 803–878). American Association for the Advancement of Science Washington, DC.
- Hansen, J. & Stevens, R. G. (2011). Night shiftwork and breast cancer risk: overall evidence. *Occupational and Environmental Medicine*, 68(3), 236.
- Harb, F., Hidalgo, M. P., & Martau, B. (2015). Lack of exposure to natural light in the workspace is associated with physiological, sleep and depressive symptoms. *Chronobiology International*, 32(3), 368–375.
- Hashimoto, S., Kohsaka, M., Nakamura, K., Honma, H., Honma, S., & Honma, K. I. (1997). Midday exposure to bright light changes the circadian organization of plasma melatonin rhythm in humans. *Neuroscience Letters*, 221(2-3), 89–92.
- Hattar, S. (2002). Melanopsin-Containing Retinal Ganglion Cells: Architecture, Projections, and Intrinsic Photosensitivity. *Science*, 295(5557), 1065–1070.
- Hattar, S., Kumar, M., Park, A., Tong, P., Tung, J., Yau, K.-W., & Berson, D. M. (2006). Central projections of melanopsin-expressing retinal ganglion cells in the mouse. *Journal of Comparative Neurology*, 497, 326–349.
- Hébert, M., Martin, S. K., Lee, C., & Eastman, C. I. (2002). The effects of prior light history on the suppression of melatonin by light in humans. *Journal of Pineal Research*, 18(9), 1199–1216.
- Hicks, A. L., Theis, T. L., & Zellner, M. L. (2015). Emergent effects of residential lighting choices: Prospects for energy savings. *Journal of Industrial Ecology*, 19(2), 285–295.
- Hirning, M. B., Isoardi, G. L., Coyne, S., Garcia Hansen, V. R., & Cowling, I. (2013). Post occupancy evaluations relating to discomfort glare: A study of green buildings in Brisbane. *Building and Environment*, 59, 349–357.
- Honma, S., Ono, D., Suzuki, Y., Inagaki, N., Yoshikawa, T., Nakamura, W., & ichi Honma, K. (2012). Chapter 8 - Suprachiasmatic nucleus: cellular clocks and networks. In A. Kalsbeek, M. Mew, T. Roenneberg, &

## References

---

- R. G. Foster (Eds.), *The Neurobiology of Circadian Timing*, volume 199 of *Progress in Brain Research* (pp. 129–141). Elsevier.
- Hopkinson, R. G. (1972). Glare from daylighting in buildings. *Applied Ergonomics*, 3(4), 206–215.
- Horne, J. A. & Ostberg, O. (1976). A self assessment questionnaire to determine Morningness Eveningness in human circadian rhythms. *International Journal of Chronobiology*, 4(2), 97–110.
- Houser, K. W., Boyce, P. R., Zeitzer, J. M., & Herf, M. (2020). Human-centric lighting: Myth, magic or metaphor? *Lighting Research & Technology*, 0, 1–22.
- Hubalek, S. (2007). *LuxBlick. Messung der täglichen Lichtexposition zur Beurteilung der nicht- visuellen Lichtwirkungen über das Auge*. PhD thesis, ETH Zürich, Switzerland.
- Hubalek, S., Brink, M., & Schierz, C. (2010). Office workers' daily exposure to light and its influence on sleep quality and mood. *Lighting Research & Technology*, 42(1), 33–50.
- Huiberts, L. M., Smolders, K. C., & de Kort, Y. A. (2015). Shining light on memory: Effects of bright light on working memory performance. *Behavioural Brain Research*, 294(July), 234–245.
- Huiberts, L. M., Smolders, K. C. H. J., & de Kort, Y. A. W. (2016). Non-image forming effects of illuminance level: Exploring parallel effects on physiological arousal and task performance. *Physiology & Behavior*, 164, 129–139.
- Iacomussi, P., Radis, M., Rossi, G., & Rossi, L. (2015). Visual Comfort with LED Lighting. *Energy Procedia*, 78, 729–734.
- Jamrozik, A., Clements, N., Hasan, S. S., Zhao, J., Zhang, R., Campanella, C., Loftness, V., Porter, P., Ly, S., Wang, S., & Bauer, B. (2019). Access to daylight and view in an office improves cognitive performance and satisfaction and reduces eyestrain: A controlled crossover study. *Building and Environment*, 165(March), 106379.
- Jang, J. & Gulley (1997). MATLAB: Fuzzy Logic Toolbox™ User's Guide. The MathWorks, Inc.
- Jenkins, D. & Newborough, M. (2007). An approach for estimating the carbon emissions associated with office lighting with a daylight contribution. *Applied Energy*, 84(6), 608–622.
- Johns, M. W. (1991). A new method for measuring daytime sleepiness: The Epworth sleepiness scale. *Sleep*, 14(6), 540–545.
- Jung, C. M., Khalsa, S. B. S., Scheer, F. a. J. L., Cajochen, C., Lockley, S. W., Czeisler, C. a., & Wright, K. P. (2010). Acute effects of bright light exposure on cortisol levels. *Journal of Biological Rhythms*, 25(3), 208–216.
- Kazilek, C. J. & Cooper, K. (2010). Rods and Cones. <https://askabiologist.asu.edu/explore/seeing-color/rods-and-cones>. Arizona State University School of Life Sciences - Ask A Biologist.
- Khalsa, S. B. S., Jewett, M. E., Cajochen, C., & Czeisler, C. a. (2003). A phase response curve to single bright light pulses in human subjects. *The Journal of Physiology*, 549(3), 945–952.



- Khan, N. & Abas, N. (2011). Comparative study of energy saving light sources. *Renewable and Sustainable Energy Reviews*, 15(1), 296–309.
- Khitrov, M. Y., Laxminarayan, S., Thorsley, D., Ramakrishnan, S., Rajaraman, S., Wesensten, N. J., & Reifman, J. (2014). PC-PVT: a platform for psychomotor vigilance task testing, analysis, and prediction. *Behavior Research Methods*, 46(1), 140–147.
- Killgore, W. D. (2010). Effects of sleep deprivation on cognition. *Progress in Brain Research*, 185, 105–129.
- Kirchner, W. (1958). Age differences in short-term retention of rapidly changing information. *Journal of experimental psychology*, 55, 352–358.
- Koo, S. Y., Yeo, M. S., & Kim, K. W. (2010). Automated blind control to maximize the benefits of daylight in buildings. *Building and Environment*, 45(6), 1508–1520.
- Kozaki, T., Miura, N., Takahashi, M., & Yasukouchi, A. (2012). Effect of reduced illumination on insomnia in office workers. *Journal of Occupational Health*, 54(4), 331–335.
- Kräuchi, K. (2002). How is the circadian rhythm of core body temperature regulated? *Clinical Autonomic Research*, 12(3), 147–149.
- Kräuchi, K., Cajochen, C., Möri, D., Graw, P., & Wirz-Justice, A. (1997). Early evening melatonin and S-20098 advance circadian phase and nocturnal regulation of core body temperature. *American Journal of Physiology*, 272(4 PART 2).
- Kräuchi, K., Cajochen, C., Pache, M., Flammer, J., & Wirz-Justice, A. (2006). Thermoregulatory effects of melatonin in relation to sleepiness. *Chronobiology International*, 23(1-2), 475–484.
- Kräuchi, K., Cajochen, C., Werth, E., & Wirz-Justice, A. (1999). Warm feet promote the rapid onset of sleep. *Nature*, 401(6748), 36–37.
- Kräuchi, K., Cajochen, C., Werth, E., & Wirz-Justice, A. (2000). Functional link between distal vasodilation and sleep-onset latency? *American Journal of Physiology - Regulatory Integrative and Comparative Physiology*, 278(3 47-3), R741–R748.
- Kräuchi, K., Cajochen, C., & Wirz-Justice, A. (2004). Waking up properly: Is there a role of thermoregulation in sleep inertia? *Journal of Sleep Research*, 13(2), 121–127.
- Kräuchi, K., Konieczka, K., Roescheisen-Weich, C., Gompfer, B., Hauenstein, D., Schoetzau, A., Fraenkl, S., & Flammer, J. (2014). Diurnal and menstrual cycles in body temperature are regulated differently: a 28-day ambulatory study in healthy women with thermal discomfort of cold extremities and controls. *Chronobiology International*, 31(1), 102–113.
- Leder, S., Newsham, G. R., Veitch, J. A., Mancini, S., & Kate, E. (2016). Effects of office environment on employee satisfaction: a new analysis. *Building Research and Information*, 44(1), 34–50.
- Lee, A., Myung, S.-K., Cho, J. J., Jung, Y.-J., Yoon, J. L., & Kim, M. Y. (2017). Night shift work and risk of depression: meta-analysis of observational studies. *Journal of Korean Medical Science*, 32(7), 1091–1096.

## References

---

- Lee, C. C. (1990). Fuzzy logic in control systems: Fuzzy logic controller, part ii. *IEEE transactions on systems, man, and cybernetics*, 20(2), 419–435.
- Lee, E. S. & Selkowitz, S. E. (2006). The New York Times Headquarters daylighting mockup: Monitored performance of the daylighting control system. *Energy and Buildings*, 38(7), 914–929.
- Lee, S. K., Sonoda, T., & Schmidt, T. M. (2019). M1 intrinsically photosensitive retinal ganglion cells integrate rod and melanopsin inputs to signal in low light. *Cell Reports*, 29(11), 3349–3355.e2.
- Léger, D., Bayon, V., Elbaz, M., Philip, P., & Choudat, D. (2011). Underexposure to light at work and its association to insomnia and sleepiness: a cross-sectional study of 13'296 workers of one transportation company. *Journal of Psychosomatic Research*, 70(1), 29–36.
- Leichtfried, V., Mair-Raggautz, M., Schaeffer, V., Hammerer-Lercher, A., Mair, G., Bartenbach, C., Canazei, M., & Schobersberger, W. (2015). Intense illumination in the morning hours improved mood and alertness but not mental performance. *Applied Ergonomics*, 46(Part A), 54–59.
- Leproult, R., Colecchia, E. F., L'Hermite-Balériaux, M., & Van Cauter, E. (2001). Transition from dim to bright light in the morning induces an immediate elevation of cortisol levels. *Journal of Clinical Endocrinology and Metabolism*, 86(1), 151–157.
- Lewis, P., Korf, H. W., Kuffer, L., Groß, J. V., & Erren, T. C. (2018). Exercise time cues (zeitgebers) for human circadian systems can foster health and improve performance: A systematic review. *BMJ Open Sport and Exercise Medicine*, 4(1), 1–8.
- Lewy, A. J. & Sack, R. L. (1989). The dim light melatonin onset as a marker for circadian phase position. *Chronobiology international*, 6(1), 93–102.
- Lewy, A. J., Wehr, T. A., Goodwin, F. K., Newsome, D. A., & Markey, S. (1980). Light suppresses melatonin secretion in humans. *Science*, 210(4475), 1267–1269.
- Li, D. H. W. & Lam, J. C. (2001). Evaluation of lighting performance in office buildings with daylighting controls. *Energy and Buildings*, 33(8), 793–803.
- Lindelöf, D. (2007). *Bayesian optimization of visual comfort*. PhD thesis, École Polytechnique Fédérale de Lausanne, Switzerland.
- Linhardt, F. (2010). *Energetic, Visual and Non-Visual Aspects of Office Lighting*. PhD thesis, École Polytechnique Fédérale de Lausanne, Switzerland.
- Lockley, S. W. (2009). Circadian rhythms: Influence of light in humans. *Encyclopedia of Neuroscience*, 2, 971–988.
- Lockley, S. W., Arendt, J., & Skene, D. J. (2007). Visual impairment and circadian rhythm disorders. *Dialogues in clinical neuroscience*, 9(3), 301–314.
- Lockley, S. W., Brainard, G. C., & Czeisler, C. A. (2003). High sensitivity of the human circadian melatonin rhythm to resetting by short wavelength light. *The Journal of Clinical Endocrinology & Metabolism*, 88(9), 4502–4502.

- Lok, R., Smolders, K. C., Beersma, D. G., & de Kort, Y. A. (2018). Light, alertness, and alerting effects of white light: a literature overview. *Journal of Biological Rhythms*, 33(6), 589–601.
- Lucas, R. J., Peirson, S. N., Berson, D. M., Brown, T. M., Cooper, H. M., Czeisler, C. A., Figueiro, M. G., Gamlin, P. D., Lockley, S. W., Hagan, J. B. O., Price, L. L. A., Provencio, I., Skene, D. J., & Brainard, G. C. (2014). Measuring and using light in the melanopsin age. *Trends in Neurosciences*, 37(1), 1–9.
- Luo, X., Hu, R., Liu, S., & Wang, K. (2016). Heat and fluid flow in high-power led packaging and applications. *Progress in Energy and Combustion Science*, 56, 1–32.
- Maierova, L., Borisuit, A., Scartezzini, J. L., Jaeggi, S. M., Schmidt, C., & Münch, M. (2016). Diurnal variations of hormonal secretion, alertness and cognition in extreme chronotypes under different lighting conditions. *Scientific Reports*, 6(May), 1–10.
- Markussen, S. & Røed, K. (2015). Daylight and absenteeism – evidence from Norway. *Economics & Human Biology*, 16, 73–80.
- Marzano, C., Fratello, F., Moroni, F., Pellicciari, M. C., Curcio, G., Ferrara, M., Ferlazzo, F., & De Gennaro, L. (2007). Slow eye movements and subjective estimates of sleepiness predict EEG power changes during sleep deprivation. *Sleep*, 30(5), 610–6.
- McCluney, R. (2003). Radiometry and photometry. In R. A. Meyers (Ed.), *Encyclopedia of Physical Science and Technology (Third Edition)* (Third Edition ed.). (pp. 731–758). New York: Academic Press.
- McIntyre, I. M. & Norman, T. R. T. R. (1989). Human melatonin suppression by light is intensity dependent. *Journal of Pineal Research*, 6, 149–156.
- Meteosuisse. Website of Meteosuisse. <http://www.meteosuisse.ch>.
- Mishima, K., Okawa, M., Shimizu, T., & Hishikawa, Y. (2001). Diminished melatonin secretion in the elderly caused by insufficient environmental illumination. *Journal of Clinical Endocrinology and Metabolism*, 86(1), 129–134.
- Moderie, C., Van der Maren, S., & Dumont, M. (2017). Circadian phase, dynamics of subjective sleepiness and sensitivity to blue light in young adults complaining of a delayed sleep schedule. *Sleep Medicine*, 34, 148–155.
- Monk, T. H. (1989). A visual analogue scale technique to measure global vigor and affect. *Psychiatry Research*, 27(1), 89–99.
- Moore, R. Y. & Danchenko, R. L. (2002). Paraventricular–subparaventricular hypothalamic lesions selectively affect circadian function. *Chronobiology international*, 19(2), 345–360.
- Moore-Ede, M. C., Sulzman, F. M., & Fuller, C. A. (1982). *The Clocks That Time Us: Physiology of the Circadian Timing System*. Harvard University Press.
- Morris, C. J., Purvis, T. E., Hu, K., & Scheer, F. A. J. L. (2016). Circadian misalignment increases cardiovascular disease risk factors in humans. *Proceedings of the National Academy of Sciences of the United States of America*, 113(10), E1402–11.

## References

---

- Motamed, A. (2017). *Integrated Daylighting and Artificial Lighting Control based on High Dynamic Range Vision Sensors*. PhD thesis, École Polytechnique Fédérale de Lausanne, Switzerland.
- Motamed, A., Bueno, B., Deschamps, L., Kuhn, T. E., & Scartezzini, J. L. (2020). Self-commissioning glare-based control system for integrated venetian blind and electric lighting. *Building and Environment*, 171(January), 106642.
- Motamed, A., Deschamps, L., & Scartezzini, J.-I. (2015). Validation and Preliminary Experiments of Embedded Discomfort Glare Assessment through a Novel HDR Vision Sensor. In LESO-PB, E. (Ed.), *Proceedings of International Conference CISBAT 2015*, (pp. 235–240).
- Motamed, A., Deschamps, L., & Scartezzini, J.-L. (2016). Toward an integrated platform for energy efficient lighting control of non-residential buildings. In *Expanding Boundaries - Systems Thinking in the Built Environment - Proceedings of the Sustainable Built Environment (SBE)*.
- Motamed, A., Deschamps, L., & Scartezzini, J. L. (2017). On-site monitoring and subjective comfort assessment of a sun shadings and electric lighting controller based on novel High Dynamic Range vision sensors. *Energy and Buildings*, 149, 58–72.
- Münch, M., Brøndsted, A. E., Brown, S. A., Gjedde, A., Kantermann, T., Martiny, K., Mersch, D., Skene, D. J., & Wirz-Justice, A. (2017). Chapter 3. The effect of light on humans. In *Changing Perspectives on Daylight: Science, technology, and Culture* (pp. 16–23). Science/AAAS, Washington, DC.
- Münch, M., Linhart, F., Borisuit, A., Jaeggi, S. M., & Scartezzini, J.-L. (2012). Effects of prior light exposure on early evening performance, subjective sleepiness, and hormonal secretion. *Behavioral Neuroscience*, 126(1), 196–203.
- Münch, M., Nowozin, C., Regente, J., Bes, F., De Zeeuw, J., Hädel, S., Wahnschaffe, A., & Kunz, D. (2017). Blue-enriched morning light as a countermeasure to light at the wrong time: effects on cognition, sleepiness, sleep, and circadian phase. *Neuropsychobiology*, 74(4), 207–218.
- Münch, M., Schmieder, M., Bieler, K., Goldbach, R., Fuhrmann, T., Zumstein, N., Vonmoos, P., Scartezzini, J.-L., Wirz-Justice, A., & Cajochen, C. (2017). Bright light delights: effects of daily light exposure on emotions, rest-activity cycles, sleep and melatonin secretion in severely demented patients. *Current Alzheimer Research*, 14, 1063–1075.
- Münch, M., Wirz-justice, A., Brown, S. A., & Kantermann, T. (2020). The role of daylight for humans: Gaps in current knowledge. *Clocks & Sleep*, (lii), 61–85.
- Mure, L. S. (2021). Intrinsically photosensitive retinal ganglion cells of the human retina. *Frontiers in Neurology*, 12, 300.
- Münch, M., Kobialka, S., Steiner, R., Oelhafen, P., Wirz-Justice, A., & Cajochen, C. (2006). Wavelength-dependent effects of evening light exposure on sleep architecture and sleep eeg power density in men. *American Journal of Physiology - Regulatory, Integrative and Comparative Physiology*, 290(5), R1421–R1428.

- New Buildings Institute, Inc. (NBI) (2003). Advanced Lighting Guidelines. <https://algonline.org/index.php?open-plan-office>.
- Newsham, G., Brand, J., Donnelly, C., Veitch, J., Aries, M., & Charles, K. (2009). Linking indoor environment conditions to job satisfaction: A field study. *Building Research and Information*, 37(2), 129–147.
- Nowozin, C., Wahnschaffe, A., Rodenbeck, A., de Zeeuw, J., Hadel, S., Kozakov, R., Schopp, H., Munch, M., & Kunz, D. (2017). Applying melanopic lux to measure biological light effects on melatonin suppression and subjective sleepiness. *Current Alzheimer Research*, 14(10), 1042–1052.
- NSVV (2003). Aanbeveling Gezond licht op de werkplek, Nederlandse Stichting voor Verlichtingskunde NSVV.
- Oakley, R. H. & Cidlowski, J. A. (2013). The biology of the glucocorticoid receptor: new signaling mechanisms in health and disease. *The Journal of Allergy and Clinical Immunology*, 132(5), 1033–44.
- Oldham, G. R. & Brass, D. J. (1979). Employee reactions to an open-plan office: A naturally occurring quasi-experiment. *Administrative Science Quarterly*, 24(2), 267–284.
- Osterhaus, W. (2001). Discomfort glare from daylight in computer offices: how much do we really know? In *Proceedings of LUX Europa*, (pp. 448–456).
- Osterhaus, W. K. (2005). Discomfort glare assessment and prevention for daylight applications in office environments. *Solar Energy*, 79(2), 140–158.
- Paas, F. G. W. C., van Merriënboer, J. J. G., & Adam, J. J. (1994). Measurement of cognitive load in instructional research. *Perceptual and Motor Skills*, 79(1), 419–430.
- Pail, G., Huf, W., Pjrek, E., Winkler, D., Willeit, M., Praschak-Rieder, N., & Kasper, S. (2011). Bright-light therapy in the treatment of mood disorders. *Neuropsychobiology*, 64, 152–62.
- Partonen, T. & Lönnqvist, J. (2000). Bright light improves vitality and alleviates distress in healthy people. *Journal of Affective Disorders*, 57(1-3), 55–61.
- Paschotta, R. Field of View. [https://www.rp-photonics.com/field\\_of\\_view.html](https://www.rp-photonics.com/field_of_view.html). RP Photonics Encyclopedia, accessed on 2021-08-12.
- Paule, B., Boutillier, J., & Pantet, S. (2015). Shading device control: effective impact on daylight contribution. In *Proceedings of International Conference CISBAT 2015*, (pp. 241–246)., Lausanne, Switzerland.
- Peeters, S. T., Smolders, K. C., & de Kort, Y. A. (2020). What you set is (not) what you get: How a light intervention in the field translates to personal light exposure. *Building and Environment*, 185, 107288.
- Petherbridge, P. & Hopkinson, R. G. (1950). Discomfort Glare and the Lighting of Buildings. *Transactions of the Illuminating Engineering Society*, 15(2), 39–79.
- Phipps-Nelson, J., Redman, J. R., Dijk, D.-J., & Rajaratnam, S. M. W. (2003). Daytime exposure to bright light, as compared to dim light, decreases sleepiness and improves psychomotor vigilance performance. *Sleep*, 26(6), 695–700.

## References

---

- Pierson, C., Wienold, J., & Bodart, M. (2017). Discomfort glare perception in daylighting: influencing factors. *Energy Procedia*, 122, 331–336.
- Prasad, S. & Galetta, S. L. (2011). Chapter 1 - Anatomy and physiology of the afferent visual system. In C. Kennard & R. J. Leigh (Eds.), *Neuro-ophthalmology*, volume 102 of *Handbook of Clinical Neurology* (pp. 3–19). Elsevier.
- Prayag, A., Münch, M., Aeschbach, D., Chellappa, S., & Gronfier, C. (2019). Light modulation of human clocks, wake, and sleep. *Clocks & Sleep*, 1, 193–208.
- Prayag, A. S., Najjar, R. P., & Gronfier, C. (2019). Melatonin suppression is exquisitely sensitive to light and primarily driven by melanopsin in humans. *Journal of Pineal Research*, 66(4), 1–8.
- Provencio, I., Jiang, G., De Grip, W. J., Hayes, W. P., & Rollag, M. D. (1998). Melanopsin: An opsin in melanophores, brain, and eye. *Proceedings of the National Academy of Sciences*, 95(1), 340–345.
- Rea, M., Figueiro, M., Bierman, a., & Hamner, R. (2012). Modelling the spectral sensitivity of the human circadian system. *Lighting Research & Technology*, 44(4), 386–396.
- Refinetti, R. (2010). The circadian rhythm of body temperature. *Frontiers in Bioscience*, 15(2), 564–594.
- Revell, V., Arendt, J., Terman, M., & Skene, D. (2005). Short-wavelength sensitivity of the human circadian system to phase-advancing light. *Journal of Biological Rhythms*, 20, 270–2.
- Richter, H. O., Sundin, S., & Long, J. (2019). Visually deficient working conditions and reduced work performance in office workers: Is it mediated by visual discomfort? *International Journal of Industrial Ergonomics*, 72, 128–136.
- Roach, G. D., Dawson, D., & Lamond, N. (2006). Can a shorter psychomotor vigilance task be used as a reasonable substitute for the ten-minute psychomotor vigilance task? *Chronobiology International*, 23(6), 1379–1387.
- Robinson, W., Bellchambers, H., Grundy, J., Longmore, J., Burt, W., Hewitt, H., Petherbridge, P., Frith, D., Hopkinson, R., & Rowlands, E. (1962). The development of the IES glare index system: contributed by the luminance study panel of the IES technical committee. *Transactions of the Illuminating Engineering Society*, 27(1\_IESTrans), 9–26.
- Roenneberg, T., Kantermann, T., Juda, M., Vetter, C., & Allebrandt, K. V. (2013). Light and the Human Circadian Clock. In *Circadian Clocks* (pp. 311–331). Springer, Berlin, Heidelberg.
- Roenneberg, T., Wirz-Justice, A., & Mrosovsky, M. (2003). Life between clocks: daily temporal patterns of human chronotypes. *Journal of Biological Rhythms*, 18(1), 80–90.
- Rosenthal, N. E., Joseph-Vanderpool, J. R., Levendosky, A. A., Johnston, S. H., Allen, R., Kelly, K. A., Souetre, E., Schultz, P. M., & Starz, K. E. (1990). Phase-shifting effects of bright morning light as treatment for delayed sleep phase syndrome. *Sleep*, 13(4), 354–361.

- Rosenthal, N. E., Sack, D. A., Gillin, J. C., Lewy, A. J., Goodwin, F. K., Davenport, Y., Mueller, P. S., Newsome, D. A., & Wehr, T. A. (1984). Seasonal Affective Disorder: a description of the syndrome and preliminary findings with light therapy. *Archives of General Psychiatry*, 41(1), 72–80.
- Rubinstein, E. H. & Sessler, D. I. (1990). Skin-surface temperature gradients correlate with fingertip blood flow in humans. *Anesthesiology*, 73, 541–545.
- Rubinstein, F., Ward, G., & Verderber, R. (1989). Improving the Performance of Photo-Electrically Controlled Lighting Systems. *Journal of the Illuminating Engineering Society*, 18(1), 70–94.
- Ruby, N. F., Brennan, T. J., Xie, X., Cao, V., Franken, P., Heller, H. C., & O'Hara, B. F. (2002). Role of melanopsin in circadian responses to light. *Science*, 298(5601), 2211–2213.
- Ruck, N., Aschehoug, Ø., Aydinli, S., Christoffersen, J., Edmonds, I., Jakobiak, R., Kischkoweit-Lopin, M., Klinger, M., Lee, E., Courret, G., Michel, L., Scartezzini, J.-L., & Selkowitz, S. (2000). *Daylight in Buildings - A source book on daylighting systems and components*. Berkeley, CA: Lawrence Berkeley National Laboratory.
- Rüger, M. & Gordijn, M. C. M. (2005). Weak relationships between suppression of melatonin and suppression of sleepiness/fatigue in response to light exposure. *Journal of Sleep Research*, 14(October), 221–227.
- Rüger, M., Gordijn, M. C. M., Beersma, D. G. M., de Vries, B., & Daan, S. (2006). Time-of-day-dependent effects of bright light exposure on human psychophysiology: comparison of daytime and nighttime exposure. *American Journal of Physiology. Regulatory, Integrative and Comparative Physiology*, 290(5), R1413–R1420.
- Santhi, N., Thorne, H. C., van der Veen, D. R., Johnsen, S., Mills, S. L., Hommes, V., Schlangen, L. J., Archer, S. N., & Dijk, D.-J. (2012). The spectral composition of evening light and individual differences in the suppression of melatonin and delay of sleep in humans. *Journal of Pineal Research*, 53(1), 47–59.
- Sarey Khanie, M., Stoll, J., Mende, S., Wienold, J., Einhäuser, W., & Andersen, M. (2013). Investigation of gaze patterns in daylit workplaces: using eye-tracking methods to objectify view direction as a function of lighting conditions. *Proceedings of CIE Centenary Conference "Towards a New Century of Light"*, (February 2015), 250–259.
- Scartezzini, J.-L. & Courret, G. (2002). Anidolic daylighting systems. *Solar Energy*, 73, 123–135.
- Scartezzini, J. L., Faist, A., & Gay, J. B. (1987). Experimental comparison of a sunspace and a water hybrid solar device using the LESO test facility. *Solar Energy*, 38(5), 355–366.
- Scheer, F. A. J. L. & Buijs, R. M. (1999). Light affects morning salivary cortisol in humans. *The Journal of Clinical Endocrinology & Metabolism*, 84(9), 855–858.
- Schmidt, C., Collette, F., Leclercq, Y., Sterpenich, V., Vandewalle, G., Berthomier, P., Berthomier, C., Phillips, C., Tinguely, G., Darsaud, A., Gais, S., Schabus, M., Deseilles, M., Dang-Vu, T. T., Salmon, E., Balet, E., Degueldre, C., Luxen, A., Maquet, P., & ... Peigneux, P. (2009). Homeostatic sleep pressure and responses to sustained attention in the suprachiasmatic area. *Science*, 324(5926), 516–519.
- Sekiguchi, H., Iritani, S., & Fujita, K. (2017). Bright light therapy for sleep disturbance in dementia is most effective for mild to moderate alzheimer's type dementia: a case series. *Psychogeriatrics*, 17(5), 275–281.

## References

---

- Skeldon, A. C., Phillips, A. J., & Dijk, D. J. (2017). The effects of self-selected light-dark cycles and social constraints on human sleep and circadian timing: a modeling approach. *Scientific Reports*, 7(September 2016), 1–14.
- Smith, K. A., Schoen, M. W., & Czeisler, C. A. (2004). Adaptation of human pineal melatonin suppression by recent photic history. *The Journal of Clinical Endocrinology and Metabolism*, 89(7), 3610–4.
- Smith, M. R., Revell, V. L., & Eastman, C. I. (2009). Phase advancing the human circadian clock with blue-enriched polychromatic light. *Sleep Medicine*, 10(3), 287–294.
- Smolders, K. & de Kort, Y. (2009). Light up my day: a between-group test of dynamic lighting effects on office workers' wellbeing in the field. In Yener, A. & Oztürk, L. (Eds.), *Lux Europa 2009 11th European Lighting Congress*, (pp. 161–168). Turkish National Committee on Illumination.
- Smolders, K., de Kort, Y., & Cluitmans, P. (2012). A higher illuminance induces alertness even during office hours: findings on subjective measures, task performance and heart rate measures. *Physiology & Behavior*, 107(1), 7–16.
- Smolders, K. C. & de Kort, Y. A. (2014). Bright light and mental fatigue: effects on alertness, vitality, performance and physiological arousal. *Journal of Environmental Psychology*, 39(April 2021), 77–91.
- Souman, J. L., Tinga, A. M., te Pas, S. F., van Ee, R., & Vlaskamp, B. N. (2018). Acute alerting effects of light: A systematic literature review. *Behavioural Brain Research*, 337(July 2017), 228–239.
- Spitschan, M., Stefani, O., Blattner, P., Gronfier, C., Lockley, S., & Lucas, R. (2019). How to report light exposure in human chronobiology and sleep research experiments. *Clocks & Sleep*, 1(3), 280–289.
- St Hilaire, M. a., Gooley, J. J., Khalsa, S. B. S., Kronauer, R. E., Czeisler, C. a., & Lockley, S. W. (2012). Human phase response curve to a 1 h pulse of bright white light. *The Journal of Physiology*, 590(13), 3035–3045.
- Stefani, O. & Cajochen, C. (2021). Should we re-think regulations and standards for lighting at workplaces? A practice review on existing lighting recommendations. *Frontiers in Psychiatry*, 12, 671.
- Stefani, O., Freyburger, M., Veitz, S., Basishvili, T., Meyer, M., Weibel, J., Kobayashi, K., Shirakawa, Y., & Cajochen, C. (2021). Changing color and intensity of LED lighting across the day impacts on circadian melatonin rhythms and sleep in healthy men. *Journal of Pineal Research*, 70(2), e12714.
- Stephan, F. K. (2002). The "other" circadian system: food as a zeitgeber. *Journal of Biological Rhythms*, 17(4), 284–292.
- Stephan, F. K. & Zucker, I. (1972). Circadian rhythms in drinking behavior and locomotor activity of rats are eliminated by hypothalamic lesions. *Proceedings of the National Academy of Sciences*, 69(6), 1583–1586.
- Stevens, R. G. & Rea, M. S. (2001). Light in the built environment: Potential role of circadian disruption in endocrine disruption and breast cancer. *Cancer Causes and Control*, 12, 279–287.
- Stewart, P. (1999). Adrenal cortex. *Current Opinion in Endocrinology & Diabetes*, 6(3), 177.



- Sundaram, S. & Croxton, R. (1998). Daylighting and Office Worker Productivity: A Case Study. In *Proceedings of the National Passive Solar Conference*, volume 23, (pp. 175–180). American Solar Energy Society Inc.
- Swiss Federal Office of Energy (2012). Energy strategy 2050. <https://www.bfe.admin.ch/bfe/en/home/politik/energiestrategie-2050.html>.
- Tahara, Y., Aoyama, S., & Shibata, S. (2017). The mammalian circadian clock and its entrainment by stress and exercise. *The Journal of Physiological Sciences*, 67(1), 1–10.
- Tähhkämö, L., Partonen, T., & Pesonen, A. K. (2019). Systematic review of light exposure impact on human circadian rhythm. *Chronobiology International*, 36(2), 151–170.
- Takasu, N. N., Hashimoto, S., Yamanaka, Y., Tanahashi, Y., Yamazaki, A., Honma, S., & Honma, K. I. (2006). Repeated exposures to daytime bright light increase nocturnal melatonin rise and maintain circadian phase in young subjects under fixed sleep schedule. *American Journal of Physiology - Regulatory Integrative and Comparative Physiology*, 291(6).
- Technical Committee CEN/TC 169 “Light and Lighting” (2018). EN 17037:2018 Daylight of Buildings.
- Terman, M. & Terman, J. (2005). Light therapy for seasonal and nonseasonal depression: Efficacy, protocol, safety, and side effects. *CNS spectrums*, 10, 647–663.
- Thapan, K., Arendt, J., & Skene, D. J. (2001). An action spectrum for melatonin suppression: evidence for a novel non-rod, non-cone photoreceptor system in humans. *The Journal of physiology*, 535(Pt 1), 261–267.
- Thorne, H. C., Jones, K. H., Peters, S. P., Archer, S. N., & Dijk, D.-J. (2009). Daily and seasonal variation in the spectral composition of light exposure in humans. *Chronobiology International*, 26(5), 854–866.
- Tsangrassoulis, A. & Li, D. (2018). Energy efficient lighting strategies in buildings. *Energy and Buildings*, 165, 284–285.
- ul Haq, M. A., Hassan, M. Y., Abdullah, H., Rahman, H. A., Abdullah, M. P., Hussin, F., & Said, D. M. (2014). A review on lighting control technologies in commercial buildings, their performance and affecting factors. *Renewable and Sustainable Energy Reviews*, 33, 268–279.
- van Bommel, W. (2019a). Non-visual Biological Mechanism. In W. van Bommel (Ed.), *Interior Lighting: Fundamentals, Technology and Application* (pp. 137–168). Cham: Springer International Publishing.
- van Bommel, W. J. (2019b). *Interior Lighting. Fundamentals, Technology and Application*. Springer.
- Van den Beld, G. (2003). What is light at the workplace? In *Proceedings 25th CIE Session*, (pp. D6.14–17).
- van Marken Lichtenbelt, W. D., Daanen, H. A., Wouters, L., Fronczek, R., Raymann, R. J., Severens, N. M., & Van Someren, E. J. (2006). Evaluation of wireless determination of skin temperature using iButtons. *Physiology and Behavior*, 88(4-5), 489–497.
- Van Someren, E. J. (2000). More than a marker: Interaction between the circadian regulation of temperature and sleep, age-related changes, and treatment possibilities. *Chronobiology International*, 17(3), 313–354.

## References

---

- Vandewalle, G., Balteau, E., Phillips, C., Degueldre, C., Moreau, V., Sterpenich, V., Albouy, G., Darsaud, A., Desseilles, M., Dang-Vu, T. T., Peigneux, P., Luxen, A., Dijk, D.-J., & Maquet, P. (2006). Daytime light exposure dynamically enhances brain responses. *Current Biology*, 16(16), 1616–1621.
- Veitch, J. A. (2006). Lighting for high-quality workplaces. In *NRC Publications Archive (NPARC)*. Taylor & Francis.
- Veitch, J. A. (2011). Workplace design contributions to mental health and well-being. *Healthcare Papers*, 11(SPEC. ISSUE), 38–46.
- Veitch, J. A., Newsham, G. R., Boyce, P. R., & Jones, C. (2008). Lighting appraisal, well-being and performance in open-plan offices: A linked mechanisms approach. *Lighting Research & Technology*, 40(2), 133–151.
- Vetter, C., Juda, M., Lang, D., Wojtysiak, A., & Roenneberg, T. (2011). Blue-enriched office light competes with natural light as a zeitgeber. *Scandinavian journal of work, environment & health*, 37, 437–445.
- Vetter, C., Phillips, A. J., Silva, A., Lockley, S. W., & Glickman, G. (2019). Light me up? Why, when and how much light we need. *Journal of Biological Rhythms*, 34(6), 573–575.
- Viola, A. U., James, L. M., Schlangen, L. J., & Dijk, D.-J. (2008). Blue-enriched white light in the workplace improves self-reported alertness, performance and sleep quality. *Scandinavian journal of work, environment & health*, 297–306.
- Walker, W. H., Walton, J. C., DeVries, A. C., & Nelson, R. J. (2020). Circadian rhythm disruption and mental health. *Translational Psychiatry*, 10(28).
- Wams, E. J., Woelders, T., Marring, I., Van Rosmalen, L., Beersma, D. G., Gordijn, M. C., & Hut, R. A. (2017). Linking light exposure and subsequent sleep: A field polysomnography study in humans. *Sleep*, 40(12).
- Weaver, D. R. & Emery, P. (2013). Circadian timekeeping. In L. R. Squire, D. Berg, F. E. Bloom, S. du Lac, A. Ghosh, & N. C. Spitzer (Eds.), *Fundamental Neuroscience (Fourth Edition)* (Fourth Edition ed.). (pp. 819–845). San Diego: Academic Press.
- Wehr, T. A., Aeschbach, D., & Duncan, J. (2001). Evidence for a biological dawn and dusk in the human circadian timing system. *Journal of Physiology*, 535(3), 937–951.
- Weitzman, E. D., Czeisler, C. A., Coleman, R. M., Spielman, A. J., Zimmerman, J. C., Dement, W., & Pollak, C. P. (1981). Delayed Sleep Phase Syndrome: a chronobiological disorder with sleep-onset insomnia. *Archives of General Psychiatry*, 38(7), 737–746.
- Weitzman, E. D., Fukushima, D., Nogeire, C., Roffwarg, H., Gallagher, T. F., & Hellman, L. (1971). Twenty-four hour pattern of the episodic secretion of cortisol in normal subjects. *The Journal of Clinical Endocrinology & Metabolism*, 33(1), 14–22.
- Wen, Y. J. & Agogino, A. (2011). Control of wireless-networked lighting in open-plan offices. *Lighting Research & Technology*, 43(2), 235–248.

- Wever, R. A. (1979). *The Circadian System of Man: Results of Experiments Under Temporal Isolation*. Springer-Verlag New York.
- Wicklin, R. (2016). Sometimes you need to reverse the data before you fit a distribution. <https://blogs.sas.com/content/iml/2016/11/02/reverse-data-before-fit-distribution.html>. SAS blogs.
- Wienold, J. & Christoffersen, J. (2006). Evaluation methods and development of a new glare prediction model for daylight environments with the use of CCD cameras. *Energy and Buildings*, 38(7), 743–757.
- Wilke, P. K., Gmelch, W. H., & Lovrich, N. P. (1985). Stress and productivity: evidence of the inverted u function. *Public Productivity Review*, 9(4), 342–356.
- Wilson, J., Reid, K. J., Braun, R. I., Abbott, S. M., & Zee, P. C. (2018). Habitual light exposure relative to circadian timing in delayed sleep-wake phase disorder. *Sleep*, 41(11), 1–9.
- Wirz-Justice, A., Benedetti, F., Berger, M., Lam, R. W., Martiny, K., Terman, M., & Wu, J. C. (2005). Chronotherapeutics (light and wake therapy) in affective disorders. *Psychological Medicine*, 35(7), 939–944.
- Wirz-Justice, A., Benedetti, F., & Terman, M. (2009). *Chronotherapeutics for Affective Disorders. A Clinician's Manual for Light and Wake Therapy*. Karger.
- Wirz-Justice, A., Bromundt, V., & Cajochen, C. (2009). Circadian disruption and psychiatric disorders: the importance of entrainment. *Sleep Medicine Clinics*, 4(2), 273–284.
- Wirz-Justice, A., Graw, P., Kräuchi, K., Sarrafzadeh, A., English, J., Arendt, J., & Sand, L. (1996). 'Natural' light treatment of seasonal affective disorder. *Journal of Affective Disorders*, 37(2-3), 109–120.
- Wittmann, M., Dinich, J., Mellow, M., & Roenneberg, T. (2006). Social jetlag: Misalignment of biological and social time. *Chronobiology International*, 23(1-2), 497–509.
- Wolf, S. (2009). LuxBlick - Mobile Langzeitaufzeichnung von Beleuchtungsstärke und Circadianer Bestrahlungsstärke am Auge. In *Lux junior 2009: Internationales Forum für den Lichttechnischen Nachwuchs*, 25. – 27. September 2009, Dörfeld/Ilm.
- Wright, K., Hull, J., & Czeisler, C. (2003). Relationship between alertness, performance, and body temperature in humans. *American Journal of Physiology. Regulatory, Integrative and Comparative Physiology*, 283, R1370–7.
- Wright, K. P., Gronfier, C., Duffy, J. F., & Czeisler, C. A. (2005). Intrinsic period and light intensity determine the phase relationship between melatonin and sleep in humans. *Journal of Biological Rhythms*, 20(2), 168–177.
- Wright, K. P., McHill, A. W., Birks, B. R., Griffin, B. R., Rusterholz, T., & Chinoy, E. D. (2013). Entrainment of the human circadian clock to the natural light-dark cycle. *Current Biology*, 23(16), 1554–1558.
- Wu, Y., Kämpf, J. H., & Scartezzini, J. L. (2019). Automated 'Eye-sight' Venetian blinds based on an embedded photometric device with real-time daylighting computing. *Applied Energy*, 252.
- Yu, X. & Su, Y. (2015). Daylight availability assessment and its potential energy saving estimation – A literature review. *Renewable and Sustainable Energy Reviews*, 52, 494–503.

## References

---

- Zaidi, F. H., Hull, J. T., Peirson, S., Wulff, K., Aeschbach, D., Gooley, J. J., Brainard, G., Gregory-Evans, K., Rizzo, J., Czeisler, C. A., Foster, R., Moseley, M. J., & Lockley, S. W. (2007). Short-wavelength light sensitivity of circadian, pupillary, and visual awareness in humans lacking an outer retina. *Current Biology*, 17(24), 2122–2128.
- Zarkadis, N. (2015). *Novel Models towards Predictive Control of Advanced Building Systems and Occupant Comfort in Buildings*. PhD thesis, École Polytechnique Fédérale de Lausanne, Switzerland.
- Zarkadis, N., Ridi, A., & Morel, N. (2014). A multi-sensor office-building database for experimental validation and advanced control algorithm development. *Procedia Computer Science*, 32, 1003–1009.
- Zeitzer, J. M. (2000). Sensitivity of the human circadian pacemaker to nocturnal light: melatonin phase resetting and suppression. *Journal of Physiology*, 526, 695–702.
- Zeitzer, J. M., Fisicaro, R. A., Ruby, N. F., & Heller, C. H. (2014). Millisecond flashes of light phase delay the human circadian clock during sleep. *Journal of Biological Rhythms*, 29(5), 370–6.
- Zhang, R., Campanella, C., Aristizabal, S., Jamrozik, A., Zhao, J., Porter, P., Ly, S., & Bauer, B. A. (2020). Impacts of dynamic LED lighting on the well-being and experience of office occupants. *International Journal of Environmental Research and Public Health*, 17(19), 1–27.

# A

## Fuzzy Logic Controller for top blind

### A.1 Fuzzy variables and membership functions

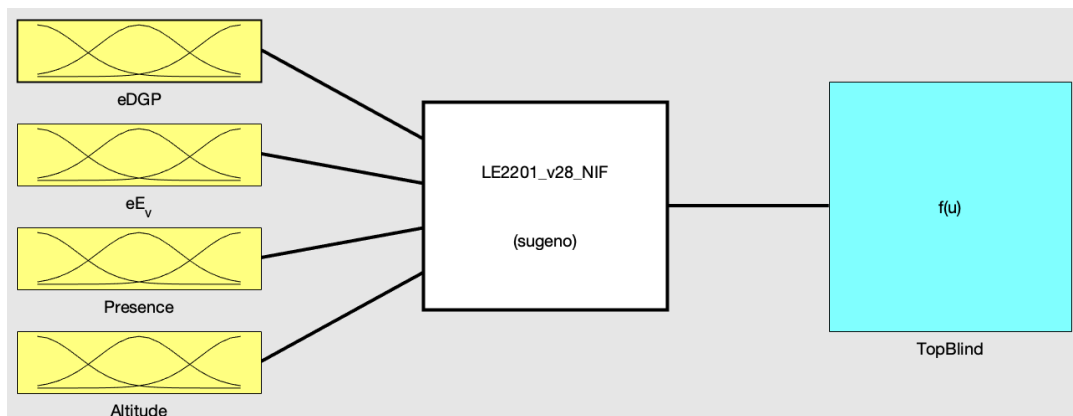


Figure A.1 – Fuzzy variable eDGP.

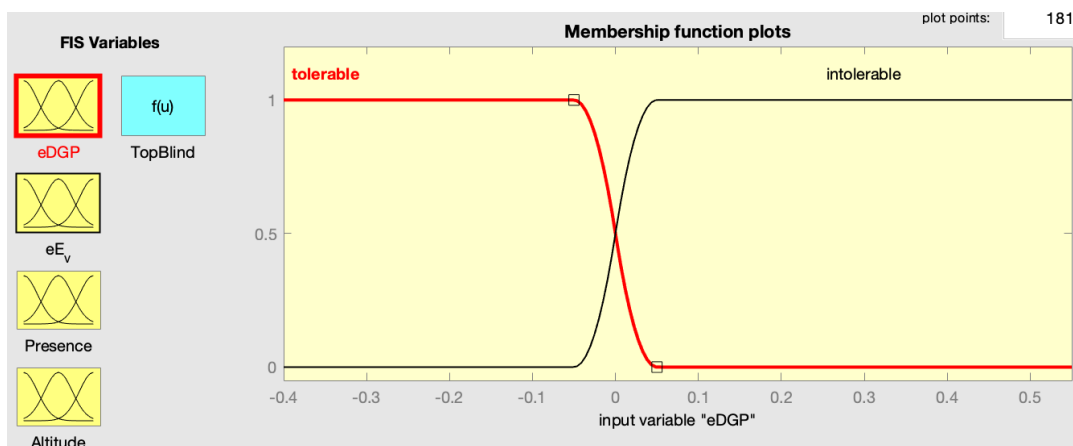


Figure A.2 – Fuzzy variable eDGP.

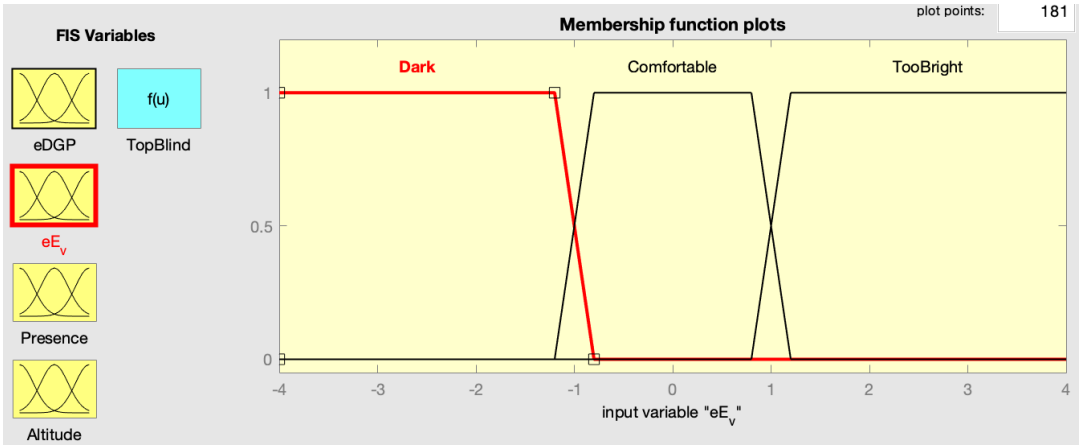


Figure A.3 – Fuzzy variable  $E_v$ .

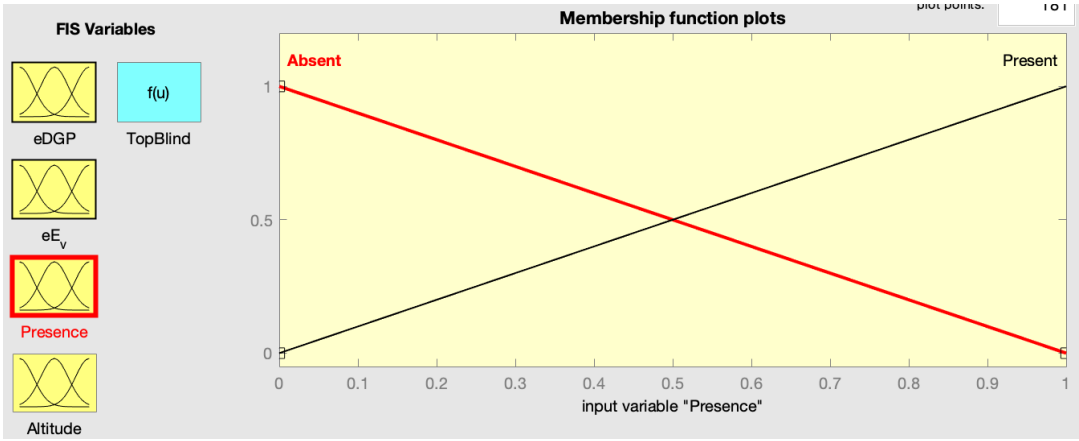


Figure A.4 – Fuzzy variable  $Presence$ .

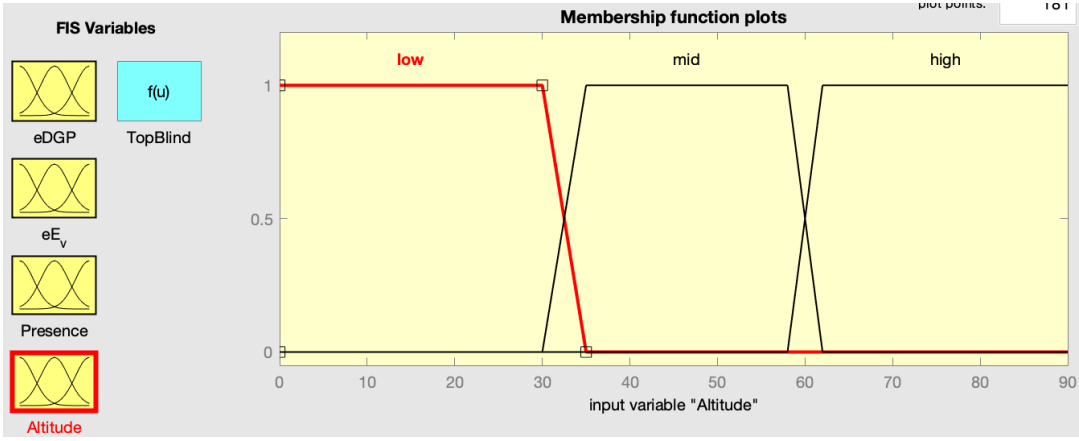


Figure A.5 – Fuzzy variable  $Altitude$ .

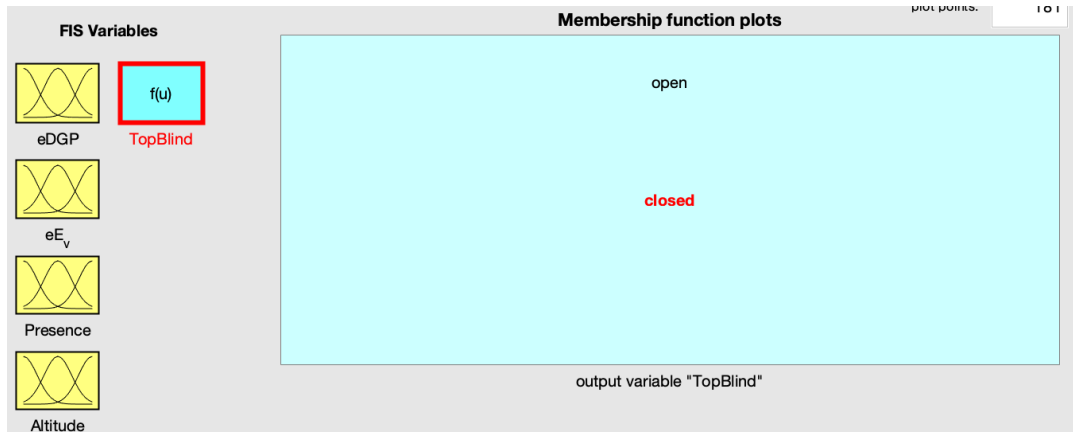


Figure A.6 – Fuzzy variable TopBlind.

## A.2 Rules of the FLC

1. If (eDGP is tolerable) and (Presence is Present) and (Altitude is high) then (TopBlind is open)
2. If (eDGP is intolerable) and (Presence is Present) and (Altitude is mid) then (TopBlind is closed)
3. If (eDGP is intolerable) and (eE<sub>v</sub> is TooBright) and (Presence is Present) then (TopBlind is closed)
4. If (eDGP is tolerable) and (eE<sub>v</sub> is Dark) and (Presence is Present) then (TopBlind is open)





# B

## Questionnaires: VAS/VCS

List of questions:

Question	Answer
1) In this moment, I like the lighting in this room (Actuellement, j'aime la lumière dans cette salle)	VAS: [no-yes = 0-100]
2) Globally, the lighting of this room is pleasant (Globalement, l'éclairage de cette salle est agréable)	VAS: [no-yes = 0-100]
3) There is not enough light to work/read properly (Il n'y a pas assez de lumière pour travailler / lire correctement)	VAS: [no-yes = 0-100]
4) There is too much light to work/read properly (Il y a trop de lumière pour travailler/lire correctement)	VAS: [no-yes = 0-100]
5) The lighting is badly distributed in this room (La lumière est mal distribuée dans cette salle)	VAS: [no-yes = 0-100]
6) How do you perceive the glare in this room (Comment ressentez-vous l'éblouissement dans cette salle)	1=imperceptible, 2=just perceptible, 3=perceptible, 4=just acceptable, 5=acceptable, 6=just uncomfortable, 7=intolerable, 8=just intolerable, 9=intolerable
7) The color of my skin looks unnatural under this lighting (La couleur de ma peau apparaît peu naturelle sous cet éclairage)	VAS [no-yes = 0-100]
8) The light in this room is too "warm" for a working environment (La lumière de cette salle est trop "chaude" pour un lieu de travail)	VAS [no-yes = 0-100]
9) The light in this room is too "cold" for a working environment (La lumière de cette salle est trop "froide" pour un lieu de travail)	VAS [no-yes = 0-100]
10) There is noise that disturbs me during my work in this room (Il y a du bruit qui me dérange pendant mon travail dans ce bureau)	VAS [no-yes = 0-100]

## Appendix B. Questionnaires: VAS/VCS

11)	If I compare the lighting condition of this office with others in which I worked before, I would say that the lighting condition here is: <i>(Si je compare la situation lumineuse de ce bureau avec d'autres dans lesquelles j'ai travaillé auparavant, je dirais que la situation lumineuse ici est:)</i>	much better, slightly better, same, slightly worse, much worse [1-4] meilleure, plutôt meilleure, plutôt pareille, plutôt pire, pire [1-4]
12)	In the context of a working day, I could imagine working in this lighting environment during... <i>(Dans le cadre d'une journée de travail, je pourrais bien m'imaginer travailler dans cet environnement lumineux pendant...)</i>	less than 2 hours, 2-4 hours, 4-6 hours, more than 6 hours [1-4] moins de 2 heures, 2 à 4 heures, 4 à 6 heures, plus de 6 heures [1-4]
Indicate how you feel in this moment <i>(Indiquez sur l'échelle comment vous vous sentez en ce moment)</i>		
13)	extremely relaxed – extremely tense <i>(extrêmement relaxé – extrêmement tendu)</i>	VAS [0-100]
14)	physically comfortable – physically uncomfortable <i>(physiquement à l'aise – physiquement pas du tout à l'aise)</i>	VAS [0-100]
15)	extremely alert – extremely tired <i>(extrêmement éveillé – extrêmement fatigué)</i>	VAS [0-100]
16)	satiated – hungry <i>(rassasié – affamé)</i>	VAS [0-100]
17)	in a bad mood – in a good mood <i>(de mauvaise humeur – de très bonne humeur)</i>	VAS [0-100]
18)	extremely warm – extremely cold <i>(extrêmement chaud – extrêmement froid)</i>	VAS [0-100]

**Table B.1** – List of questions included in the surveys (VAS/VCS) to which participants were required to answer at regular intervals during the days in the office rooms. The questions were presented to the participants in French (here in italics).

## Échelle de confort visuel

Voici quelques questions concernant l'environnement lumineux de cette salle.  
Veuillez marquer votre consentement avec chaque déclaration sur la ligne correspondante.

1. Actuellement, j'aime la lumière dans cette salle:

Non  Oui

Question suivante

Question 1 sur 18:

6. Comment ressentez-vous l'éblouissement dans cette salle:

Imperceptible Juste perceptible Perceptible Juste acceptable Acceptable Juste inconfortable Inconfortable Juste intolérable Intolérable

Question suivante

Question 6 sur 18:

15. Indiquez sur l'échelle comment vous vous sentez en ce moment:

Extrêmement éveillé  Extrêmement fatigué

Question suivante

Question 15 sur 18:

Figure B.1 – Example of questions (screenshots) included in the surveys with Visual Analogue Scale (VAS).

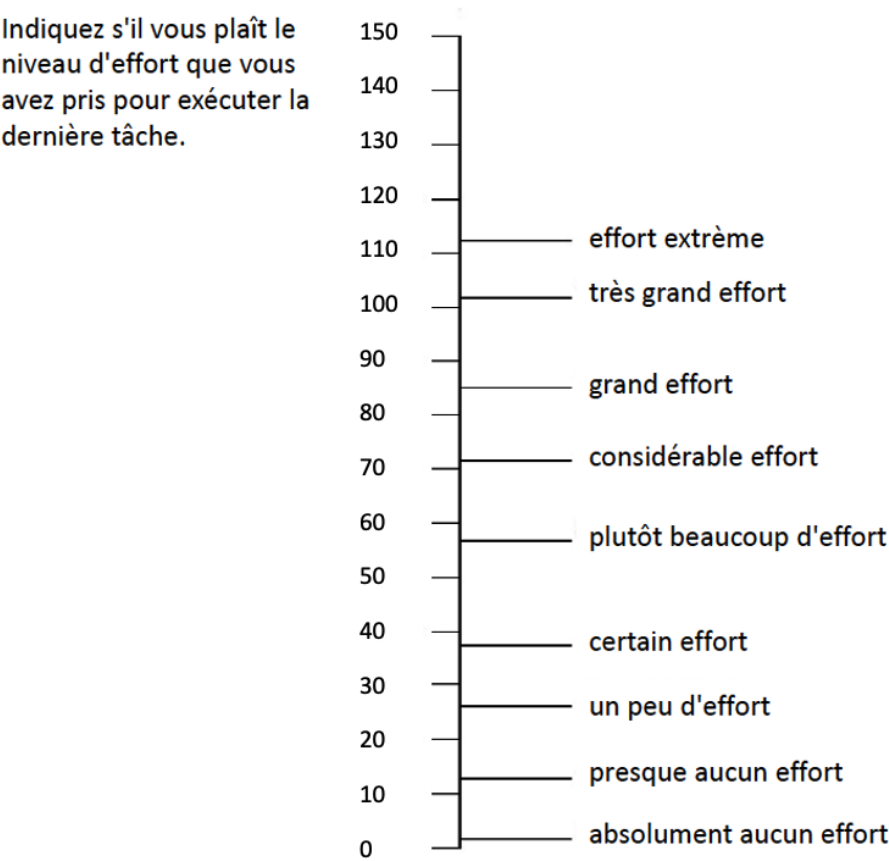
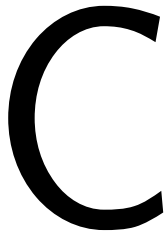


**Figure B.2** – Mental Effort Rating Scale (MERS). During the study, participants were asked to indicate their perceived effort in executing the cognitive task session.



## Correlation analysis and subjective comfort

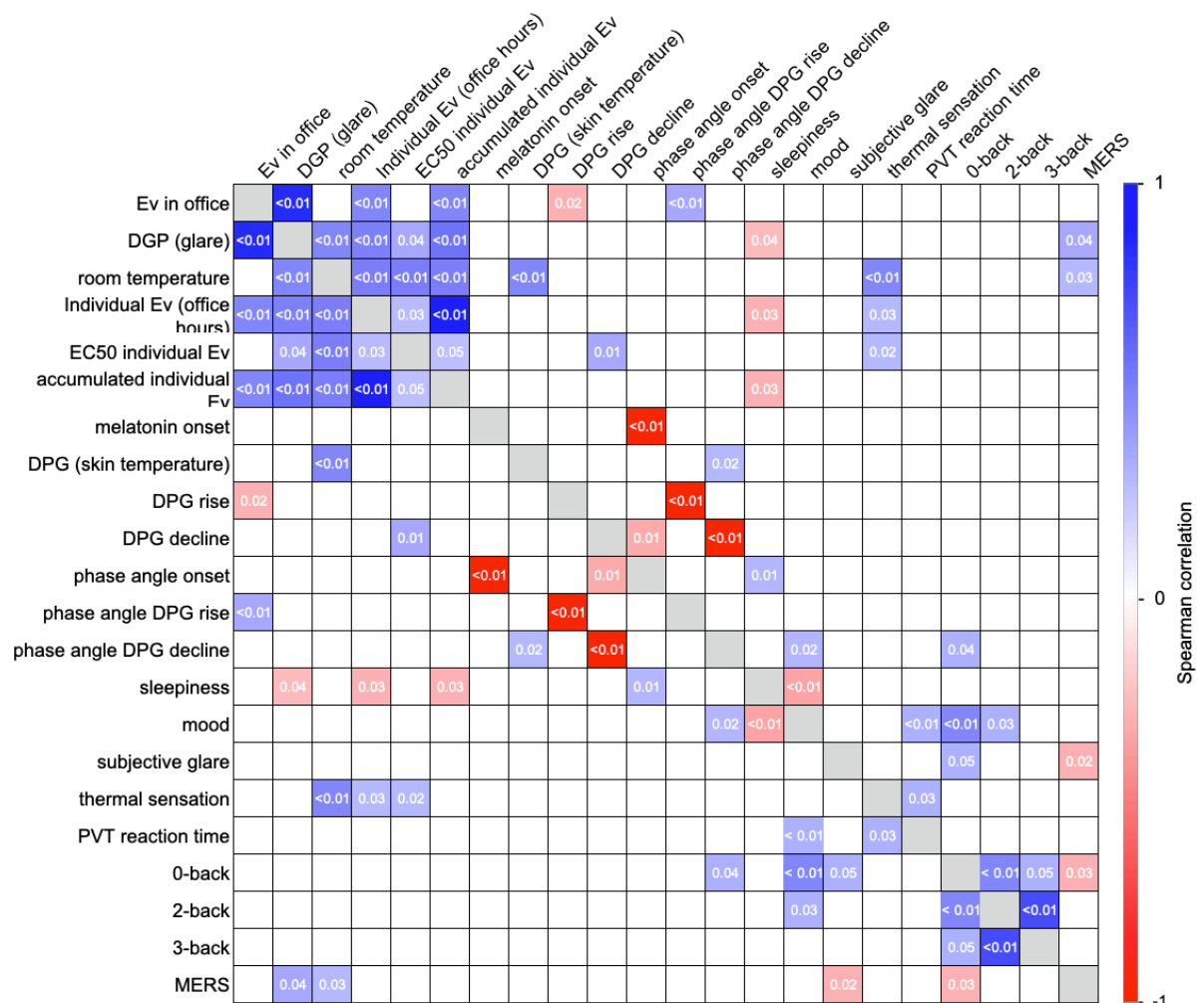


**Figure C.1** – Correlation table. Colours indicate the Spearman's correlation coefficient (as shown in the colour legend on the right). Only p-values lower than 0.05 are indicated, whereas blank cells denote  $p > 0.05$  (no significant correlation).  $E_v$  in office = assessed by VIP vision sensor during office hours; DGP = Daylight Glare Probability; Individual Ev = from wearable light sensors during office hours; phase angle onset = (sleep onset - melatonin onset); phase angle DPG rise = (sleep onset - DPG rise); same for DPG decline; PVT reaction time = 10% fastest RTs.

## Appendix C. Correlation analysis and subjective comfort

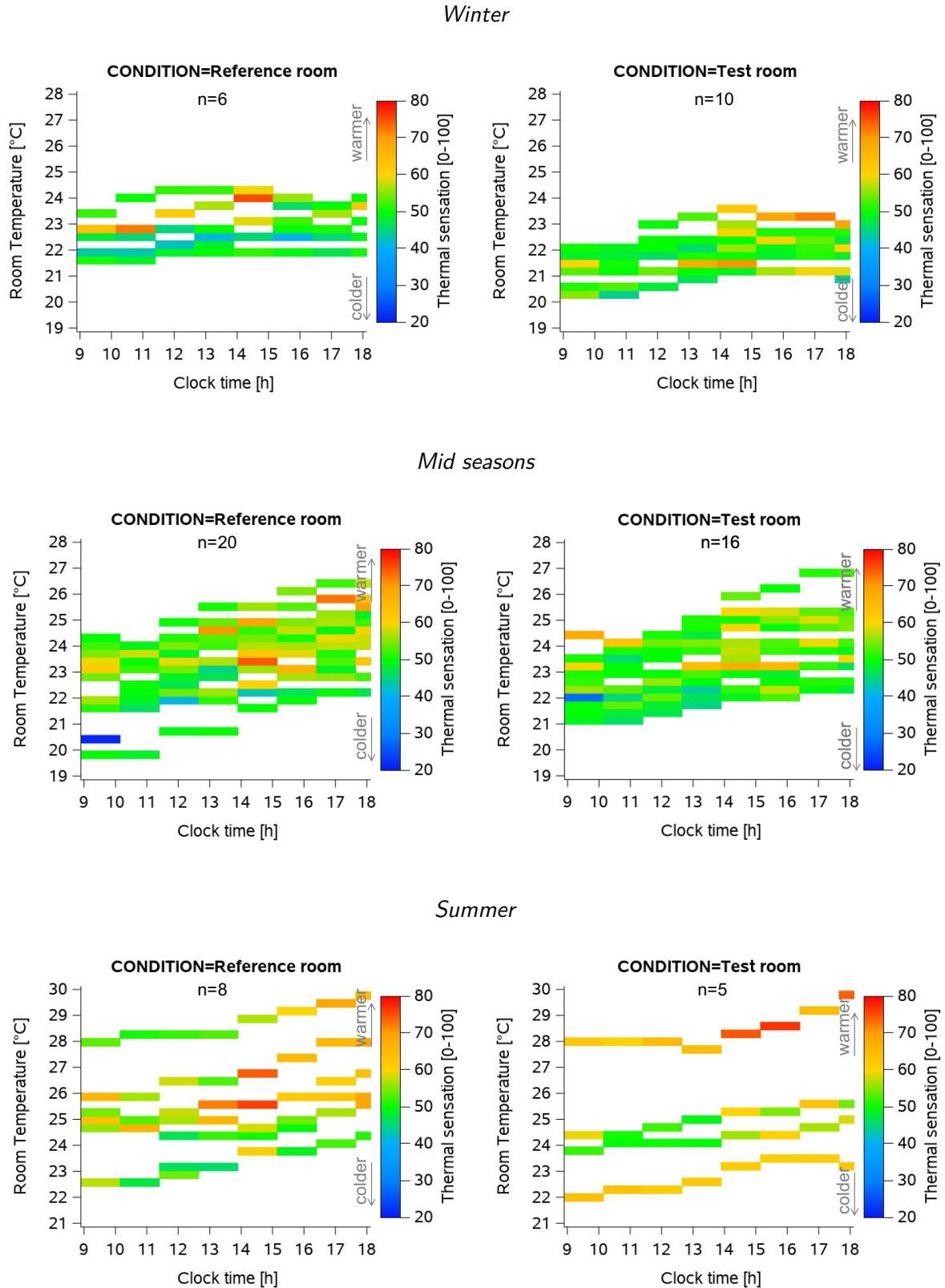


**Figure C.2** – Heat plots of room temperatures (left y-axis) and subjective thermal comfort assessments (right y-axis) in all seasons (winter: top; mid-seasons: middle; summer: bottom); averaged across 5 days and shown for both conditions (Reference room left and Test room right; all aligned to clock time). The colour bars on the right side of the Figures indicate the direction of subjective thermal sensation (=perception), from colder (blue) to warmer (red); n = number of participants.

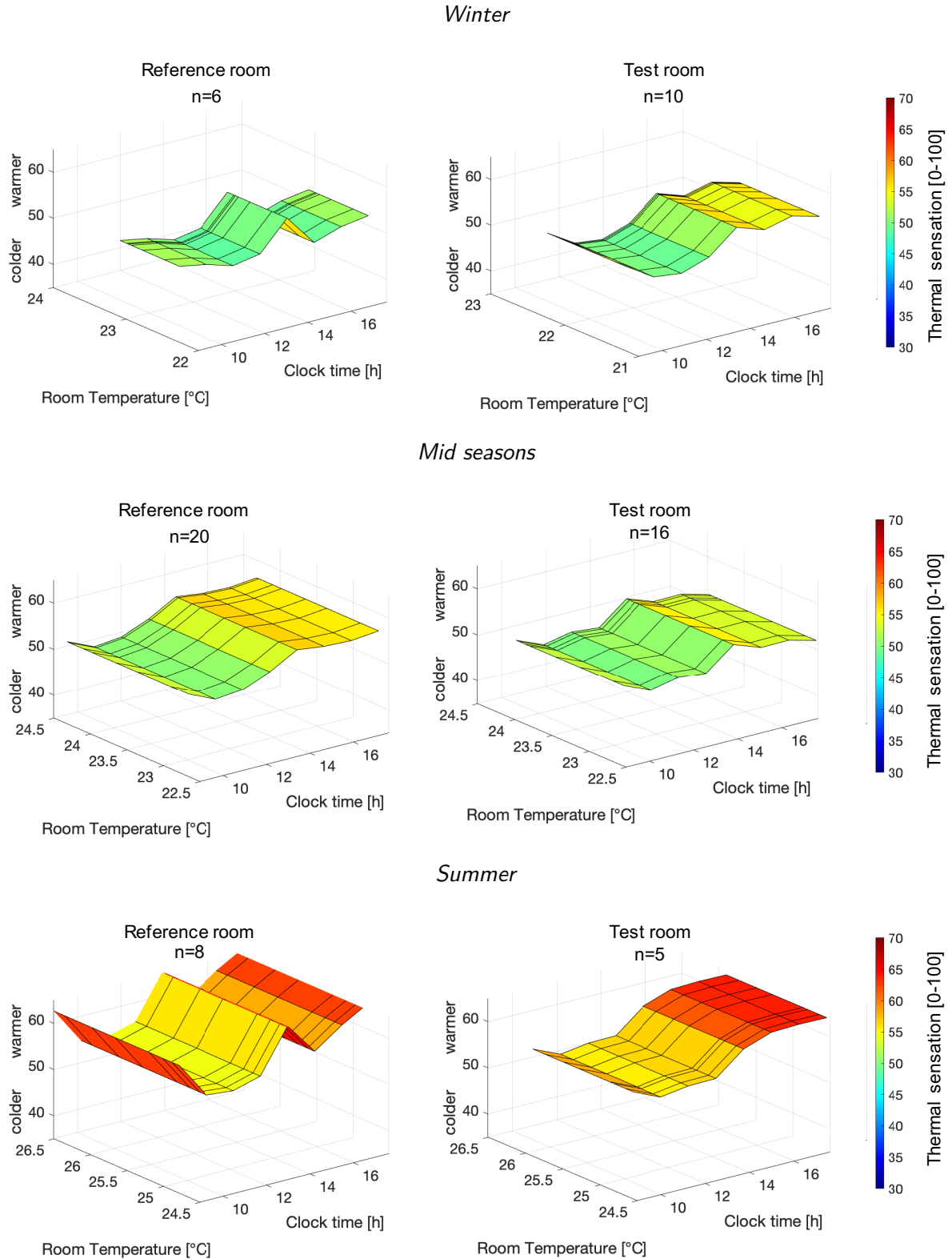


**Figure C.3** – 3D plots for subjective thermal comfort in all seasons averaged across 5 days for both conditions (left = Reference room, right = Test room). X-axis: room temperature (°C); y-axis: clock time (h); z-axis: subjective thermal comfort (thermal sensation, 0-100). The colours indicate subjective thermal comfort [see the legend on the right sides of the Figures; warmer colors (reddish) = warmer temperature sensations; colder (bluish) colours = colder temperature sensations]; n = number of participants.

Heat maps: visual comfort in all seasons and conditions

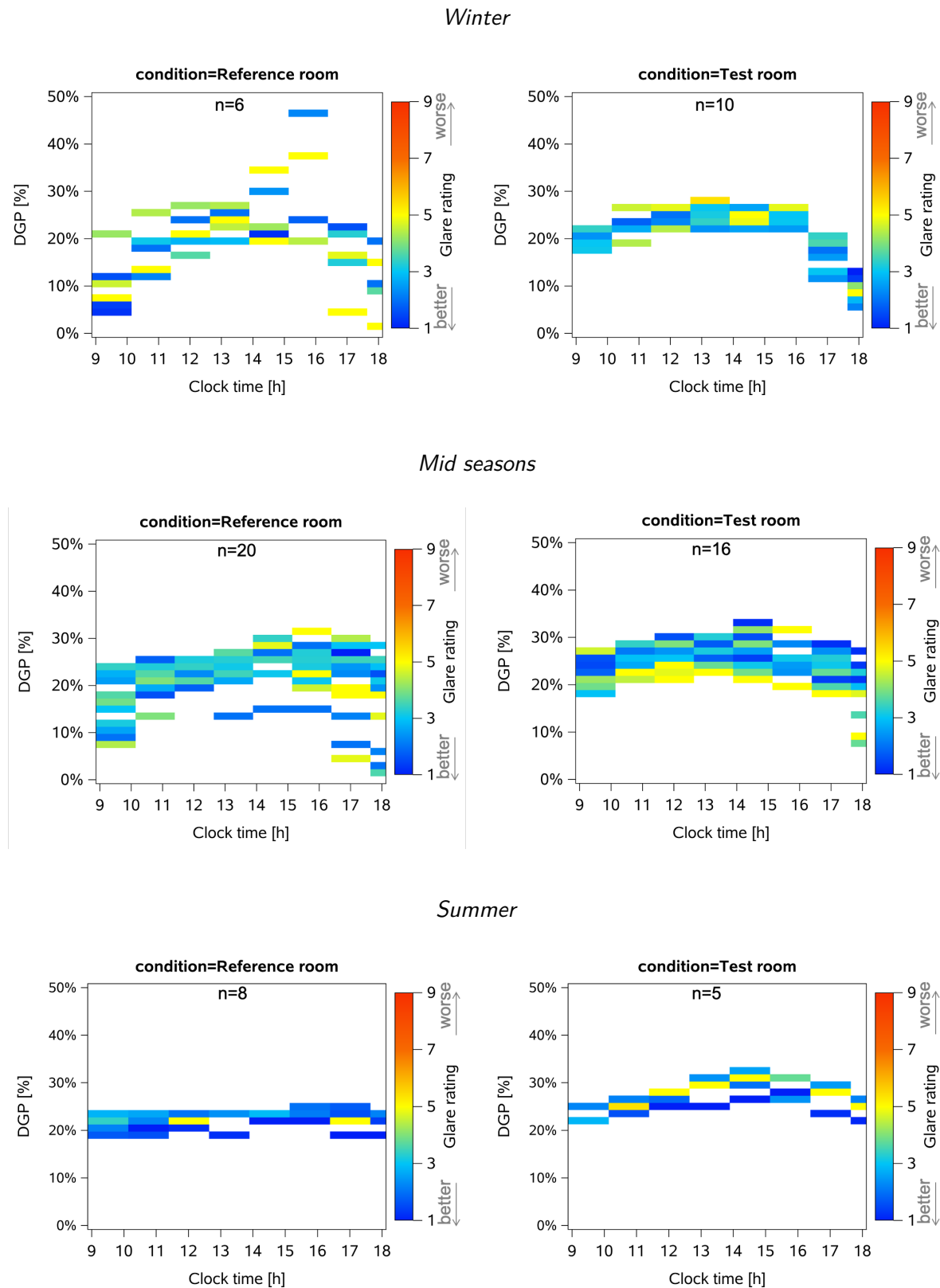


**Figure C.4** – Heat plots representing DGP and subjective visual comfort (glare rating) in all seasons and conditions for all participants, averaged across 5 days and aligned to clock time. The colour bars on the right side of the Figures indicate subjective glare ratings, from imperceptible (blue) to intolerable (red).



# D

## Control platforms at LESO-PB and NEST

---

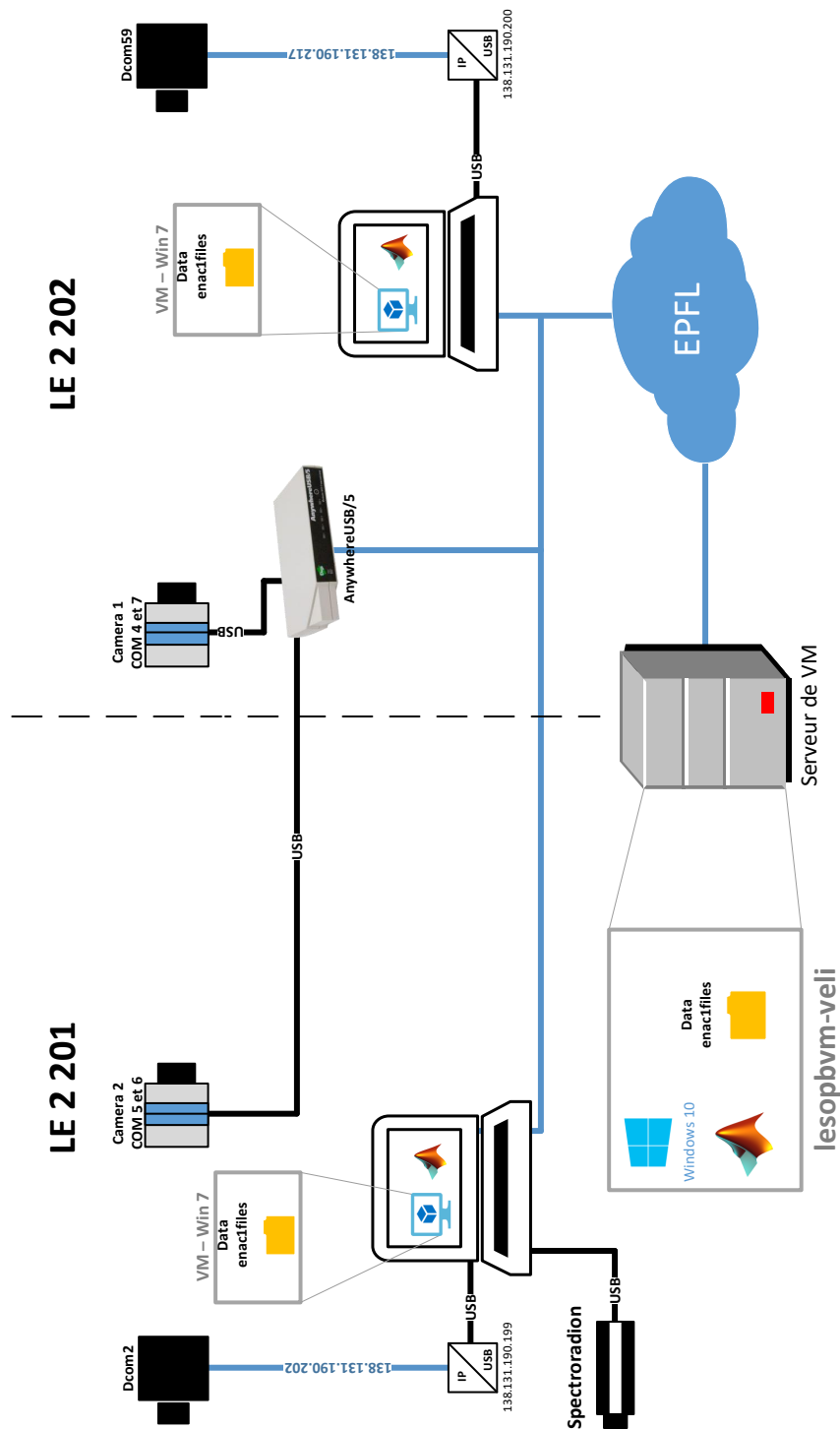


**Figure D.1** – Schematic overview of the physical platform of the control system applied in the two rooms in LESO-PB: LE2201 and LE2202 (courtesy of Michael Divià and Laurent Deschamps). The two IcyCams and the spectrometer are connected to local laptops in each room via USB cables, while the VIP sensors are connected to the DIGI Anywhere USB. All data (from both the local laptops and the DIGI) is transmitted and stored in the internal server of LESO-PB (grey box at the bottom). On the virtual machine (named "lesopbvm-veli") the control algorithm reads data on the server in real-time and sends the commands to the actuators of venetian blinds and electric lighting.

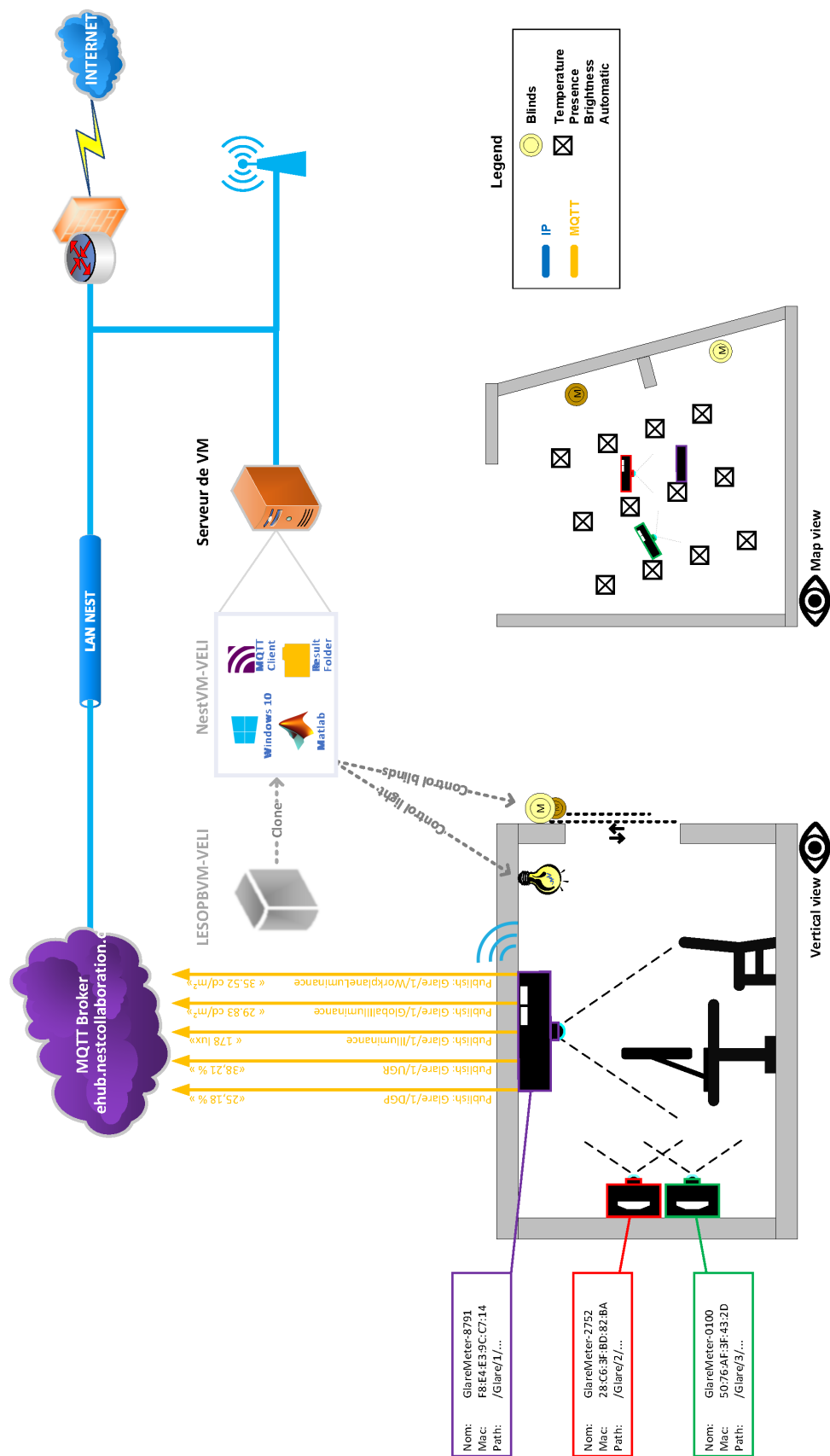


**Figure D.2** – Schematic overview of the data communication platform set up for the control of blinds and lighting at SolAce (courtesy of Valentin Trana and Laurent Deschamps). The Glare Meters (each one identified by a code and a path, as shown in the purple, red and green rectangles) monitor the lighting conditions and send data to the NEST database via the network protocol Message Queuing Telemetry Transport (MQTT), as indicated by the yellow arrows. The MQTT runs over the Internet by Protocol (IP). The controller is installed on a virtual machine on the NEST server (grey rectangle): here, data stored on the database is read and processed in real time by the algorithm, which then sends the commands to blinds and electric lighting. The "map view" also shows the positions of luminaires and blinds in the open plan office.



# MARTA BENEDETTI

[martabenedetti@live.com](mailto:martabenedetti@live.com)

+41 76 528 98 75

<https://www.linkedin.com/in/benedettimarta/>



## EMPLOYMENT HISTORY

---

2017 – present	Swiss Federal Institute of Technology (EPFL) - Solar Energy and Building Physics Laboratory (LESO-PB) PhD candidate, research & teaching assistant
2016 – 2017	Swiss Federal Institute of Technology (EPFL) - Solar Energy and Building Physics Laboratory (LESO-PB) Scientific assistant/engineer
2011 – 2012	WSC Studio Environmental Engineering - Trento, Italy Intern

## EDUCATION

---

2016	Free University of Bozen, Faculty of Science and Technology Master in Energy Engineering
2012	University of Trento   Department of Civil, Environmental and Mechanical Engineering Bachelor in Environmental Engineering

## AWARDS & SCHOLARSHIPS

---

2017 – present	9 <sup>th</sup> IAQVEC conference, Seoul (KR) Best paper award Motamed, M. Benedetti, J.-L. Scartezzini, "On the impact of integration of Non-Image-Forming (NIF) effect of light on electrical lighting control in non-residential buildings" <a href="https://infoscience.epfl.ch/record/222924">https://infoscience.epfl.ch/record/222924</a>
2019	Swiss National Foundation (CH) Doc Mobility fellowship for a 6-months research stay in Wellington, New Zealand

## SCIENTIFIC PUBLICATIONS

---

M. Benedetti, L. Maierová, C. Cajochen, A. Motamed, M. Münch, J.-L. Scartezzini, "Impact of dynamic lighting control on light exposure, visual comfort and alertness in office users" – Journal of Physics: Conference Series 2019  
<https://infoscience.epfl.ch/record/274116?ln=en>

M. Benedetti, A. Motamed, Laurent Deschamps, Jean-Louis Scartezzini, "On the integration of Non-Image-Forming effects of light on venetian blinds and electric lighting control" - Energy Procedia 122:1039-1044, 2017  
<https://doi.org/10.1016/j.egypro.2017.07.475>

A. Motamed, M. Benedetti, J-L. Scartezzini, "On the Impact of Integration of Non-Image Forming ( NIF ) Effect of Light on Electrical Lighting Control in Non-Residential Buildings" – Best Paper Award at IAQVEC conference in Seoul, South Korea, 2016

<https://infoscience.epfl.ch/record/222924>

## SCHOOLS AND WORKSHOPS

---

Jan. 2019	ETH Sustainability Winter School "Perspectives on Daylight" Rigi Kaltbad (CH)
Aug. 2018	LumeNet: A Research Methods Workshop for PhD Students of Lighting, Colour, Daylight and Related Subjects Aalborg University Copenhagen (DK)
Aug. 2018	CIE Expert Tutorial and Workshop On Research Methods For Human Factors In Lighting Copenhagen (DK)
Feb. 2018	Eurotech Winter School Swiss Federal Institute of Technology (EPFL) Lausanne (CH)
Nov. 2017	Daylight Academy (DLA) Annual Conference and General Assembly Lausanne (CH)
Oct. 2017	SCCER Summer School "Shaping the energy transition" Swiss Competence Center for Energy Research Engelberg (CH)
Aug.-Sept. 2017	Zero Energy Buildings Summer School (ZEBSS) Politecnico di Milano Mantova (IT)
June 2017	Continuous Medical Education (CME) course in Annual SLTBR meeting "Impacts of Light on Humans and Chronobiological Approaches" Berlin (DE)
May 2017	7 <sup>th</sup> Velux Daylight Symposium Berlin (DE)

## APPROVED RESEARCH PROJECTS

---

2018-2020	NEST (Next Evolution in Sustainable Building Technologies) SolAce EMPA (Swiss Federal Laboratories for Materials Science and Technology) <a href="https://www.empa.ch/web/nest/solace">https://www.empa.ch/web/nest/solace</a> (section: Dynamic & Circadian LED lighting)
-----------	--

## SOFTWARE SKILLS

---

- |  |   |
|--|---|
| <ul style="list-style-type: none"> <li>• Matlab, Python</li> <li>• Data analysis and statistics: SAS, SPSS, R</li> </ul> | <ul style="list-style-type: none"> <li>• MS Office, LaTeX, AutoCAD</li> <li>• Dialux, SketchUp</li> </ul> |
|--|---|

## LANGUAGES

---

Italian: mother tongue  
English: proficient (B2/C1) – First Certificate English (FCE)  
French: independent (B2)  
German: independent (B1/B2)

## EXTRA-CURRICULAR ACTIVITIES

---

2011-2020 Schweizer Skischule St. Moritz (CH), New Generation Ski School Méribel-3 Vallées (FR), Scuola Italiana Sci Moena Dolomiti (IT)  
Ski instructor

2012-2016 Topflight (Ireland)  
Tour operator assistant (summer seasons)

## HOBBIES

---

Strong passion for sports: alpine ski, road cycling, triathlon (taking part in competitions), windsurfing, sailing, fitness

## PERSONAL DETAILS

---

Birth date: 25.01.1989  
Citizenship: Italian  
Residence permit: B